Thermal up-rating of transmission lines and substation equipment

---

A dissertation submitted to
The School of Electric, Electronic and Computer Engineering
North West University

In partial fulfilment of the requirement for the degree
Magister Ingeneriae in Electrical and Electronic Engineering

by

Pieter Schalk van Staden

Supervisor: Prof. Jan A de Kock

Date: November 2012
Potchefstroom Campus

Declaration

In accordance with the requirements for the Masters degree in Engineering and the school of Electric, Electronic and Computer Engineering, I present the following dissertation entitled “Thermal up-rating of transmission lines and substation equipment.” The research and work of this project was performed under the supervision and guidance of Prof Jan A de Kock.

I declare that the work submitted in this dissertation is my own, except the parts as acknowledged in the references.

Pieter Schalk van Staden

Note: The Northwest University postgraduate management committee approved the title of this dissertation as “Thermal up-rating of transmission lines and substation equipment”, however the spelling of up-rating must reflect as uprating. From here on forward uprating will be used in the text.

Abstract

The new regulated electricity supply industry of South Africa is undergoing a major transformation that requires a redefined approach to increase the utilisation of existing transmission line assets. South Africa's existing 275 kV transmission line network was designed conservatively. It is suspected that the lines are being operated at temperatures well below than which they were designed for. Therefore, in certain cases they could be uprated by operating them above their present power rating such that more power is transmitted without the requirement for new lines.

The country is currently experiencing challenging times as additional capacity is needed by the growing economy, increasing the power demands of Eskom's customers. However, economic and environmental pressures contribute to the difficulty in obtaining new servitudes and the regulatory approval for the construction of new transmission lines. Uprating the 275 kV power network may partly alleviate these predicaments.

Thermal uprating a line results in an increase in ampacity, which is the maximum current carrying capacity of a particular transmission line. This means that the power flow will be increased by allowing more current through the conductor which in turn increases the thermal rating (operating temperature) of the conductor, but the resulting increase in power transfer influences the sag which reduces the line clearance.

It is possible by means of a non-intrusive method to increase the power transfer capability of transmission assets and at the same time maintaining the safety of the transmission line for the public. Any increase in power transfer will occur without any risk in power equipment or system.

Dedication

This work is dedicated to my lovely wife-to-be Lené, my parents Pieter and Nelie van Staden, and Tallie and Leonie White for all the sacrifices, endless support and encouragement. Also a special dedication in the memory of my friend Gerrit Grobler.

Acknowledgements

The work presented in this dissertation could not have been completed without the assistance of a number of key people and organisations. The author wish to express his gratitude to all the people who made this dissertation possible and especially to the following:

- Prof. Jan A de Kock from the North-West University for his mentorship and insightful advice.

- Thank you to all the members of Eskom Central Grid live line team for their dedication and hard work during the installation of the measurement equipment.

- Shelley le Roux for her guidance and advice with the power line modelling.

- Arthur Burger and Rob Stephen for their guidance regarding heat balance equations and conductor thermal ratings.

- Adri de la Rey and Dumisani Sibande, who on short notice arranged for light detection and ranging surveys.

- Thank you to Eskom Research, Test and Development for financial support to perform this research.

- A special thank you to family and friends for all their support and encouragement.

Table of Contents

List of figures

List of tables

Nomenclature
Terms and Definitions

Ampacity	-	The ampacity of a conductor is that current that will meet the design, security and safety criteria of a particular line on which the conductor is used.
Annealing	-	A process that causes a decrease in a conductor's strength and performance due to heating and slow cooling of the material.
Clearance	-	The distance between two objects or the space between them. The distance by which one object clears another.
Creep	-	The continuous deformation or elongation of a conductor under tension or load at modest operating temperatures.
Deterministic method	-	The assumption of worst-case cooling for bare overhead conductors to determine operating temperature.
Electrical clearances	-	The minimum clearances prescribed by statutory law for electrical clearance between objects, conductors and the ground. Prescribed by the Operational, Health and Safety Act of South Africa.
Exceedence	-	The time when the conductor operating temperature is greater than the design temperature.
Laser	-	A laser generates a highly focused narrow beam with a single wavelength and high radiant intensity used for the measurement of distances.
LIDAR	-	Light detection and ranging system used to measure distance as well as to compute co-ordinates.
Loadability	-	The maximum power that a transmission line can convey.
Meteorological	-	Atmospheric phenomena that include weather conditions.
Non-intrusive	-	A type of technique used to increase power transfer without physical modifications to a transmission line and hardware.
Operating temperature	-	The actual temperature of the loaded conductor under prevailing weather conditions.
Probabilistic method	-	The actual weather data and conditions prevailing on the line or in the area to determine the likelihood or probability of a certain condition occurring based on statistical probabilities.
Reliability	-	The probability of satisfactory operation in the long term.
Right of way	-	Servitude.
Sag	-	The vertical distance between the points where the conductor

		is joined (points of support) at the tower and the lowest point of the conductor.
Servitude	-	A right belonging to Eskom in the property of another person, which refers in the context of transmission lines to the land required to construct and operate an overhead transmission line.
Statutory	-	Defined by national laws and regulation.
Steady state conditions	-	A condition in a power system that does not change or vary as time progress.
Strain	-	Refers to material science where deformation takes place in terms of relative displacement of particles in a body.
Strain rate	-	The rate of change in strain with respect to time.
Template	-	A transparent template used to simulate the sag of a conductor under statutory clearance curves and weather conditions. It is used as a scale for conductor catenaries between towers.
Templating temperature	-	The line templating (templated) or design temperature is the maximum conductor temperature during normal operational load at which the height of the conductor above the ground is as prescribed by statutory law.
Templated temperature	-	Templating temperature.
Thermal rating	-	The maximum current that power equipment or transmission circuits can transport continuously.
Thermal limit	-	The maximum load current that the transmission asset can transport continuously.
Thermal uprating	-	A process to increase the power transfer capability of transmission circuits by allowing increased operating temperature.
Uprating	-	To increase power transfer capacity of transmission circuits.

List of abbreviations

3D	-	Three-dimensional
A	-	ampere
AAAC	-	All aluminium alloy conductor
AAC	-	All aluminium conductor
AC	-	Alternating current
ACAR	-	Aluminium conductor aluminium alloy reinforced
ACSR	-	Aluminium conductor steel reinforced
ANSI	-	American National Standards Institute
CADD	-	Computer aided design and drafting
CB	-	Circuit breaker
CIGRE	-	International Council on Large Electric Systems
CT	-	Current transformer
CVT	-	Capacitor voltage transformer
DC	-	Direct current
EPRI	-	Electric Power Research Institute
HVAC	-	High voltage alternating current
HVDC	-	High voltage direct current
HTLS	-	High temperature low sag
IEC	-	International electro-technical commission
IEEE	-	Institute of electronic and electrical engineers
K	-	kelvin unit for measurement of temperature
kA	-	kiloampere
kHz	-	kilohertz
km	-	kilometre
kV	-	kilovolt
kV/m	-	kilovolt per metre
LIDAR	-	Light detection an ranging
m	-	metre
ms	-	millisecond
MVA	-	Megavolt-Ampere
MW	-	Megawatt
PLS CADD	-	Power line systems computer aided design and drafting
P	-	Power
p.u.	-	Per unit value
SF6	-	Sulphur hexafluoride
SIL	-	Surge impedance loading

TxSIS	-	Transmission spatial information system
V	-	volt
VA	-	Voltampere
var	-	voltampere reactive
VT	-	Voltage transformer
W	-	watt

List of symbols

α	-	Temperature co-efficient of resistance per kelvin
α_s	-	The absorptivity of the conductor surface
Δ	-	Delta
δ_s	-	Sending end voltage angle
δ_r	-	Receiving end voltage angle
ε	-	Emissivity of conductor
η	-	The angle of the solar beam with respect to the axis of the conductor
λ_f	-	Thermal conductivity of air around the conductor
Ω	-	Resistance of conductor
ω	-	Angular frequency in radians
π	-	Pi
ρ	-	Relative air density
σ_B	-	Stefan-Boltzmann constant
τ	-	Thermal time constant
τ_w	-	Winding thermal time constant
τ_0	-	Oil thermal time constant
θ_a	-	Ambient temperature
θ_C	-	On load tap changer contact temperature rise over oil
$\theta_{C,R}$	-	On load tap changer contact temperature rise over oil at rated load
θ_{FL}	-	Full load top oil rise temperature
θ_g	-	Hottest spot rise over top oil
θ_{HR}	-	Winding hottest spot temperature
θ_{HS}	-	Hottest spot temperature
$\theta_{HS.R}$	-	Rated hot spot rise over oil
$\theta_{HS.U}$	-	Ultimate hot spot temperature rise over oil
$\theta_{HS,1}$	-	Hot spot rise over oil at the previous time step, *t*1
$\theta_{HS,2}$	-	Hot spot rise over oil at the present time step, *t*2
θ_i	-	Initial oil rise temperature from prior loading

$\theta_{O.R}$	-	Rated oil temperature rise
θ_r	-	Limit of observable temperature rise at rated continuous current
θ_{U}	-	Ultimate temperature rise
θ_{u}	-	Ultimate oil rise temperature for overload
$\theta_{O.U}$	-	Ultimate oil temperature rise
$\theta_{\max n}$	-	Normal maximum allowable temperature
$\theta_{\max}$	-	Maximum allowable temperature of switch part
$\theta_{\max_{e24}}$	-	Emergency allowable maximum temperature
θ_0	-	Top oil temperature rise over ambient
θ_1	-	Temperature rise at step i
θ_2	-	Contact temperature rise at present time step, *t*2
$\theta_{O.1}$	-	Oil temperature rise at the previous time step, *t*1
$\theta_{O.2}$	-	Oil temperature rise at the present time step, *t*2
A_s	-	Cross-sectional area of the steel core
B_1	-	Constant used to determine Nusselt number
B_m	-	The peak value of magnetic induction in a steel core
C	-	Transmission line capacitance
$^{\circ}C$	-	Degrees celsius
C_p	-	Specific heat capacity of the conductor per unit length
Dia	-	The diameter of the conductor
Δt	-	Time step
d_s	-	Diameter of steel wires in the core of ACSR conductors
f	-	Rated frequency
F	-	Skin-effect coefficient
F_{aaf}	-	Ageing accelerated factor
G	-	Thermal time constant
G_r	-	Grashof number
H_s	-	The solar altitude
i	-	Initial quantity

I	-	Per unit rated bushing current
I^2	-	Effective conductor current
I_A	-	Allowable continuous current
I_d	-	The intensity of the diffuse sky radiation to a horizontal surface
I_D	-	The intensity of the direct solar radiation on a surface normal to the beam
I_{cth}	-	Continuous thermal current
I_{e24}	-	Emergency rating of greater than 24 hours duration
I_f	-	Final step change in current
I_i	-	Initial current value before step change
I_{th}	-	Thermal current
I_I	-	Initial current prior to overload
I_n	-	Normal current rating,
I_p	-	Current capability at actual ambient temperature
I_R	-	Rated continuous current at a temperature rise θ_r
I_r	-	Rated continuous current
I_s	-	Short-time permissible overload
I_{tapr}	-	Rated continuous current of specific current transformer
I_{tap}	-	Adjusted rated continuous current of specific current transformer tap
I_2	-	Current at the present time step
K_i	-	Per unit initial loading, prior to overload
k_j	-	Correction factor for skin and magnetic effect
K_u	-	Per unit overload intended.
$K_{1,2}$	-	Specific bushing constant
L	-	Transmission line inductance
L_{air}	-	Loadability of a line isolator
L_p	-	Inductance at the power frequency
M	-	Mass of the conductor per unit length
m	-	Exponent, generally between 1.5 and 2.0

n	-	Constant used to determine Nusselt number
Nu	-	The Nusselt number (Nuforced)
$Nu_{de-rated}$	-	De-rated Nusselt number
P_{acc}	-	Probability of an accident or flashover occurring
$P(CT)$	-	Probability of a certain temperature being reached by the conductors
P_C	-	Convective cooling
P_{gain}	-	Sum of the Joule heating P_J and solar heating P_S
$P(I)$	-	Probability of the assumed current being reached
P_i	-	Corona heating
P_J	-	Joule heating
P_M	-	Magnetic heating
$P_{n1,2,3}$	-	Natural convective cooling
$P(obj)$	-	Probability of decreasing the electrical clearance by an object under or in the vicinity of the servitude
$P_{prandtl}$	-	Prandtl number
P_r	-	Radiative cooling
$P(surge)$	-	Probability of a voltage surge occurring
P_S	-	Solar heating
P_w	-	Evaporative cooling
q_C	-	Convective heat loss
q_{cond}	-	Conductive heat loss
q_r	-	Radiative heat loss
q_s	-	Solar heat gain
R_{ac}	-	AC resistance of conductor
R_{dc}	-	DC resistance of conductor
RF	-	Continuous thermal current rating factor
R_f	-	Conductor roughness factor
R_r	-	Ratio of load losses at rated current to no-load losses
R	-	Reynolds number
$Strand_{diameter}$	-	Outer layer aluminium conductor
$S_{measured}$	-	Radiation level of the sun

T_2	-	Winding hot spot temperature at the present time step, t_2 .
t	-	Intended overload
t_s	-	Allowable short-time period
$t1$	-	Previous time step
$t2$	-	Present time step
T_a	-	The ambient temperature
T_{avg}	-	Average temperature of the conductor
T_c	-	Steel core temperature of ACSR conductor
T_f	-	Air film temperature around the conductor
T_h	-	Maximum design temperature for different insulation classes
T_o	-	Design ambient temperature.
T_s	-	Surface temperature of the conductor
U_m	-	Highest system voltage
v	-	Kinematic viscosity of air around the conductor
v_r	-	Voltage and receiving end
v_s	-	Voltage at sending end
X_L	-	Series reactance
Z_C	-	Characteristic impedance

Chapter 1
Introduction

This chapter serves as an introduction to and the motivation for the research discussed within this dissertation. The topic of the dissertation is briefly introduced and explained in this chapter, followed by the methods used to achieve the required outcome. An overview of the structure of the dissertation is also provided.

1.1 BACKGROUND INFORMATION

Through discovery, invention and innovative engineering applications, engineers have contributed towards making electricity useful for and available to a larger section of the population. Historically, electricity was confined to powering large cities but nowadays electricity is used to power industry as well as to promote economic growth and the well-being of countries. A power utility must continually expand its generating capacity to meet the increasing demands of the customer. In some cases, power utilities struggle to meet the demand with the existing capacity in the network and therefore seek to expand their capacity.

Increasing demand for electrical energy drives the need to utilise existing networks closer to their thermal limits. Both electricity researchers and manufacturers seek solutions to increase utilisation. New methodologies and technologies aiming at identifying solutions to support system planners and operators to optimise the use of existing lines and substation equipment are investigated [1].

South Africa is experiencing challenging times as additional capacity is needed. Previously the increase in demand was matched by expanding the transmission line network to satisfy the increase in demand [3]. However, the solution of building new lines is limited by the regulation of the electricity supply industry as well as the influence of economic and environmental constraints. The difficulty of obtaining new servitudes is resulting in a corresponding requirement to increase the power transfer of existing overhead transmission lines and substation equipment.

Electricity is the key component that fuels all economic development globally. Eskom's annual 2010 report states that South Africa has to build an extra generating capacity of 40 000 MW by 2025 to ensure an adequate electricity supply for the future [4]. Figure 1.1.1 displays the existing generating capacity of Eskom. To optimise the transmission network in this rapidly expanding environment, system operators and network planners have to expand the transmission network or improve the reliability and utilisation of the existing network.

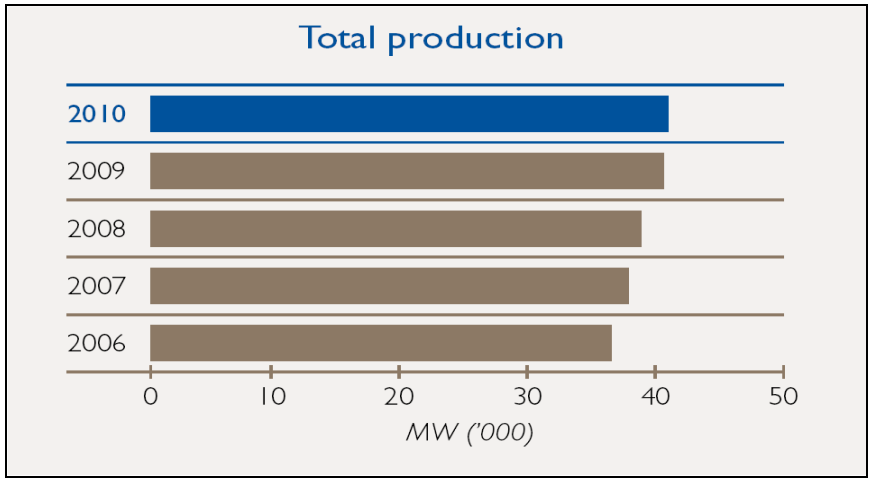

Figure 1.1.1: Existing generating capacity of the South African power pool [4]

The transmission line network improves the access to electricity, stimulates healthy economic growth, and contributes to the social, ecological and environmental upliftment of the country [5]. Additionally the transmission line network plays a very important role in ensuring a reliable and secure electricity supply to connected customers. Eskom is currently expanding its generating capacity at a rapid rate to meet the increasing demand; new transmission lines have to be constructed to transport the generated power from new power stations to the respective load centres within Southern Africa. In some cases, the existing infrastructure has to be exploited to convey the increase in power through existing rights of way.

It is postulated that South Africa's existing 275 kV transmission network was designed very conservatively. It is suspected that the lines are operating at temperatures well below those for which they were designed. In light of the above,

the existing power network within South Africa requires the re-evaluation of the conservative design practises as well as the determination of optimal conductor ampacity ratings to meet the challenges of increased power flow in existing electrical circuits [6].

To establish a firm increase in power flow, new technologies have to be innovatively integrated into the transmission environment. Most of the new generating capacity will rely on the present electrical circuits and servitudes for delivering electricity to customers. Figure 1.1.2 displays an example of an integrated programme for increasing existing transmission line capacity [7]. The need to construct new transmission lines exists and also forms part of the programme but requires special environmental and regulatory approval.

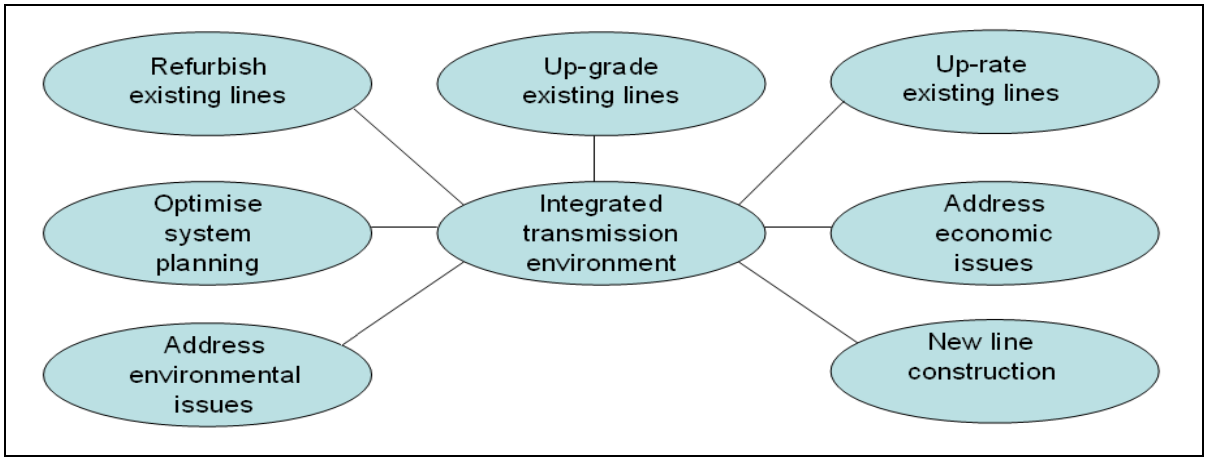

Figure 1.1.2: An example of an integrated programme to increase power flow [7]

A well-structured transmission infrastructure is one of the most important elements in the electricity supply industry for maintaining a reliable and secure electricity supply. Energy consumers and infrastructures are dependent on high quality electricity from the network to sustain, operate, maintain and develop businesses. Inevitably, electricity networks are vital for the functioning of societies and our economy [8]. Figure 1.1.2 illustrates a generic plan on how to establish a safe increase in power transfer. The techniques in Figure 1.1.2 can be used as a guide to assist system operators and planners to alleviate congestion in power networks.

The research discussed in this dissertation aims to relieve pressure on system operators and planners by increasing the loadability and power transfer of lines by fully utilising the thermal capability of existing transmission line circuits.

1.2 DEFINITION OF THE RESEARCH PROBLEM

1.2.1 **Problem statement**

The power supply industry in South Africa has undergone a dramatic change in the last decade. The general increase in demand for electricity reassigned the focus of system operators to re-evaluate the loading of existing transmission line assets. The objective of this dissertation is to provide and implement a non-intrusive method to achieve a reliable and safe increase in power transfer using existing rights of way. To achieve this, this dissertation will identify and discuss the thermal uprating of transmission lines and substation equipment. A section on the constraints and limitations of thermal uprating is also included in this dissertation. Additionally, an investigation into the behaviour of substation terminal equipment during short-time emergency loads under uprated conditions is researched. The optimisation of the loading of existing transmission circuits will result in the optimal use of existing transmission assets.

1.2.2 **Aim of the research**

The thermal uprating of existing transmission lines and substation equipment is, in most cases, possible and the easiest way of establishing a reliable increase in power transfer capability without any power equipment failures. In this context, increasing the load flow capacity in existing transmission circuits is a valid alternative to the construction of new transmission circuits. The aim of the research discussed within this dissertation is to investigate the possible increase in power transfer capability of existing transmission circuits. It will show how system operators will be able to increase the loading of transmission lines safely, if sufficient margin exists. Thermal uprating of transmission lines will result in higher templating and operating temperatures of overhead transmission lines and substation equipment. The

resulting increase in operating temperatures will fully utilise the thermal capability of existing transmission circuits, again provided that sufficient margin exists.

1.2.3 **Hypothesis**

South Africa's existing 275 kV transmission line circuits are operated well below their optimal thermal rating and loading capability.

Hypothesis extension – Thermal uprating of overhead transmission lines are thermally limited by the substation and terminal equipment.

1.3 DESCRIPTION OF PROCESS

The power transfer capability of overhead power lines is limited by economic, physical and statutory constraints [1]. One of these constraints is conductor temperature. The maximum temperature at which a conductor can safely operate is determined by: (a) permissible sag, governed by statutory requirements; (b) annealing and long-term creep; and (c) the reliability of current carrying parts, joints and fittings [6].

The temperature of a conductor is affected by the current flowing through the line as well as radiation from the sun. In the same way, cloud cover, wind speed, wind direction (angle of attack) and rain have a cooling effect. The sag of a conductor is proportional to the temperature and the tension of the conductor, which affects safe ground clearances. In the past, the temperature ratings of lines have been estimated using various methods, i.e. deterministic and probabilistic rating methods. The worst case in terms of ambient conditions was used to determine the thermal limits of a line. These worst-case conditions, however, only exist for a short-time during an entire year. In this way, the full use of the maximum capacity of the overhead transmission line is not used [9].

"As built" plans of lines have also not been reviewed and consequently the position of the conductor in space is not known to any degree of certainty. Through the years,

sag and the construction of physical features under the line encroached on safe clearances.

As it is possible to simultaneously determine the exact position of the conductor and its temperature, the direct relationship between the conductor position and ground surface can be established. Real time measurement of the conductor temperature enables the system operator to safely increase the power transfer capability of the system within the existing ambient conditions without compromising safe clearances. This method determines the actual thermal rating of a transmission line.

For the purpose of the research discussed in this dissertation the national system operator identified transmission lines that are heavily loaded and considered as critical under “system healthy” or during N-1 contingencies. Before the loadability of the lines is increased, it is important to understand and evaluate the history and the physical integrity of these lines. Power system issues pertaining to the thermal uprating of overhead lines and substation terminal equipment will be discussed in subsequent sections of this dissertation. The loadability of a transmission line refers to the maximum power the transmission line can transfer. Bottlenecks might be alleviated by thermally uprating the transmission lines together with the power equipment located within substation boundaries. The thermal models used to determine the templating temperature of the transmission lines together with the terminal equipment is also discussed in this dissertation. By implementing progressive methods together with real-time weather parameters, a higher transfer limit may be established from rating calculations, provided that sufficient margin exists to achieve this.

1.4 ISSUES TO BE ADDRESSED

In the light of the above, the research discussed within this dissertation will strive to address the following issues:

a. Establish the present loading of the identified transmission lines in relation to the designed loading.
b. Determine the prospective maximum loading of these lines.

c. Establish line-to-ground clearances under present loading versus the prospective maximum loading.
d. Identify constraints imposed by the possible thermal uprating of the lines.
e. Determine whether present thermal models can be used to effectively determine the rating of the lines and substation terminal equipment.
f. Establish the primary reasons for temperature limits of lines.
g. Identify the consequences of over-temperature of the transmission lines and substation terminal equipment.
h. Estimate how sensitive the lines and substation terminal equipment are to weather parameters.
i. Investigate how substation terminal equipment would respond to short-time emergency loads when thermal uprating is implemented.

1.5 METHODOLOGY

The following section describes several methods implemented in the study.

1.5.1 **Literature review**

The literature review is documented in Chapter 2 of this dissertation. The main objective of the literature review is to provide insight into relevant aspects of the thermal uprating of transmission circuits. This section will review various uprating methods available that can be implemented to relieve pressure within congested power networks as well as providing justification for the need to increase the power transfer capability of overhead transmission lines. The general uprating of substation equipment in comparison with transmission lines is also discussed in the literature review.

1.5.2 **Transmission line profile modelling**

This section of the dissertation will discuss the modelling of transmission lines in a three-dimensional (3D) field by means of a flight light detection and ranging data (LIDAR) survey together with load and weather based data. The 3D modelling of

transmission lines will assist system operators to do conclusive sag and clearance analysis on bare overhead conductors. In addition to the load and weather data, the conductor temperature is measured during flight by means of temperature sensors that are installed on the conductors. The LIDAR survey data will enable line profilers to establish a representative “as is” model of the transmission line. The transmission line model will include accurate information on the towers, ground wires, transmission line hardware and the exact catenary and position of the conductor in space. The 3D CADD (computer aided design and drafting) model will then be calibrated to allow users to graphically sag and raise the conductor to different positions by means of changing the conductor temperature. Through this method the permissible sag of the conductor for templating, normal and emergency ratings can be established. Subsequently the analysis is used to identify and address any infringements on conductor-to-ground clearances that might occur if power transfer is increased.

1.5.3 **Thermal analysis**

Planning and designing tools based on deterministic, probabilistic and mathematical techniques are used to accurately calculate thermal ratings of existing transmission lines. An evaluation between historical conservative design practices and static equations will be done. The evaluation will identify any shortcomings and drawbacks with previous historical design practices and will re-evaluate existing power transfer ratings with a modern approach. The approach will allow system operators and grid planners to make informed decisions on which method to implement to fully unlock any spare capacity within existing transmission circuits. In addition, engineers will be able to quantify the increase in power transfer by establishing higher conductor ratings.

1.5.4 **Validation and verification of results**

The approach described in Section 1.5.3 will be used to evaluate normal, templated and emergency current ratings that will result in a certain operating temperature of the conductor and vice versa. A mathematical model using Mathcad®, software

package will be implemented to assist with mathematical calculations. Calculated conductor operating temperatures will be validated and verified against measured operating temperatures. Additionally, the temperature of the conductor has a direct relationship to the sag that will be verified by using LIDAR data with the PLS CADD 3D (power line system computer aided design and drafting) model.

1.5.5 **Evaluation and conclusion**

The exact position of the conductor will be determined from the three dimensional transmission line models. The calculated temperature from Mathcad® will be used for the sag and clearance analysis of the conductor under various loading conditions. In conclusion, the position of the conductor in space will be known to a high degree of certainty. The results obtained from the modelling will be used to evaluate the condition of the transmission lines under study and the direct relationship between the conductor position and ground topography. Finally, recommendations for future work are made.

1.6 DISSERTATION OVERVIEW

Chapter 1 serves as a brief introduction to the research that is documented within this dissertation. The chapter forms the foundation of the research that is further discussed in subsequent chapters. The problem statement, aim of the research and hypothesis are defined and issues to be addressed with the research and the methodology are explained.

Chapter 2 consists of an in-depth literature review that discusses various uprating techniques as well as differentiating between invasive and non-invasive methods for uprating. The objective of the literature review is to give insight into the thermal uprating of transmission circuits. Power system issues and constraints that influence transfer capacity and thermal limits are discussed. Finally, fundamental principles as well as modern innovative concepts with the ultimate goal of increasing the power transfer capability of transmission circuits are demonstrated.

The objective of Chapter 3 is to focus on the 3D modelling, temperature, sag and clearance analysis of overhead transmission lines. By means of inflight light detection and ranging survey data, together with 24-hour based weather and load data, a representative “as is” transmission line model can be designed with the ability to sag and raise the conductors graphically under different loading conditions. Sag and clearance analysis of every span within the existing servitude can easily be done.

Chapter 4 focuses on identifying existing loading conditions of the transmission circuits under study and comparing the existing ratings against designed ratings. The operating temperatures of the lines under study are also determined and the ampacity rating methods discussed in the literature review are used to determine if the transmission lines are under-utilised. Results from the sag and clearance analysis are also discussed. In addition, the practicality of uprating strategies is demonstrated.

In Chapter 5, a conclusion is drawn based upon the results. In addition, recommendations are given for further study.

1.7 SUMMARY

The amounts of power a transmission line can transfer are largely affected by the maximum thermal limit, surge impedance loading, voltage limit and the steady state stability limit of the transmission line. By making use of various thermal uprating techniques discussed in this dissertation, it is possible to increase the loadability and power transfer capacity of transmission circuits where sufficient margin is available. This chapter serves as an introduction to the thermal uprating of overhead transmission lines and substation equipment. The definition of the research problem and the research methodology are defined. The ability to safely increase the current carrying capability of existing transmission circuits will prove to be enormously beneficial to power utilities. The accuracy, reliability and dependability of methods as well as the technology discussed in this dissertation will provide significant justification for the uprating of overhead transmission lines and substation terminal equipment.

Chapter 2
Literature review

The main objective of the literature review is to provide insight into the relevant aspects of the thermal uprating of transmission circuits. This section of the dissertation will review various uprating methods available that can be implemented to relieve pressure within congested power networks as well as providing justification for the need to increase the power transfer capability of a power network. In addition, there is a continuous need to support national system operators and grid planners to alleviate problems within the national transmission network. To further extend our knowledge in the field of thermal uprating of transmission circuits, new trends have to be explored that will enable operators to make informed decisions on the thermal uprating of overhead transmission lines and substation equipment. The demand for higher power transfers exists and by thermally enhancing the conductors' templating values, higher loading of the existing lines can be established without infringing on safety clearances and the security of supply. The loadability and transfer capacity of transmission networks is of major concern; therefore, it is very important to have comprehensive information available on the criteria used for the thermal uprating of overhead head transmission lines and substation equipment [6]. Together with the theoretical relationship of thermal uprating methodologies, supporting technology and engineering principles, the literature reviewed within this section provides and summarises best practises to establish an increase in power flow [11].

2.1 INTRODUCTION

Uprating methodologies are a significant fast and attractive way used by power utilities globally to enhance the possibility of increasing the loadability of their existing power lines. An urgent need exists within South Africa's power supply industry to establish methods to fully utilise the thermal capability of existing transmission assets. The strategic grid review of the country calls for the implementation of new ways to transport power from the new northern generation pool of South Africa. The difficulty in obtaining new rights of way is a constraint to the construction of new transmission lines. Different trends have to be explored to optimise the loading of existing transmission lines and substation equipment.

2.2 HISTORICAL REVIEW

The maximum allowable conductor temperature of a transmission line is normally selected in terms of the minimum ground clearance requirements, regulated by statutory laws [6]. The specific power transfer of a transmission line is affected by the current flowing through the conductor together with prevailing weather parameters. The temperature of the conductor affects the sag, which influences the conductor-to-ground clearance. Table 2.2.1 summarizes minimum clearances for electric conductors as stipulated in the Occupational Health and Safety Act and Regulations, (Act 85 of 1993) [34]. These figures are based on the assumption that clearances shall be determined for a minimum conductor temperature of 50 °C and a swing angle corresponding to wind pressure of 500 Pa. In addition, power line conductors templated to operate at a temperature higher than 50 °C shall also be in accordance with the minimum clearances indicated in table 2.2.1 [34].

Table 2.2.1 Minimum clearances for power lines in metres[34]

Highest system r.m.s. voltage	System nominal r.m.s. voltage	Safety clearance phase- to-earth	Safety clearance phase - to - phase	Minimum vertical clearances (m)					Minimum live-line working clearance (m)		Tower-top clearances (m)		
kv	kV	m	m	Outside town-ships	In town-ships	Roads intownships, and proclaimed roads, railways, tramways	To comminica-tion lines or between power lines and cradles	To buildings, poles and structures, not part of power lines	Phase-to-earth	Phase-to-phase	Still air con-ditions	Normal swing	Maximum swing
<1	-	-	-	4,9	5,5	6,1	0,6	3,0	-	-	-	-	-
7,2	6,6	0,15	0,2	5,0	5,5	6,2	0,7	3,0	-	-	-	-	-
12	11	0,20	0,3	5,1	5,5	6,3	0,8	3,0	-	-	-	-	-
24	22	0,32	0,4	5,2	5,5	6,4	0,9	3,0	-	-	-	-	-
36	33	0,43	0,5	5,3	5,5	6,5	1,0	3,0	-	-	-	-	-
48	44	0,54	0,61	5,4	5,5	6,6	1,1	3,0	0,8	1,1	5,4	0,5	0,15
72	66	0,77	0,89	5,7	5,7	6,9	1,4	3,2	0,9	1,3	7,7	7,1	0,20
100	88	1,00	1,14	5,9	5,9	7,1	1,6	3,4	1,0	1,5	1,00	9,2	0,24
145	132	1,45	1,68	6,3	6,3	7,5	2,0	3,8	1,2	1,9	1,45	1,30	0,35
245	220	2,1	2,7	6.7	6.7	8,2	2,7	4,5	1,7	2,8	2,1	1,88	0,6
300	275	2,5	3,6	7.2	7.2	8,6	3,1	4,9	2,0	3,4	2,5	2,2	0,7
362	330	2,9	4,3	7,8	7,8	9,0	3,5	5,3	2,3	4,1	2,9	2,6	0,86
420	400	3,2	4,8	8,1	8,1	9,3	3,8	5,6	2,8	4,8	3,2	2,9	1,0
800	765	5,5	8,9	10,4	10,4	11,6	6,1	8,5	5,5	9,7	5,5	5,2	1,9

During the 1970s Eskom had limited information available on the thermal behaviour of their bare overhead conductors [6]. For this reason, the philosophy of rating the lines at 75 °C was used, but the line was templated to operate at a maximum of 50 °C. Until recently, conservative weather conditions were used to determine the conductor ratings. As explained in Eskom's overhead line design procedure, worst case ambient conditions of 40 °C, solar radiation of 1120 W/m², together with wind speeds of 0.44 m/s were used to determine the thermal limits of transmission circuits [12]. It is important to mention that line ratings for emergency conditions were calculated as well and were quantified at 90 °C for short periods of time. In terms of existing practice and legislation, if the line was hypothetically operated at the rated value of 75 °C it would result in an infringement on the minimum permissible conductor-to-ground clearance. Therefore, by rating the line at 75 °C and templating under normal conditions at 50 °C the probability was deemed very low that any under-clearance issues would arise [12]. This method of approach served Eskom very well, as the tactics used ensured that the thermal limit was not exceeded.

Theoretically the conductor temperature in some cases may exceed the 50 °C templated temperature. In light of the above and due to the low probability and occurrences of under-clearances the scope exists to rerate the lines to 80 °C. This can be done by decreasing span lengths and introducing higher towers to the line

design. However, both solutions will need special permission, regulatory approval and the sanction of funds to allow for the capital expenditure [6].

2.3 POWER SYSTEM ISSUES

In South Africa, commercial power is generated as alternating current (AC), which is then transported through a complex power transmission system from the generating sources to the end users. The power transmission system within any region of the country is a combination of electrical circuits and components, each subjected to high electrical, mechanical and thermal stresses. Each element within the electrical circuit (i.e. the conductors, insulators and substation terminal equipment such as transformers, line traps, circuit breakers, bushings and bus-bars) has a certain power flow limit that allows for their safe and reliable operation.

In recent years, many factors converged to contribute to the instability of a national power network. Safe operating limits of power equipment are often stretched to their limits. In some cases, even the smallest system disturbances may aggravate the instability of a transmission network. Additional contingencies in a power system can also produce large system perturbations that eventually can lead to nationwide blackouts [14]. It is essential to have a clear understanding of the power system issues that in some cases can aggravate small system disturbances which in turn can influence the reliability of supply when thermal uprating is implemented. Critical factors related to severe system disturbances include:

a. Voltage transients
b. Interruptions
c. Under voltages
d. Overvoltages
e. Waveform distortion
f. Transmission line loadability
g. Environmental limits

Each one of the above-mentioned disturbances can have an influence on the reliability and security of supply. Before implementing thermal uprating an investigation into the

performance history of the line is recommended to ensure that no over-loading of the network occurs. The power system issues mentioned are very important and cannot be neglected. In general, power system disturbances require some study in order to understand the operational behaviour of the transmission system under normal, emergency and fault conditions.

2.3.1 **Voltage transients**

In a modern interconnected power system, transfer limits of a power network are sometimes stretched to meet customer demand. Small, unexpected transients manifested in the power system can lead to large system disturbances that subsequently can lead to system instability and at worst voltage collapse. Transients can be described as events that can suddenly raise the voltage peak of an electrical system in a very short period [15]. Transients manifest a sudden change in the behaviour of electrical circuits that can lead to enormous stresses on power equipment due to excessive voltages. The thermal response of transmission lines and substation equipment may be greatly affected when experiencing transients and in some cases may exceed the average power rating of the electrical system for short periods. The thermal limits of a transmission line and the terminal substation equipment is dependent on the voltage and the elevated current that is flowing during the transient period coupled with the weather parameters. Power equipment has voltage, current and thermal limits. These limits maintain transient stability and synchronism of the network and equipment when subject to a severe disturbance. The main effect of voltage transients is an insulation failure due to insulation overheating or excessive sags of conductors due to increased loading.

2.3.2 **Interruptions**

Interruptions within a power utility are defined as the complete loss of supply to customers within a given region. Transmission lines transmit large amounts of power, which generally can be routed by national system operators in any desired direction on the various links of the transmission system to achieve the desired power delivery in an economic way [17]. Temporary loss of supply and interruptions are bound to occur

as the result of damage to the national grid caused by lightning strikes, harsh weather conditions including high winds, animals, trees and equipment failure.

The duration of interruptions can be labelled and categorised into groups based on their duration.

The categories include [61]:

- Voltage dips:1 cycle to 15 cycles,
- Temporary interruptions: 3 seconds to 2 minutes,
- Sustained interruptions: greater than 2 minutes.

Voltage dips and temporary loss of supply can be due to network switching, utility faults or circuit breakers tripping. These are the most common interruptions that occur in a power system and the utility infrastructure is designed to automatically compensate for many of these problems by means of auto reclosers [15]. Sustained interruptions in most cases are due to component failure. The IEEE Standard 100-1992 describes sustained interruptions as a situation where the infrastructure cannot compensate for the fault and field personnel have to investigate before power is restored. Once the power is restored the col load pick-up may overload the power system.

Solutions to help prevent interruptions exist but vary both in effectiveness and in cost. Furthermore, when uprating a transmission line attention must be paid to the ratings of automatic fault clearing infrastructure and protection to ensure both the dependability and reliability of the equipment.

2.3.3 **Undervoltage**

An undervoltage or a voltage dip in a power system is often the result of system faults or switching of large loads, e.g. large induction motor. An undervoltage is also defined as a decrease in rms (root means square) AC voltage to less than 90% of the nominal voltage. Capacitive and inductive loads require excessive current on start-up that will result in a significant voltage drop influencing the supply to the rest of the network on

which it resides. Overheating in motors, failures of nonlinear loads and equipment failure of the power utility are typically the result of undervoltages. If an undervoltage remains on the system, induction motors will draw excessive currents and might result in equipment failure or mal-operation [15]. Higher ampacity levels coupled with voltage disturbances can also result in a under voltage.

2.3.4 **Overvoltage**

An overvoltage is a voltage that is greater than the upper design limit of the power equipment or transmission circuit. The increase in rms AC voltage during overvoltage conditions is generally greater than 110% of the nominal voltage. Commonly an overvoltage is known as a swell and is mostly experienced in areas where there is a sudden reduction in load, e.g. when a large induction motor or furnace is switched off. Overvoltage stresses coupled with increased loading may influence the reliability of transmission equipment and shorten insulation lifespan of power equipment.

2.3.5 **Waveform distortion**

Waveform distortion is the alteration in the characteristic of a specific power frequency that contributes to the non-uniformity of an AC signal. Distortion in a power network is an unwanted phenomenon that contributes to the overheating and saturation of both transformers and power equipment.

2.3.5.1 DC offset

Commonly a direct current offset occurs when DC is re-introduced back into the AC transmission system. The cause of a DC offset is coupled together with the failure of rectifiers or geo-magnetically induced currents.

2.3.5.2 Harmonic distortion

Harmonic distortion can be described as the corruption of or change in the waveform of the supply voltage from the sinusoidal waveform. The saturation of transformers and

substation equipment poses a constraint on their performance. The power rating of substation equipment is the maximum amount of power it can handle before it overheats and is damaged. Harmonic distortion mostly affects; transformers and power factor correction capacitors. The magnetic saturation of power equipment can also lead to the generation of harmonics.

2.3.6 **Transmission line loadability**

AC transmission lines are generally economical and the most reliable means of electrical energy transmission. Nevertheless traditional design practice limits their transfer distance and capacity. Four major line-loading limits include: (1) the surge impedance loading; (2) the thermal limit; (3) the voltage drop limit; and (4) the steady state stability limit. Overhead line transfer capacities can be increased by evaluating the existing line loadability and by observing some new line design criteria [12]. Rules for increased transfer capacity and line design criteria include:

a. The most traditional rule for line design is that the greater the transmitted power or line length, the greater the number of sub-conductors needed per phase.
b. Non symmetrical spacing of sub-conductors in a bundle will allow for an increase in permissible field strength if compared against a symmetrical bundle.
c. Lowering the inductive impedance of a transmission line will facilitate a decrease in the power angle between the line terminals and ensure greater steady state stability, which in turn allows for higher power transfer capacity [12].

2.3.6.1 Surge impedance loading

The electricity reserve margin in South Africa is steadily declining due to higher demand for electricity. Higher load factors result in the need to increase existing transfer capacity. One of the factors limiting the increase in power transfer along existing power lines is the surge impedance loading (SIL) of the particular line. The SIL is the capability of a transmission line to support the flow of energy. The SIL of a transmission line provides a useful measure of transmission line loading limitations because of the effects of series reactance. The SIL of a transmission line is the MW (megawatt) loading of a transmission line at which a natural reactive power balance

occurs. To define the load transfer capability of a transmission line it is very useful to consider two important features characterising the loadability of an overhead power line [12]. Commonly one of the features is the surge impedance or the characteristic impedance Z_C of a transmission line.

The following formulae will briefly explain the concept of surge impedance

$$z = j\omega L \ \ \Omega/m \tag{2.3.6.1}$$

$$y = j\omega C \ \ S/m \tag{2.3.6.2}$$

where:

j = Imaginary unit,
ω = Angular frequency,
L = Inductance per unit length,
C = Capacitance per unit length.

From (2.3.6.1) and (2.3.6.2), the characteristic impedance Z_c of a transmission line is defined as:

$$Z_C = \sqrt{\frac{z}{y}} = \sqrt{\frac{j\omega L}{j\omega C}} = \sqrt{\frac{L}{C}}\Omega \tag{2.3.6.3}$$

From (2.3.6.3) the surge impedance of an overhead line is numerical equal to, $\sqrt{\frac{L}{C}}$ and is a function of line inductance L and capacitance C and is independent of line length [22]. The power that is transferred across a transmission line.

$$SIL = \frac{kV_{L-L}^2}{Z_C} \tag{2.3.6.4}$$

where:

SIL = Surge impedance loading,
kV_{L-L}^2 = Square of the line-to-line voltage,

Z_c = Surge impedance.

The surge impedance loading in MW (megawatt) is equal to the square of the line voltage (in kV) divided by the surge impedance (in ohm). It measures the amount of reactive power absorbed or supplied by the power network. If a transmission line is loaded above its SIL, it acts as a shunt reactor by absorbing reactive power from the system. When a line is loaded below its SIL, it acts a shunt capacitor supplying reactive power to the system [16].

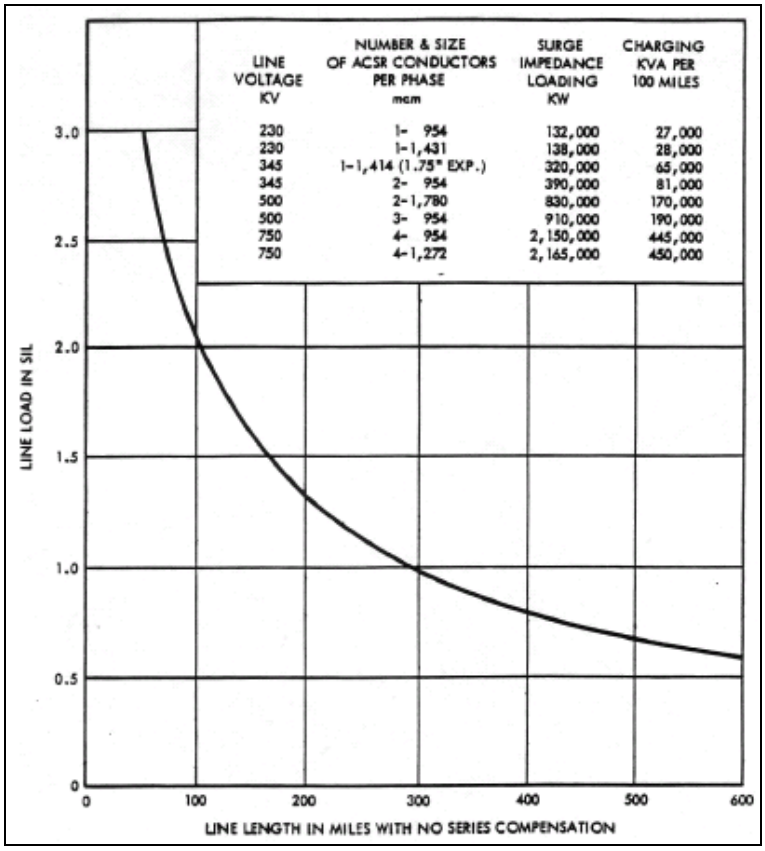

Figure 2.3.1: Transmission line transfer capability in terms of the surge impedance loading [24]

2.3.6.2 Thermal limit

The maximum operating temperature of a conductor is its thermal limit [16]. There is a direct relationship between the temperature of a conductor and the sag of the conductor between towers. If the temperature of a conductor is too high it might infringe on prescribed conductor-to-ground clearances. Furthermore, higher operating

temperatures affect the tensile strength of the conductor due to annealing of the conductor material. In most cases, the thermal limit of conductors denotes the current carrying capacity of a transmission line [24]. The thermal limit of a conductor depends on the current magnitude and duration, weather conditions, certain conductor parameters, surface conditions and the maximum allowable conductor temperature. Some of the thermal rating parameters include [24]:

- Conductor geometry: outside diameter, conductor strand diameter, core strand diameter, number of conductor strands, and number of core strands;
- AC conductor resistance, which is a function of the conductor diameter;
- Conductor surface conditions: emissivity and solar absorptivity;
- Weather conditions: solar radiation, ambient air temperature, wind speed and direction;
- Line topography and location: longitude, latitude, inclination and elevation above sea level.

Generally, the thermal rating and limit of a transmission line are determined by the safety of the public with a calculated probability of an unsafe condition arising. This, in turn, depends on the conductor sag between towers and as previously, explained the mechanical or tensile strength of the conductor. As the current flow through a conductor increases, the conductor's temperature increases and it elongates. The elongation of the conductor increases the sag between supporting towers and influences the conductor-to-ground clearance. In the light of the above, it is important to determine the thermal behaviour and temperature of overhead conductors in the steady state. The steady state behaviour of conductors is discussed in subsequent sections of this chapter.

Power flow patterns constantly change as the demand for electricity increases or decreases. Figure 2.3.2 displays a step change in current from an initial current I_1 to a final current I_f. Immediately after the step change in current the sum of the heat generated by solar radiation and ohmic losses equals the heat loss of convection and radiation and can be described by a heat balance equation: Heat gain equals heat loss. For this reason, it is assumed that no heat is stored in the conductor and immediately prior to the step changes the conductor experiences thermal equilibrium.

In addition, after a certain period the conductor temperature reaches a final steady state temperature T_f .

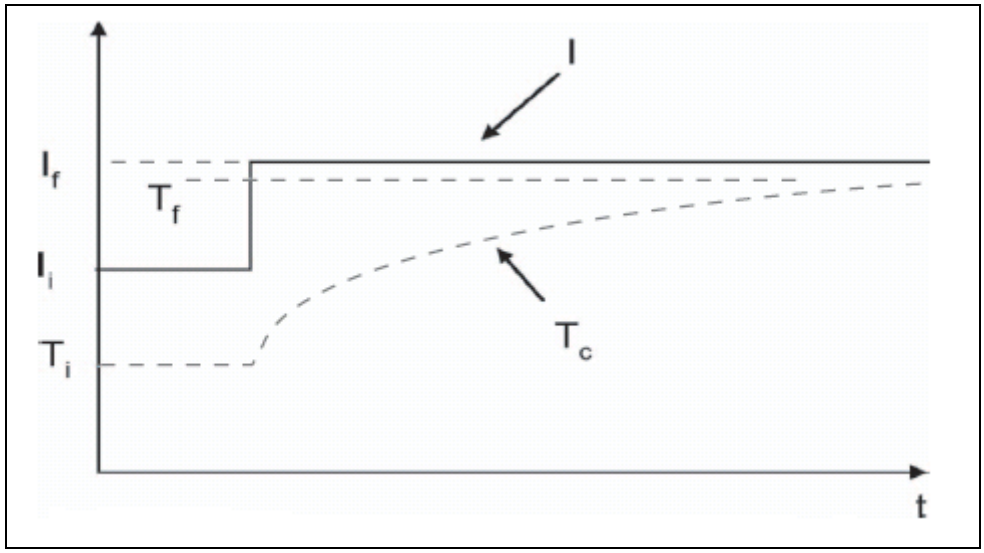

Figure 2.3.2: Temperature response of a bare overhead conductor to a step increase in current [24]

Figure 2.3.3 displays the temperature change after a step decrease in current from a value I_I to a final value I_f . After the step decrease in current the conductor again approaches a final steady state temperature T_f . The thermal limit or rating of overhead conductors is dependent on the duration of elevated electrical current, the maximum safe operating temperature and the initial temperature T_I of the conductor. Sustained periods of excessive elevated current flows on transmission lines may lead to the loss of tensile strength and excessive sags due to high temperature of the conductor. The key aspect of thermal uprating is to increase the thermal rating of overhead lines to a safe operating point where an increase in transfer capacity is experienced without negatively influencing supply of electricity.

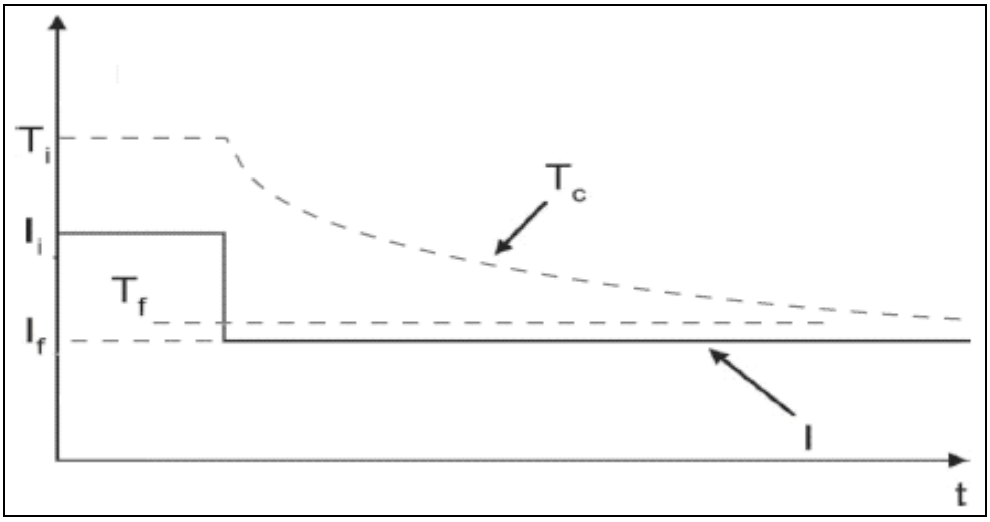

Figure 2.3.3: Temperature response of a bare overhead conductor to a step decrease in current

2.3.6.3 Voltage limit

The equipment of both the power utility and the connected customers are designed to operate at certain rated voltage limits. The voltage limit of the national power system is of high concern to system operators as system loading increases. The system voltage of a transmission network is affected by the series inductance and shunt capacitance of the transmission line [24]. The transmission network has an array of different voltage levels interconnected via transformers and power equipment. In practice, transmission line voltages decrease when heavily loaded and increase when lightly loaded. The general standard is to maintain voltage levels within ± 5% of the rated system voltage to ensure that unusual operating problems are not encountered [16].

Thermal uprating a transmission circuit implies an increase in power transfer capability of transmission circuits by increasing loading. The increase in loading on a transmission line may produce unacceptably large voltage drops at the receiving end of the line when the line is uprated. If there is not sufficient reactive power to support the voltage the system voltage may drop below the 95% of the rated system voltage and cause momentary loss of supply or voltage collapse.

Figure 2.3.4 displays the power transferred through the line in relation to the voltage level at the receiving bus. The graph shows that if the power transfer is increased, the voltage decreases and at some stage reaches a critical point.

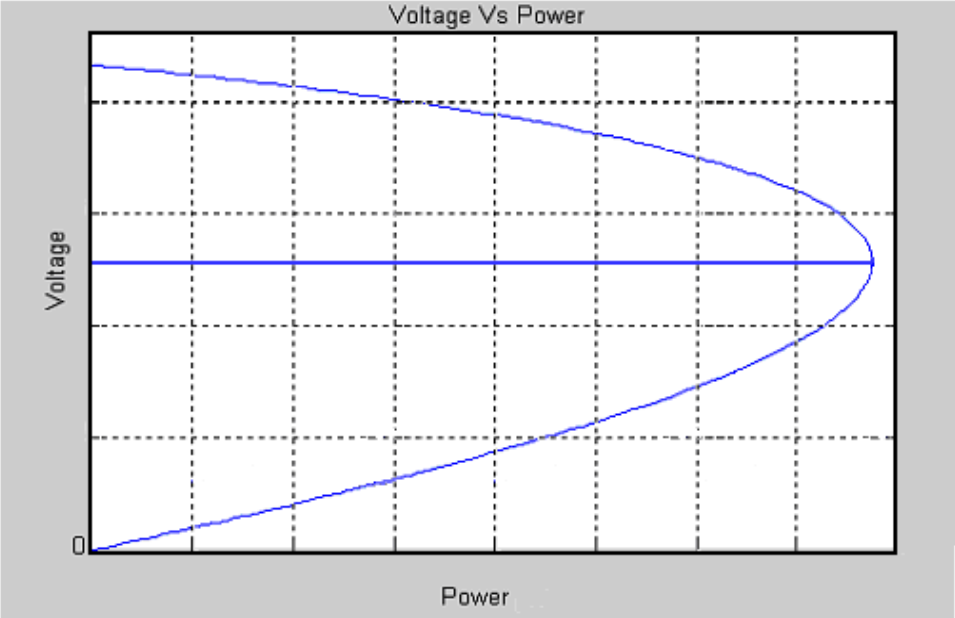

Figure 2.3.4: The relationship between transferred power and voltage at the receiving bus [2]

2.3.6.4 Steady state stability limit

Power system stability refers to the ability of a power system to remain in equilibrium under normal operating conditions by ensuring that phase angles across transmission lines are not too large, bus voltages are close to nominal values, and that the generators, transmission lines and power equipment are not overloaded [16]. The stability limit of power networks is influenced by various system disturbances that are manifested in different ways depending on the system configuration. The steady state stability of large-scale power networks is of great importance to system operators and can be divided into two categories, namely the voltage stability and the angle stability. In large interconnected power systems, the voltage stability and angle stability are interlinked, but in certain aspects differ from each other.

Angle stability limits are imposed to ensure that synchronous machines (e.g. generators) would not lose synchronism and that power and torque angles remain controllable in the power network.

Figure 2.3.5 displays a basic layout of an AC transmission system. The power transmitted between the sending end and receiving end is given by:

$$P = \frac{V_s V_r}{X_L} \sin(\delta_s - \delta_r) \quad (2.3.6.5)$$

where V_s and V_r are the respective voltage at each side. The angle difference between the sending and receiving end is reduced to the following equation:

$$\delta = (\delta_s - \delta_r) \quad (2.3.6.6)$$

Equation (2.3.6.5) is then expressed as:

$$P = \frac{V_s V_r}{X_L} \sin(\delta) \quad (2.3.6.7)$$

where δ is the angle difference and X_L is the series reactance of the transmission line [16].

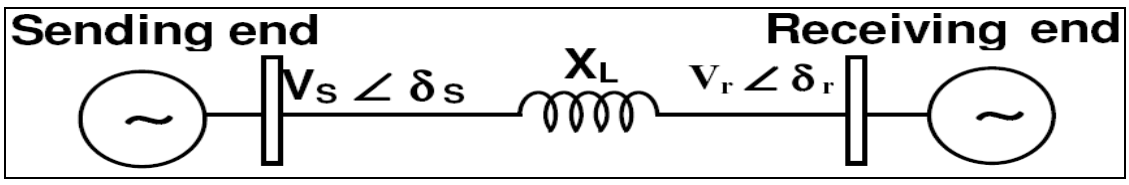

Figure 2.3.5: Basic interpretation of a transmission system [25]

Equation (2.3.6.5) describes very important properties of transfer limits and the performance of an overhead line. The power that can be transmitted by a transmission

line is directly proportional to the product of V_s and V_r. The voltage of the sending and receiving end is usually more or less the same and therefore the power limit is proportional to the square of the operating voltage. It is for this reason that power utilities generally use higher voltages to transmit higher amounts of power [12].

In relation to angle stability, the voltage stability of a power system is the ability of the system to maintain a steady voltage after a manifested system disturbance with an extended capability to restore equilibrium between the connected load and supply. The power transmitted from one end of the line to the other is a function of $\sin\delta$ and a power transfer curve can be drawn [26].

If Figure 2.3.6 is examined closely, it appears to make sense to use $\delta = 90^\circ$ to maximise the power flow of a transmission line. However, in practice this is not feasible. This is because the generators connected to the transmission network may fall out of synchronism and trip if a small disturbance occurs. The angular displacement or load angle δ is typically maintained between $30^\circ \text{ to } 45^\circ$ to ensure steady state stability and allowing for an adequate steady state stability margin to recover from a system disturbance or when higher power transfer is required to provide relief to emergency conditions. At $\delta = 90^\circ$ any increase in power transfer will be exhausted and a further increase in power transfer will result in the power input exceeding the power that can be safely transferred. Generator pole slip will occur and the generator will no longer remain in synchronism. Instability then occurs with the result of voltage collapse.

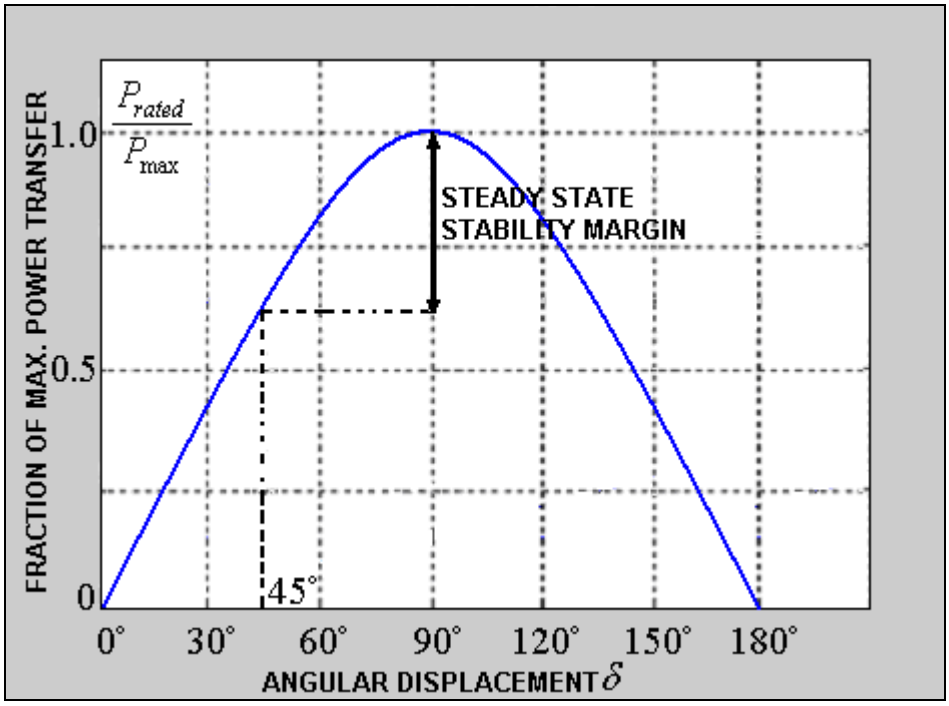

Figure 2.3.6: Power angle curve

In contrast with the steady state stability limit, it is important to give proper emphasis to the available steady state stability margin of the entire network and not just the transmission line alone in need of uprating. The steady state stability limitation is defined in terms of the available margin between the maximum power transfer ability of the power system $P_{\max}$ and the operating limit P_{rated} [20]. The percentage steady state stability margin in Figure 2.3.6 is given by:

$$\%\text{Stability margin} = \frac{P_{max} - P_{rated}}{P_{max}} \cdot (100) \qquad (2.3.6.8)$$

The desired available amount of stability margin is dependent on many factors. Generally, line designers allow for a 30% to 35% reserve margin for heavy loaded transmission lines. From Figure 2.3.6, this corresponds to an angular displacement of approximately 45°. Voltage stability in power networks is load driven. Steady state problems can be identified by means of various software programmes during the design stage and the problem of voltage and angular stability is well understood by system operators and planners. Overall, power transfer of transmission circuits can be increased by safely exploiting operating margins together with the load angle δ. The

following case study will be used as an example to illustrate that the power transfer of a particular transmission line can be increased without influencing the steady state stability.

Case study [26]: A generator is operating at a load angle of 30° and is transmitting power over two parallel lines. The load angle across the lines is 10°. If the entire load is slowly shifted to one power line, will the line and generator remain stable?

Using (2.3.6.5) and re-arranging the equation gives:

$$\sin(\delta) = \frac{PX_L}{V_s V_r}$$

If $P,\ V_s$ and V_r remain constant then $\sin(\delta)$ is proportional to X .When $\delta = 10^\circ$, $\sin(\delta) = 0.173$ with reactance X. When X increases to $2X$, $\sin(\delta)$ will increase to $2(0.173) = 0.347$. This gives a new value for δ, where $\delta = \arcsin(0.347) = 20^\circ$. This means that the line load angle approximately doubled. The combined load angle for the generator and the line is $30^\circ + 20.3^\circ = 50.3^\circ$, which is considerably less than 90° and so the generator and line will remain stable with an increase in power transfer.

2.3.6.5 Summary of transmission line loadability

The overall line loadability is set out in the operating criteria during the design stages of the transmission line. Conservative design practice limits power transfers of existing overhead transmission lines. Figure 2.3.7 displays line loadability estimated by the surge impedance loading as the transfer capacity in megawatt (MW) versus the line length. In addition, Figure 2.3.7 also displays superimposed curves of the thermal limit, the voltage limit and the steady state stability of the transmission line [11].

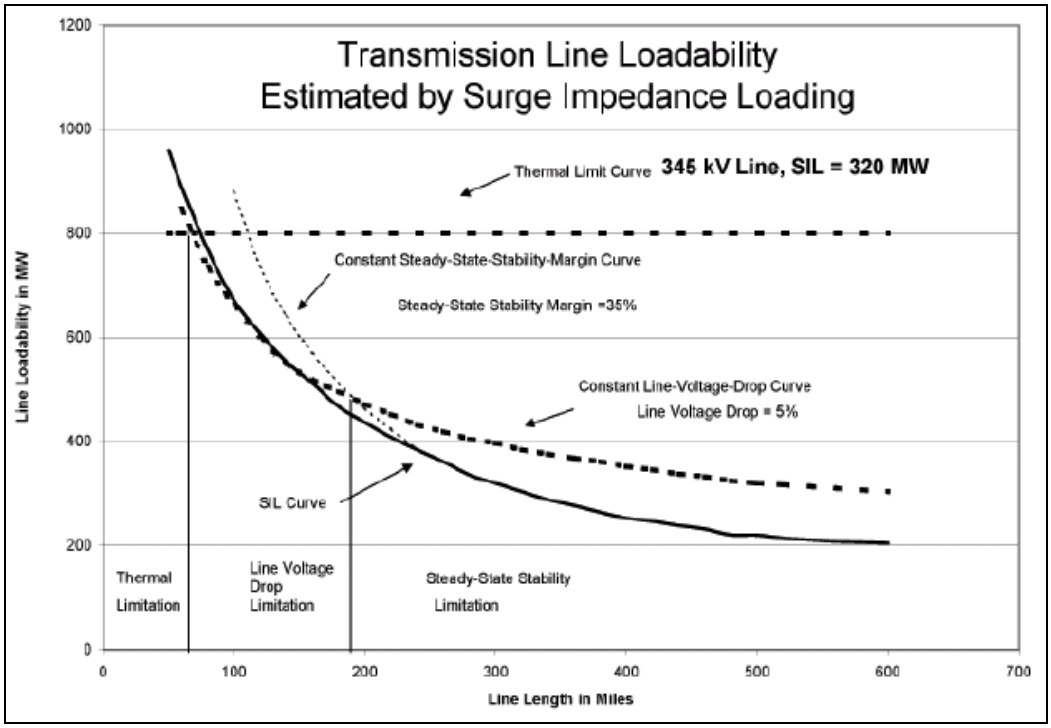

Figure 2.3.7: Transmission line loadability curve displaying the thermal limit, voltage limit and steady state stability limit [11]

From Figure 2.3.7 it is clear that the thermal limit and the voltage drop limit roughly intersects at 110 miles or 177 km. In addition, the voltage drop and the stability limit curves cross at 190 miles or 306 km. Based on the above-mentioned three regions in Figure 2.3.7 are identified:

- Thermal limit – at less than 177 km in line length the line is thermally limited.
- Voltage drop limit – between 177 km and 306 km line length the line is limited by voltage drop.
- Stability limit – beyond 306 km line length the line is limited by the stability criteria.

St. Clair [11] defined and introduced transmission line loadability and how it influences the maximum load carrying capability of a transmission line in 1953. Line designers and system operators adopted the concept worldwide and in the present, the St. Clair curve is still used to express the loadability of overhead lines in per unit of SIL [21]. The curve was derived empirically based upon practical considerations and experiences [20].

Modern challenges to satisfy the electricity demand of the country remains and the need to increase the loadability and power transfer of existing transmission circuits. Thermally uprating a transmission circuit may be influenced by line loadability limitations. It is possible to overcome network limitations and alleviate congestion within transmission circuits by implementing thermal uprating.

2.3.7 **Environmental limits**

The emphasis put on the use of land, the visual impact of transmission lines, pollution, energy efficiency, global warming aspects and various hazards (like induced voltages and currents, noise, electromagnetic fields) is continuously increasing. These environmental legislation and regulatory issues also contribute to the difficulty in obtaining new rights of way for the construction of new transmission lines. Due to the difficulty in acquiring servitudes, the present regulated electricity supply industry of South Africa requires stringent environmental impact studies for approval to construct or modify existing transmission lines. One of the biggest benefits of thermal uprating is that no special permission or regulatory approval is required before implementation.

Higher current flow in a transmission line has a direct effect on the electric and magnetic fields of the transmission line. The electric field of a transmission line is measured in kilovolts per metre (kV/m). The electric field levels of a transmission line are limited by regulations and jurisdiction. If the current on a particular transmission line is going to be increased, it is recommended to confirm the electrical field of a transmission line to ensure that limits is not exceeded or infringed upon [11].

In addition to the electric field, the magnetic field of a transmission line is measured in ampere-turn per meter (A/m). The magnetic field is affected by the same criteria as the electric field. In cases such as parallel fences or railroads, the induced voltages and currents may be significant and may require special attention. If the existing transmission line in need of thermal uprating is already operated near magnetic field limits set by regulation, the ability to increase the line current may be impaired unless measures are taken to reduce the magnetic field levels [11].

2.4 CONSTRAINTS AND LIMITATIONS TO THERMAL UPRATING

Power utilities worldwide are challenged to create additional power capacity in existing rights of way without the investment of large capital funding. By increasing the thermal rating of existing transmission lines, additional concerns are the mechanical and electrical safety of the line. The uprated line must remain safe under all power flow conditions without compromising the safety integrity of the line. This section of the dissertation will focus on the issues and limitations of the thermal uprating of transmission lines.

2.4.1 **Sag and tension of the conductor**

When a transmission line is designed, the height of the conductor above the ground is one of the main considerations. The height of the conductor above the ground is primarily governed by regulations and other safety aspects such as the probability of an object present underneath the line, the size of the object, voltage surges, magnitude of the surge and the likelihood of a flashover occurring when these factors occur simultaneously [27]. In addition, the effects of the magnetic and electric field discussed in Section 2.3.7 of this dissertation also influence the safety of the transmission line as the conductor sags closer to the ground.

To maintain the minimum distance to nearby objects and people within the servitude boundaries it is important to limit the sag of the conductor under elevated operating temperatures and high mechanical stresses. The thermal rating or ampacity of a conductor is mainly a function of the maximum allowable conductor current. Uprating sometimes requires re-tensioning of the conductor to raise the conductor above the ground to establish the required clearances needed for higher temperature operation.

Figure 2.4.1 illustrates a basic sag variation diagram of a loaded conductor under various operational temperatures and load conditions. The position of loaded conductors above the ground at all times of operation is critical to system operators. The temperature of the conductor at the various labels of Figure 2.4.1 is:

- Init - is the initial installed un-energised and unloaded sag of the conductor. During construction, the conductor is typically stringed at ambient temperature and the remaining weather conditions are measured to compensate for any error.
- Final short-time creep (STC) - is the final sag of the conductor after a wind-loading event has occurred for a short time – typically an hour.
- Final long time creep (LTC) - is the final sag of the conductor after an extended period being in service, typically 10 years.
- TC max - is the sag of the conductor when the temperature is at the maximum for which the line was designed – typically Eskom's older transmission lines were designed for 75°C and templated to operate at a maximum temperature of 50°C.

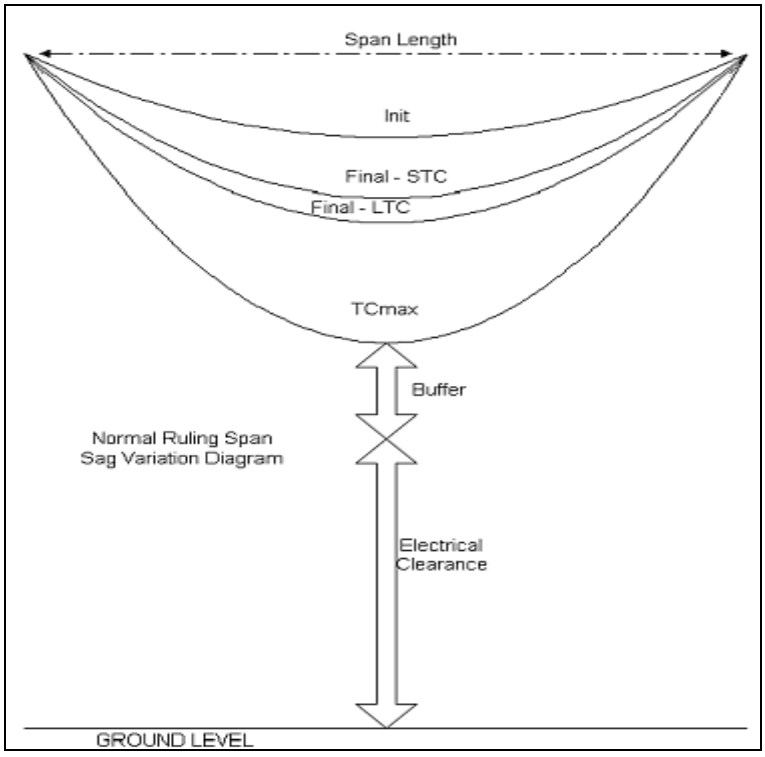

Figure 2.4.1: Example of conductor sag at various operational temperatures and load conditions [11]

The highest system voltage (U_m) of the line determines the electrical clearance of the line. The requisite clearance distance along the route of the line must be maintained at all times of operation. Different operating voltages of transmission lines require different conductor-to-ground and phase-to-phase clearances as summarized in table

2.2.1. The spacing and phase clearances of conductors are determined during line design stages by considerations which are electrical and partly mechanical.

2.4.2 **Annealing, conductor creep and the loss of tensile strength**

The manufacturer generally specifies the operating limits of a conductor. The limits are divided into normal and emergency ratings. The conductor's normal rating specifies the loading of the conductor for continuous operation and the emergency rating the loading for short periods, usually around 15 minutes to 30 minutes.

Annealing of the conductor material is a constraint that limits higher power transfers. For uprating to higher temperatures, the potential impacts of annealing, conductor creep, loss of tensile strength and the reliability of joints and fittings needs to be assessed [28]. Annealing is a process that causes a decrease in a conductor's strength and performance due to heating and slow cooling of the material.

The minimum tensile strength of aluminium conductors is specified by various IEC (International Electrotechnical Commission) and ASTM (American Society for Testing and Materials) standards [11].

The graph in Figure 2.4.2 displays the reduction in tensile strength of 1350-H19 hard drawn aluminium wire when operated at higher temperatures. In general, it is deduced from Figure 2.4.2 that the tensile strength reduction of 1350-H19 at operating temperatures less than 90 °C is negligible. In addition, annealing in the material is experienced when the aluminium wire is operated at temperatures exceeding 100 °C for significant periods. After 5000 hours of operation at 100 °C, there is a 10% reduction in tensile strength and at 125 °C a 10% reduction in tensile strength is experienced at 250 hours of operation. The effects of annealing are irreversible and lead to permanent cumulative damage that will result in premature replacement of the conductor [11].

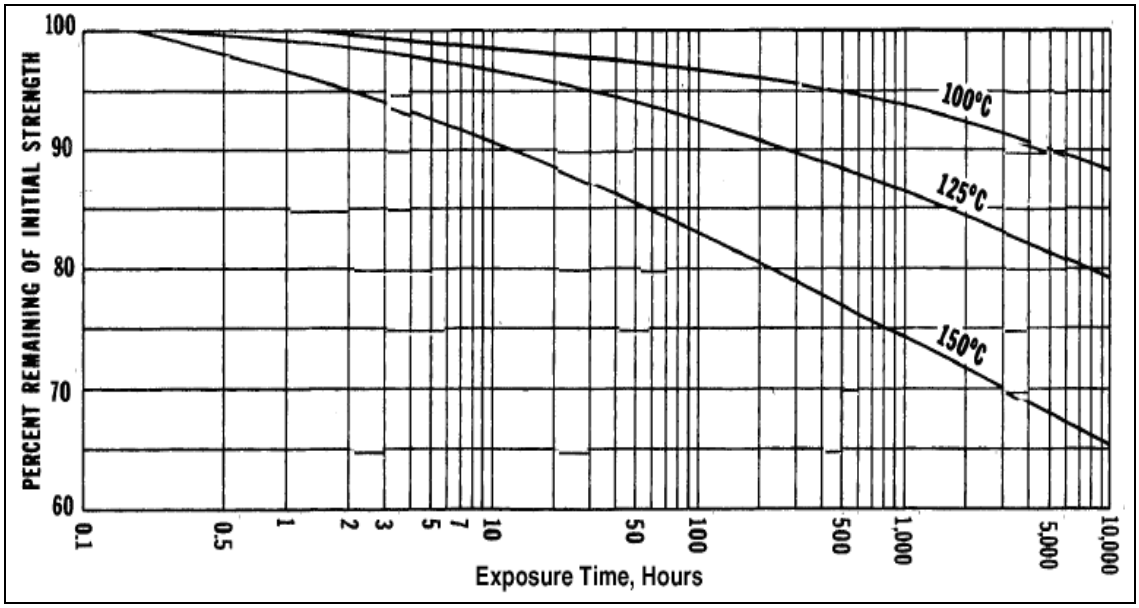

Figure 2.4.2: Annealing of 1350-H19 hard drawn aluminium wire [11]

Conductor creep is another constraint that ultimately limits higher power transfers. Conductor creep at high temperatures is a critical factor in the long-term performance of loaded conductors and contributes to the sag of the conductor. The definition of creep is the continuous deformation or elongation of a conductor under tension or load at modest operating temperatures [29]. Creep is determined by long-term creep tests and the results are used to generate creep-time curves that document the relationship of creep deformation of the conductor material versus time. The temperature ranges in which creep deformation occurs may differ for various materials and occurs in three distinct stages.

Figure 2.4.3 illustrates creep deformation as a function of time at a constant temperature. The curve is divided into three distinct phases. The primary stage includes both elastic and plastic deformation of which the strain rate is relatively high but also shows a decreasing creep rate, which is primarily due to strain hardening. In the second stage, the strain rate reaches a minimum or a steady state due to the annealing effect. In the final stage, the material under test displays a reduction in area and the strain exponentially increases.

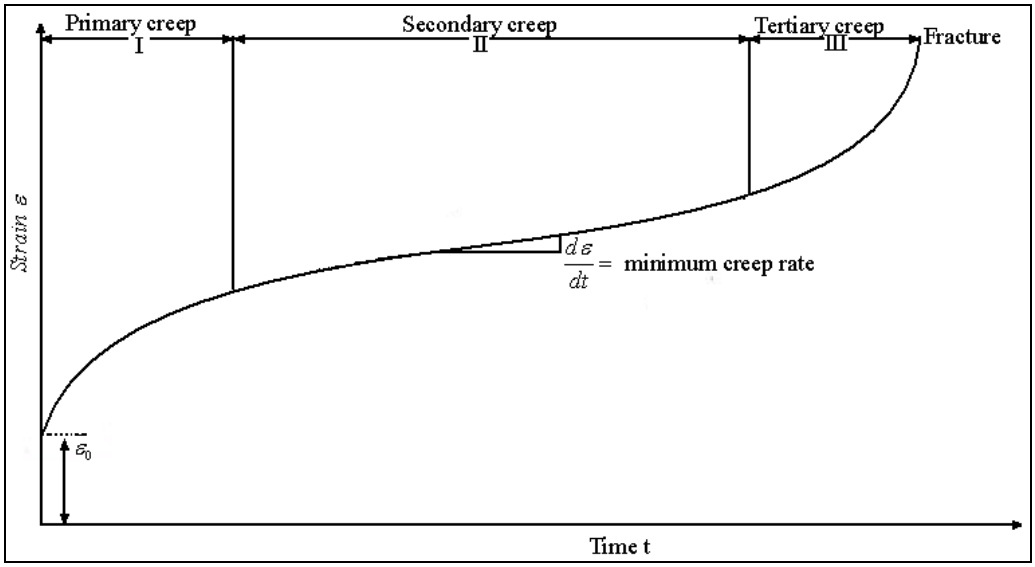

Figure 2.4.3: Creep time curve [29]

Aluminium conductors such as AAC (All Aluminium Conductor), AAAC (All Aluminium Alloy Conductor), and ACAR (Aluminium Conductor Alloy Reinforced) are much more susceptible to high-temperature creep and therefore exhibit higher rates of creep elongation that lead to fractures in the material. Steel reinforced conductors or ACSR (Aluminium Conductor Steel Reinforced) conversely exhibit lower rates of creep. In addition, the sag and tension behaviour of ACSR conductors are less affected by higher operating temperatures. Loaded conductors experience creep under everyday tension levels, which is directly proportional to the type of conductor, various material characteristics, the tension, the ratios between stranding, and the operating temperature. In case of an uprated transmission line the conductor might be operated in circumstances resulting in the maximum tension and creep levels. The extent to which annealing and creep can occur on overhead transmission lines determines the maximum safe operating temperature. For this reason it is advisable that the effects of annealing and conductor creep are taken into consideration to ensure that the conductor's operating temperature does not exceed the safe temperature limits imposed by line designers.

2.4.3 **The reliability of connectors, clamps, joints and fittings**

Substation terminal equipment consists of different interconnected power equipment, including links, connections, joints and compression fittings. The integrity of these components is of high concern and critical to the reliable operation of a transmission circuit. Secondly, the utility may experience outages that will result in a loss of revenue, and sustained outages, which will require expensive repairs to restore supply. Due to their reliability and convenience, connectors have become widely used to make electrical connections between conductors and power equipment. Higher temperature operation of a transmission circuit greatly increases the mechanical, electrical and thermal stresses on connections. When connectors are subjected to higher temperature operations the performance and service life of the connector can be adversely affected, and this could lead to premature failure and replacement.

When operating transmission lines at higher ratings a breakdown effect in the connectors occurs. The purpose of a connector is to allow the transfer of current through numerous contact surfaces between substation hardware and the conductor. Higher current flows and temperature operations cause higher current densities between the contact points of the connector and the conductor that lead to a considerable build-up of resistance between the connecting surfaces. The build-up of resistive compounds reduces contact surfaces and in some cases restricts the flow of current completely. The electrical load on a transmission line is expected to fluctuate from full load and sometimes to heavy overloads. This will cause a wide fluctuation in the operating temperature and the stresses experienced by connectors, which will further affect the restricted contact surfaces, until a point where all the contact points are exhausted. The connector is then forced to maintain proper contact at points, which are experiencing very high resistive compounds. Contact choking contributes to the increase and build-up in resistance, current density and operating temperatures that will eventually lead to thermal failure and eventually to the mechanical failure of hardware equipment.

Figure 2.4.4 displays a typical impending failure on connections caused by higher current densities and higher temperatures of which any additional increase in loading will contribute to thermal and mechanical failure.

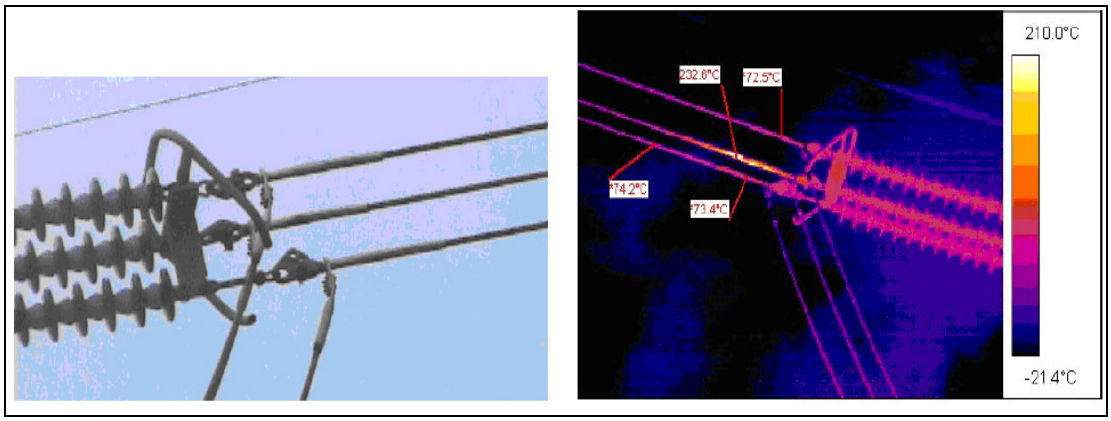

Figure 2.4.4: Visual and infrared image displaying an impending failure [11]

In addition to the thermal and mechanical stresses, a connector in some cases can experience galvanic corrosion. Galvanic corrosion refers to corrosion that is the result of two dissimilar materials that are in contact with each other and in which one metal corrodes the other. Generally, dissimilar materials have different electrode potentials and when they encounter each other, a galvanic couple is set up. For galvanic corrosion to occur three conditions have to be present:

- Dissimilar metals (e.g. different types of conductors);
- The dissimilar metals must be in electrical contact with each other; and
- A corrosive medium or electrolyte has to be present. (e.g. oxygen content, moisture, pollution level and the conductivity thereof).

The conditions mentioned will then drive the galvanic current flow or ion migration from the anode to the cathode. This will then encourage the dissimilar anodic material corroding to the cathode material. Figure 2.4.5 illustrates a typical ion migration from the anode to the cathode.

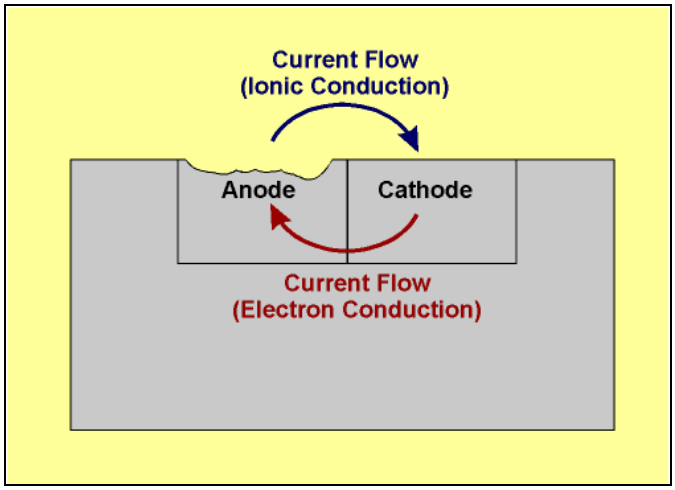

Figure 2.4.5: Illustrates the phenomenon of galvanic corrosion and ion migration [30]

After several premature connection failures due to galvanic corrosion power utilities developed guidelines which led to the development of the massive anode principle that is displayed in Figure 2.4.6.

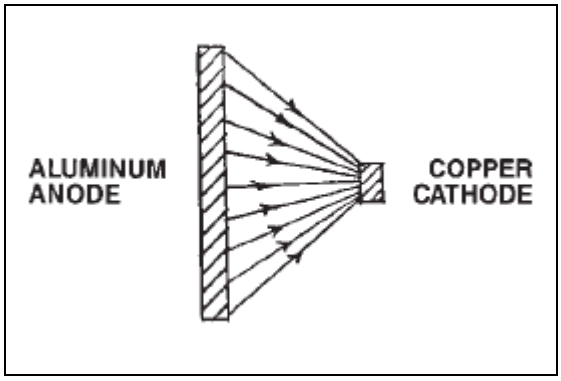

Figure 2.4.6: Illustrates the massive anode principle [31]

Figure 2.4.6 schematically illustrates the massive anode principle. By making the aluminium contact surface bigger in relation to the copper current carrying parts' contact surface, where the copper conductor emerges from the connector, the current density over the exposed face of the aluminium connector is greatly reduced. Since the rate of corrosion is directly related to the current density on the surface of the anode material, this will reduce corrosion; in addition the relatively large face of the aluminium connector will only experience a small loss of metal due to minor galvanic attack. The effectiveness of the massive anode principle is confirmed by means of the

results obtained from exposing connections to salt spray and evaluating their performance for change in their contact resistance. The general experience globally is that there is virtually no change in the contact resistance of connections after exposure to rigorous testing. The same principle applies throughout any other connection within the transmission network, whether it is splices, compression joints or fittings. The method is used effectively to prevent the effect of electrolytic attack.

Figure 2.4.7 displays the infrared analysis of a clamp and a joint within the substation boundaries. In (a) a substation clamp is displayed and in (b) a joint of a conductor. This is the typical normal behaviour of clamps and joints.

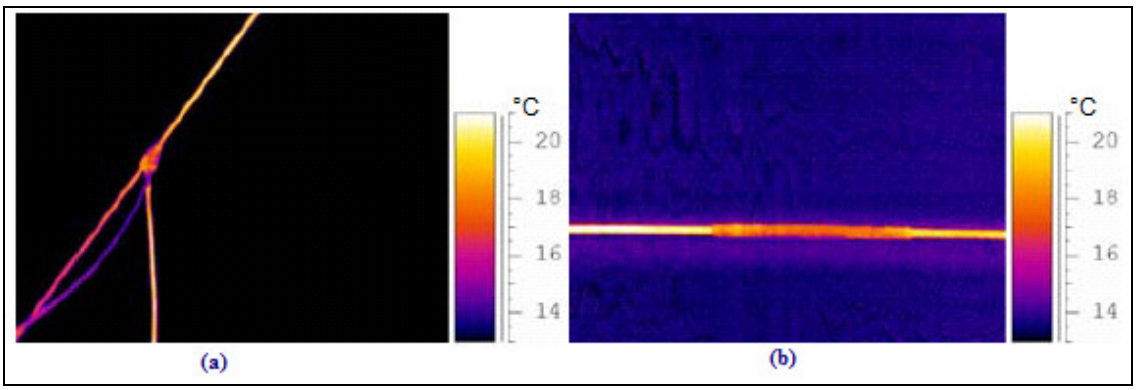

Figure 2.4.7: Infrared analysis of a clamp and joint [11]

The infrared analysis of the joint in Figure 2.4.8 revealed a hot spot in the range of about 120 ℃. This is a typical effect of corrosion between a joint and conductor. If the loading on this particular line is increased without rectifying the hot spot, it will lead to thermal and permanent mechanical failure [11].

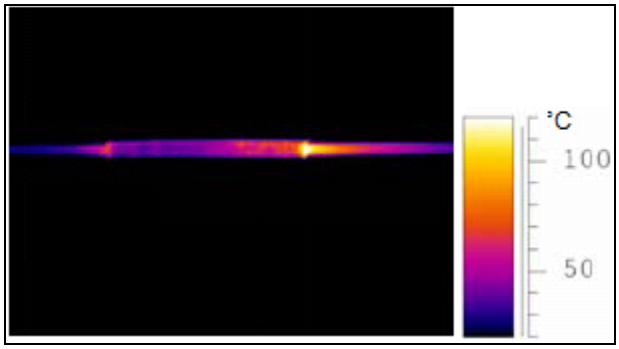

Figure 2.4.8: Infrared analysis of a damaged joint [11]

2.4.4 **Current carrying capacity (ampacity) of overhead conductors**

The ampacity of conductors is primarily limited by the maximum permissible temperature rise of the conductor under normal operating conditions. High temperature operations affect the integrity of conductors and result in annealing of the material. Bare overhead ACSR (Aluminium Conductor Steel Reinforced) conductors traditionally can tolerate more heat than AAC (All Aluminium Conductor) and therefore can withstand higher current flows but are not totally unaffected by annealing.

The ampacity of a conductor mainly depends upon the following criteria:

- Weather conditions and environmental conditions (ambient temperature, wind speed, wind direction and heat sources such as solar radiation);
- Mechanical and electrical conductor properties (i.e. resistance);
- Frequency, in the case of alternating current;
- Ability to dissipate heat (i.e. power dissipation ability);
- Geometry (includes conductor size, and bundle arrangement);
- Maximum allowable temperature of the conductor.

Figure 2.4.9 illustrates the relationship between the current flow and conductor temperature for three different sized conductors with a cross sectional area that varies from 200 mm² to 800 mm². As an example, a thermal rating of 1000 A is selected from Figure 2.4.9 to obtain the respective conductor temperature for each cross sectional area. The weather conditions used to calculate the thermal rating are described in the caption of Figure 2.4.9. Conductor (A) with a cross sectional area of 800 mm² allows

for a current flow of 1000 A with a temperature of around 70 ℃, (B) 400 mm² conductor at around 100 ℃ and (C) 200 mm² conductor at 200 ℃. It is commonly accepted that aluminium begins to anneal at a temperature in excess of 90 ℃; therefore only conductor (A) is suitable to accommodate the thermal rating of 1000 A.

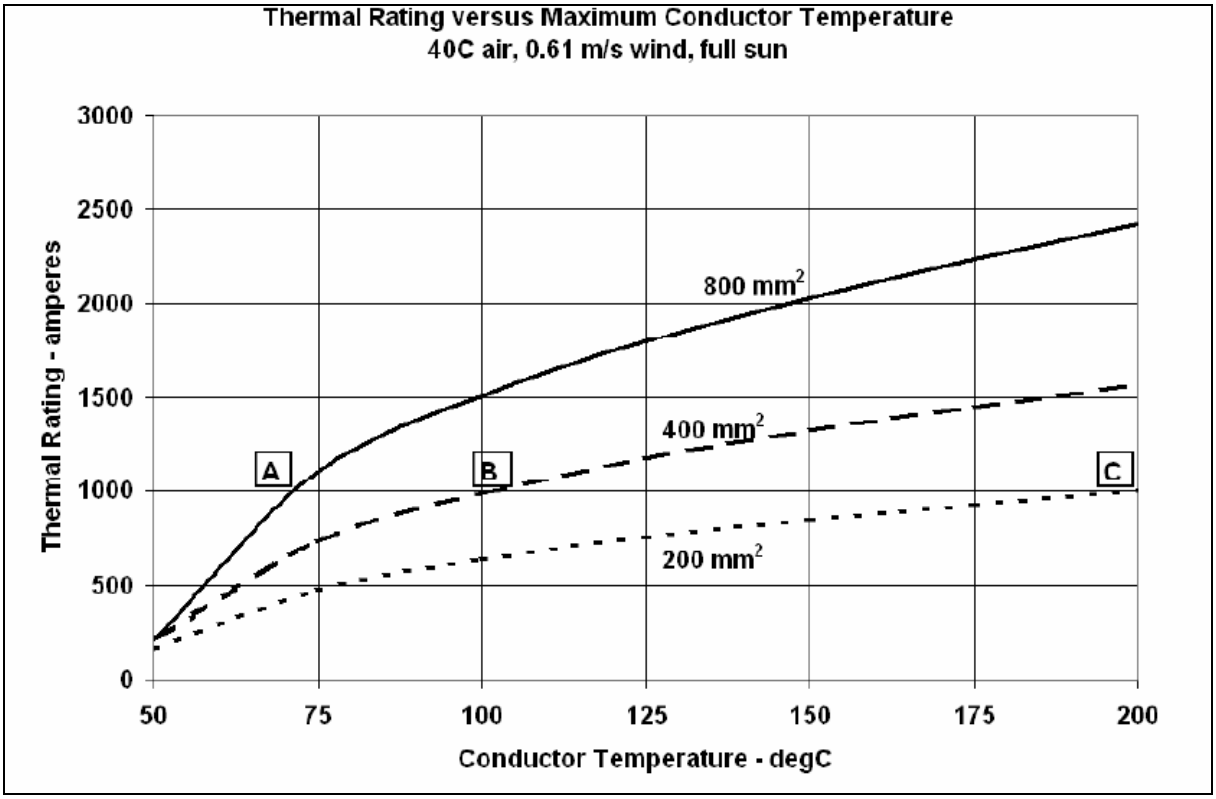

Figure 2.4.9: Line thermal rating as a function of maximum allowable conductor temperature and cross-sectional area [33]

Eskom tends to operate their newer transmission lines at temperatures of up to 80 ℃, with emergency conditions, which are usually 10 ℃ -15 ℃ higher that previous guidelines. However, the older 275 kV network has a templated temperature of 50 ℃ and the emergency ratings also lower than those of the newer transmission network.

An internal Eskom directive, EED 15/6/1-1 1970, allowed line ratings to be calculated for normal and emergency conditions at 75 ºC and 90 ºC [red]. The lines were then templated at 50 ºC according to the internal Eskom directive. Presently three line ratings, A, B and C, are used internally by Eskom for the rating of overhead conductors. They are:

- Rate A is the maximum operating current under normal conditions. The risk of exceedence according to the Eskom standard is 8.60% (Conductor operating temperature > Templating temperature).
- Rate B is the maximum operating current under contingency conditions. Not limited in time and the risk of exceedence is determined as 42.97%.
- Rate C is the ultimate maximum operating current under emergency conditions preceding load shedding. It has a maximum of a 15-minute period only.

Note: The exeedence is defined as the time when the conductor operating temperature is greater than the templated temperature [33].

Table 2.4.1 displays a typical table used to capture various current ratings for a particular conductor at different templating temperatures, for example Bear conductor. The probability of an unsafe condition arising associated with each rating is quantified and displayed. The probability of an unsafe condition arising is kept constant for the conductor and rate A, B and C are determined at different operating temperatures.

Table 2.4.1 Typical thermal rating table for overhead conductors [33]

ACSR Double layer Aluminium				
Percentage		8.60%	42.97%	70.05%
Probability of unsafe condition arising		-1.05E-06	5.25E-06	8.56E-06
Type	Templated Temperature ℃	Rate A (A)	Rate B (A)	Rate C (A)
Bear	50	510	735	1080
Bear	60	613	842	1225
Bear	70	691	928	1354
Bear	80	758	1002	1430

Table 2.4.1 is used for line design purposes, but is also used as a guideline by system operators to quickly determine the thermal rating of a particular conductor given a certain set of weather parameters. In conclusion, given the “worst case” atmospheric conditions, the maximum allowable temperature of loaded conductors determines the thermal rating of an overhead line.

2.5 DETERMINATION OF CONDUCTOR TEMPERATURE

The availability of electrical energy is steadily declining as the demand increases and supply decreases. The national power supplier of South Africa is increasing its generating capacity to meet the demand but in the interim transmission assets lack the ability to convey any increases in power transfer due to conservative design margins. By exploiting both design margins and conservative thermal ratings of existing transmission infrastructure, an optimal increase in transfer capacity can be established. One of the most important factors that influence any increase in transfer capacity is the operating temperature of a loaded conductor. The conductor temperature will mainly depend upon the relationship of the load current, the electrical characteristics of the conductor and atmospheric conditions such as ambient temperature, solar radiation, wind speed and wind direction [12]. By simultaneously incorporating the above-mentioned parameters into an equation the operating temperature of a loaded conductor can be determined successfully. This section of the dissertation will examine different methods available in determining the operating temperature of a conductor given a certain set of parameters or circumstances.

2.5.1 **Conductor temperature in the steady state**

The maximum transfer capacity of longer transmission lines is usually dictated by power system stability constraints, percentage voltage regulation and electrical losses usually in the form of I^2R losses. The power transfer capability of shorter lines is determined by the maximum thermal rating and operating temperature. In addition, the transmission line hardware, such as current carrying clamps, fittings and joints, must be in a good condition. The relationship between the conductor temperature, load current and atmospheric parameters of a transmission line are known as a heat balance equation [35]. The approach of the equation assumes that no heat is stored in the conductor and therefore a heat balance equation can be defined [35]:

Heat gain = Heat loss

$$P_J + P_M + P_S + P_i = P_C + P_r + P_w \quad (2.5.1)$$

where:

Heat gain = $P_J + P_M + P_S + P_i$ and Heat loss = $P_C + P_r + P_w$ and:

P_J = Joule heating

P_M = Magnetic heating

P_S = Solar heating

P_i = Corona heating

P_C = Convective cooling

P_r = Radiative cooling

P_w = Evaporative cooling

All parameters that form part of the heat balance equation are fixed in steady state and therefore all quantities calculated are referred to in units of W/m [12].The heat gain and heat loss of the equation are discussed separately in subsequent sections.

2.5.1.1 Heat gain

This section discusses the heat gain of the heat balance equation. For specific reasons corona heating is omitted for the heat gain side of the equation because it is negligible. During line design and conductor selection stages special care is given to the type of conductor that will be used on the transmission line to minimise corona activity. Corona heating is a phenomenon that occurs when the voltage gradient at the surface of the conductor exceeds that of the critical gradient. The air around the conductor surface ionises, giving rise to the frictional impact heating of air molecules near the surface. The result produces heat dissipation known as corona heating. Corona heating mostly occurs during rainy seasons or under wet conditions [12]. The moisture then provides additional cooling to the conductor. For this reason the heat gain side of the equation reduces to [35]:

$$\text{Heat gain} = P_J + P_M + P_S \quad (2.5.2)$$

2.5.1.1.1 Joule heating (P_J)

The largest part of South Africa's electrical energy is generated via synchronous generators that produce alternating current (AC) and the greater part of the power network is operated under AC conditions. Joule heating is mainly caused by the effect of current flow and resistance against the flow of current [35]. In addition to the resistance of a conductor, magnetic and skin effects also contribute to the heating of the conductor. The magnetic phenomenon is mainly caused by eddy currents and the inherent effect of hysteresis that is due to the time varying magnetic flux, and only occurs under AC conditions of power transmission. The skin effect refers to the increase in current density as a function of frequency that increases the AC conductor resistance. Under AC conditions, the skin effect is a significant factor as the current density increases from the interior of the conductor towards the surface. Figure 2.5.1 illustrates the skin effect phenomenon in conductors under AC conditions. It is noted that there is a much higher current density distribution towards the surface of the conductor.

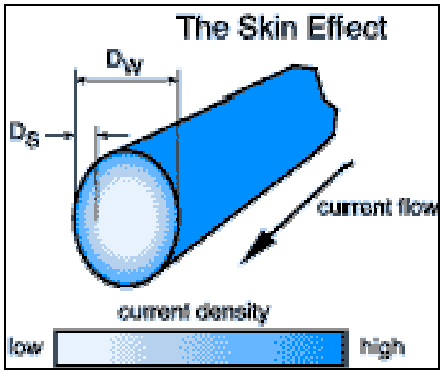

Figure 2.5.1 Illustration of the skin effect under AC conditions [60]

Additionally, manufacturers specify the DC resistance at an ambient temperature of around 20 °C from which engineers can calculate the AC resistance of a conductor by means of the following equation [35]:

$$R_{ac} = k_j R_{dc} \quad (2.5.3)$$

where:

R_{ac} = AC resistance of conductor at 20℃ (Ω/km),

k_j = Correction factor for skin and magnetic effect, i.e. a constant of 1.01,

R_{dc} = DC resistance conductor at 20℃ (Ω/km).

The joule heat gain is determined using the following equation [35]:

$$P_J = k_j I^2 R_{dc}[1 + \alpha(T_{avg} - 20)] \quad (2.5.4)$$

where:

k_j = Correction factor for skin and magnetic effect,

I = effective conductor current (A rms),

R_{dc} = DC resistance per unit length (Ω/km),

α = temperature co-efficient of resistance per degree kelvin,

T_{avg} = average temperature of the conductor (℃).

2.5.1.1.2 Solar heating (P_S)

Solar radiation largely affects the conductor temperature. Figure 2.5.2 illustrates a direct plot of the solar radiation for Johannesburg.

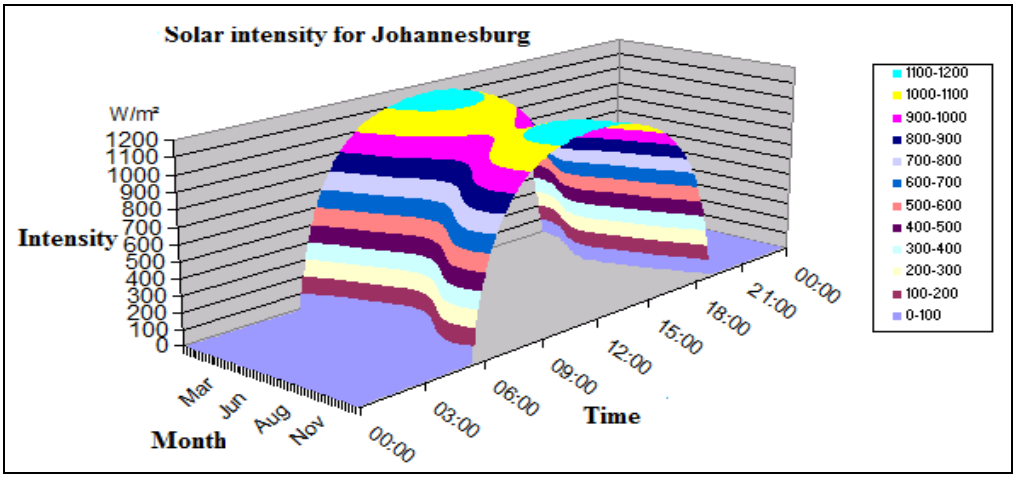

Figure 2.5.2: Typical solar radiation for Johannesburg [12]

Figure 2.5.2 was obtained from an Eskom database that recorded accurate solar radiation data at sites throughout South Africa. The solar heat gain mainly depends upon the following parameters [12]:

Dia = The diameter of the conductor,

α_s = the absorptivity of the conductor surface,

I_D = the intensity of the direct solar radiation on a surface normal to the beam (W/m²),

I_d = the intensity of the diffuse sky radiation to a horizontal surface (W/m²),

H_s = the solar altitude,

η = the angle of the solar beam with respect to the axis of the conductor (degrees),

F = the reflectance of the ground beneath the conductor.

The direct solar radiation is given by:

$$I_D = 1280 \sin \frac{H_s}{\sin H_s + \pi} \qquad (2.5.5)$$

where H_s is the solar altitude.

As an alternative to the calculation of the solar radiation, an inexpensive weather station with solar radiation sensor may be used to measure the amount of solar radiation of a particular area. The Davis Vantage Pro II weather station is used for the purpose of this research and is included in annexure A of this dissertation. If the solar radiation is measured then the solar heat gain P_S is expressed by [12]:

$$P_S = \alpha_s \cdot S_{measured} \cdot \frac{Dia}{1000} \tag{2.5.6}$$

where:

α_s = the absorptivity of the conductor surface,

Dia = the diameter of the conductor (m),

$S_{measured}$ = radiation level of the sun W/m².

2.5.1.1.3 Magnetic heating (P_M)

The theory surrounding the heat balance equation allows for the discussion of the magnetic heating effect of loaded conductors. It was very difficult to estimate the temperature of conductors prior to the advent of the heat balance equation. The magnetic heating P_M , of a conductor is also affected by the core temperature of a conductor. Composite ACSR conductors rely on a steel core for the greater part of the conductor's tensile strength and this affects the magnetic heating of the conductor. The steel core temperature of ACSR conductors is determined by [12]:

$$T_c = T_s + \frac{P_{gain}}{4\pi}\left[0.5 - \frac{d_s^2}{\frac{Dia^2}{1000} - d_s^2}\left(\ln\left(\frac{\frac{Dia}{1000}}{d_s}\right)\right)\right] \tag{2.5.7}$$

where:

T_c = steel core temperature of ACSR conductor (°C),

T_s = surface temperature of the conductor (°C),

P_{gain} = sum of the Joule heating P_J and solar heating P_S ,

Dia = outside diameter of the conductor (m),

d_s = diameter of the steel wires in the core of the ACSR conductor (mm).

By using Morgan's empirical equation the magnetic heating P_M is defined by [12]:

$$P_M = 4.9\times10^6 \times \frac{A_s}{10^6} \times B_m^{1.82} \times e^{(-2.5xT_C x10^{-3})} \times \sqrt{\frac{d_s}{1000}} \quad (2.5.8)$$

where:

A_s = cross-sectional area of the steel core (mm²),

T_c = the core temperature (℃),

B_m = the peak value of magnetic induction in steel core (tesla) [12].

2.5.1.2 Heat loss

This section of the report discusses the parameters of the right side of equation (2.5.1). The heat loss of a conductor is a combination of convective, radiative and evaporative cooling. Each effect contributes in its own way to the cooling of loaded conductors.

2.5.1.2.1 Convective cooling (P_C)

Convective cooling is responsible for the largest part of heat transferred from a conductor and plays the biggest part in determining the thermal rating of a transmission line. It is a function of conductor temperature, ambient air temperature, wind speed, the direction thereof, the air film and the geometry of the conductor [6]. Current flows generate heat within the conductor. The heat of the conductor heats the air adjacent to and near the conductor surface which leads to the density of the air decreasing. The decrease in the air density around the conductor allows air to rise in the case of natural convection or to be blown away in the case of forced convection. This allows cooler air to replace the much hotter air, which results in the cooling of the

conductor. Convective cooling is the most complex cooling effect of equation (2.5.1) and consists of two components that need to be discussed separately. They are:

- Forced convection and
- Natural convection cooling.

Forced convection cooling takes place when the wind is blowing. Wind that blows at right angles or perpendicular to the conductor results in optimal cooling of the conductor, compared with winds blowing at angles that range between 0 ° to 90 °. At zero degrees, the wind is blowing parallel to the conductor. Before the forced convective heat loss can be determined, a few parameters that influence forced cooling P_C need to be determined. They include [12]:

- The air film temperature around the conductor T_f;
- Conductor roughness factor R_f;
- Relative air density ρ;
- The Nusselt number Nu (Nuforced);
- Kinematic viscosity of air around the conductor v;
- Thermal conductivity of air around the conductor λ_f;
- Prandtl number $P_{prandtl}$;
- The Reynolds number R; and
- Grashof number G_r.

The air film temperature around the conductor T_f is a function of the ambient temperature measured by means of a weather station and the surface temperature of the conductor. Temperature sensors can measure the surface temperature of the conductor and the method is discussed in Section 2.8 of this dissertation. The air film temperature is determined by [12]:

$$T_f = \frac{(T_s + T_a)}{2} \tag{2.5.9}$$

where T_s is the surface temperature and T_a the ambient temperature. The roughness factor R_f is a function of the outer layer aluminium conductor strands measured in millimetres and is determined by [12]:

$$R_f = \frac{Strand_{diameter}}{[2\times(Dia - 2\times Strand_{diameter})]} \quad (2.5.10)$$

where $Strand_{diameter}$ is the outer layer aluminium conductor (in mm) and Dia is the diameter of the conductor (in mm). These values are typically obtained from tables provided by the conductor manufacturer. The relative air density ρ is an exponential function and is defined by [12] as:

$$\rho = e^{\left(-1.16x10^{-4}\times altitude\right)} \quad (2.5.11)$$

The altitude used to determine the relative air density is the altitude of the transmission line in need of uprating and is measured in meters (m) above mean sea level. This might differ along the right of way and is dependent on the topography. Optimal cooling of the conductor takes place when the wind is blowing at right angles (90 °) to the conductor. Nusselt defined a new parameter, Nuforced, that enables engineers to determine the cooling effect when wind angles are less than 90 ° [35]. Nuforced is defined by [12]:

$$Nuforced = 0.42 + 0.58\sin(windangle) \quad (2.5.12)$$

It is now possible to determine the kinematic viscosity of air v around the conductor which is defined by [12] as:

$$v = 1.32\times10^{-5} + 9.5\times10^{-8}\times T_f m^2 \quad (2.5.13)$$

The thermal conductivity of air around the conductor λ_f is a function of the air film temperature T_f and is defined by [12] as:

$$\lambda_f = 2.42\times10^{-2} + 7.2\times10^{-5}\times T_f \quad (2.5.14)$$

In addition, the Prandtl number $P_{\mathrm{Pr}andtl}$ is also a function of the air film temperature T_f and is defined by [12] as:

$$P_{\mathrm{Pr}andtl} = 0.715\times2.5\times10^{-4}\times T_f \quad (2.5.15)$$

The Reynolds number R is a function of relative air density ρ, wind speed, the diameter of the conductor and the kinematic viscosity of air v around the conductor and is defined by:

$$R = \rho\times windspeed\times\frac{Dia}{1000\times v} \quad (2.5.16)$$

The Grashof number is defined by:

$$G_r = \frac{\left[\frac{Dia}{1000}\right]^2\times(T_s - T_a)\times9.807}{(T_f + 273)\times v^2} \quad (2.5.17)$$

The Grashof number is a function of the surface, ambient, and air film temperatures as well as the diameter and the viscosity of air.

Table 2.5.1: Constants for the calculation of forced convective heat transfer [12]

Reynolds number R	Roughness factor R_f	B_1	n
$100 \le R \le 2650$	All stranded surfaces	0.641	0.471
$R \ge 2650$	$R_f \le 0.05$	0.178	0.633
$R \ge 2650$	$R_f \ge 2650$	0.048	0.800

The Nusselt number is defined by using the constants pre-determined in the caption of Table 2.5.1 and is given by [12]:

$$Nu = B_1 \times R^n \tag{2.5.18}$$

where B_1 and n are constants depending on the Reynolds number and the roughness factor. After determining the Nusselt number is it possible to define the forced convective cooling P_c as [12]:

$$P_c = \pi \times \left[\lambda_f \times (T_s - T_a) \right] \times Nusselt \times Nuforced \tag{2.5.19}$$

Natural convection or cooling is an effect that takes place during still weather conditions in which wind speed is less than 0.5 m/s. The density of air at low wind speeds is different from the density at higher wind speeds. At low winds speeds a phenomenon called buoyant forces occurs and is mainly due to the density difference between the air near the conductor surface and that of the main body of air. The density of air near the conductor surface is less than that of the main body of air, thus causing natural convection to occur around the conductor. Understanding the cooling effect of natural convection is required to enable line designers and engineers to determine the cooling effect when there is no forced convection present [12].

CIGRE working group WG 22.12 [35] pre-determined certain constants needed for the determination of natural convective heat transfer from conductors. The constants are presented in Table 2.5.2 and are determined using the Grashof and Prandtl numbers.

Table 2.5.2: Constants for the determination of natural cooling of conductors [12]

Gr x Pr = GP	A_2	m_2
$100 \leq GP < 10000$	0.85	0.188
$10000 \leq GP < 10^6$	0.48	0.250

The Nusselt number NuGP is a function of the constants presented in Table 2.5.2 and the Grashof and Prandtl numbers. NuGP is defined by [35] as:

$$NuGP = A_2 \times (Gr \times \Pr)^{m_2} \tag{2.5.20}$$

Working group 22.12 defines three different methods for the calculation of natural convective cooling. They include $P_{n1}, P_{n2}\ and\ P_{n3}$. Each one of these uses different criteria to determine the natural convective heat loss of conductors. P_{n1} is determined by assuming a wind direction of 45° to the conductor and is defined by [12] as:

$$P_{n1} = \pi \times \lambda_f \times (T_s - T_a) \times Nu45 \tag{2.5.21}$$

To determine P_{n2} the Nusselt number first has to be de-rated as follow:

$$Nu_{de-rated} = 0.55 \times Nusselt \tag{2.5.22}$$

Note: The Nusselt number needs to be de-rated due to changing conditions for instance altitude correction.

P_{n2} is then determined by:

$$P_{n2} = \pi \times \lambda_f \times (T_s - T_a) \times Nu_{de-rated} \tag{2.5.23}$$

WG 22.12 and references [35, 36] describe how the third value for natural convective cooling P_{n3} is calculated by multiplying the Nusselt number by the product of the Grashof and Prandtl numbers GP as in Table 2.5.2. P_{n3} is then defined by:

$$P_{n3} = \pi \times \lambda_f \times (T_s - T_a) \times Nusselt \times GP \tag{2.5.24}$$

The highest value as determined by equations (2.5.21), (2.5.23 and 2.5.24) are used as the natural convective heat loss for conductors.

2.5.1.2.2 Radiative cooling (P_r)

Radiative cooling is a function of conductor external diameter D, conductor surface temperature T_s, ambient air temperature T_a, the emissivity ε of a conductor and in the CIGRE case the Stefan-Boltzmann constant, σ_B, is included. The radiative cooling is defined by [35] as:

$$P_r = \pi D \varepsilon \sigma_B \left[(T_s + 273)^4 - (T_a + 273)^4 \right] \quad (2.5.25)$$

2.5.1.2.3 Evaporative cooling (P_w)

Evaporative cooling does not alter with relative humidity or with the presence of water vapour. However, as soon as the conductor is wetted then significant changes are notable. Generally, evaporative cooling is omitted when determining the heat balance.

2.5.1.3 Summary of the heat balance equation

The heat balance equation is a unique method used by power utilities globally to calculate thermal ratings of their respective transmission circuits. The equations mentioned in Section 2.5.1 contribute in one way or another to the successful determination of conductor temperatures and thermal ratings. If all parameters in equation (2.5.1) are satisfied, the heat balance is obtained. Software modules can be created, for instance in Mathcad®, that speed up the iterative process when determining the heat balance equation [12]. For the purpose of the research discussed in this dissertation the loading on the line is available as well as the measured operating temperature of the conductor. The operating temperature of lines obtained from heat balance equations are compared with measured temperatures obtained from temperature sensors.

2.5.2 **Deterministic method for thermal uprating**

This section of the dissertation focuses on the deterministic method for thermal uprating. The particular method is being used globally by utilities during the design stages of a transmission network to establish conservative safe thermal ratings. The deterministic method assumes the worst cooling conditions expected along the right of way coupled with the highest line loading. “Worst case” weather and cooling conditions are assumed to which the heat balance equation in (2.5.1) is applied to determine the operating temperature or the line loading. It is thus possible to calculate the line loading, which will result in the design or templated temperature or vice versa. Previously weather conditions during the 1960s were used for deterministic calculations which were generally decided based on what was considered conservative at the time [6]. Nowadays, power utilities globally define their own conservative parameters that are dependent on their environmental and climatic conditions. Table 2.5.3 defines conservative parameters used for the calculation of conductor thermal ratings in Southern Africa.

Table 2.5.3: Deterministic parameters used for thermal rating calculation [12]

Parameters influencing conductor cooling	Value of deterministic parameters
Wind Speed	0.5 m/s
Wind direction	Parallel with conductor (0°). The optimal cooling at 90°.
Ambient temperature	40ºC
Solar radiation	1120 W/m² (or sometimes 980 W/m²)
Current loading	100% duty cycle
Altitude	1500 m or worst case along servitude

The deterministic method for thermal uprating defers capital investment and generally avoids re-conductoring of transmission lines. By evaluating conservative parameters and re-calculating thermal ratings, moderate increases in power flow of 5% to 25% are possible depending on the original conditions, type of existing conductor and the overall condition of the line [28]. Recent field studies during this research revealed that the deterministic method is very conservative and that transmission lines are not operated to their maximum power transfer ability. Transmission capacity is therefore adversely affected. However, this method is particularly suitable and effective with older lines. With minor modifications in the conservative parameters a safe increase in power can be establish that might alleviate existing constraints within the network, therefore conservatively allowing for an increase in power transfer. For thermal uprating and higher power transfer purposes the probabilistic method supersedes the deterministic method [12] and is discussed in the subsequent section.

2.5.3 **Probabilistic method for thermal rating**

The largest part of Eskom's 275 kV network is believed to operate at temperatures well below the temperatures for which they were designed. Thermal ratings that are based upon the deterministic method result in the under-utilisation of transmission lines. Deterministic thermal ratings limit power transfer and therefore in some cases are replaced by the more effective probabilistic approach, which allows for the determination of higher thermal ratings. Three main probabilistic methods are of growing interest among line designers and system operators, and take into account the stochastic nature of the meteorological parameters [6].

The probabilistic approach uses actual weather conditions prevailing in the geographical area of the line at the time to determine the likelihood or probability of an unsafe condition occurring. The method identifies the risk of an unsafe condition arising as well as the current or the operating temperature that will result in the risk. A risk is the probability of a negative action occurring, including something that creates a hazard. A risk can be avoided through pre-emptive action. A possible identified risk could be the conductor operating temperature exceeding that of the design temperature or the possible risk of the loaded conductor infringing upon prescribed

conductor-to-ground clearances. One of the major advantages of the probabilistic method is that risk is identified during line design stages or prior to thermal uprating. Therefore, the ampacity can be changed to meet the level of the specific risk. Furthermore, weather conditions vary across geographical areas. One of the disadvantages of the probabilistic approach is the need for large amounts of data to determine the rating of the line. However, the benefits of increasing the transfer capacity outweigh the drawbacks. The three most common probabilistic approaches used are

- Absolute probabilistic method,
- Standard exceedence method,
- Modified exceedence method.

2.5.3.1 Absolute probabilistic method

The absolute probabilistic method quantifies the probability of an unsafe condition occurring and ensures that an absolute measure of safety is achieved. Previous drawbacks in determining the nature of parameters presented a difficulty in determining the probabilistic thermal ratings of a transmission lines. However, methods in determining the nature of parameters progressed. The absolute probabilistic approach simulates the safety of a line by incorporating all relevant influencing factors and confirming the probability of each factor [12]. Each factor is independent from each other. The probability of an un-safe condition arising is defined by [11] as:

$$P_{acc} = P(CT) \times P(I) \times P(obj) \times P(surge) \tag{2.5.26}$$

where:

P_{acc} = probability of an accident or flashover occurring,

$P(CT)$ = probability of a certain temperature being reached by the conductors and is calculated from existing weather parameters, conductor characteristics and types. A loading current is assumed. However, it is possible to obtain the load current for existing lines from the system operator. P(CT) is determined by a Monte Carlo simulation;

$P(I)$ = probability of the assumed current being reached and can be determined from the actual current measured on the system;

$P(obj)$ = probability of decreasing the electrical clearance by an object under or in the vicinity of the servitude,

$P(surge)$ = probability of a voltage surge occurring on the line and is determined from previous fault records or surge overvoltage simulations of the power system. If the surge occurs simultaneously with an object under the line the likelihood of a flashover or accident happening is increased.

2.5.3.2 Standard exceedence method

The method uses historical weather data to determine the operating temperature of conductors for a given conductor current. The standard exceedence method allows for the design temperature of the line to be exceeded for a small percentage of time and occurs without infringing on the safety of the public. In addition, the probability of $P(I)$, $P(obj)$ and $P(surge)$ occurring is deemed very low. The exceedence level is the amount of time the operating temperature exceeds the design temperature of the conductor.

Figure 2.5.3 displays the exeedence graphs for work performed on the Eskom Majuba – Pegasus 400 kV transmission line. The line route starts at Majuba coal-fired power station near Volksrus, in the Mpumalanga provinceand terminates at Pegasus transmission substation near Dundee in the KwaZulu-Natal. The line is approximately 154 km long and various weather parameters can occur along the right of way. The line rating at the sending end can therefore differ from the rating at the receiving end and vice versa due to the varying weather parameters. The exeedence graph in figure 2.5.3 shows results for the sending end represented by the dotted line and the receiving end represented by the solid black line. Higher wind speeds at the sending end results in increased cooling, hence the lower exeedence level for the same current. With reference to figure 2.5.3, if the exeedence limit is set to 5% two different ratings are obtained. The rating at Pegasus will be 1000A and the rating at Majuba will be 1400A for the same conductor due to varying weather conditions. The deterministic method results in 946A rating [11]. The benefit of the standard exeedence method is

realized when the results of the standard exeedence method and the deterministic method are compared. The percentage difference between results reveals that increases in rating of 5% to 38% can be expected when using the standard exeedence method.

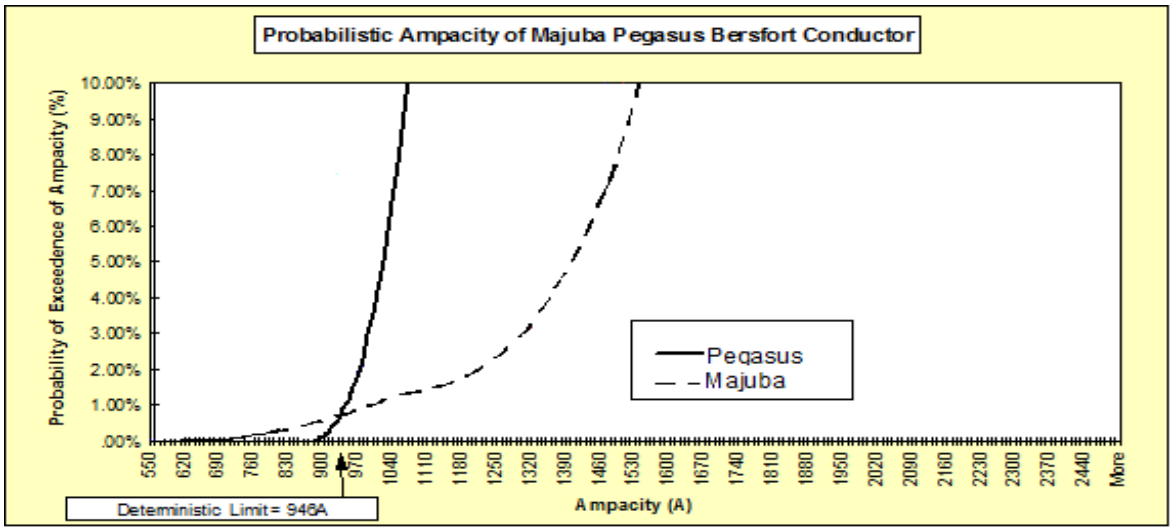

Figure 2.5.3: Exeedence graph generated by means of the standard exceedence method [11]

2.5.3.3 Modified exceedence method

The method discussed in the previous section assumes a flat current profile to determine the thermal rating. The modified exceedence method allows for a more dynamic approach in determining the exceedence level by means of the actual load profile. The actual profile is normalized and the current that would result in the design temperature being reached is determined. The modified exeedence method is a more sophisticated method and results in higher current transfers.

Figure 2.5.4 show the results for the modified exceedence method. The exceedence level was set at 5% and the ampacity was determined for Hare conductor. With reference to figure 2.5.4, the light blue line was obtained by using a flat current profile and the solid black line was obtained using the actual load profile. The graph in figure 2.5.4 shows the benefit of using the modified exeedence method as the current rating was increased from 280 A to 340 A with a 5% exeedence.

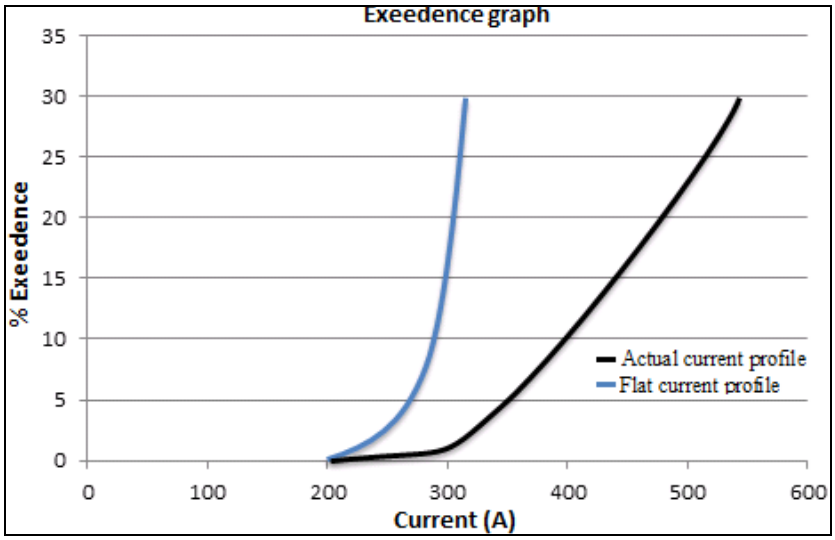

Figure 2.5.4: Results for the modified exceedence method [11]

2.5.4 **Dynamic behaviour of conductor temperature**

Dynamic line ratings generally result in higher thermal ratings than conventional static ratings as a result of changing input parameters. This creates a dynamic process of heat balance where the average conductor temperature is expressed by a differential equation. The dynamic rating of conductor temperature may be used to maximise load flow and simultaneously minimise the likelihood of infringements [12]. The average conductor temperature is defined by the conductor surface and core temperature and is given by [12]:

$$T_{avg} = \frac{T_S + T_C}{2} \tag{2.5.27}$$

The differential equation is defined by [35] as:

$$M \times C_p \times \frac{dT_{avg}}{dt} = P_J + P_S + P_M - P_r - P_C \tag{2.5.28}$$

where:

M = mass of the conductor per unit length (kg/m);

C_p = specific heat capacity of the conductor per unit length (J/℃/m).

2.6 LIGHT DETECTION AND RANGING TECHNOLOGY (LIDAR)

In order to accommodate higher current transfer, information on the existing “as-is” condition of the line must be gathered. Analysis of the available clearances and safety margins must be done before the rating of the transmission lines can be increased.

Generally, traditional survey techniques have been used in transmission line design to collect terrain data for the uprating of existing lines or the design of new lines. However traditional surveying techniques are relatively time-consuming and expensive. In flight LIDAR surveying is a modern technique which allows for high speed and effective data acquisition of existing rights of way. By implementing laser surveying technology accurate information on the terrain, structures, conductors and any other obstacle along the right of way is obtained. The principle behind PLS CADD and the three-dimensional profile modelling is discussed and demonstrated in chapter 3 of this dissertation.

2.6.1 **Working principle of LIDAR**

LIDAR technology is a well-proven technology that is used for cost effective gathering of high density and accurate topographic data. This technology allows fast surveying of transmission lines which makes it very attractive. Aerial laser surveying of power corridors is becoming increasingly common. LIDAR systems operate in the near infrared band emitting high-energy pulses that can be realised in short intervals on a narrow optical spectrum. The principle of laser ranging is to measure distances from the sensor to the ground or desired feature. A laser beam is projected onto a scanning mirror that sends a brief pulse of light out onto the terrain surveyed. The LIDAR system projects thousands of pulses per second creating a dense population of points on the ground. The reflected pulse is detected by the LIDAR system together with the integrated GPS (global positioning system), the POS (Position orientation system) and control unit. Based on the speed of travel of the aircraft and the position and altitude of the system, it computes the x, y and z coordinates and position of each reflected point.

LIDAR data received by the control system are continually monitored for quality during data acquisition.

The representative three-dimensional model of the transmission line is created with the help of modelling software. The data that were stored during the aerial survey is imported into PLS CADD, converted and merged with conductor characteristics, tower geometry and attachment heights. A direct representation of the “as-is” condition of the existing line and surroundings is obtained. In addition, the exact conductor-to-ground clearances are also established from the model.

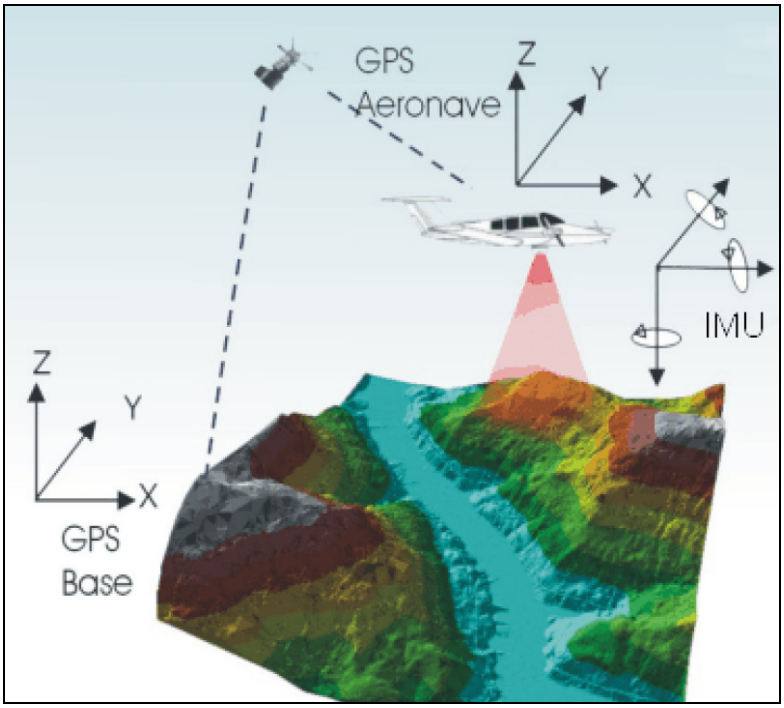

Figure 2.6.1: Typical LIDAR system components [37]

The different systems in Figure 2.6.1 are

- Airborne GPS is needed to determine the x, y, and z coordinates of the moving LIDAR sensor in the air, surveyed relative to one or more GPS base stations.
- The Inertial Measuring Unit (IMU) directly measures the roll, pitch, and heading of the aircraft, establishing the angular orientation of the LIDAR sensor about the x, y, and z axes in flight.

- The LIDAR sensor measures the scan angle of the laser pulses. Combined with the MU data, this establishes the angular orientation of each laser pulse.
- The LIDAR sensor measures the time needed for each emitted pulse to reflect off the ground or the conductor and return to the sensor.

2.6.2 **LIDAR advantages and drawbacks**

Light detection and ranging technology can be used to generate a direct representation of the transmission line in 3D. Accurate data and information are available to establish conductor-to-ground clearances from the 3D model. The main advantage of LIDAR technology is the high-speed data acquisition of transmission line networks in relation to time consuming traditional survey methods. The use of LIDAR technology in transmission line uprating studies allows for fast and accurate collection of terrain, structures and cable data as well as obstacles along the power line corridor.

Some of the drawbacks of LIDAR include that it does not provide a real time solution, so that post processing of the surveyed data is needed. Also, not all LIDAR equipment is the same in regard to the wavelengths needed to penetrate different levels of surveying terrain, i.e. open land, water and forestry. For surveying transmission lines it is very important to choose the appropriate LIDAR equipment, which will yield the desired results.

2.7 PLS CADD AND THE 3D MODELING OF TRANSMISSION LINES

Power line system computer aided design and drafting (PLS CADD) is a transmission overhead line design software packages that seamlessly integrates line design into a single software packages [38]. It allows line design engineers to create sophisticated three-dimensional engineering models of transmission lines and is used for new line design purposes or for evaluating existing transmission lines. During this research three individual transmission line models were created in PLS CADD to establish whether the transmission lines are capable of carrying additional load. The functionality of PLS CADD and the profile modelling of the lines under study are discussed in chapter 3.

2.8 CONDUCTOR TEMPERATURE MEASUREMENT

It is expected that the temperature of a conductor will increase if the amapacity is increased. Higher temperature operations will contribute to the increase in sag of the conductor. It is very important to accurately determine the temperature of conductors during a LIDAR survey. One method is to measure the temperature of the conductor directly. The conductor temperature is measured at multiple points along the transmission line by means of temperature sensors.

A temperature sensor that is commonly used for measurement of conductor temperatures is commonly known as an i-Button®. The i-Button® is an integrated chip enclosed in a small stainless steel container (16 mm in diameter) is rugged enough to withstand harsh environmental conditions and is able to operate in a high voltage environment. The sensor is small and portable enough to be attached to an overhead conductor to measure the temperature of the conductor. The sensor has a temperature measurement range of -40 °C to 85 °C with a selectable measuring resolution of either 0.5 °C or 0.0625 °C. Additionally, the user is able to specify the temperature sample rate as well as the start and stop times for measurement.

Figure 2.8.1: Representation of a DS1922L i-Button temperature sensor [39]

Programming and data retrieval are done through a specialised software and USB (universal serial bus) hardware bus. It is possible to view the data on the sensor by means of the software or the user can export the data to a Microsoft Excel file for data

analysis. Figure 2.8.2 illustrates the interface of the software used for programming and data retrieval purposes.

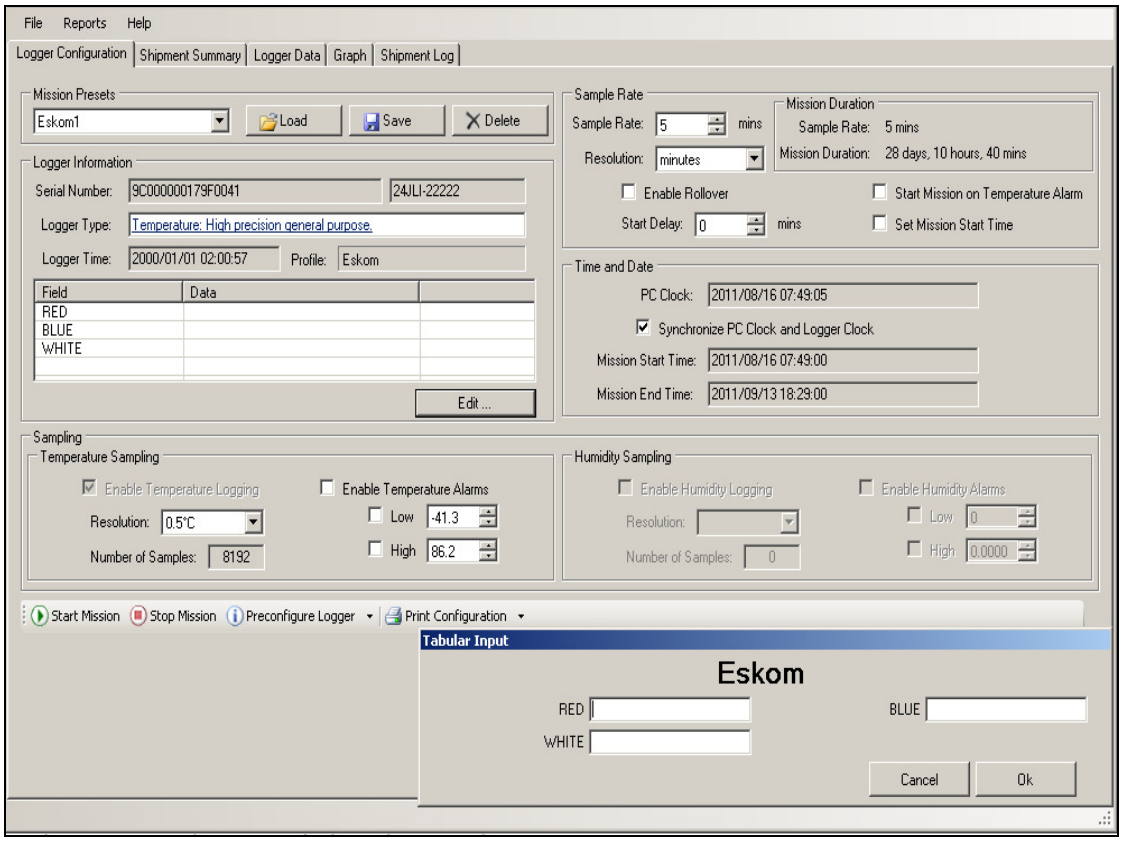

Figure 2.8.2: Setup of temperature sensor prior to live line installation

2.9 INTRODUCTION TO THE THERMAL UPRATING OF SUBSTATION EQUIPMENT

Eskom's existing generating capacity at times has proven to be inadequate. This is due to the rapid increase in economic and industrial growth. Generally, the solution to such a crisis is to expand the generating capacity to meet demand. This requires the need for new transmission infrastructure to transmit electrical energy from power stations to load centres. As previously explained, environmental pressures, the lack of space and public opposition restrain this possibility. It is impossible to obtain new rights of way in heavy populated areas. Existing infrastructure in many cases is heavily loaded, which causes bottlenecks in the network. Thermal uprating may alleviate heavily loaded lines and increase transfer capacity.

Power system equipment is an important aspect in the supply of electricity and is generally located within the substation boundaries. Substations throughout the South African power network face various challenges that necessitate the need to uprate power equipment. Power equipment must be able to handle the increase in power transfer expected from thermal uprated transmission lines. Nonetheless, the benefits of increasing the rating of transmission lines may be limited by the thermal ratings of power equipment. The maximum current that substation equipment can conduct without violating any safety criteria is called the rating. Higher power transfers of substation equipment, as with transmission lines, are limited by the operating temperature and thermal ratings. Excessive overloading of substation equipment adversely affects the performance and operating life of equipment. The life span of substation equipment varies between components for differing reasons. In certain cases power equipment can be refurbished but must then be taken out of service for the refurbishment period. Refurbishing equipment is different from thermal uprating in the sense that thermal uprating of substation equipment increases the transfer capacity while the equipment is in-service with minor modifications. Thermal uprating of substation equipment defers the capital investment for refurbishment by unlocking spare thermal capacity.

One of the key operational aspects for power utilities is to increase the utilization of their transmission circuits. Substation plant availability and reliability is ranked as one of the top priorities in ensuring the security of supply. It is becoming necessary to look into the uprating of existing substation equipment to alleviate congestion in transmission circuits. In contrast to the power transfer increase of equipment, the thermal uprating of power equipment aims to provide a cost effective solution with minimal capital expenditure to increase the performance and utilisation of substation equipment.

2.9.1 **Thermal response of substation equipment**

The main objective of this section of the dissertation is to discuss the thermal response of power equipment to an increase or change in current flow. The risks of overloading associated with power transfer increases are also discussed and thermal models used

for the determination of substation equipment ratings are examined. In addition, the sensitivity of substation equipment ratings to weather parameters is discussed. There is a strong case in South Africa for the implementation of the thermal uprating of substation equipment. Substation equipment ratings are generally dictated by the fixed voltage limit, thermal limit, the rated continuous current and the rated short circuit current.

Changing trends in the power sector necessitate that substation equipment has higher transfer capacity, higher thermal ratings and reliability. Higher equipment rating parameters allow for increased power transfer. Substation terminal equipment is manufactured according to IEC (International Electro-technical Commission), IEEE (Institute of Electronic and Electrical Engineers) or ANSI (American National Standards Institute) standards. The standards are used as a guideline for the determination of thermal ratings and specify maximum operating temperatures of equipment.

2.9.1.1 Power transformers

Thermal uprating of substation equipment requires the use of higher operating temperatures than recommended by manufacturers. The nameplate rating of a power transformer provides a normal life expectancy under continuous operation at rated load [40]. The life span of power transformers is generally dependent on the loading specification of the power utility. Power utilities load their substation equipment differently when compared with one another. The equipment is designed to suit the loading requirements of the utility.

Power transformers are able to sustain short periods of overloading with negligible losses in insulation and equipment lifetime. It is possible to calculate short-time overload characteristics for power transformers to increase the thermal rating. Increased power flows influence the operating and hotspot temperatures of a transformer. The life expectancy of transformer insulation is a function of the hotspot temperature and the operating time at that temperature [41]. The IEC 60076-2 describes maximum permitted temperature rise limits for transformers as [43]:

- Average winding temperature rise = 65 K (with oil directed (OD) cooling an additional 5 K is allowed);
- Top oil rise = 60 K (for normal conservator transformer types).

The temperature rise limits of the IEC 600076-2 are based on an annual average ambient temperature of 20 ℃. Various modes of cooling are employed on transformers. The IEC 600076-1 developed a four-letter designation depicting the various cooling options. They are [59]:

- 1st letter: internal cooling medium
  O = Oil
- 2nd letter: method of internal cooling medium circulation
  N = natural
  D = directed
  F = forced
- 3rd letter: external cooling medium
  A = air
  W = water
- 4th letter: method of external cooling medium circulation
  N = natural
  F = forced, usually with fans (air) and pumps (oil).

An example of this four-letter designation could be an ODAF cooled transformer (oil directed, air forced). This means that the transformer has an internal oil-cooling medium that is pumped through the windings with forced cooled air being blown on the heat exchanger externally [42].

Thermal models are developed based on the maximum permitted temperature rise limits of the IEC 600076 – 2 [43]. The IEC limits were determined in assuming an maximum ambient weather condition of 40 ℃. These assumptions are essential to the specification and design of power transformers but can result in conservative thermal ratings. It is possible to unlock spare thermal capacity of transformers safely by

determining higher allowable top oil temperatures. Figure 2.9.1 illustrates the typical distribution of transformers' temperatures along the winding.

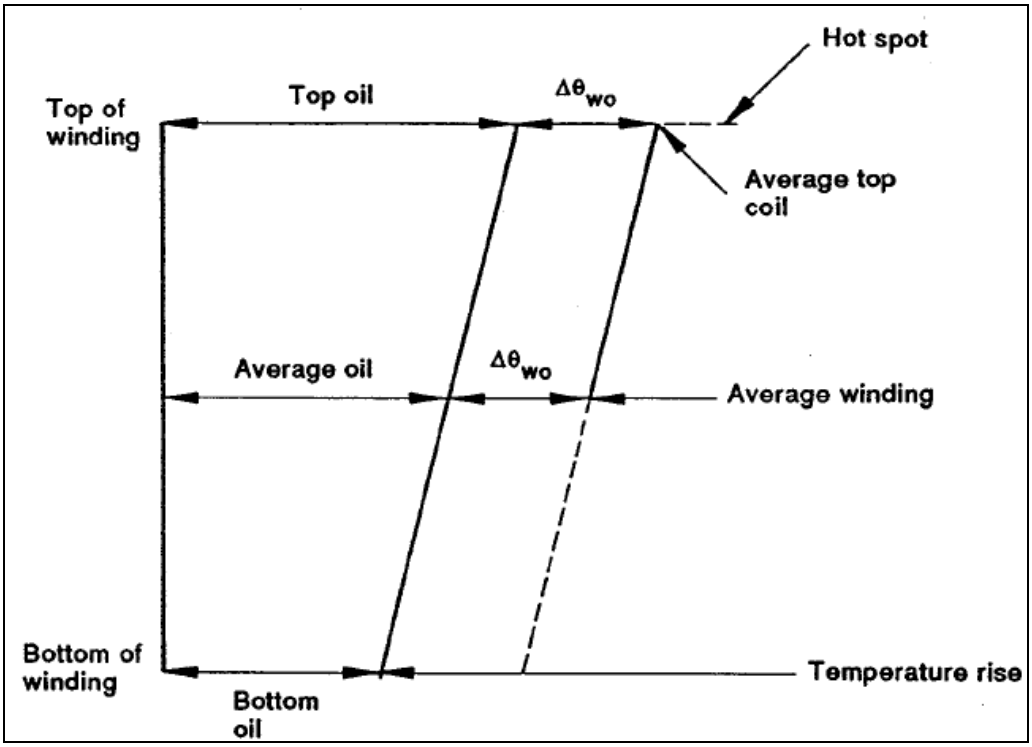

Figure 2.9.1: Temperature distribution model along a typical transformer winding [43]

The thermal model and equations used to determine short-time overloads are defined by [40]:

$$\theta_{HS} = \theta_a + \theta_0 + \theta_g \tag{2.9.1}$$

$$\theta_0 = (\theta_u - \theta_i)(i - e^{\frac{-t}{\tau}}) \tag{2.9.2}$$

$$\theta_u = \theta_{FL}\left[\frac{K_u^2 R_r + 1}{(R_r + 1)}\right]^n \tag{2.9.3}$$

$$\theta_i = \theta_{FL}\left[\frac{K_i^2 R_r + 1}{R_r + 1}\right]^n \tag{2.9.4}$$

$$\theta_g = K_u^{2n}\theta_{gFL} \tag{2.9.5}$$

$$\theta_{gFL} = (\text{average winding rise}) - (\text{top oil rise}) + (\text{industry allowance}) \tag{2.9.6}$$

$$\text{n} = 0.8 \text{ for OA, OW, OA/FA and } 1.0 \text{ for FOA, FOW, OA/FOA, OA/FA} \tag{2.9.7}$$

where:

θ_{HS} = Hottest spot temperature in ℃,

θ_a = ambient temperature in ℃,

θ_0 = top oil rise over ambient in ℃,

θ_g = hottest spot rise over top oil in ℃,

θ_u = ultimate oil rise for overload in ℃,

θ_i = initial oil rise (t=0) from prior loading in ℃,

t = intended overload in hours (hr),

τ = thermal time constant in hours (hr),

θ_{FL} = full load top oil rise in ℃,

K_u = per unit overload intended,

K_i = per unit initial loading, prior to overload,

R_r = Ratio of load losses at rated current to no-load losses

i = initial quantity.

The thermal time constant for the determination of short-time overloads is defined by [40] as:

$$\tau = \frac{C(\theta_u - \theta_i)}{P} \tag{2.9.8}$$

C/P is a relation between transformer mass and change in total power loss, due to load change.

Power transformers are a strategically important part of power networks and are sometimes exposed to adverse operating conditions including overvoltages, transient voltage surges, fault currents, overloading and under frequency operation. A combination of these adverse conditions could result in overexcitation of the transformer. Overexcitation is a phenomenon that occurs in power transformers where the core is subject to greater than normal flux when the voltage to frequency ratio (Volts/Hz) exceeds 1.05 p.u. at full load and 1.10 p.u. at no load [60]. The flux in the

transformer core is directly proportional to the applied voltage and inversely proportional to the frequency. Permissible levels of over-excitation for power transformers are generally specified by international standards. Figure 2.9.2 displays a permissible short-time transformer over-excitation capability curve under light-load conditions. Transformers are susceptible to thermal damage from excitation beyond the coloured region in Figure 2.9.2 [40].

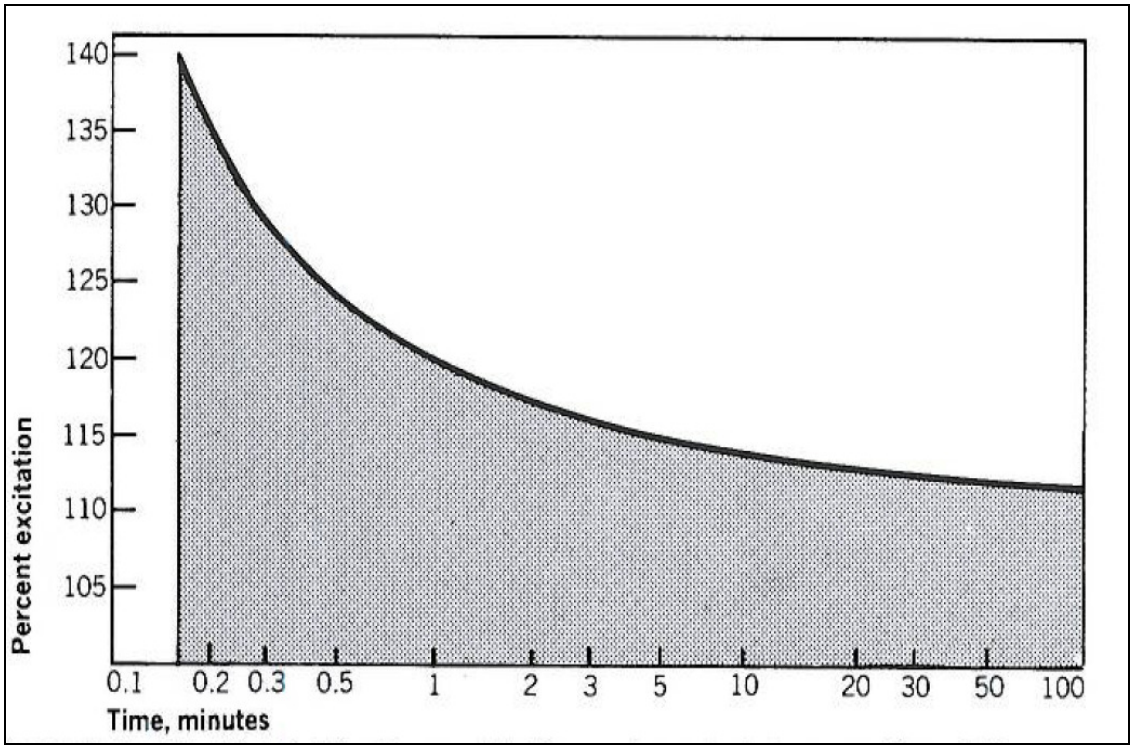

Figure 2.9.2: Permissible short-time transformer over-excitation capability curve [40]

Additional heat generated by increased current transfers may reduce the expected life of insulation. Therefore, the insulation of a transformer is of utmost importance when considering over-load capability [11]. Overloading power transformers beyond nameplate ratings can cause a rise in temperature of both transformer oil and windings [60] Figure 2.9.3 displays a typical loss of insulation graph against hottest spot temperature for oil-immersed transformers.

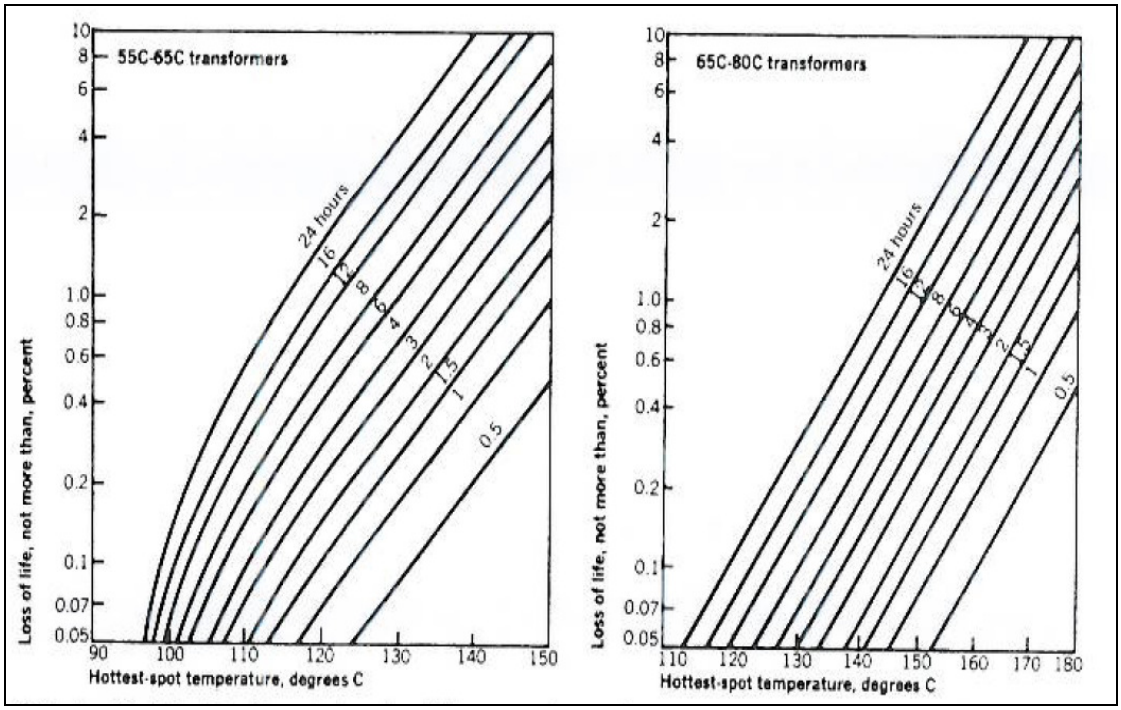

Figure 2.9.3: Loss of insulation graph versus hottest spot temperature [40]

It is possible to determine a short-time overload for an oil-immersed transformer using the parameters in Figure 2.9.3. A general case study is discussed for this purpose [40]:

The initial conditions prior to determining the short-time overload are assumed as θ_a = 25 ℃ and the per unit initial loading, prior to overload, K_i = 85%. The transformer characteristics on which the load is to be increased are

- FOA cooling allowance = 5℃,
- Hottest spot rise = 65 K,
- Top oil rise = 45 K,
- Time constant = 1.5 hr,
- C/P ratio = 5.0,
- Average winding temperature rise = 55 K, and
- n = 1.0.

An allowable loss of insulation life of 0.2% is assumed from Figure 2.9.3. For an overload of 30 minutes to result in a hot spot temperature of approximately 140 ℃ it is

possible to solve the value for θ_{HS} and K_u. By solving the overload equations (2.9.1 to 2.9.7) the hottest spot temperature is determined as 140 ℃, which results in an overload of around 185% [40].

The performance of power transformers is a function of time and temperature. The manner in which the overloading of a transformer is approached results in short-time power transfer increases with minimal sacrifice in the loss of insulation. The IEC standards mentioned [43] in this section suggest safe loading guidelines for power transformers. Guidelines are necessary to prevent premature failure of equipment, to recognise distinctions in thermal capability and to permit the selection of thermal ratings that will result in increased loading. The risks associated with the safe overloading of transformer are low. The challenge with un-locking spare thermal capacity in power transformers is to determine increased loading levels that represent an acceptable risk level given the circumstances of the increase [11].

Thermal ratings play a big role in the uninterrupted continuous operation of power transformers. Transformer ratings are generally determined over a 24 hour period. The method employs the calculation of critical operating temperatures and loss of insulation life over a 24-hour period as displayed in Figure 2.9.3. The thermal ratings of transformer are generally a function of weather parameters, the load and the duration of the load. The steps to calculate the rating of a transformer are [11]:

a. Gather information on the loading requirements as suggested by the manufacturer.
b. Assess the condition of the transformer. The method of checking the condition is generally specified by guidelines of manufacturers' and international standards.
c. Determine the initial temperature. The initial temperature prior to the rating is important and is generally estimated. The temperature can also be determined directly by calculating the temperatures at the end of a 24 hour period of assumed loading.
d. Calculate transformer temperatures and loss of life for the rating period using equations (2.9.1) to (2.9.7).

e. Compare the maximum temperatures and loss of insulation life from point 2 with transformer limits.
f. Examine the risks of loss of insulation at point 5.
g. Check the ratings of auxiliary equipment (bushing etc.).
h. Adjust the load level once the decision is made. Real time monitoring of operational temperatures must accompany the decision when increasing the loading. Note: The loading is also generally cyclic in nature. The peak loading may only be present for 2 hours in a 24-hour cycle.

The effects of weather conditions influence the thermal ratings of power transformers as in the case for overhead lines. Ambient temperature conditions play a vital part in the rating of transformers. High ambient air temperatures influence the operating temperature of the transformer drastically. The transformer is generally de-rated in cases of surrounding high ambient air temperatures. Different transformer ratings for day and night could exist and are dependent on the surrounding ambient air temperatures. In addition, wind speed and direction influence the cooling of transformers. Historically, power utilities assumed conservative wind conditions of approximately 0.61 m/s [41]. This generally results in convective cooling of the transformer. Weather conditions have a varying influence on the overall temperature of the transformer. The sensitivity of power transformers to outdoor weather conditions must be recognised when determining thermal ratings.

2.9.1.2 Transformer auxiliary equipment

The discussion on the loading criteria of transformers in the preceding section requires discussion on the loading of auxiliary power transformer equipment. The increased loading on transformers could influence the loss of life for transformer auxiliary equipment such as bushings, tap changers and internal current transformers. It is therefore important to evaluate the loading criteria and risks associated with the overloading of transformer auxiliary equipment.

High voltage transformer bushings require capacitive grading to control the internal electrical field both radially and longitudinally. Many power transformer bushings

consist of Kraft paper layers impregnated with oil. Hence the method of rating transformer bushings is similar to that used on transformers. Bushings are designed to operate with a hot spot temperature of around 105 ℃ and top oil temperatures of 95 ℃. The same principle applies in determining the loss of life over a 24-hour period for bushings as with transformers. Overloading of bushings is plausible when determining higher hotspot temperatures. The method and thermal model used to determine the hotspot temperature of transformer bushings are defined by [40]:

$$\Delta\theta_{HS} = K_1 I^n + K_2 \Delta\theta_O \tag{2.9.9}$$

where:

$\Delta\theta_{HS}$ = bushing hotspot temperature,

K_1 = specific bushing constant ranging from 15 to 32,

K_2 = specific bushing constant ranging from 0.6 to 0.8,

I = per unit rated bushing current,

$\Delta\theta_O$ = transformer top oil temperature,

n = bushing constant ranging between 1.6 and 2.0.

Overload limits for transformer bushings are specified by international standards, for example the ANSI standard C57.19.100-1995 [44]. Manufacturers and power utilities use standards as a guideline to the rating and loading of transformer bushings. The general over load limits as specified by the ANSI standard are [44]:

- 40℃ ambient temperature,
- 110℃ transformer top oil temperature,
- 2 x rated bushing current,
- 150℃ bushing hot spot temperature.

Transformer bushings experience the same environmental, mechanical and electrical stresses as power transformers. With higher hotspot temperatures, associated risks are relevant and important to identify. The risk of bushing failure is an inherent effect of severe overloading. However, it is possible to determine safe overload criteria with moderate risks in loss of insulation life. The risks associated with the overloading of bushings include:

- Cellulose ageing of insulating Kraft paper (Kraft paper is an insulating medium with very good mechanical, chemical and electrical characteristics);
- Ageing of oil;

As in the case of power transformers, the risk of increasing the loading is dependent on an economic decision. Increasing the loading of a bushing may defer capital investment and allow for increased power transfers but the risk of premature failure exists. The loss of life for bushings can be determined in the same way as for power transformers. Bushing ageing is also affected by the voltage level. The transformer insulation loss of life curve in figure 2.9.3 is generally used as the basis for determining the ageing acceleration factor over a 24-hour period. The factor is usually determined for a given load and temperature or a changing load and temperature. The ageing factor is defined by [40] as:

$$F_{aaf} = e^{\left(\frac{15000}{\theta_{HR}+273} - \frac{15000}{\theta_{HS}+273}\right)} \tag{2.9.10}$$

where:

F_{aaf} = ageing accelerated factor;

$\Delta\theta_{HS}$ = bushing hotspot temperature;

θ_{HR} = winding hottest spot temperature.

Accurate determination of the constants used in equation 2.9.9 and 2.9.10 is necessary. This type of information can be requested from the manufacturer.

Another important piece of auxiliary power transformer equipment is the tap changers. Different types of tap changers are used in the transmission system. The most common tap changers are on-load tap changers (OLTC) and de-energised tap changers (DETC). Recent advances in power technology lead to the introduction of vacuum tap changers. Tap changers evolved from normal fixed transformer tap technology. Taps along the winding of a transformer allow for easy regulation of the output voltage. Historically, taps were designed as fixed. Changes in the power supply

industry necessitated the need for variable taps. Innovative engineering designs lead to the development of tap changing technology or commonly known as tap changers. Tap changers are used to select different winding ratios. This method allows for easy voltage regulation in transmission circuits.

Power utilities are obliged to ensure the uninterrupted supply of electricity. On-load tap changers allow for on-load voltage control. OLTC's are generally equipped with multiple selectors and a diverter switch. The contacts of the selector generally degrade normally over time at rated load. However, higher current transfers accelerate the ageing of selector contacts and therefore are regarded as a thermal constraint. ANSI standard C57.91-1995 specifies general safe overload limits for current carrying contacts as [44]:

- 120 ℃ contact temperature. The contacts can tolerate higher operating or contact temperatures but will result in regular maintenance;
- Have to break twice the rated current of the OTLC (for at least 40 times).

The temperature rise of contacts is determined by [11] as:

$$\Delta\theta_C = \Delta\theta_{C,R} I^n \tag{2.9.11}$$

where:

$\Delta\theta_C$ = the OLTC contact temperature rise over oil,

$\Delta\theta_{C,R}$ = the OLTC contact temperature rise over oil at rated load,

I = the OLTC rated per unit current,

n = an exponent that varies from 1.6 to 1.85.

The total contact temperature is defined by [11] as:

$$\theta_C = \theta_A + K\theta_{TO} + \Delta\theta_C \tag{2.9.12}$$

where:

θ_C = the total contact temperature,

θ_A = the ambient air temperature,

θ_{TO} = the transformer top oil temperature,

K = a constant to account for the difference between transformer top oil temperature and OLTC compartment oil temperature, typically around 0.8.

The risks associated with higher temperature operations and short-time overloading of OLTC includes:

- Contact coking which increases electrical resistance across contacts.
- Higher contact resistances result in elevated operating temperatures that adversely influence thermal ratings.
- Elevated contact temperatures further increase contact coking that increases wear and tear during break operations (regular maintenance is required).
- Higher resistance results in prolonged arcing during break operations.
- Arcing may short-circuit the regulating winding, which leads to transformer failure and loss of supply.

Another type of tap changer is the de-energised tap changer (DETC). This type of tap changer requires that the transformer must be de-energised between tap changes. The thermal characteristics of the DETC are similar to the OLTC. The same risks associated with higher temperature operations for the OTLC apply to the DETC.

2.9.1.3 Current and voltage transformers

As previously explained in Section 2.9.1, a substation consists of a combination of different types of power equipment that are designed according to the requirements of the power utility and industry. Current transformers are used in transmission circuits for protective relaying and metering purposes. CTs are generally rated according to ANSI or IEC standards. In addition, the standards provide general limitations, thermal ratings and tables for determining CT loading based on average characteristics. The thermal capacity of a freestanding CT can be increased by calculating the permissible short-time over load.

The rating plate of a freestanding CT displays the following important information necessary to determine short-time overloads [45]:

- the rated primary and secondary current;
- the rated frequency (e.g. 50 Hz);
- the rated output and the corresponding accuracy class;
- the highest voltage for equipment (e.g. 1,2 kV or 145 kV);
- the rated insulation level (e.g. 6/–kV* or 275/650 kV);
- the rated short-time thermal current (I_{th}) and the rated dynamic current if it differs from 2,5;
- the class of insulation, if different from class A type insulation;
- on transformers with two secondary windings, the use of each winding and its corresponding terminals; and
- the rated continuous thermal current (for example I_{cth} = 150 %).

The maximum allowable operating temperature of a CT is a function of the prevailing ambient air temperature θ_a. The temperature rise of a current transformer when carrying a primary current equal to the rated continuous thermal current shall not exceed the values as defined in the IEC 60044-1 [45]. Additionally, the ANSI standard C57.13-1993 [46] also defines thermal limits for freestanding oil immersed CTs.

Table 2.9.1 summarises the thermal limits for free-stranding oil immersed current transformers. Historically, the limits specified in Table 2.9.1 remained the same from 1954 to 1993 when power utilities required the need for current transformers with higher temperature rise limits. The 65 K temperature rise limit for current transformers was then defined.

Table 2.9.1: Free-standing oil immersed CT operating temperature and thermal limits [46]

Year	CT Type	CT temperature rise (K)	Normal allowable maximum temperature (K)	Winding rise (K)	Hot spot temperature rise (K)
1954	Oil immersed	55	95	55	65

1968	Oil immersed	55	95	55	65
1978	Oil immersed	55	95	55	65
1993	Oil immersed	55	95	55	65
1993 onwards	Oil immersed	65	110	65	80

The normal continuous current I_a of a CT is a function of the continuous current loading I_{tap} and the ambient air temperature θ_a. The continuous current loading I_{tap} of a CT is defined by [11] as:

$$I_{tap} = I_{tapr} \times \left(\frac{I_r}{I_{tapr}} \right)^{\frac{1}{n}} \times RF \qquad (2.9.13)$$

where:

I_{tap} = adjusted rated continuous current of specific current transformer tap under consideration,

I_r = rated continuous current (full ratio rating),

I_{tapr} = rated continuous current of specific current transformer tap under consideration,

RF = continuous thermal current rating factor. Assume 1.0 if not available,

n = winding rise exponent (typically a conservative value of 2 is used).

The normal continuous current rating for free standing CTs I_a is defined by [11] as:

$$I_a = I_{tap} \times \left(\frac{30 + \theta_r - \theta_a}{\theta_r} \right) \qquad (2.9.14)$$

where:

I_a = normal current rating,

θ_a = ambient air temperature,

θ_r = rated maximum temperature rise.

Equation (2.9.14) can be used to determine current ratings at various ambient air temperatures other than 30 ℃. In addition, manufacturers generally do not determine emergency ratings for current transformers. Existing practice is to specify and use a CT with a continuous thermal current rating that is sufficient to handle unforeseen emergency loading conditions [47]. Figure 2.9.4 expresses the normal loading as a function of the time loading. It is possible to load CTs at more than 100% normal current for short periods. The graph displayed in Figure 2.9.4 is a helpful way to determine the percentage overload. The overload is a function of the prevailing ambient conditions and the period for which the overload is needed.

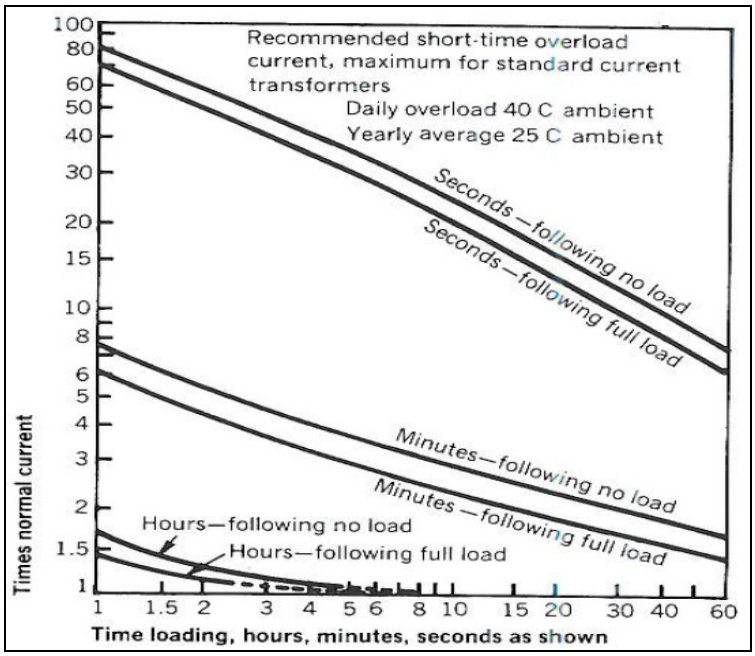

Figure 2.9.4: Short time overload curves for current transformers [40]

Voltage transformers (VT's) are instrument transformers in which the secondary voltage, in normal conditions of use, is substantially proportional to the primary voltage. The primary purpose of a VT is to isolate and protect control and measurement equipment from the high voltages present within transmission circuits, while producing reduced voltages to measuring and protection equipment. Voltage transformers are divided into two groups, magnetic (inductive) voltage transformers

and capacitor voltage transformers (CVT). VT's and CVT's are voltage related equipment and are not affected by thermal uprating.

2.9.1.4 Line Isolator

Line isolators are used in transmission circuits to isolate and separate electric circuits by means of opening contacts under no load conditions. The isolator relies on air for its insulation between open contacts. The switch provides a protective function by means of a visible break in the electrical circuit and is generally used during routine maintenance by isolating or sectionalising power equipment to ensure personnel safety. The rating of line isolators is guided by international standards. The thermal rating of a switch is based on weather conditions and equipment operating temperatures. Historically, the current carrying parts of switches were manufactured from copper, bronze castings and hard-drawn copper. The largest parts of modern switches rely on silver alloy contacts, castings and joints. The temperature rise limits of silver current carrying parts are higher than for conventional current carrying parts.

Silver contact current carrying parts are rated for continuous operation at a temperature rise of 53 K [11]. Ambient temperatures have a very big impact on the thermal rating of isolators. Table 2.9.2 summarises a few ambient values and the effect it has on the thermal rating of silver contacts with a temperature rise of 53 K.

Table 2.9.2: Impact of ambient air temperature on thermal rating of line isolators [11]

Ambient temperature (°C)	Thermal rating (53 K rise in silver contact temperature)
45	95
40	100
35	105
30	109
25	113

The largest part of line isolator manufacturers nowadays use materials that are able to withstand higher operating temperatures. Older line isolators still rely on copper for

their current carrying parts. Copper current carrying parts do not accommodate high operating temperatures well and are not desirable to support higher power transfers. Copper oxidises rapidly in air which results in copper oxide. Copper oxide has a very high resistance that causes increased heating on the current contacts and contributes to the acceleration of the oxidation process. Cumulative oxidation of the current carrying parts can result in the annealing of the material that adversely affects the performance of the switch. In addition, the spring used to keep proper switch contact must also be considered and is subjected to the same oxidation effects as the current carrying parts. The oxidation effect on springs is solved for instance by replacing copper springs with stainless steel springs of type 17-7, which are not adversely effected at high operating temperatures [50].

Two types of line isolators are generally used in power networks. They are enclosed and non-enclosed isolators. The latter are designed to operate in a maximum ambient condition of 40 °C and are used predominant in power utilities. Enclosed isolators can operate in higher ambient conditions of up to 55 °C and are able to be operated indoors or outdoors. The demand for higher power transfer recognises the need for line isolators with higher temperature limitations. New technology and the improvement in material sciences contributed to the development of materials and alloys that have the ability to be operated at temperatures in excess of 60 °C. In addition, these materials have greater electrical and thermal properties under higher power transfers. International standards and IEEE guidelines provides acceptable methods to determine thermal ratings for line isolators. The rating of isolators is a function of the continuous current, the allowable maximum temperature, ambient temperature and the temperature rise limit of the switch.

The thermal or allowable continuous current I_A is defined by [11] as:

$$I_A = I_R \left[\left(\frac{\theta_{\max} - \theta_a}{\theta_r} \right) \right]^{0.5} \tag{2.9.15}$$

where:

I_A = allowable continuous current,

I_R = rated continuous current at a temperature rise θ_r,

$\theta_{\max}$ = allowable temperature of switch part,

θ_a = ambient air temperature,

θ_r = limit of observable temperature rise at rated current of switch part.

Figure 2.9.5 displays various parameters that can be used to determine the allowable continuous current I_A for enclosed and non-enclosed isolators with different material types for current carrying parts, contacts and other mechanical conducting parts. The loadability L_{air} of an isolator gives an average measure of the allowable continuous current over a range of ambient conditions. As in the case with overhead lines, the loadability of line isolators gives an indication of the power transfer capability of the power equipment. The loadability of isolators is:

$$L_{air} = \frac{I_A}{I_R} = \left[\left(\frac{\theta_{\max} - \theta_a}{\theta_r} \right) \right]^{0.5} \quad (2.9.16)$$

Switch Part	Allowable Max Temperature, θ max	Limit of Observable Temperature Rise at Rated Current (θ_r) (°C)	
		Nonenclosed Indoor and Outdoor Switches (see Note 1)	Enclosed Indoor and Outdoor Switches
	Col 1	Col 2	Col 3
(1) Contacts in air (see Note 2)			
(a) Copper or copper alloy	75	33	20
(b) Copper or copper alloy to silver or silver alloy, or equivalent	90	43	33
(c) Silver, silver alloy, or equivalent	105	53	43
(d) Other (see Note 3)	—	—	—
(2) Conducting mechanical joints			
(a) Copper or aluminum	90	43	33
(b) Silver, silver alloy, or equivalent	105	53	43
(c) Other (see Note 3)	—	—	—
(3) Switch terminals with bolted connections	90	43	33
(4) Welded or brazed joints or equivalent	105	53	43
(5) Other current-carrying parts			
(a) Copper or copper alloy castings	105	53	43
(b) Hard drawn copper parts (see Note 4)	80	37	25
(c) Heat treated aluminum alloy parts	105	53	43
(d) Woven wire flexible connectors	75	33	20
(e) Other materials (see Note 3)	—	—	—
(6) Insulator caps and pins and bushing caps	110	57	47
(7) Current-carrying parts in contact with insulating materials (see Note 5)			
(a) Insulation Class 90°C	80	37	25
(b) Insulation Class 105°C	95	47	37
(c) Insulation Class 130°C	120	63	53
(d) Insulation Class 155°C	145	80	70
(e) Insulation Class 180°C	170	97	87
(f) Insulation Class 220°C	210	123	113
(g) Oil (see Note 6)	90	43	33
(8) Nonenergizable parts subjected to contact by personnel			
(a) Handled by operator	50	10	10
(b) Accessible to operator	70	30	30
(c) Not accessible to operator	—	—	—

Figure 2.9.5: ANSI Temperature limitations for line isolators [51]

2.9.1.5 Circuit breakers

Circuit breakers are very important pieces of power equipment used to control power flow, protect transmission networks and ensure the highest network reliability. Circuit breakers that are commonly used in transmission circuits include:

- Oil filled,
- SF_6 (Sulphur hexafluoride),
- Air blast, and
- Vacuum circuit breakers.

For the purpose of this study, only oil filled and SF_6 circuit breakers are discussed. The rating criteria of circuit breakers are governed by international standards, which in some cases present a conservative approach to the thermal, electrical and mechanical loading of the equipment. High voltage circuit breakers should be able to fulfil the following requirements under operational conditions [52]:

- In the stationary closed position, the circuit breaker must be able to conduct its rated current without exceeding the permissible temperature rise in any of its components;
- In its stationary positions, open as well as closed, the circuit breaker must be able to withstand any type of over-voltages within its rating; and
- The circuit breaker must, at its rated voltage, be able to make and break any possible current within its rating, without becoming unsuitable for further operation.

Power circuit breakers experience identical cumulative annealing effects, as is the case with line isolators when operated excessively under higher temperatures. Historically, current carrying parts and contacts of circuit breakers were manufactured using copper. Circuit breakers with copper current carrying parts experience deterioration in the hardness of the parts when subjected to higher operating temperature. It is common to expect at least a 25% loss of life when circuit breakers are continuously operated beyond nameplate ratings. To neutralise the annealing effects of copper carrying parts, copper alloys and silver are used in the manufacturing process of current carrying parts for circuit breakers. In addition, contact springs are replaced with stainless steel springs to maintain adequate contact pressure. High resistance joints and contacts are not considered a potential problem with these materials. An excellent article by Conway [53] discusses the basic factors on the load capability and temperature limiting criteria of power circuit breakers, which include:

- Annealing of copper current carrying parts as being cumulative;
- High operating temperatures affect the mechanical strength of materials such as aluminium and copper;
- Oxidation of current contacts results in higher resistance which subsequently cascades into runaway temperature situations;
- Actual loading or real time loading of circuit breakers can result in higher power transfers and are influenced by temperature rise limits, maximum operating temperatures and the ambient air temperature; and
- Different types of circuit breakers (oil, vacuum, SF_6 etc.) are capable of operating under separate loading criteria.

Industry standards and loading criteria of circuit breakers have been in place since the early 1940s [11]. Methodologies have been developed to determine the thermal rating of circuit breakers for the steady state conditions and during a transient loading period. In addition, short-time overloads for circuit breakers can be determined that are permissible for normal life expectancy. It is possible to increase the continuous current of an oil-filled circuit breaker by using different ambient air temperatures. The steady state expression used to determine the continuous thermal rating is defined by [11] as:

$$I_a = I_r \left(\frac{\theta_{HS} - \theta_a}{\theta_r} \right)^{1/n} \tag{2.9.17}$$

where:

I_a = the allowable continuous load current at a given ambient, with a maximum operating temperature of $\theta_{\max}$,

I_r = the nameplate rated current for a particular piece of equipment,

θ_{HS} = the maximum hottest spot temperature or the ultimate temperature rise,

θ_a = the ambient temperature at which the rating is being calculated,

θ_r = the allowable or rated temperature rise (hottest spot rise),

n = an exponent usually between 1.6 and 2.0.

The transient formulation used to determine the operating temperature of an oil-filled circuit breaker during transient loading periods is given by [48]:

$$\theta_{O.U} = \theta_{O.R} \left(\frac{I_2}{I_R} \right)^m \tag{2.9.18}$$

$$\theta_{O.2} = \theta_{O.1} + (\theta_{O.U} - \theta_{O.1})(1 - e^{-\Delta t/\tau_0}) \tag{2.9.19}$$

$$\theta_{HS.U} = \theta_{HS.R} \left(\frac{I_2}{I_R} \right)^n \tag{2.9.20}$$

$$\theta_{HS,2} = \theta_{HS,1} + (\theta_{HS.U} + \theta_{HS,1})(1 - e^{-\Delta t/\tau_W}) \tag{2.9.21}$$

$$T_{HS,2} = T_A + \theta_{O.2} + \theta_{HS.2} \tag{2.9.22}$$

where:

$\theta_{O.U}$ = the ultimate oil temperature rise,

$\theta_{O.R}$ = the rated oil temperature rise,

I_2 = current at the present time step, *t*2,

I_R = the rated current,

m = an exponent, generally between 1.5 and 2.0 (default 1.8),

$\theta_{O.2}$ = the oil temperature rise at the present time step, *t*2,

$\theta_{O.1}$ = the oil temperature rise at the previous time step, *t*1,

Δt = the time step,

τ_0 = the oil thermal time constant,

$\theta_{HS.U}$ = the ultimate hot spot temperature rise over oil,

$\theta_{HS.R}$ = the rated hot spot rise over oil,

n = an exponent, generally between 1.6 and 2.0 (default 1.8),

$\theta_{HS,2}$ = the hot spot rise over oil at the present time step, *t*2,

$\theta_{HS,1}$ = the hot spot rise over oil at the previous time step, *t*1,

τ_w = the winding thermal time constant (default 5.0 min),

$T_{HS,2}$ = hot spot temperature at the present time step, *t*2,

T_A = the ambient temperature.

The short-time overload for oil-filled circuit breakers can be determined by using the following expressions [40]:

$$I_s = I_I \left[1 + \left(\frac{\theta_{HS} - \theta_a - Y}{\left(1 - e^{t_s / G} \right) Y} \right) \right]^{1/n} \tag{2.9.23}$$

and

$$Y = \left(\theta_{HS} - 40^{\circ}C \right) \left(\frac{I_I}{I_R} \right)^n \tag{2.9.24}$$

where:

I_s = short-time permissible overload,

I_1 = initial current prior to overload,

G = thermal time constant,

t_s = allowable short-time period,

n = an exponent, generally between 1.5 and 2.0 (default 1.8).

Figure 2.9.6 displays a summary of temperature limitations for circuit breakers used to determine continuous thermal and short-time overload ratings.

Component	Temp rise limit, C	Hottest-spot limit, C
Parts handled by operator*	10	50
Copper contacts; copper to copper conducting joints; external surfaces accessible to operator*; external terminal connected to bushing	30	70
Top oil	40	80
Terminals to be connected to 85C insulated cable	45	85
Hottest-spot temperature of parts where they contact oil, silver (or equal) contacts or conducting joints in oil	50	90
Silver (or equal) contacts or conducting joints in air, hottest spot of bushing conductor or metal parts in contact with class A insulation or with oil, hottest-spot winding temperature rise of current transformer with 55C rise	65	105
External surfaces not accessible to operator*	70	110
Hottest-spot winding temperature of 80C dry-type current transformer	110	150

Figure 2.9.6: Temperature limits for oil circuit breakers [40]

SF_6 circuit breakers are unique and do not use oil for cooling. SF_6 gas circuit breakers are superior to oil circuit breakers and are the preferred choice for protection of new transmission networks. A major economic advantage of SF_6 breakers is that they

require less maintenance than oil circuit breakers and have better switching and thermal properties. The IEC 62271-1 standard [54] specifies temperature rise limits and maximum operating temperatures for SF6 circuit breakers. Figure 2.9.7 displays an excerpt from the IEC standard and summarises the maximum operating temperature and temperature rise limits.

	Maximum temperature °C	Maximum temperature rise (Ambient temperature 40 °C.) K
Contacts in SF_6 (silver-plated or bare copper)	105	65
Connections in air (bolted or equivalent) (Bare copper, bare copper alloy, bare aluminum alloy)	90	50
High voltage terminals		
Bare	90	50
Silver or tin-coated	105	65

Figure 2.9.7: Temperature limits for SF6 circuit breakers [54]

The thermal model used to determine the thermal rating of a SF_6 circuit breaker is defined by [11] as:

$$\theta_U = \theta_R \left(\frac{I_2}{I_R} \right)^n \tag{2.9.25}$$

and:

$$\theta_2 = T_A + \theta_1 + (\theta_U - \theta_1)(1 - e^{-\Delta t/\tau}) \tag{2.9.26}$$

where:

θ_U = ultimate temperature rise,

θ_R = rate temperature rise,

I_2 = breaker current at time step, *t*2,

I_R = rated current,

n = exponent, generally between 1.6 and 2.0 (default 1.8),

θ_2 = contact temperature rise at present time step, *t*2,

T_A = actual ambient temperature,

θ_1 = contact temperature rise at previous time step, $t1$,

Δt = time step,

τ = thermal time constant (default 5.0 min).

2.9.1.6 Air core reactor

The on-going trend of increasing transfer capacity of existing power systems, especially by thermal uprating, led to the change of operational requirements of power equipment. An air core reactor is a device used in a transmission network for power system compensation. Compensation is used to increase and improve voltage quality, regulate voltage magnitude and enhance the system stability of the network. As explained in Section 2.3.6 reactors are used to reduce line over-voltages by consuming reactive power while shunt capacitors are used to boost voltage levels.

Air core reactors are generally used for:

- Compensation in power networks, e.g. to off-set the capacitive charging current during light loaded conditions;
- Reactors for capacitor banks;
- Smoothing reactors;
- Used for harmonic filtering in filtering reactors;
- Neutral grounding reactors; and
- Fault current limiting.

The rating of reactors is governed by international IEC and ANSI standards. The hot spot temperature rise of air core reactors is a function of the conductor in contact with the insulation material or encapsulation material. Operating temperature limits are generally dependent on the insulation material, as is the case with the majority of power equipment. Table 2.9.3 summarises specific operating temperature limits for air core reactors.

Table 2.9.3: Operating temperature limits for air core reactors [11]

Insulation Temperature Index (°C)	Average Winding Rise by Resistance (°C)	Hottest-spot Winding Temperature Rise (°C)
105	55	85
130	80	110
155	100	135
180	115	160
220	140	200

Advanced design and manufacturing of power equipment led to the innovative design of the air core reactor. In addition, dry-type air core reactors form part of the new generation of reactors and do not utilise oil for insulation or cooling. They are virtually maintenance free and have the benefit of having a low fire risk due to the absence of oil. Air core reactors can facilitate the highest voltage and power levels, making them attractive for thermal uprating. However, no specific thermal model is outlined in applicable standards. EPRI (Electric Power Research Institute) developed a simple thermal model to determine the ultimate winding hot spot temperature and is defined by [11] as:

$$\theta_U = \theta_R \left(\frac{I_2}{I_R} \right)^{2n} \tag{2.9.28}$$

where:

θ_U = the ultimate winding hot spot temperature rise,

θ_R = the rated winding hot spot temperature rise,

I_2 = winding current at present time step, t_2 ,

I_R = the rated current,

n = a predetermined exponent, generally between 0.7 and 1.0.

I_2 is increased during thermal uprating that will increase θ_U . Increases in transfer capacity can be satisfied by determining higher winding hot spot temperatures with minimal loss of insulation. In addition, the hotspot temperature T_2 is a function of the ambient temperature and the temperature rise θ_2 and is defined by [11] as:

$$\theta_2 = \theta_1 + (\theta_U - \theta_1)(1 - e^{\frac{-\Delta t}{\tau}}) \quad (2.9.29)$$

and

$$T_2 = T_A + \theta_2 \quad (2.9.30)$$

where:

θ_2 = winding hot spot temperature rise at present time step, t_2,

θ_1 = winding hot spot temperature rise at the previous time step, t_1,

Δt = time step,

τ = winding thermal time constant,

T_A = the ambient temperature,

T_2 = winding hot spot temperature at the present time step, t_2.

2.9.1.7 Line traps

Power utilities use their high voltage transmission systems for the transmission of power carrier signals. Power line carrier technology is used to transmit carrier signals between 30 kHz and 100 kHz. Power line carrier signals are generally used for protection signals over transmission lines. It can also be used for data and speech between power stations, sub-stations and system control centres. Line traps are used in high voltage transmission systems to provide known blocking impedances to the carrier signals, for all power conditions. The signals are then diverted to the tele-protection or the telecommunications panel for processing. The line trap is mounted in series the station busbar and in series with the transmission circuit and is designed to be exposed to the system voltage, the maximum continuous load current and to high levels of fault current.

.

Line traps must generally operate under the following conditions:

- Outdoors (exposed to harsh environmental conditions);
- At an altitude above sea level up to 1800 m;
- At the following ambient air temperatures:
  - — Maximum temperature of 40 °C
  - — Daily average temperature of 30 °C

— Yearly average temperature of 20 °C
— Minimum temperature of –10 °C
— Maximum diurnal temperature variation 35 °C;

- Severe incidence of lightning induced overvoltages.

The temperature rise limits for line traps varies between manufactures. Table 2.9.4 summarises and compares various temperature rise limits as well as maximum operating temperatures of line traps from a sample set of manufacturers.

Table 2.9.4: Recommended temperature limits for substation line traps [11]

Line trap manufacturer	Limit of temperature rise for rated continuous current (K)	Normal maximum temperature (°C)
GE type CF (1954-1965)	90	130
Trench type L	110	150
Westinghouse type M	110	150
GE type CF (after 1965)	115	155

The temperature rise of any part of the line trap under rated continuous current shall not exceed the limits specified by the manufacturer. The temperature rise limit is determined by the ambient conditions and the loading current. Temperature rises in excess of 150 K may be adopted and agreed upon between manufacturer and the user.

Changing operating conditions in the electricity supply industry led to the recognition that various designs of line traps are required to suit the specific needs of a power utility. Operating conditions, which include different voltage limits, normal, continuous and emergency load currents, led to the formation of basic ratings methods based upon line trap capabilities, utility operating procedures, environmental conditions and special conditions [55].

Rating methods for line traps are generally developed based upon the following criteria [55]:

- Ambient temperature θ_a,
- Temperature rise as a function of the square of the current,
- Maximum temperature determined to be acceptable for various line traps under normal and emergency conditions,
- Acceptable loss of life and insulation, and
- Line trap short circuit withstands capability for emergency conditions.

It is possible to determine normal and emergency ratings for line traps. The normal rating I_n of a line trap reflects the continuous current without the line trap exceeding its normal allowable maximum operating temperature. The emergency rating I_e of a line trap is the current, which can be carried for a specified time without the line trap exceeding its emergency allowable maximum temperature. The thermal model used to determine the normal rating of a line trap is defined by [55] as:

$$I_n = I\left(\frac{\theta_{\max n} - \theta_a}{\theta_r}\right)^{\frac{1}{n}} \tag{2.9.32}$$

where:

I_n = normal current rating,

I = adjusted rated continuous current,

θ_a = ambient temperature,

$\theta_{\max n}$ = normal maximum allowable temperature,

θ_r = limit of temperature rise at rated continuous current,

n = pre-determined exponential value between 1.8 and 2.0.

The emergency thermal model is defined by [55] as:

$$I_e = I\left(\frac{\theta_{\max_{e24}} - \theta_a}{\theta_r}\right)^{1/n} \tag{2.9.32}$$

where:

I_{e24} = emergency rating of greater than 24-hours duration,

θ_r = limit of temperature rise at rated continuous current,

$\theta_{\max_{e24}}$ = emergency allowable maximum temperature.

Line traps are designed within temperature rise limits to permit optimal life expectancy. Higher operating temperatures in excess of the recommended manufacturer values may shorten the life expectancy of the line trap. However, it is possible to determine short-time overloads for line traps with a maximum ambient temperature of 40 °C. It is assumed that the line trap has reached its full load temperature under these ambient conditions. Figure 2.9.8 displays rated current graphs for the line traps as a function of the overload capability and the time the overload is needed.

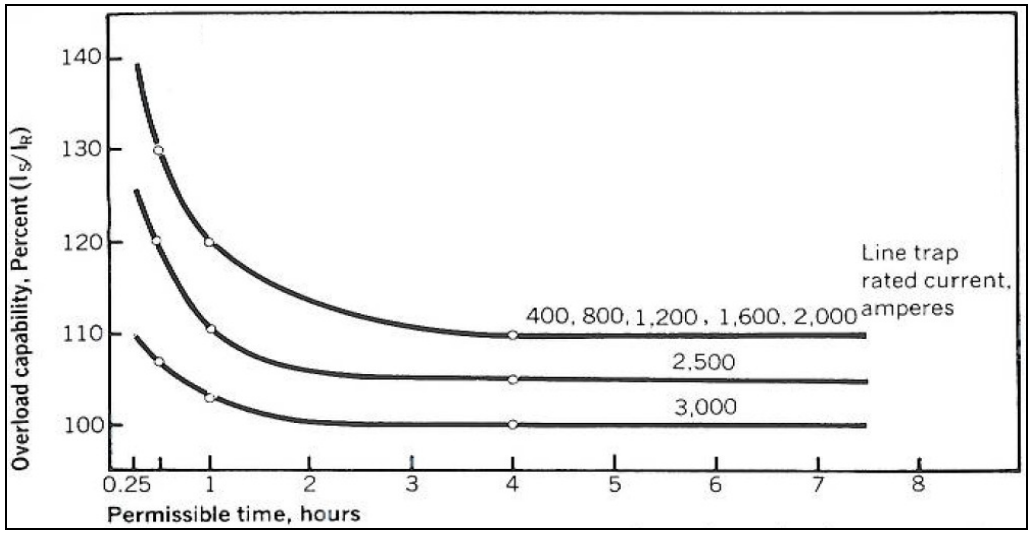

Figure 2.9.8: Short-time overload curves based on the rated continuous load current [40]

The continuous load current capability at a given actual ambient temperature without exceeding the maximum design limit is defined by [40] as:

$$I_p = I_r\left[\frac{(T_h - T_a)}{(T_h - T_o)}\right]^{0.5} \tag{2.9.33}$$

where:

I_p = capability at actual ambient temperature or the continuous loading capability,

I_r = rated continuous current,

T_h = maximum design temperature for different insulation classes,

T_a = actual ambient temperature,

T_o = design ambient temperature.

The criteria in this section can be used to determine short-time overloads for line traps.

For example, a short-time overload is needed for a line trap with a 2500 A continuous rating operating in a 30 ℃ ambient environment and with a maximum design temperature of 150 ℃. The overload is required for 30 minutes. The continuous loading I_a of the line trap is determined by equation (2.9.33):

$$I_a = 2500\left[\frac{(150-30)}{(150-40)}\right]^{0.5}$$
$$= 2611\,A$$

From Figure 2.9.8, a 30-minute overload allows for:

$$\frac{I_s}{I_a} = 120\%,\ I_s = (1.20)(2611) = 3133\,A,$$

The percentage overload capability for a 30-minute overload is:

$$\frac{I_s}{I_p} = \frac{3133}{2500} = 125\%\,.$$

2.9.1.8 Substation busbar conductors

The secure supply of electricity from power stations to load centres is only as reliable as the interconnecting transmission network and substations. Substation busses (bus bars) interconnect loads and sources via a complex arrangement of power equipment in a power system. Busbars are electrical conductors that allow for numerous power connections and current taps. A substation bus system must be designed and built to ensure electrical flexibility, reliability and power supply continuity [11]. Substation busses support large power flows and are subjected to very high thermal and abnormal electromechanical stresses. Three common types of busbars used in substations are:

- Rigid bus – an aluminium, copper or copper alloy bar (normally tubular), which is supported by insulators and used in a low, medium or high voltage environment.
- Strain bus – stranded aluminium wires with a steel wire core (ACSR) usually identical to stranded conductor used in overhead transmission lines. Generally under tension and used in high voltage environments.
- Jumper bus – stranded aluminium wires (AAC or AAAC) not under tension.

Some important items to consider when determining the thermal rating of substation bus conductors are:

- Current carrying capacity,
- Thermal expansion,
- Allowable voltage drop,
- Short circuit current rating, and
- Conductor strength.

The rating of substation bus conductors is based on temperature rise limits above a 40 °C ambient. The thermal model used for substation bus conductors is similar to that of overhead lines. The steady state temperature of substation bus conductors is defined by the heat input and output given by [11] as:

$$I^2RF + q_S = q_C + q_r + q_{cond} \tag{2.9.34}$$

where:

I^2 = current for allowable temperature rise,

F = skin-effect coefficient,

R = direct current resistance at the operating temperature (Ω/m),

q_s = solar heat gain (W/m),

q_C = convective heat loss (W/m),

q_r = radiative heat loss (W/m),

q_{cond} = conductive heat loss (W/m).

By re-arranging the expression in (2.9.34) the current for a given conductor temperature rise is obtained:

$$I = \sqrt{\frac{q_C + q_r + q_{cond} - q_S}{RF}} \qquad (2.9.34)$$

2.9.2 **Summary of substation terminal equipment**

A substation is a complex system consisting of many interconnected power equipment items and requires large amounts of capital investment. Power utilities want to maximise their return on capital investment and simultaneously increase revenue. One possibility is to increase the loading and transfer capacity of existing assets by increasing current flow through existing transmission circuits. The loss of life and insulation of substation equipment is of major concern when operating substation equipment at higher loading and operating temperatures. This chapter reviewed the literature to identify methods to increase the current and electrical transfer, in transmission lines and terminal equipment whilst remaining within all criteria of safety.

2.10 CONCLUSION

There is an operational need to operate existing transmission circuits safely and reliably at higher loadings. The thermal rating of transmission lines and substation

equipment can be safely increased to alleviate demand in highly congested networks while maintaining system reliability. The literature presented in this dissertation demonstrates best practices to increase power transfer of existing transmission line assets by means of a non-intrusive method. The knowledge obtained in the literature review can now be used, in the next chapters, to investigate several existing transmission lines and terminal equipment on the possibilities to increase the electrical current to higher levels.

.

Chapter 3
Transmission line profile modelling

The modelling of transmission lines in a three-dimensional field by means of implementing in flight light detection and ranging (LIDAR) data together with actual load and meteorological data is explained in detail in this chapter. Initially a brief introduction on transmission line modelling is given. The 3D modelling of transmission lines will assist designers and system operators to do conclusive sag and clearance analysis on overhead line bare conductors. In addition to the load and weather data, the conductor temperature is also measured during flight by means of temperature sensors that are installed on the conductors. The LIDAR data will enable engineers to establish a representative "as is" model of the transmission line that was surveyed. Furthermore, the transmission line model will include accurate information on the towers, ground wires, transmission line hardware and the exact catenary and position of the conductor in space. The 3D CADD (computer aided design and drafting) model will then be calibrated to allow users to graphically sag and raise the conductor to different positions by means of changing the conductor temperature. Through this method the permissible sag of the conductor for templating, normal and emergency ratings can be established. Subsequently the method is implemented to identify and address any infringements on conductor-to-ground clearances that might occur if current transfer is increased.

3.1 INTRODUCTION

Three-dimensional transmission line modelling is a method used to establish whether the transmission line is capable of carrying additional load. A computer package (PLS CADD) is used to model lines in a three dimensional field by implementing existing terrain information obtained from remote sensing and geospatial technology. In this chapter, the necessary steps towards modelling transmission lines are discussed. Three individual PLS CADD models were created. One for the Jupiter – Prospect line, one for the Apollo – Croydon line and one for the Esselen – Jupiter line. The Jupiter – Prospect line is used during this chapter to illustrate the transmission line profile modelling that was performed in PLS CADD. The same methodology was used to model the other two lines and therefor the modelling of the Apollo – Croydon and the Esselen – Jupiter line is omitted from the discussion in this chapter. However, the transmission line profile modelling of the Apollo – Croydon and the Esselen – Jupiter line is both included in Annexure B and C.

The overall concept behind PLS CADD is illustrated in Figure 3.1.1. The Figure illustrates that the 3D model includes the terrain, structures, and obstacles within the right of way as well as libraries including any other design criteria, which are stored in the library file. PLS CADD also allows for the easy calculation of any sag, conductor tension and clearances.

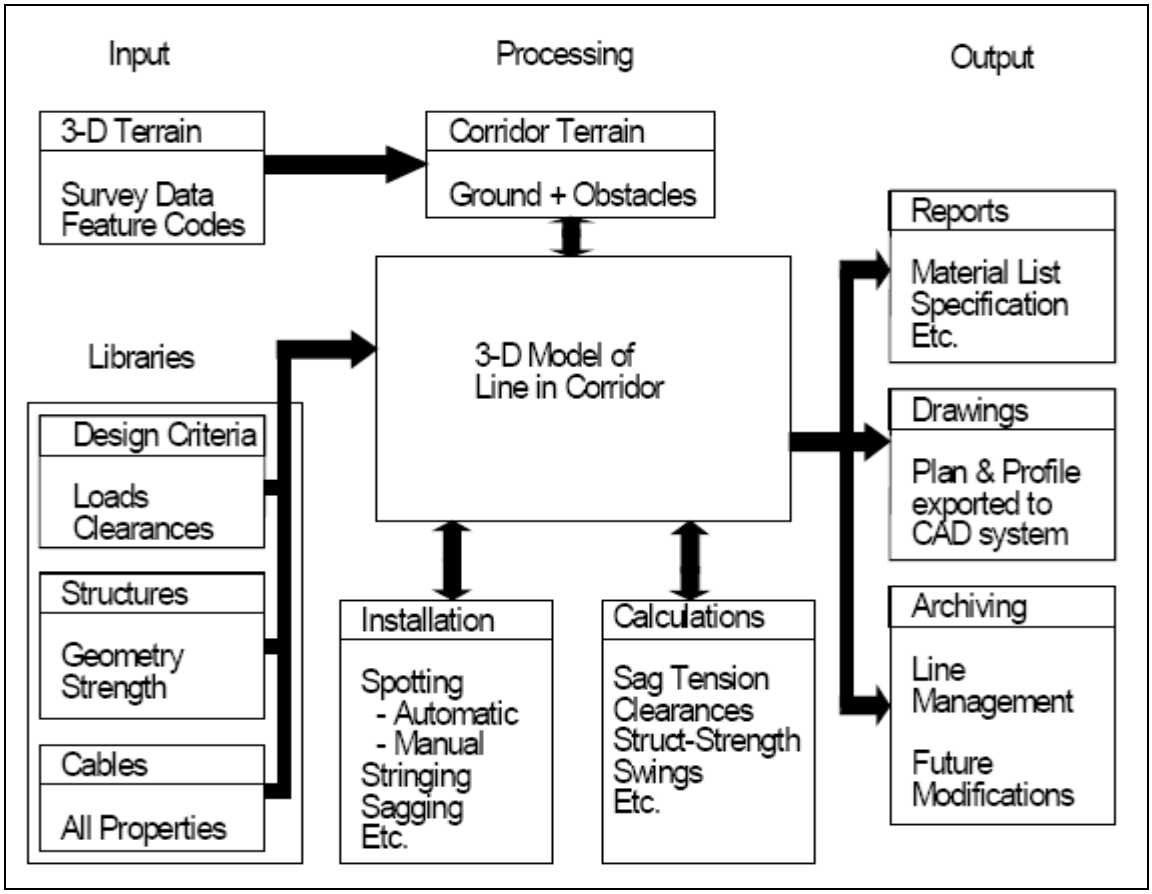

Figure 3.1.1 Flow diagram of the overall 3D line design in PLS CADD [38]

3.2 MODEL DEVELOPMENT

The following section will discuss the profile modelling of the Jupiter – Prospect 275 kV transmission line. The profile model will be created from LIDAR data as input.

3.2.1 **Jupiter – Prospect 275 kV transmission line model**

Building a three-dimensional line model involves three basic steps: a) loading a terrain model and defining the alignment, b) spotting the structures, and c) stringing and sagging the conductors [38]. At the beginning of every new PLS CADD project the engineer has to decide if existing transmission line information, such as feature codes, design criteria, towers and conductor information stored in library files, is suitable to model the line that was surveyed, or must the files be created. For the purpose of this research, all library files had to be created as they did not exist.

The first step is to import the terrain data into the design software package, assign the correct required clearance voltage, and feature code data. Once the terrain data are imported, the terrain widths and side profile criteria must be selected and assigned. For this specific simulation a voltage of 275 kV was used. Table 3.2.1 display the feature code file where various clearances for a 275 kV power line are defined. Each data point within the surveyed right of way is grouped together, for instance existing vegetation, power lines, water hazards, buildings, power lines bend points, telecommunication lines and railways. A special feature code number is then assigned to each group that allows for easy data management during the modelling stage. It is generally a good idea to maintain a master feature code file in a situation where more than one transmission line is modelled.

The feature code file in table 3.2.1 defines a symbol and number for each group of data points. Additionally a description is assigned to each plot point within the feature code file. For instance:

- grounds points or ground profile are displayed in red dots,
- vegetation in green dots,
- clearance lines with a dotted line,
- Water course or rivers with a blue triangle.
- 275 kV power lines and structures with a dense cloud of pink points etc.

The feature codes can be changed at any stage during the modelling or additional feature codes can be assigned to the data. The feature code file is used to distinguish between the various data obtained from the LIDAR survey. Once the raw data is imported into PLS CADD the feature codes are assigned and a visual imagery is given to the data. The visual imagery is then used to model the transmission line.

Table 3.2.1 Master feature code file

	Feat. Code	Feature Description	Prof Symbol	Plan Symbol	Line From Feature Top To Bottom	Aerial Obst-acle	Point is on Ground	Req Vert Clear 0kV (m)
18	101	WATER COURSE/RIVER - EDGE	▲	▲	No	No	Yes	5.9
19	102	Navigable WATER	△	△	No	No	Yes	18.4
20	132	132kV power line	✳	✳	No	Yes	No	2.4
21	200	Ground points	·	·	No	No	Yes	5.9
22	220	220kV power line	✳	✳	No	Yes	No	3.1
23	275	275kV power line	✳	✳	No	Yes	No	3.5
24	400	400kV power line	✳	✳	No	Yes	No	4.2

Figure 3.2.1 displays the sophisticated three-dimensional view of the Jupiter – Prospect line that was modelled. The model includes a 3D view of the terrain, power lines, wire positions and structures. The 3D view allows for the easy alignment of the LIDAR points with the superimposed designed model. The 3D visual imagery is obtained by assigning a symbol pre-defined in the feature code file as previously explained. The dense cloud of pink points provides an image of the structure 5 and 6 of the Jupiter – Prospect line and the plot points are defined in table 3.2.1.

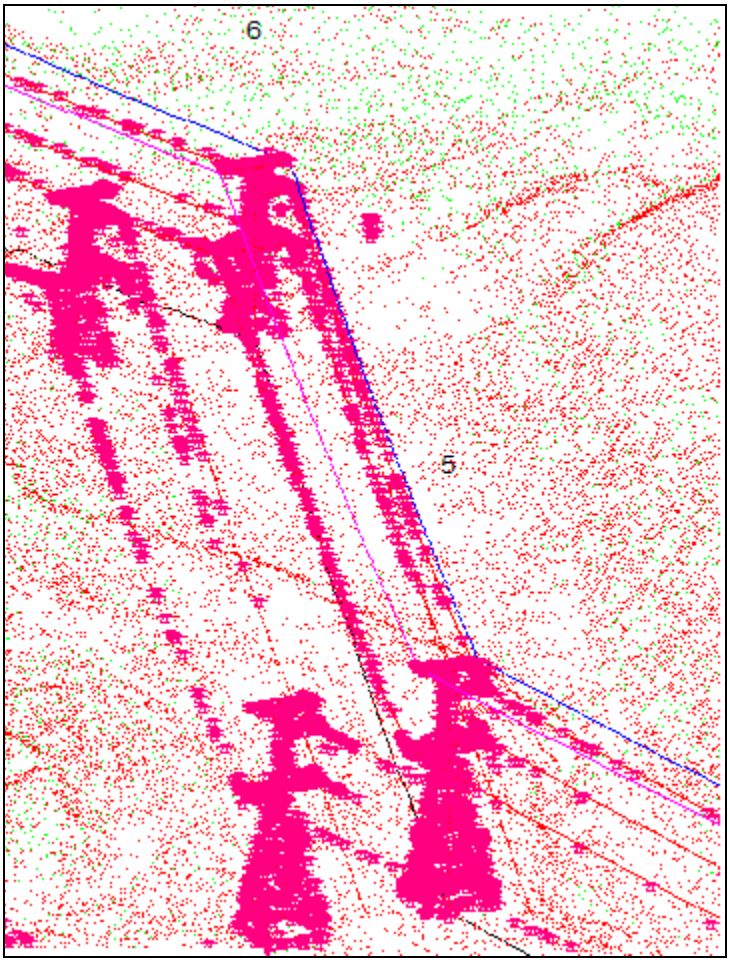

Figure 3.2.1 PLS CADD three dimensional image of the Jupiter – Prospect line

PLS CADD has a flexible engineering environment with functions that is easily adapted to the power utilities' design requirements. IEEE and CIGRE engineering standards form the basis for advanced three-dimensional transmission line modelling. Sag, tension and conductor-to-ground clearances are easily obtained by means of built-in sag-tension routines. The modelled line can be quickly adapted for different weather cases that have an influence on the conductor sag, insulator swing and blowouts. In addition, spacing between conductors and between phases can also be calculated under any weather conditions.

The next step in the modelling process is to define the correct alignment of the terrain data. In addition, the centreline [38] of the project is also defined. Figure 3.2.2 displays the concept of alignment and centreline for the 275 kV Jupiter-Prospect transmission line. The alignment of the model consists of straight-line sections between the points

of inflection (PI points) of the corridor. The same principle applies for the rest of the lines studied during this research.

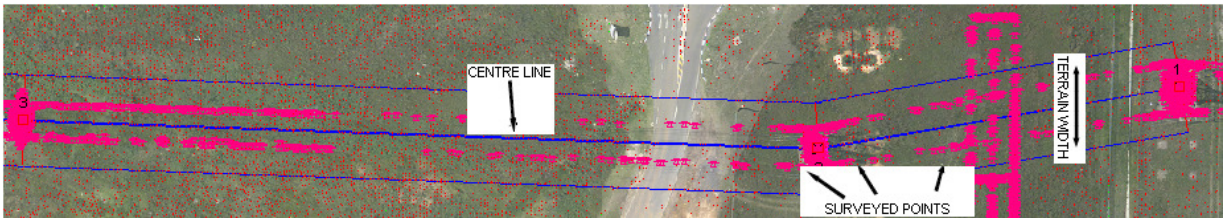

Figure 3.2.2: Plan view displaying concept of alignment, surveyed points, terrain width and centre line

The second step in the modelling process is to create the transmission towers from geometry or existing tower drawings. Transmission towers are classified as strain towers or suspension towers. A strain tower is where a conductor is terminated by dead end joints on a string of one or more horizontal insulators. A suspension tower is generally used in straight-line corridor sections. On a suspension tower the conductor passes through and is suspended from the tower by means of one or more strings of insulators arranged to create an suspension assembly. Towers or structures can be located or moved around the terrain data. The geometry of the structure is entered in a structure file. A typical structure file is displayed in Figures 3.2.3 and 3.2.4. The files contain information on the tower geometry that includes structure height, insulator weight and conductor attachment heights. After the structures are created, they are superimposed on terrain data.

Structure Data Editor

Structure file name g:\eskom\projects\275 kv line uprating\d...\424n 4 bear.122
Description strain tower 424 N
Height (ground to top of structure) (ft) 75.13
Embedded length (for report purposes only) (ft)
Lowest wire attachment point height above ground (ft) 41.14

	Set #	Phase #	Dead End Set	Set Description	Insulator Type	Insul. Weight (lbs)	Insul. Wind Area (ft^2)	Insul. Length (ft)	Attach. Trans. Offset (ft)	Attach. Dist. Below Top (ft)	Attach. Longit. Offset (ft)	Min. Req. Vertical Load (uplift) (lbs)	Allowable Suspension Swing Angles and 2-Part Load Angles min,max for 4 conditions (deg)
1	1	1	Yes	gw1	Clamp	NA	NA	NA	-10.99			No Uplift	NA
2	2	1	Yes	gw2	Clamp	NA	NA	NA	10.99			No Uplift	NA
3	3	1	Yes	c1	Strain				-13.94	12.01		No Uplift	NA
4	3	2	NA	NA	Strain				-13.94	33.99		No Uplift	NA
5	3	3	NA	NA	Strain				13.94	33.99		No Uplift	NA

Figure 3.2.3: Structure file for a strain tower

Structure Data Editor

Structure file name g:\eskom\projects\275 kv line uprating\d...\424a 4 bear.152
Description suspension tower 424 A
Height (ground to top of structure) (ft) 84.22
Embedded length (for report purposes only) (ft)
Lowest wire attachment point height above ground (ft) 49.99

	Set Description	Insulator Type	Insul. Weight (lbs)	Insul. Wind Area (ft^2)	Insul. Length (ft)	Attach. Trans. Offset (ft)	Attach. Dist. Below Top (ft)	Insul. Length Side 2 (ft)	Attach. Trans. Offset Side 2 (ft)	Attach. Dist. Below Top Side 2 (ft)	Attach. Longit. Offset Side 2 (ft)	2-Part Tension Only Side 1	2-Part Tension Only Side 2	2-Part Bottom Right
1	gw1	Clamp	NA	NA	NA	-8.99		NA	NA	NA	NA	NA	NA	NA
2	gw2	Clamp	NA	NA	NA	8.99		NA	NA	NA	NA	NA	NA	NA
3	c1	2-Part			12.47	-20.51	3.94	12.47	-2.46	3.94		Yes	Yes	Yes
4	NA	2-Part			12.47	-20.51	25.62	12.47	-2.46	25.62		Yes	Yes	Yes
5	NA	2-Part			12.47	20.51	25.62	12.47	2.46	25.62		Yes	Yes	Yes

Figure 3.2.4: Structure file for a suspension tower

The third step in the modelling process involves creating the wire system between sections. The wire system includes conductors, ground wires and overall 3D geometry. The modelling of the wire system involves superimposing a single wire representative of a conductor bundle between strain sections over LIDAR data. A transmission line generally consists of three phase conductors with two shield (ground) wires suspended at the top of the tower to shield against lighting and to carry fault currents. Wind load, ice load and phenomena that generate longitudinal forces and conductor blow out were ignored from the scope of this modelling.

It is very important to define the correct characteristics of the conductor in a cable file. A cable file includes essential data on the properties of the conductor as displayed in Figure 3.2.5. The following data are stored in the cable file [38]:

- A description of the conductor obtained from the manufacturer,
- The stock number of the conductor suitable for future use in design reports,
- The total cross-section area, including core and outer strands of the conductor,
- The outside diameter of the conductor,
- The weight per unit length of bare conductor,
- The ultimate (rated) conductor mechanical tension,
- The number of separate cables in a group of wires,
- The temperature at which the polynomial coefficients and data were obtained,
- The final modulus of elasticity of outer and inner conductor strands,
- The thermal expansion coefficient of outer material and inner strands,
- The stress-strain polynomial coefficients for both the outer and inner strands,

- The creep polynomial coefficients for both the outer and inner strands,
- The final modulus of elasticity of core material,
- The thermal expansion coefficient of core material,
- The stress-strain polynomial coefficients of core material,
- The core stress-elongation,
- The creep polynomial coefficients of core material,
- The behaviour for temperatures above the transition point,
- The thermal Rating Properties,
- The resistances at two temperatures,
- The emissivity coefficient,
- The solar absorption coefficient,
- The outer strands' heat capacity, and
- The core heat capacity.

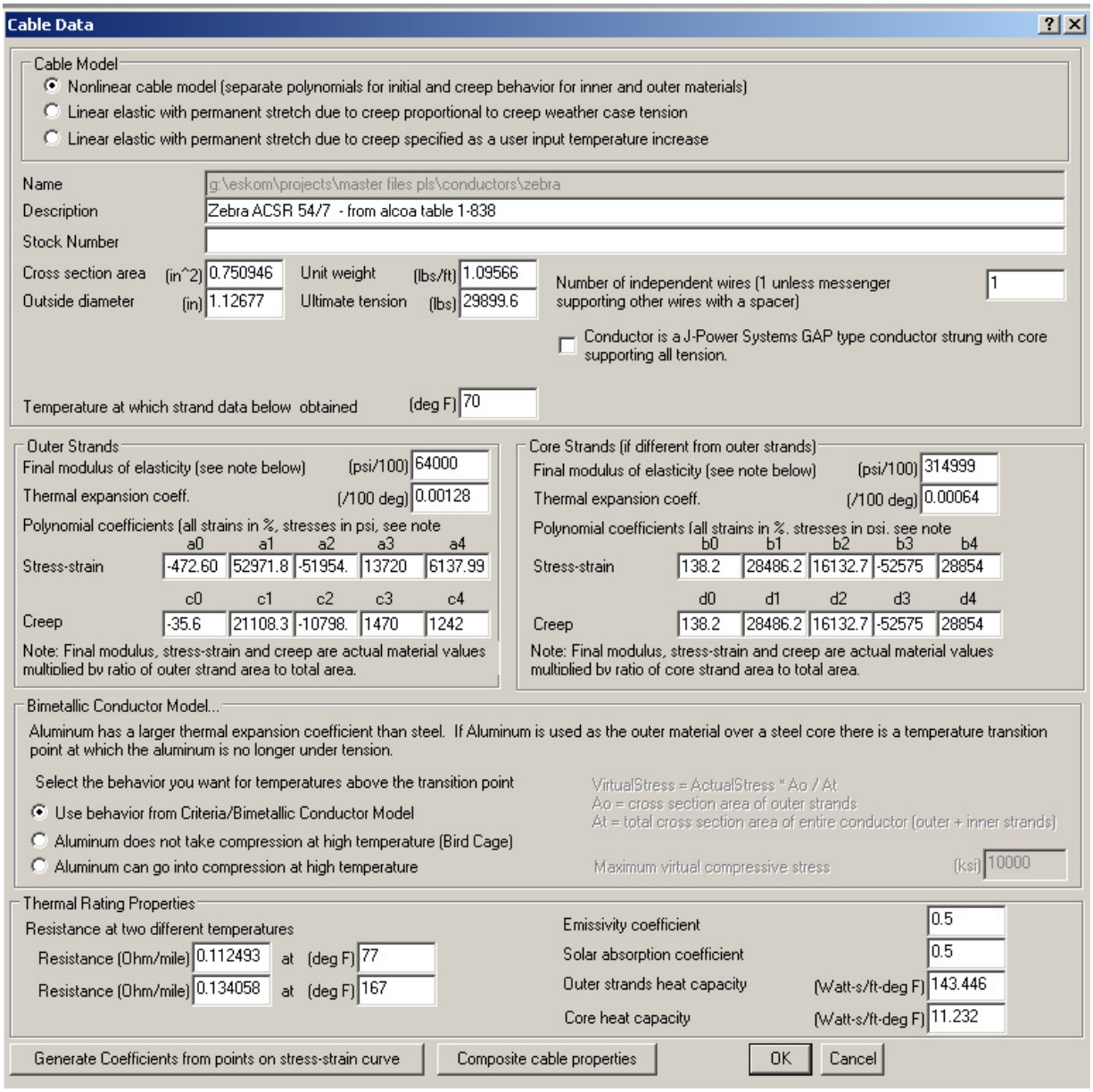

Figure 3.2.5: Cable file for zebra conductor

Once the conductor files and cable criteria are prepared it is possible to string the phase conductors. The characteristics of shield wires are defined in a similar cable file. Conductors are strung between strain towers of a transmission line. By using the add section functionality in PLS CADD, conductors can be added to towers. Once the function is selected, a dialogue box as displayed in Figure 3.2.6 will appear and the software will detect that the user has selected a strain tower. The conductor will then automatically be attached to the selected tower and by sequentially moving from one tower to the next the conductor will be attached to the attachment positions created in step 2. The same procedure applies for the remaining phases and ground wires.

Within the dialogue box in figure 3.2.6 various information of the conductor is included for instance the number of conductors in the bundle is specified, the voltage level, creep conditions as well as the temperature at which the conductor is initially stringed before calibration.

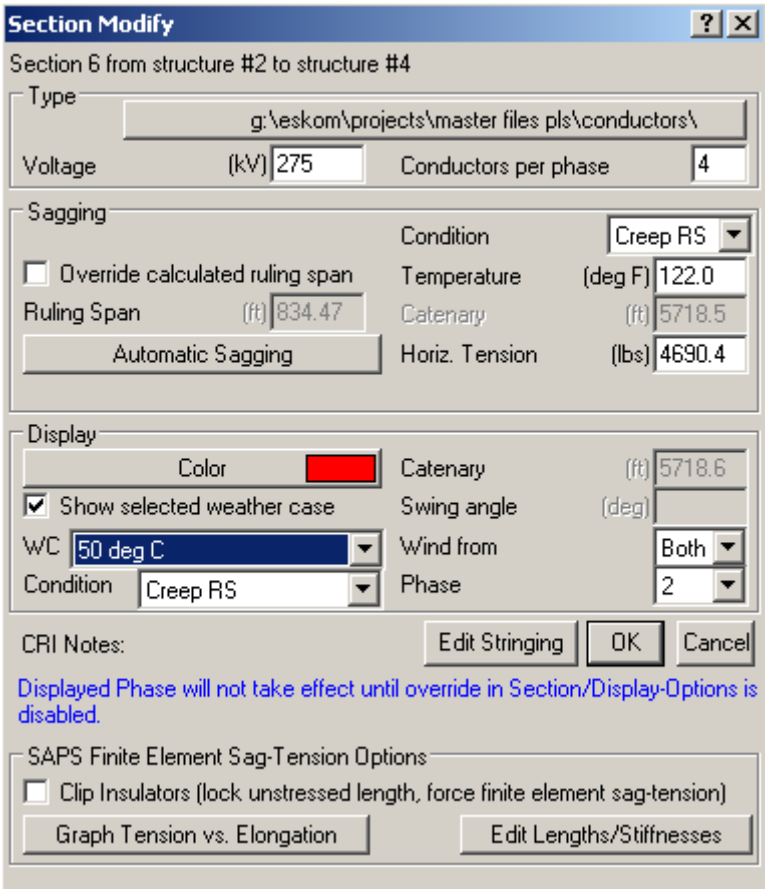

Figure 3.2.6: Dialogue box displaying information of a strung span

Once the entire corridor is strung, the automatic sagging function is implemented. The function specifies a sufficient number of conditions so that the computer can determine what the unstressed length of cable in each span at 0 °C is under no electrical loading. Figures 3.2.7 and 3.2.8 display the result of the automatic sagging function. The temperature of the conductor is automatically set as 0 °C. Then information on the ground profile, clearance line, ground wires and the conductor position during LIDAR survey is displayed. It is now possible to calibrate the model so that the newly strung conductors match the catenary of the conductor as during the LIDAR survey.

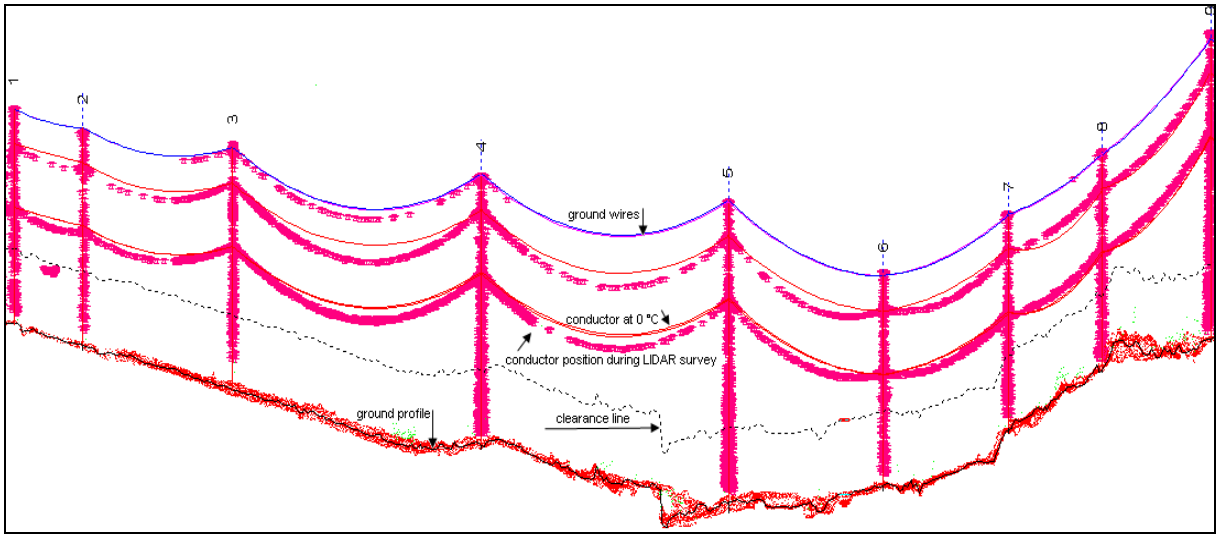

Figure 3.2.7: Profile view of spans 1 – 8

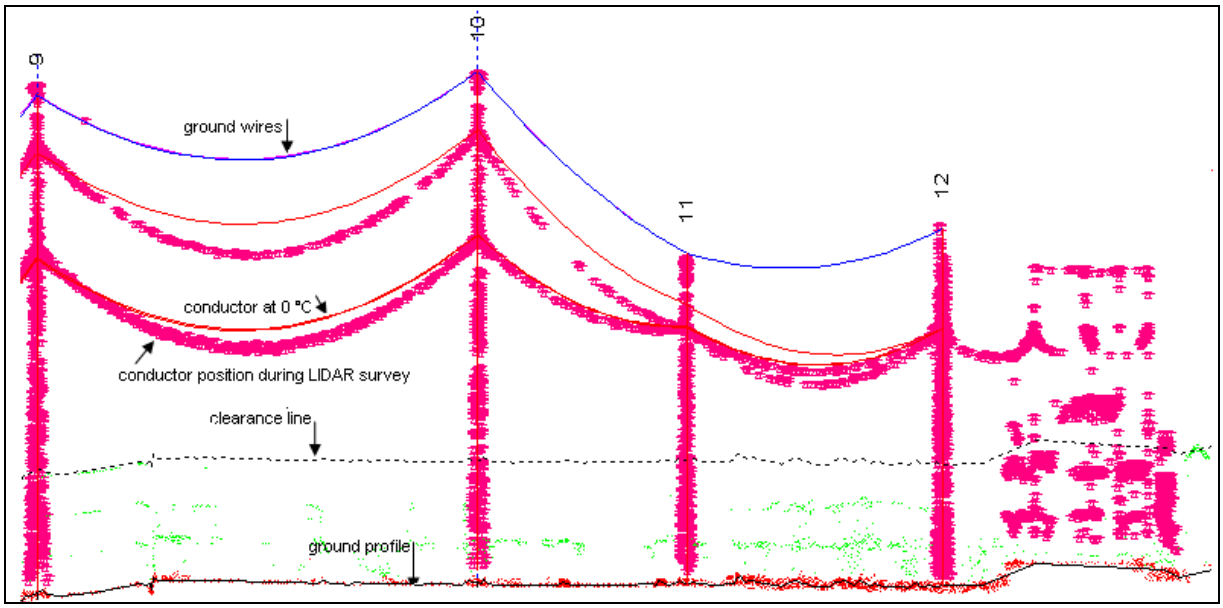

Figure 3.2.8: Profile view of spans 9 – 12

A transmission line is subjected to a given combination of weather conditions. These include wind speed, wind direction, solar radiation and ambient temperature. The weather conditions have to be defined to calibrate the PLS CADD model and to match the stringed conductors with LIDAR data. PLS CADD defines a combination of weather conditions as a weather case. All weather cases used during this modelling are described in the weather case table displayed in Figure 3.2.9 and include various weather cases needed for displaying the conductors at various operating temperatures.

Weather Cases

See Criteria/Code Specific Wind and Terrain Parameters for more information on height adjustments and gust response factors.

	Description	Air Density Factor (Q) psf/mph^2	Wind Velocity (mph)	Wind Pressure (psf)	Wire Ice Thickness (in)	Wire Ice Density (lbs/ft^3)	Wire Ice Load (lbs/ft)	Wire Temp. (deg F)	Ambient Temp. (deg F)	Weather Load Factor	NESC Constant (lbs/ft)	Wire Wind Height Adjust Model	Wire Gust Response Factor
1	EDT No Wind	0.00256	0	0	0	0	0	59.0	59.0	1	0	None	1
2	EDT Slight Wind	0.00256	31.2978	2.50626	0	0	0	59.0	59.0	1	0	None	1
3	-5 deg C	0.00256	0	0	0	0	0	23.0	23.0	1	0	None	1
4	20 deg C	0.00256	0	0	0	0	0	68.0	68.0	1	0	None	1
5	35 deg C	0.00256	0	0	0	0	0	122.0	122.0	1	0	None	1
6	40 deg C	0.00256	0	0	0	0	0	122.0	122.0	1	0	None	1
7	50 deg C	0.00256	0	0	0	0	0	122.0	122.0	1	0	None	1
8	60 deg C	0.00256	0	0	0	0	0	140.0	140.0	1	0	None	1
9	70 deg C	0.00256	0	0	0	0	0	158.0	158.0	1	0	None	1
10	75 deg C	0.00256	0	0	0	0	0	167.0	167.0	1	0	None	1
11	80 deg C	0.00256	0	0	0	0	0	176.0	176.0	1	0	None	1
12	High wind - Conduc	0.00256	90.349	20.8855	0	0	0	59.0	59.0	1	0	None	1
13	Moderate Swing	0.00256	31.2978	2.50626	0	0	0	59.0	59.0	1	0	None	1
14	Max Swing	0.00256	63.8864	10.4427	0	0	0	59.0	59.0	1	0	None	1

Figure 3.2.9: Weather cases for Jupiter – Prospect 275 kV

After defining the correct weather cases, it is possible to graphically sag the conductors. This functionality allows the engineer to match the position of the conductor with the LIDAR data. The PLS CADD model is calibrated with an operating temperature of 35 °C. The operating temperature was obtained from direct temperature measurement as the LIDAR survey took place. The method and sensors used for measuring the operating temperature are described in Section 2.8 of this dissertation. In addition, the measured conductor operating temperature is compared with the calculated operating temperature and is discussed in the subsequent chapter. When selecting the graphical sag function the user can select any predefined weather case at which the conductor must be sagged. The same functionality is used to raise the conductor. When selected, the phase conductors or shield wires will move interactively up and down with the cursor. Once the conductor position is matched with the conductor position of the LIDAR data with a measured operating temperature of 35 °C, the model is calibrated. This option is very useful as it is now possible to raise and sag the conductor at any operating temperature or loading condition.

Figure 3.2.10 displays the calibrated PLS CADD model for the Jupiter-Prospect 275 kV transmission line. Note that the conductors, ground wires and structures are superimposed over the LIDAR data. The exact method used to model and calibrate the Jupiter – Prospect 275 kV transmission line is implemented to model and calibrate

the Apollo - Croydon and Esselen – Jupiter lines. As previously explained the profile models of these two lines are displayed in Annexure B & C. Due to the repeatability of the modelling procedure it was only necessary to demonstrate the modelling of one line in this chapter.

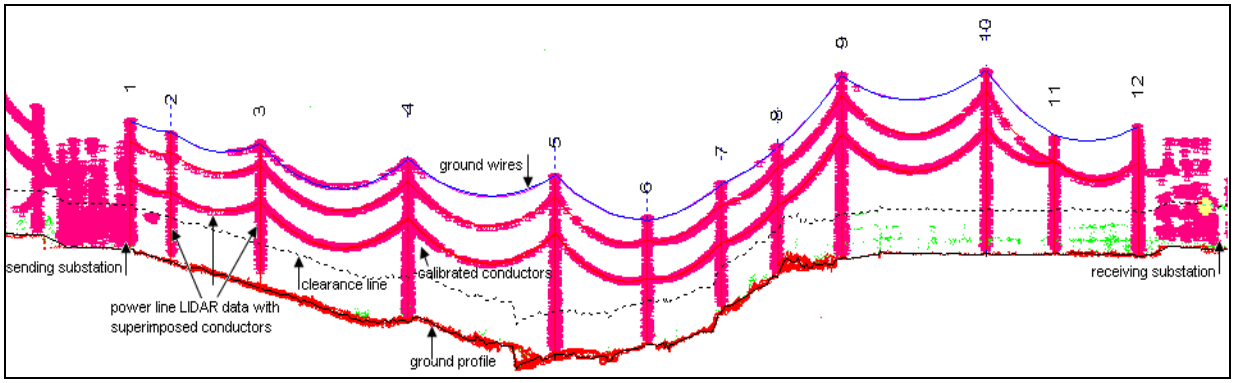

Figure 3.2.10: Profile view of calibrated PLS CADD model at an operating temperature of 35 °C

3.3 GRAPHICAL SAG ANALYSIS

This section will demonstrate the graphical sag analysis of the Jupiter – Prospect 275 kV transmission line by sagging the calibrated PLS CADD model at various operating temperatures. No under clearance issues or infringements were identified on the line, therefore it is possible to proceed to graphically sag or raise the conductor at various operating temperatures and conditions. The PLS CADD model was calibrated for 35 ℃, which enables the user to graphically sag the conductors accurately. The conductors are sagged at multiple temperatures with 10 ℃ intervals, starting at 25 ℃ and ramping up to the line design temperature of 75 ℃. By selecting different predefined weather cases in the section table of PLS CADD, the conductors automatically sag or rise. The conductors will only rise and increase ground clearance under low operating temperatures. Figure 3.3.1 displays the section table for the calibrated model. Selecting and sorting the information in the section table according to a cable file name will numerically sort all the spans from the first span to the last. This facilitates an easy selection of different weather cases for all the spans.

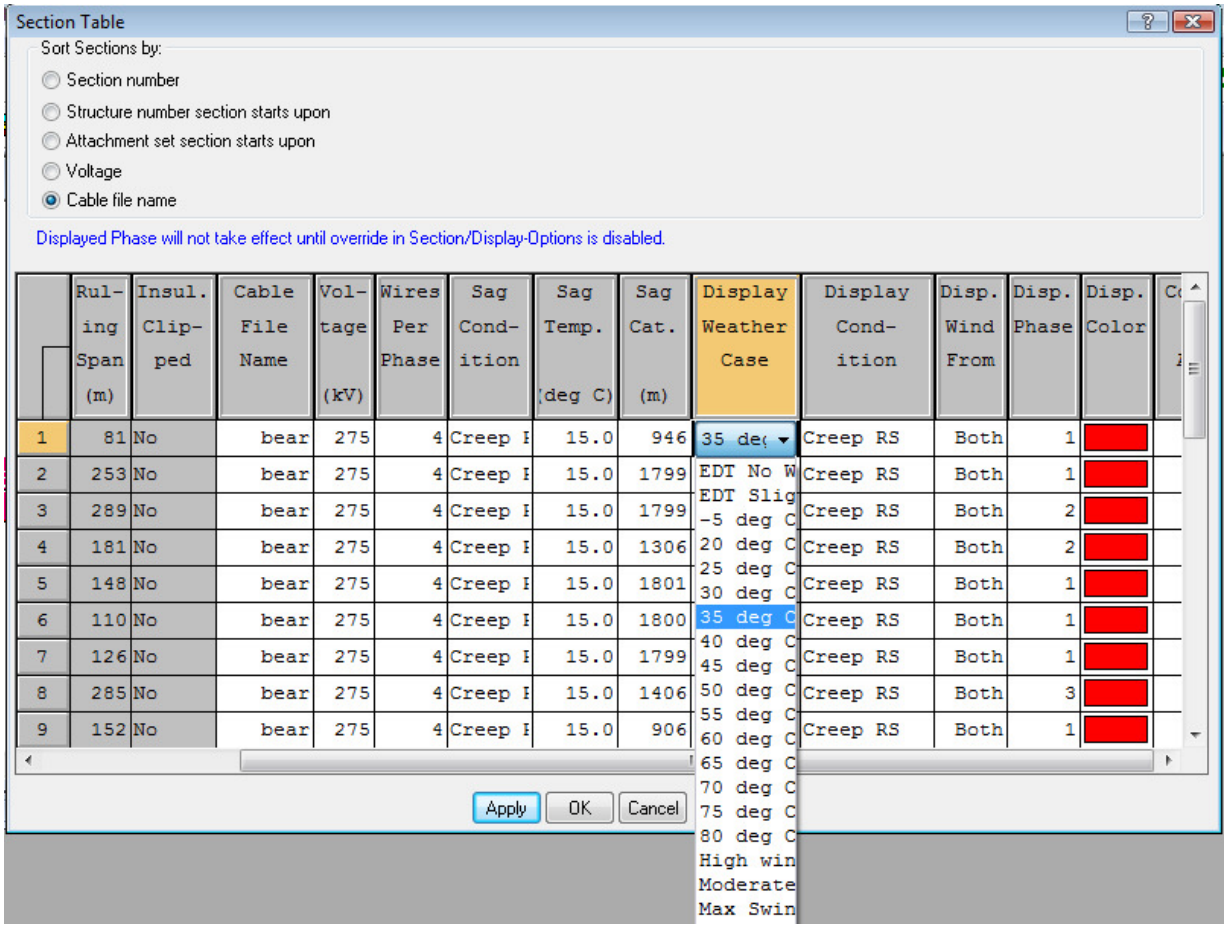

Figure 3.3.1: Section table displaying various weather cases

Figure 3.3.2 displays the graphical sag analysis when the operating temperature of the conductor is set at 25 ℃. Note that the conductor position raised as expected due to the lower operating temperature.

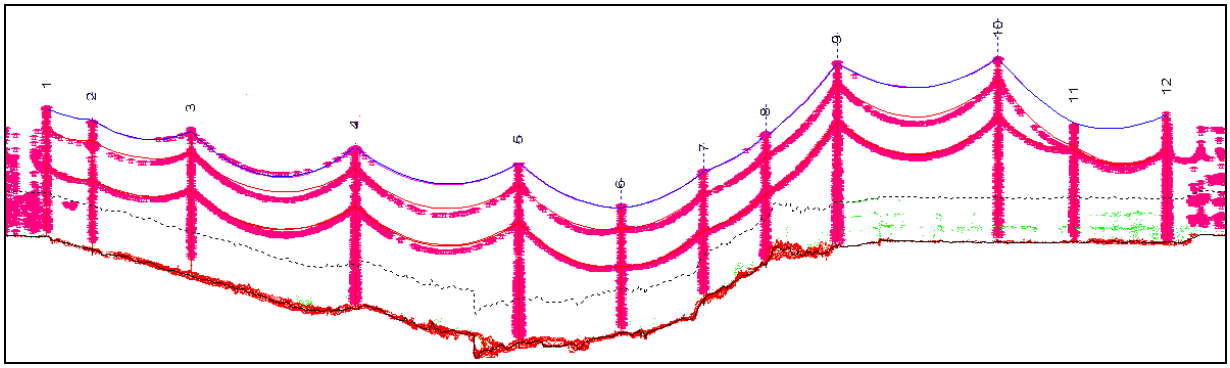

Figure 3.3.2: Conductor position at 25 °C

Following Figure 3.3.3, Figures 3.3.4 to 3.3.7 display the outcome in terms of clearance for the conductors when they are sagged at various operating temperatures.

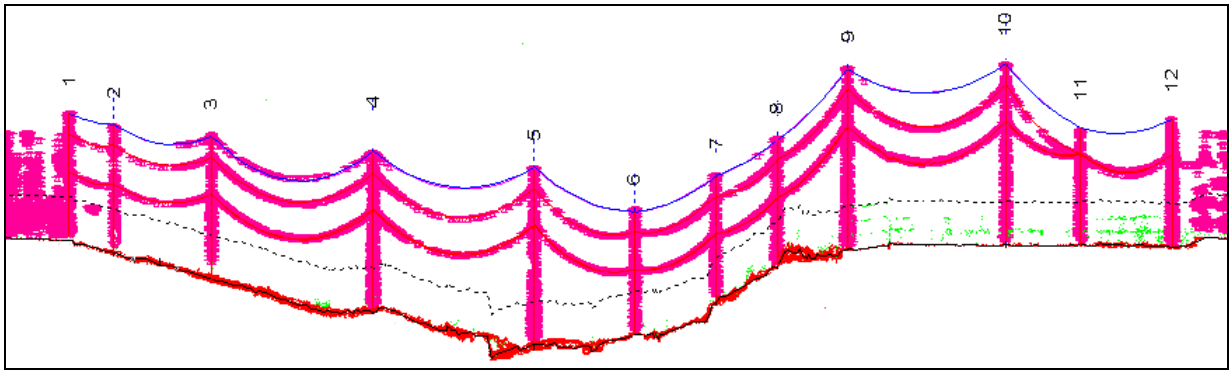

Figure 3.3.3: Conductor position at 35 °C

Figure 3.3.4 displays conductor clearances at an operating temperature of 45 °C. One of the major advantages of the Jupiter – Prospect 275 kV line is that it is a very short transmission line with short spans and numerous strain sections. This feature minimises conductor sag. Minimal conductor sag with no infringements occurred between spans 9 and 10.

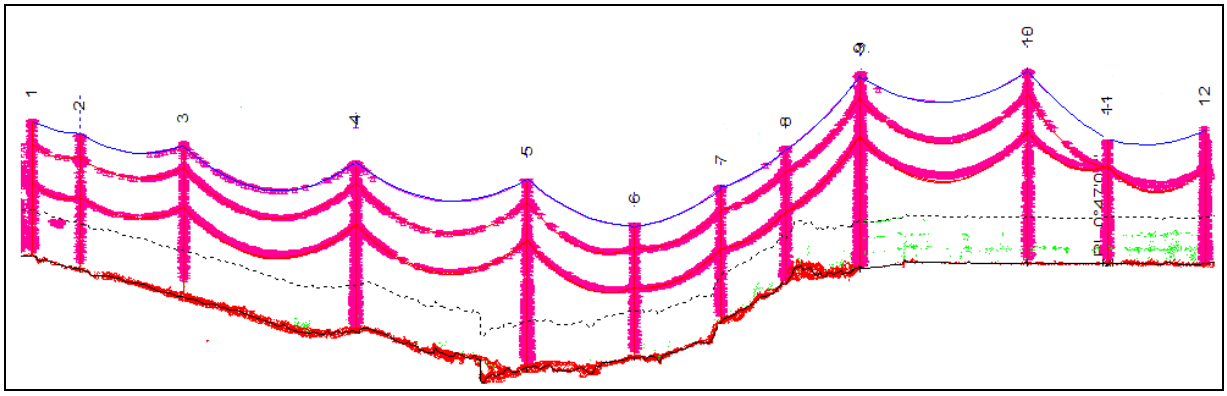

Figure 3.3.4: Conductor position at 45 °C

Figure 3.3.5 displays conductor clearances at an operating temperature of 55 ℃. Minimal conductor sag with no notable infringements occurred between spans 4 and 5 and spans 9 and 10.

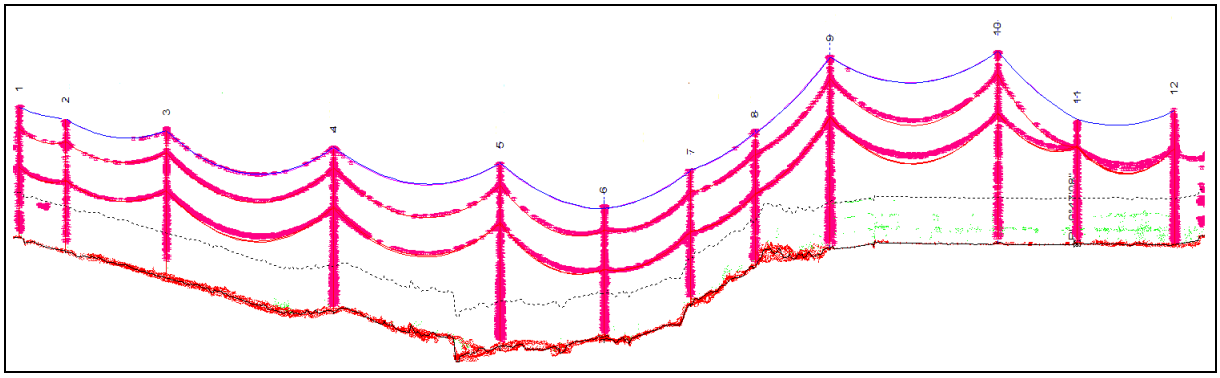

Figure 3.3.5: Conductor position at 55 °C

Figure 3.3.6 displays conductor clearances at an operating temperature of 65 ℃. Minimal conductor sag with no notable infringements occurred between spans 4 and 5 and spans 9 and 10. The graphical sag and clearances analysis up to this point emphasise that the Jupiter – Prospect line has the capability to be thermally uprated.

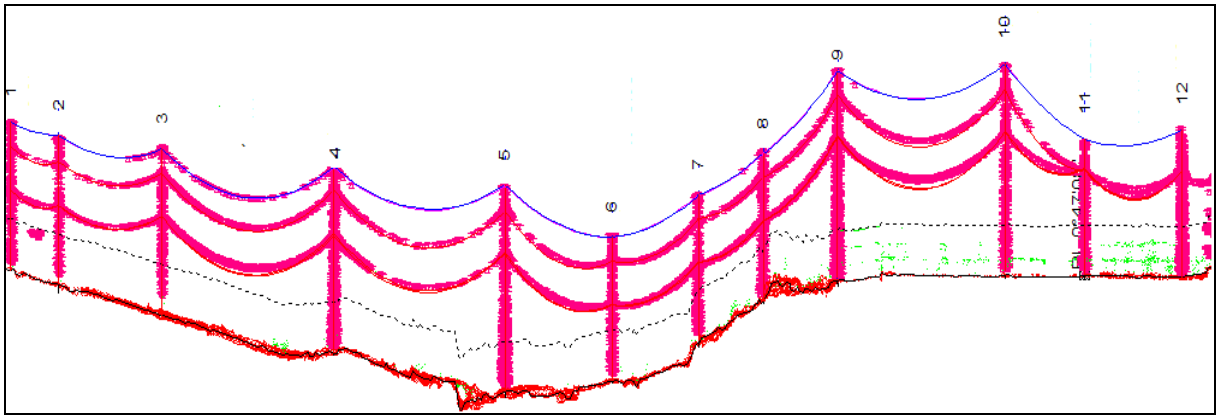

Figure 3.3.6: Conductor position at 65 °C

The original design temperature for the Jupiter – Prospect line is 75 ℃. Figure 3.3.7 displays conductor clearances at the line design temperature with no clearance violations or infringements. The graphical sag and clearance analysis further presents

that the Jupiter – Prospect 275 kV transmission line consists of sufficient spare thermal capacity which can be unlocked to accommodate higher power transfers. The conductors are able to support an increase in the rated, design and templated temperature.

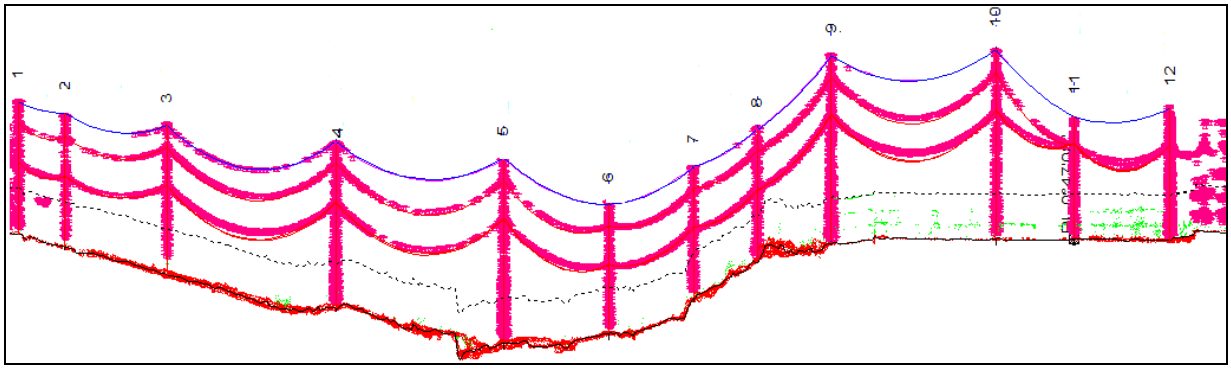

Figure 3.3.7: Conductor position at 75 °C

3.4 PLS CADD THERMAL RATINGS

The thermal rating functionality of PLS CADD allows the user to determine the steady state or the transient behaviour between conductor temperature and electrical current based on weather conditions [38]. Ampacity calculations coupled with the ability to check conductor clearances as performed in Section 3.3 provide necessary tools to examine the existing ratings of the transmission lines. The thermal calculations used are based on the methods presented in Section 2.5. PLS CADD allows the user to determine the conductor temperature for a given electric current or to determine the current that causes a given conductor temperature. This process implements conservative design parameters or measured weather parameters along the line route together with the loading on the line. The weather parameters used to calibrate the PLS CADD model are used to demonstrate the thermal rating functionality. The thermal rating for the line is determined for the temperatures at which the model was graphically sagged. The steady state thermal rating dialogue box is used to enter the weather parameters and conductor temperature that are used to determine the ampacity or thermal rating of the conductors. The weather parameters entered into the dialogue box was obtained by measurement during LIDAR survey.

Figure 3.4.1 displays the relationship between the conductor operating temperature and current loading. An operating temperature of 35 ℃ results in a thermal rating of approximately 660 A per quad bundle, or 165 A per conductor. Figure 3.4.1 also displays the current for all the temperatures at which the conductors were graphically sagged. For instance, a conductor temperature of 55 ℃ results in a thermal rating of 1200 A per quad bundle, or 300 A per conductor.

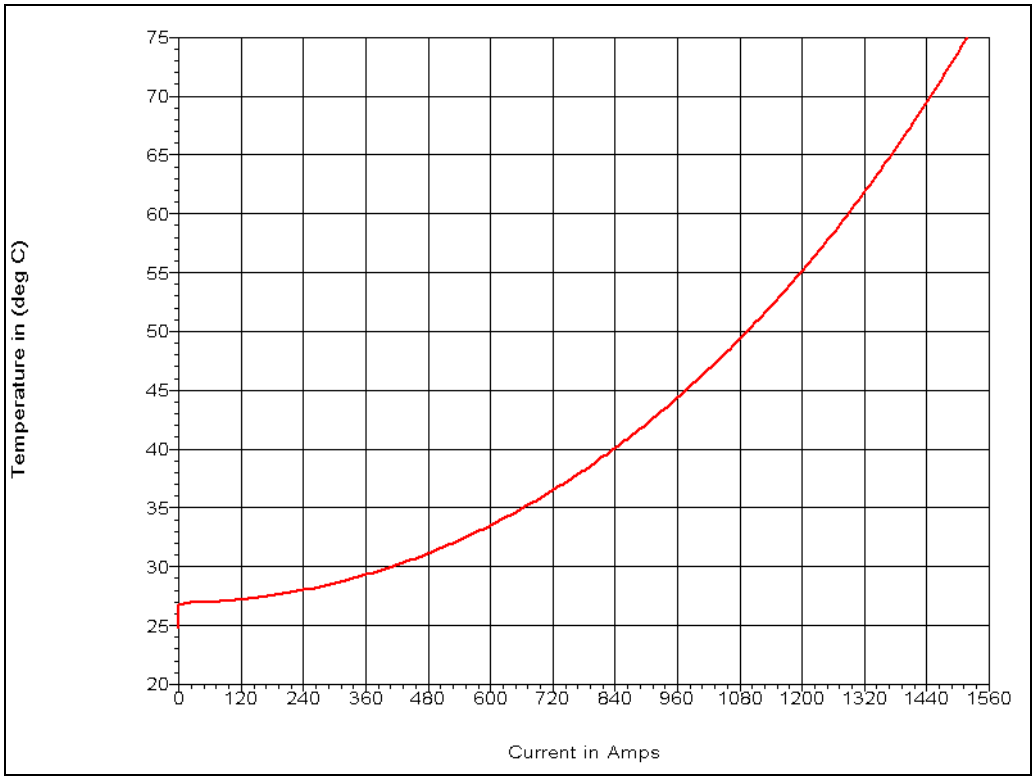

Figure 3.4.1: Relationship between temperature and electrical loading

The combination of operating temperature, electrical loading and the graphical sagging of the conductors identifies if the transmission line is underutilised. In the case of the Jupiter – Prospect 275 kV transmission line the modelling identified margin to increase the current carrying capability and transfer capacity while maintaining safe clearances. The thermal rating analysis presented in this section is used to determine the ampacity or the operating temperature of the line in any given combination of weather parameters and conditions while simultaneously maintaining safe conductor operating limits and safe conductor-to-ground clearances.

3.5 CONCLUSION

The value of modelling transmission lines in a three dimensional field by means of implementing in flight LIDAR data with actual load and meteorological data was demonstrated. The confidence that is developed from knowing the “as is” condition of the line contributes to the decision-making process of whether to uprate a particular line. The benefits of increasing the utilisation of an existing transmission circuit empower system operators to increase thermal limits safely. Transmission line profile modelling and identifying the existing condition of the line is a non-negotiable requirement when intending to uprate an existing transmission circuit.

The ability to sag and raise the conductors graphically under different loading conditions while assessing clearances presents a unique method of clarifying whether a transmission circuit will manage or fail to support higher power transfers. The three-dimensional modelling, graphical sag and thermal analysis of the Apollo – Croydon and Esselen – Jupiter lines are documented in Annexures B and C.

Chapter 4
Thermal rating analysis and results

The focus of Chapter 4 is to identify existing loading conditions of the transmission circuits under study and compare the existing ratings with designed and increased ratings. The operating temperatures of the lines under study are also determined and verified against measurement. In addition, the ampacity rating methods discussed in the literature review are used to determine whether the transmission lines are underutilised in terms of operating temperature. In addition, the practicality of thermal uprating techniques is demonstrated. The aspects of operating temperatures and how they affect the transfer capacity are emphasised.

4.1 INTRODUCTION

The present practice in power utilities is to predict the operating temperature of loaded conductors by means of deterministic and probabilistic methods. The actual operating temperature of a loaded conductor is therefore not known and it is apparent that a need exists to compare estimated temperatures with calculated operating temperatures and to verify with direct measurements. Weather conditions are known to have a significant influence on the operating temperature of transmission lines and are used to determine the operating temperature of loaded conductors.

It is expected that the temperature of a conductor will increase if the ampacity is increased. Higher temperature operations will contribute to the increase in sag of a loaded conductor. The sag and clearance analysis was discussed in Chapter 3. It is important to determine the temperature of conductors accurately. One method is to measure the temperature of the conductor directly at mutiple points along the right of way and compare it with calculated values. Figure 4.1.1 shows workers installing sensors to measure conductor operating temperature under de-energized conditions. These sensors are installed at various spans along the right of way. In addition,

weather stations as displayed in Figure 4.1.2 are also installed for the purpose of measuring meteorological data along the right of way.

Figure 4.1.1: Workers installing temperature sensors onto conductors

Figure 4.1.2 Weather station used to measure atmospheric conditions

4.2 JUPITER – PROSPECT 275 kV THERMAL RATING ANALYSIS

Each high voltage transmission line is rated to a maximum operating temperature to ensure safe transfer of electrical power. Increasing this operating temperature to a higher temperature will result in available additional capacity without infringing on the safe conductor-to-ground clearances. This section will determine the operating temperature under existing operating conditions of the Jupiter – Prospect 275 kV transmission line. Next, a comparison between the measured operating temperature and calculated temperature is performed, after which a conclusion is drawn based upon the result.

The Jupiter - Prospect line is the shortest of the lines considered while performing this research. Two additional lines identified for possible thermal uprating were also studied during this research. Their thermal rating analysis and results are discussed subsequently to that of the Jupiter – Prospect line.

Figure 4.2.1 displays the topography of the Jupiter – Prospect 275 kV line. The term MSL (mean sea level) refers to the elevation of the topography relative to the average sea level. Because it is a very short line, it was decided that only one weather station (installed at tower 5) was needed to measure atmospheric conditions along the right of way. Temperature sensors were installed on each conductor within the quad bundle arrangement: four on the red phase, four on the blue phase and four on the white phase. Therefore, twelve temperature sensors were installed overall to measure operating temperature.

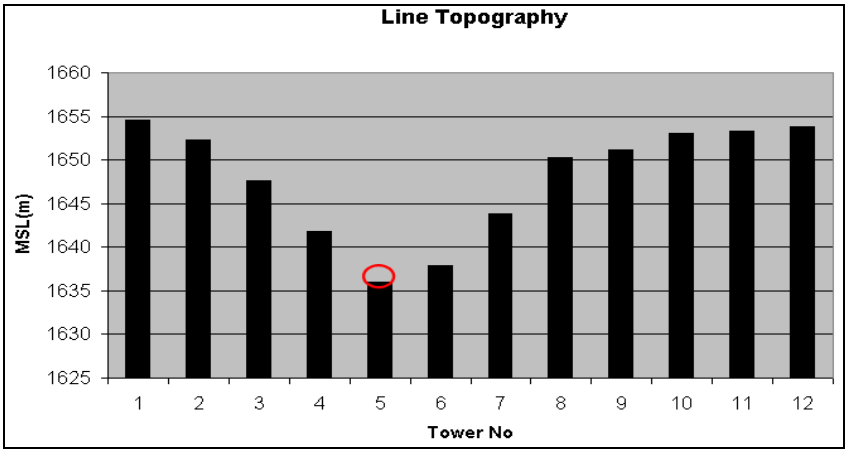

Figure 4.2.1:Jupiter – Prospect line topography

Figures 4.2.2, 4.2.3 and 4.2.4 display the conductor temperature measured during the LIDAR survey that took place on the 23 March 2011 at around 9h00. The figures show that the maximum operating temperature was around 37 ℃ with a minimum of around 14 ℃. The templated temperature of 50 ℃ for the Jupiter – Prospect line was never reached. The temperature while the LIDAR survey took place is required to calibrate the PLS CADD model as discussed in Chapter 3 of this dissertation. This temperature is also compared against calculation and is displayed in Table 4.2.1.

The temperature sensors measured the temperature of the conductor for 2 months from 30 January 2011 to 28 March 2011. The results are displayed in Annexure D.

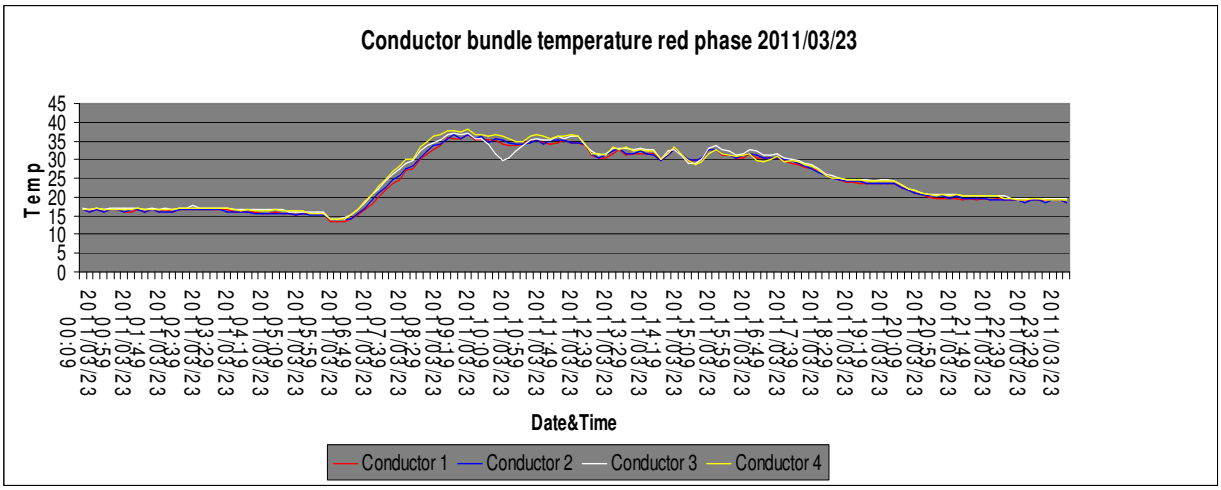

Figure 4.2.2: Actual conductor temperature red phase measured at tower 5

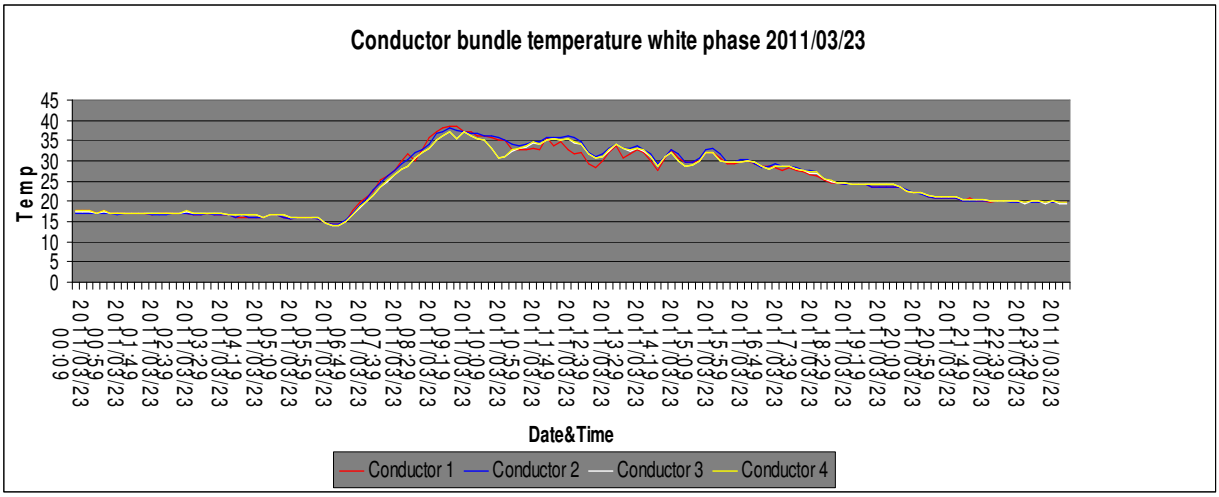

Figure 4.2.3: Actual conductor temperature white phase measured at tower 5

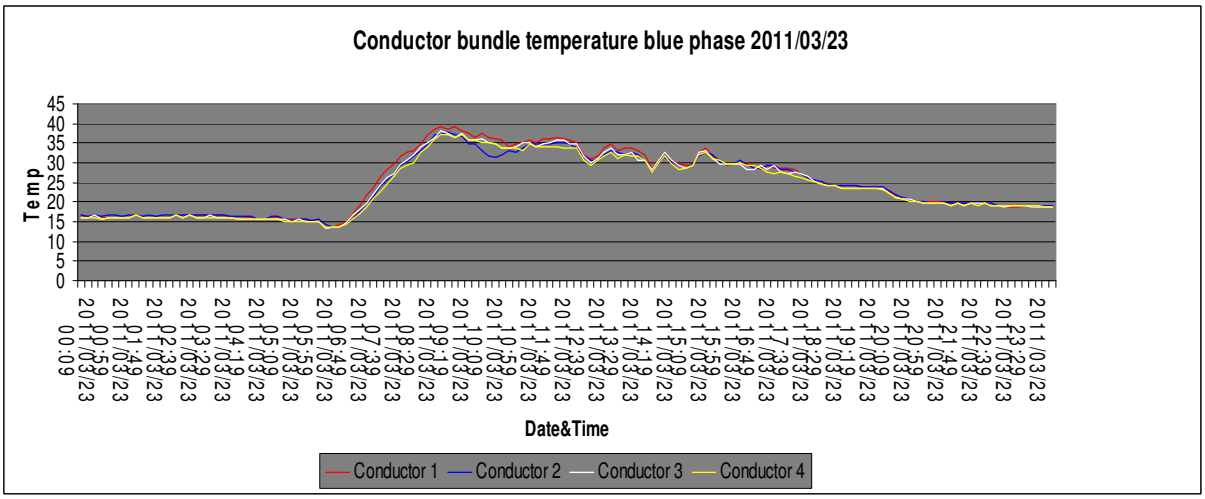

Figure 4.2.4: Actual conductor temperature blue phase measured at tower 5

The calculated temperature as per PLS CADD and Mathcad is verified by the measured temperature. Mathcad is used to speed up the intensive iterative process involved when determining conductor temperatures. Figures 4.2.2, 4.2.3 and 4.2.4 display the measured temperature of each individual conductor within the quad bundle arrangement. The calculated temperatures show that there is good agreement between measured temperatures. These results prove that the Jupiter – Prospect line is being operated at temperatures well below those for which it was designed.

Figure 4.2.5 displays the result for the temperature of the conductor as calculated in Mathcad module. The module allows the user to calculate the conductor temperature with a given current flow or to calculate the current flow given an existing operating

temperature. Both methods depend on measured weather parameters and conditions for calculation.

From Figure 4.2.5 two matrices are identified. The first matrix is I (35.951978, 1500, 0.3, 18, 614, 24.8) and allows for the calculation of the current flow in a conductor given certain operating temperature and weather conditions. The second matrix is T (117.95, 1500, 0.3,18, 614, 24.8) and allows for the calculation of conductor temperature given certain weather parameters and an existing current flow.

$$CondName = \text{" Bear "}$$

$$I(35.951978, 1500, 0.3, 18, 614, 24.8) = \begin{pmatrix} 118.34892 & 0 & 0.943029 & 8.78634 \\ 0.000816 & 3.17579 & 6.525021 & 0 \\ 0 & 9.729369 & 9.700811 & 0 \end{pmatrix}$$

$$T(117.95, 1500, 0.3, 18, 614, 24.8) = \begin{pmatrix} 35.951978 & 0 & 0.936681 & 8.78634 \\ 0.000493 & 3.17579 & 6.525021 & 0 \\ 0 & 9.723021 & 9.700811 & 0 \end{pmatrix}$$

Pm Pjoule Psolar
Prad Pconv
Pgain Ploss

Figure 4.2.5: Mathcad result displaying operating temperature and loading

Note that the phase current was 471 A, as obtained from the national system operator. Hence the single conductor current in Figure 4.2.5 is approximately 118 A. This is due to the current sharing principle between the conductors within the quad bundle arrangement. This is confirmed by similar temperature values measured between the conductors within the bundle arrangement.

Table 4.2.1 shows the comparison between the measured conductor temperature during survey as well as the temperature calculated with Mathcad and PLS CADD. From the results presented in Figures 4.2.2 to 4.2.5 it is possible to determine that there is good agreement between calculated temperatures obtained from PLS CADD and Mathcad, which were verified by actual measured temperature on loaded transmission lines. The operating temperature for the line on average was around 37 °C at the time of survey. In addition, it is possible to establish a confidence level in the use of temperature sensors for measuring conductor temperature. Weather stations are the preferred method of use but are more capital intensive than

temperature sensors. Temperature sensors are therefore a more cost-effective way to determine the operating temperature.

Table 4.2.1: Temperature comparison table for Jupiter – Prospect 275 kV

	PLS CADD	Mathcad	Measured
Wind speed (m/s)	0.3	0.3	0.3
Direction/Angle with conductor (degrees)	18	18	18
Ambient temperature (°C.)	24.8	24.8	24.8
Solar radiation (Watt/m²)	614	614	614
Load current (A)	471	471	471
Single conductor current (A)	117.95	117.95	117.95
Conductor height above sea level (m)	1500	1500	1500
Conductor Temperature (°C.)	36.7	35.95	36.98

4.2.1 **Jupiter – Prospect line ratings**

An internal Eskom directive EED 15/6/1-1 1970 [62] allowed for transmission line ratings to be calculated for normal and emergency conditions at 75 ºC and 90 ºC by using methods discussed in Section 2.5. The lines were then templated at 50 ºC according to the internal directive. Recently a new system operator guideline defined new line ratings as rating A, rating B and rating C [33]. Rating A specifies the level of electrical loading that a transmission circuit can withstand without loss of equipment life. Rating B specifies the electrical loading that the circuit can withstand under contingency situations without the loss of equipment life. Rating C specifies the level of electrical loading that the circuit can withstand for a predetermined period of 15 minutes with an acceptable loss of equipment life.

The existing steady state thermal ratings of overhead lines documented in this guideline were determined based on a probabilistic approach with historical weather data. This method in some cases still results in the lines being underutilised in terms of thermal criteria and operating temperature as displayed in Section 4.2. Table 4.2.2 displays the thermal rating for the conductor used on the Jupiter – Prospect line. The exceedence is defined as the time when the conductor operating temperature is greater than the design temperature. The ratings dictate the maximum current rating transfer at various operating temperatures. The ratings are for a single conductor with a double aluminium layer. For a conductor arrangement, consisting of four conductors (quad bundle) the rating must be multiplied by four. E.g. a single conductor at a 50 °C template temperature has a current rating, rate A of 510 A. Four conductors or a quad bundle arrangement at a 50 °C templated temperature will have a current rating, rate A of 2040 A.

Table 4.2.2 Thermal ratings determined by means of probabilistic approach [33]

ACSR Double layer Aluminium				
Percentage		8.60%	42.97%	70.05%
Probability of unsafe condition arising		-1.05E-06	5.25E-06	8.56E-06
Type	Templated Temperature °C	Rate A (A)	Rate B (A)	Rate C (A)
Bear	50	510	735	1080
Bear	60	613	842	1225
Bear	70	691	928	1354
Bear	80	758	1002	1430

Figure 4.2.6 displays the 24-hour loading or current flow of the line for the day that the LIDAR survey took place. The loading for the line during the survey is circled in red. The measured and calculated temperature results for this instance are documented in Section 4.2.

Please note that Figure 4.2.6 only displays the loading on the line for the white phase. The flow was obtained from System Operator that only records the white phase on the Jupiter - Prospect line. The white phase represents a good agreement of the flow on

the remaining phases and only assumes an imbalance of around 3 % between phases. Figure 4.2.6 displays the actual loading of the line.

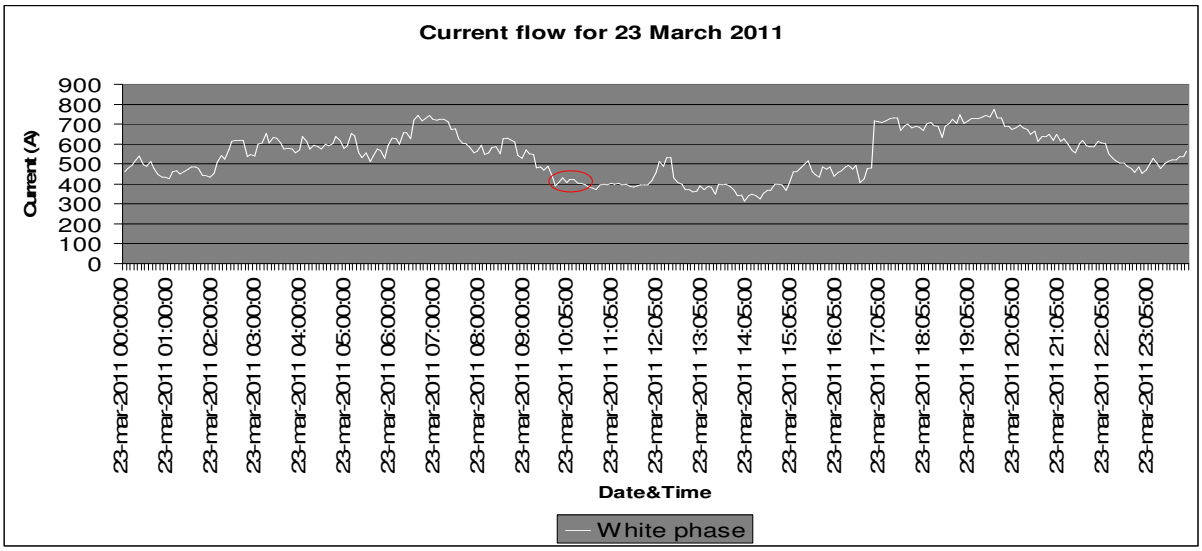

Figure 4.2.6: Actual loading of line during day of survey

The confidence that was established in the use of temperature sensors for the measurement of conductor temperature allows the evaluation of the temperature of the conductor at different times and loading. The actual loading and operating temperature can be compared with the designed and templated values. As an example, the time for verification is chosen at around 18h00 from Figure 4.2.6 when the loading on the line is relatively high. The temperature of the conductor was determined by PLS CADD and Mathcad, and verified against the measured temperature. The results for the comparison are summarised in Table 4.2.3.

The results obtained for the conductor temperature from PLS CADD, Mathcad and the sensors again show a good agreement. It is noted from the results in Table 4.2.3 that the temperature rise of the conductors above ambient is much less than in Table 4.2.1. This is mainly due to the difference in weather parameters. Higher forced cooling is obtained in Table 4.2.3 due to the higher wind speed and angle. In addition, there is no solar heat gain. The loading of the line in Figure 4.2.6 suggests that at 718 A the line was operated between rating A and Rating B. That should result in a probabilistic temperature of around 50 °C, which is the templated temperature for the line. The measured temperature during this time was approximately 26 °C. This highlights the

fact that the line at this stage is actually underutilised and therefore is a very good candidate for thermal uprating. It is also important to mention that there are no clearance issues or infringements on the conductor-to-ground clearance for the Jupiter - Prospect 275 kV line.

Table 4.2.3: Temperature comparison for Jupiter – Prospect 275 kV at higher loading

	PLS CADD	Mathcad	Measured
Wind speed (m/s)	1	1	1
Direction/Angle with conductor (degrees)	58	58	58
Ambient Temperature (°C)	24.3	24.3	24.3
Solar radiation (Watt/m²)	0	0	0
Load current (A)	718	718	718
Single conductor current (A)	179.5	179.5	179.5
Conductor height above sea level (m)	1500	1500	1500
Conductor Temperature (°C)	26.27	26.36	26.2

4.2.2 **Jupiter – Prospect substation equipment ratings**

Substation equipment is deemed as critical components in a transmission circuit that may affect the reliability and the security of supply when overloaded. Generally, the benefits of increasing the rating of transmission lines may be limited by the thermal ratings of power equipment that further contributes to transfer capacity constraints. Power utilities are inclined to operate substation equipment within manufacturer criteria to avoid failure and unnecessary insurance complications. Any overloading beyond nameplate values is deemed a loss of life and insulation of substation equipment. The loading of substation equipment is therefore an economic decision. The gains of increasing the loading capability beyond the equipment's maximum rating must be balanced against the risk of failure, loss of capital investment and the

alleviation of power flow constraints within the network. Power equipment is generally matched to the line rating and the type of equipment that is available at the time of design and the cost thereof. An important step is to identify the power equipment ratings and limitations of both Jupiter and Prospect substations.

Table 4.2.4 displays the 275 kV equipment ratings at Jupiter substation. The thermal limits, short circuit current rating and the MVA rating are displayed. The highest current rating is that of the circuit breaker and the lowest current rating is that of the current transformer followed by the pantograph line isolator of the second busbar. Based on the power equipment ratings the Jupiter – Prospect line cannot operate at the designed line ratings due to underrated terminal equipment and is therefore thermally limited by the substation equipment. As displayed in Table 4.2.5, rating A for the line is 2040 A. The rating of the current transformer at Jupiter substation is 2000 A, which is below that of line rating A. This is clearly a constraint to the operation of the line. By replacing underrated terminal equipment to match line ratings thermal capacity is unlocked and power transfer is increased.

Table 4.2.4: Jupiter substation equipment ratings

Equipment	**Thermal ratings**	**MVA rating**
Isolator BB1	2500A, 31.5 kA ,1s	1191 MVA
PG Isolator BB2	2400A, 31.5 kA, 1s	1143 MVA
Circuit breaker	3150A, 50 kA ,1s	1500 MVA
Line trap	2500A, 50 kA ,1s	1191 MVA
Isolator line	2500A, 31.5 kA ,1s	1191 MVA
Current transformer	2000A, 40 kA, 1s	952 MVA
Capacitor voltage transformer	Voltage related equipment	Voltage related equipment
Surge Arrester	Voltage related equipment	Voltage related equipment

Note: The rated duration for fault currents of substation equipment were obtained from Eskom specification TSP41-595 [63], IEC 60694:2002 [64], IEEE Std C37.06:2009 [54].

Table 4.2.5 displays the 275 kV equipment ratings at Prospect substation. The thermal limits, short circuit current rating as well as the MVA rating are displayed. The current

ratings of the power equipment at Prospect substation are all equal except the rating of the busbars. However, the busbar ratings at both substations are similar.

Table 4.2.5: Prospect substation equipment ratings

Equipment	**Thermal ratings**	**MVA rating**
Isolator BB1	2500A, 31.5 kA ,1s	1191 MVA
Isolator BB2	2500A, 31.5 kA, 1s	1191 MVA
Circuit breaker	2500A, 31.5 kA, 1s	1191 MVA
Current transformer	2500A, 50 kA, 1s	1191 MVA
Isolator line	2500A, 31.5 kA, 1s	1191 MVA
Line trap	2500A, 40 kA,1s	1191 MVA
Capacitor voltage transformer	Voltage related equipment	Voltage related equipment
Surge Arrester	Voltage related equipment	Voltage related equipment

Table 4.2.6 displays the line ratings for the Jupiter – Prospect 275 kV overhead transmission line. In addition, the current rating of the limiting piece of terminal equipment is well below the designed ratings of the line. This limits power flow, as the transmission line cannot be operated at the designed line ratings.

Table 4.2.6: Jupiter – Prospect line ratings

Line	Conductor rating (A) Quad Bear			Busbar rating (A) Twin bull			Terminal equipment (A)
Jupiter-Prospect 275 kV	Rate A	Rate B	Rate C	Rate A	Rate B	Rate C	Lowest equipment rating
	2040	2939	4321	2305	3307	6091	2000

The substation equipment ratings for both Jupiter and Prospect are well below that of rating B and C of the line. The substation equipment thermally limits this line. However, by replacing underrated equipment to match line ratings increases in transfer capacity is obtained and bottlenecks alleviated.

4.3 APOLLO – CROYDON 275 KV THERMAL ANALYSIS

The Apollo – Croydon line is approximately 33 km long and is the second line identified for possible thermal uprating by the system operator. Figure 4.3.1 displays

the topography of the line obtained from Eskom's transmission spatial information system (TxSIS). Seven weather stations were installed at pre-identified spans at which the temperature of the conductor was also measured for the red, white and blue phases. The spans where the equipment was installed are:

- Spans 1 – 2 (12 temperature sensors and 1 weather station),
- Spans 8 – 9 (3 temperature sensors and 1 weather station),
- Spans 28 – 29 (3 temperature sensors and 1 weather station),
- Spans 59 – 60 (3 temperature sensors and 1 weather station),
- Spans 65 – 66 (3 temperature sensors and 1 weather station),
- Spans 81 – 82 (3 temperature sensors and 1 weather station),
- Spans 141 – 142 (3 temperature sensors and 1 weather station).

Note: The weather stations were installed at the conductor level as displayed in Figure 4.1.2.

The rationale behind the number of temperature sensors installed was defined as follows: one span on the line was selected where the temperature on each of the conductors within the quad bundle arrangement was measured. This allowed for the verification of the current sharing principle between the conductors in the bundle and comparison of the temperatures of conductors within a bundle arrangement with each other. The conductor temperature was then monitored on only one conductor in the bundle for the red, white and blue phases for the remainder of the spans. This method allowed a cost saving as fewer temperature sensors were needed. Figure 4.3.1 displays the topography of the Apollo – Croydon 275 kV line. The positions circled in red identify the tower numbers where the weather stations were installed.

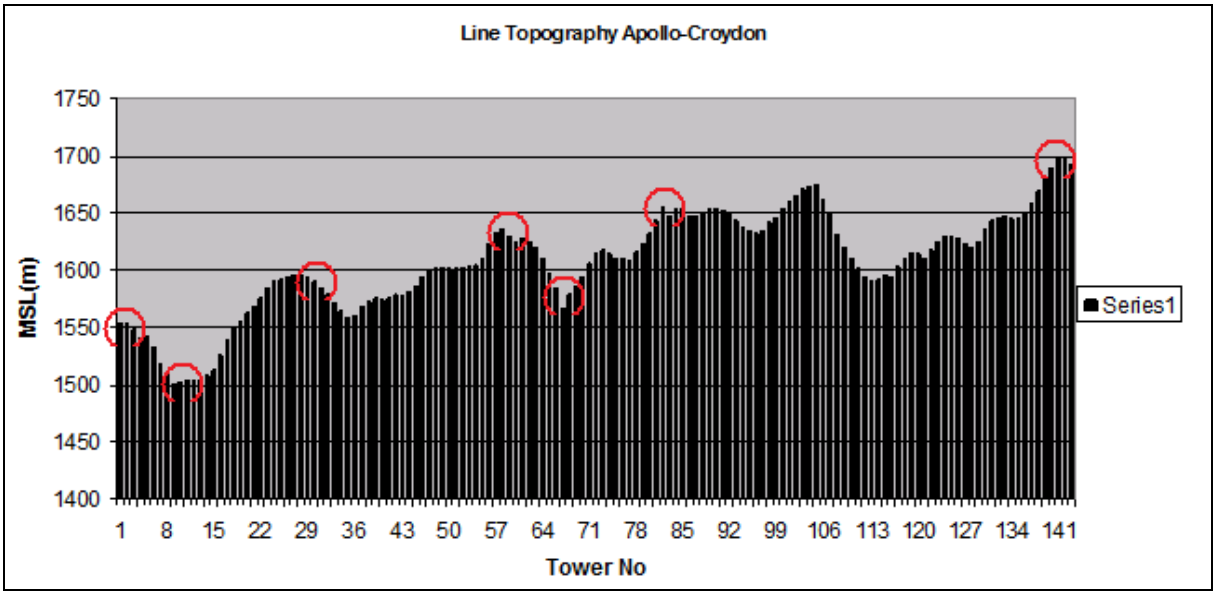

Figure 4.3.1: Line topography of Apollo – Croydon 275 kV

Figures 4.3.2 to 4.3.10 display the conductor temperatures measured during the LIDAR survey for the Apollo-Croydon 275 kV line that took place on 23 January 2011 from approximately 10:00 to 11:30. The figures show that the maximum operating temperature was experienced at spans 65 – 66 which was around 40 ℃. The rest of the spans experienced maximum temperatures that ranged between 35 ℃ to 40 ℃. On average, the minimum temperature was consistent across all the monitored spans with an average minimum of approximately 15 ℃. The templated temperature of 50 ℃ was never reached.

The temperature sensors measured the temperature of the conductors for approximately 3 months from 20 December 2010 to 15 March 2011. The results for the duration of the installation are displayed in Annexure E.

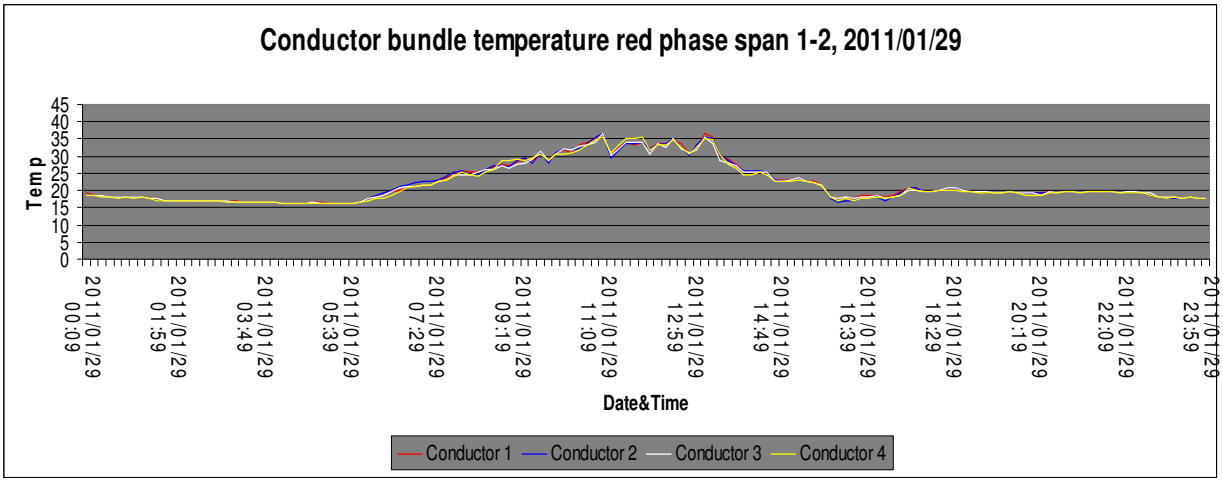

Figure 4.3.2 Actual measured conductor bundle temperature red phase, spans 1 – 2

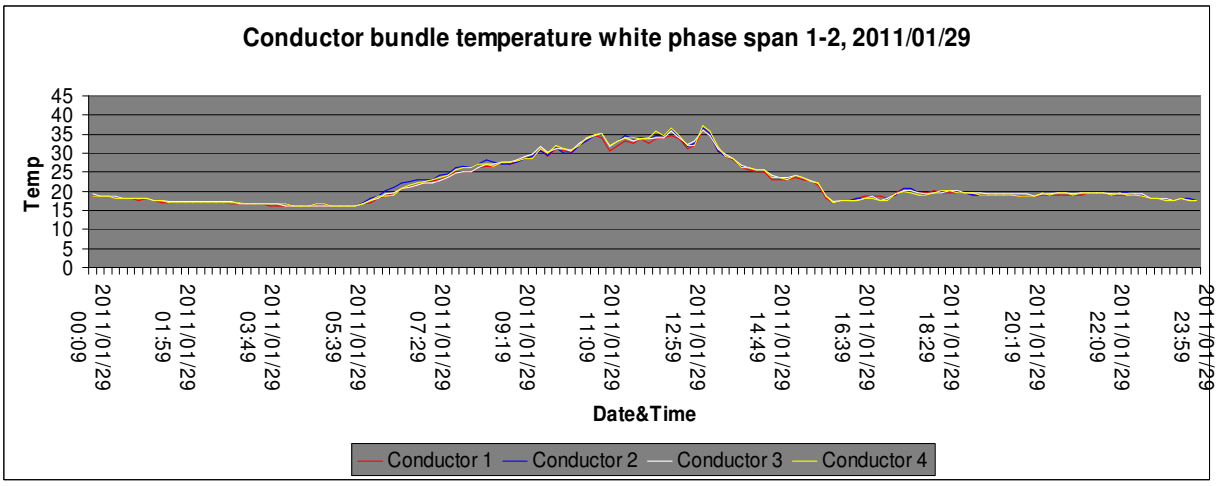

Figure 4.3.3: Actual measured conductor bundle temperature white phase, spans 1 – 2

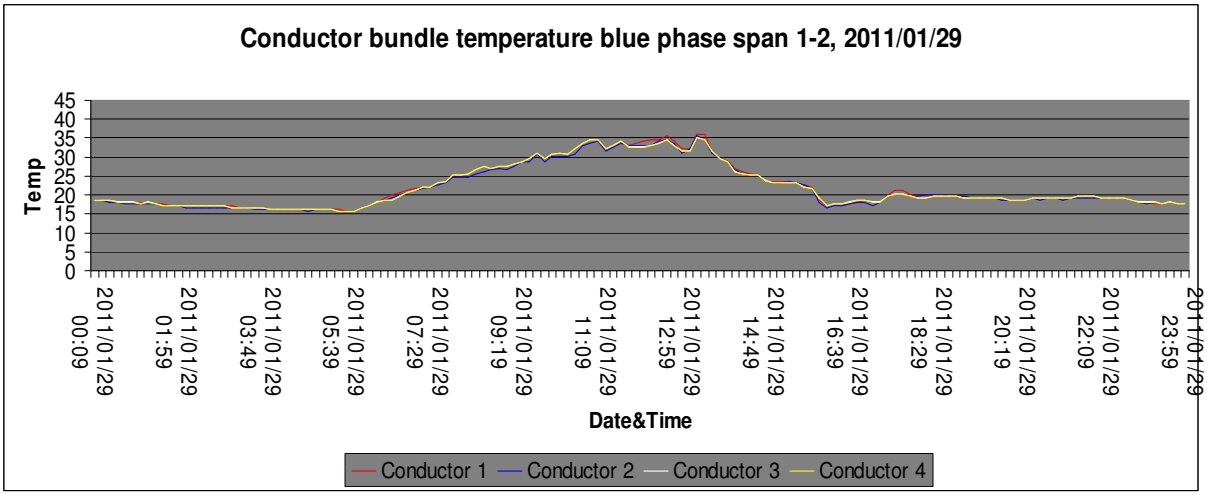

Figure 4.3.4: Actual measured conductor bundle temperature blue phase, spans 1 – 2

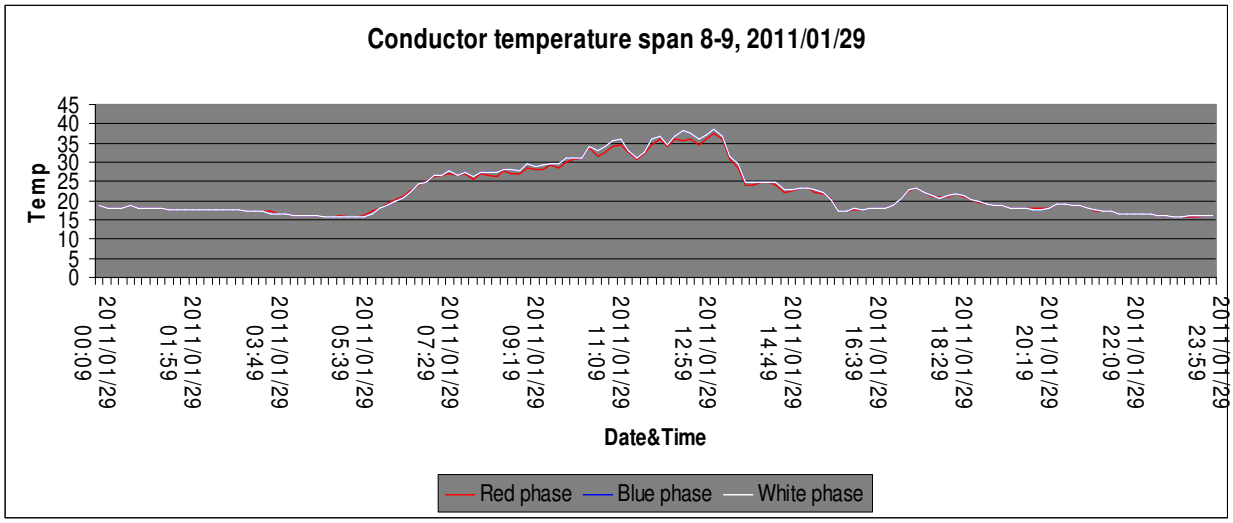

Figure 4.3.5: Actual measured conductor temperature, spans 8 – 9

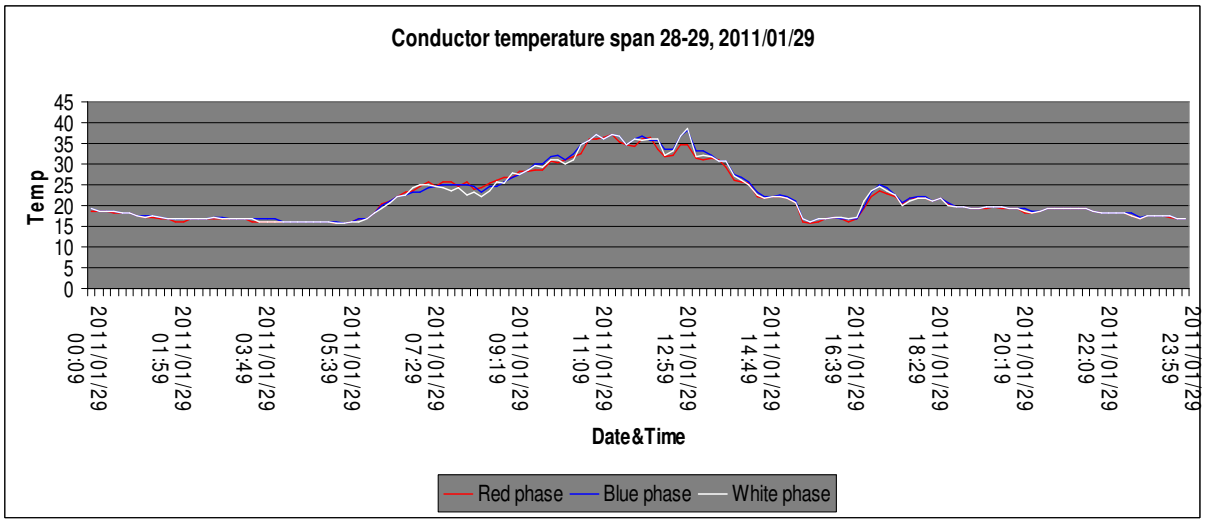

Figure 4.3.6: Actual measured conductor temperature, spans 28 – 29

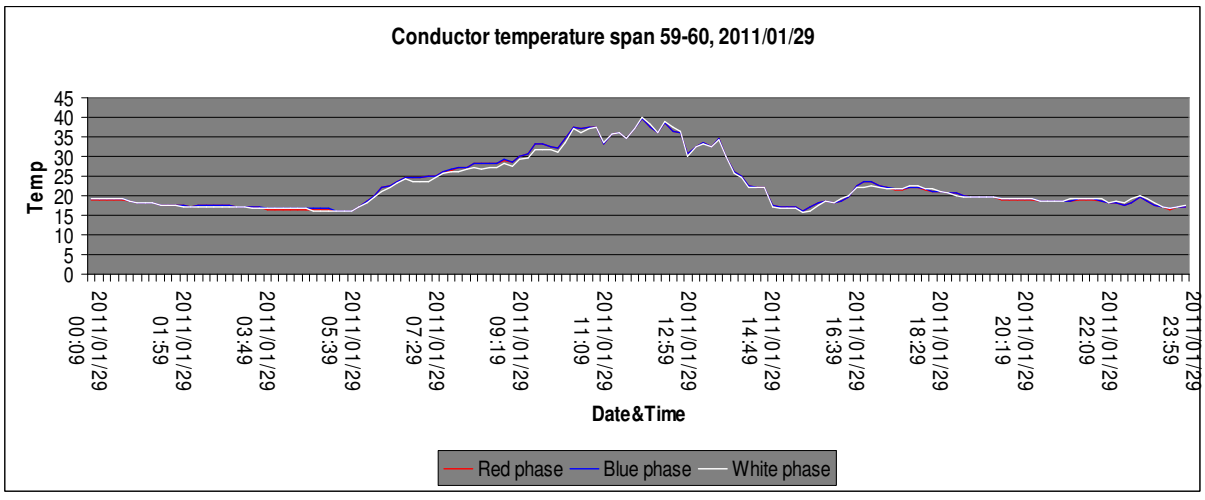

Figure 4.3.7: Actual measured conductor temperature, spans 59 – 60

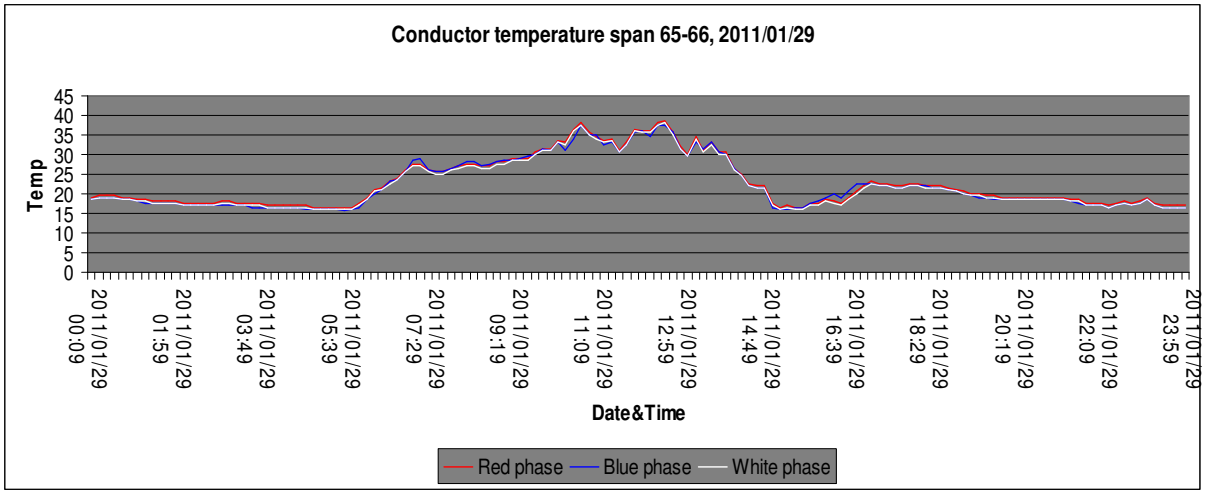

Figure 4.3.8: Actual measured conductor temperature, spans 65 – 66

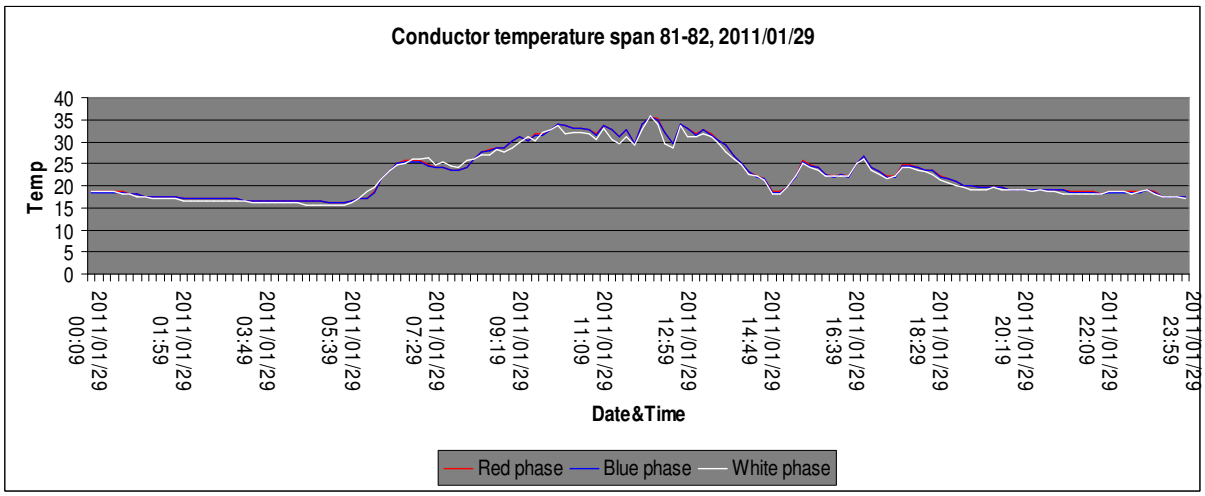

Figure 4.3.9: Actual measured conductor temperature, spans 81 – 82

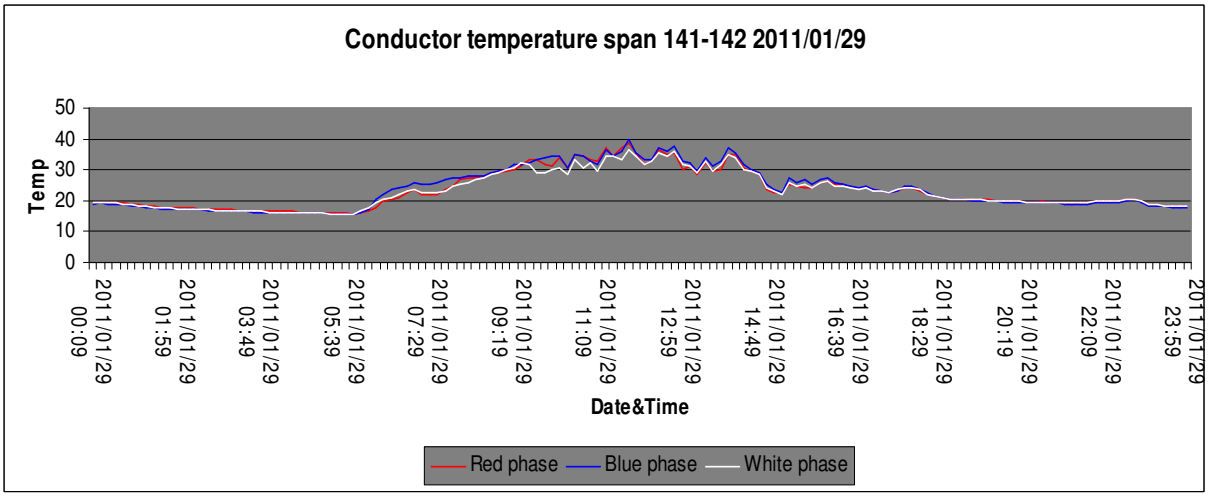

Figure 4.3.10: Actual measured conductor temperature, spans 141 – 142

Table 4.3.1 displays the comparison between the measured conductor temperature and the temperature calculated with Mathcad and PLS CADD for the various spans. The results in Table 4.3.1 present a good agreement between the temperatures measured and temperatures obtained by calculation. The biggest influence on the temperature of the conductor was that of the surrounding weather parameters. Higher wind speeds and greater angle of attack provided higher forced and convective cooling. The results of Table 4.3.1 emphasise that the Apollo – Croydon line is underutilised in terms of operating temperature. The templated temperature of 50 °C is not reached and this demonstrates that spare capacity is available in terms of operating temperature.

Table 4.3.1: Temperature comparison for Apollo – Croydon 275 kV

	Span 1-2			**Span 8-9**		
	PLS CADD	**Mathcad**	**Measured**	**PLS CADD**	**Mathcad**	**Measured**
Wind speed (m/s)	2	2	2	2	2	2
Direction/Angle with conductor (degrees)	50	50	50	58	58	58
Ambient temperature (°C.)	21.8	21.8	21.8	22.7	22.7	22.7
Solar radiation (Watt/m²)	889	889	889	960	960	960
Load current (A)	802	802	802	800	800	800
Single conductor current (A)	200.5	200.5	200.5	200	200	200
Conductor height above sea level (m)	1500	1500	1500	1500	1500	1500
Conductor Temperature (°C.)	28.7	29.18	29.96	29.4	29.22	30.67

	Span 28-29			Span 59-60		
	PLS CADD	**Mathcad**	**Measured**	**PLS CADD**	**Mathcad**	**Measured**
Wind speed (m/s)	1	1	1	1	1	1
Direction/Angle with conductor(degrees)	67	67	67	20	20	20
Ambient Temperature (℃.)	22	22	22	22.4	22.4	22.4
Solar radiation (Watt/m²)	981	981	981	1032	1032	1032
Load current (A)	779	779	779	795	795	795
Single conductor current (A)	194.75	194.75	194.75	198.75	198.75	198.75
Conductor height above sea level (m)	1500	1500	1500	1500	1500	1500
Conductor Temperature(℃.)	31.4	30.88	31.11	35.8	36.55	34.23
	Span 65-66			**Span 81-82**		
	PLS CADD	**Mathcad**	**Measured**	**PLS CADD**	**Mathcad**	**Measured**
Wind speed (m/s)	1	1	1	2	2	2
Direction/Angle with conductor (degrees)	67	67	67	10	10	10
Ambient Temperature (℃.)	22.8	22.8	22.8	22.1	22.1	22.1
Solar radiation (Watt/m²)	1018	1018	1018	960	960	960
Load current (A)	795	795	795	793	793	793
Single conductor current (A)	198.75	198.75	198.75	198.25	198.25	198.25
Conductor height above sea level (m)	1500	1500	1500	1500	1500	1500
Conductor Temperature (℃.)	29.6	31.96	32.23	30.6	32.67	32.75

	Span 141-142					
	PLS CADD	**Mathcad**	**Measured**			
Wind speed (m/s)	1	1	1			
Direction/Angle with conductor (degrees)	28	28	28			
Ambient Temperature (°C.)	24	24	24			
Solar radiation (W/m^2)	1130	1130	1130			
Load current (A)	752	752	752			
Single conductor current (A)	188	188	188			
Conductor height above sea level (m)	1500	1500	1500			
Conductor Temperature (°C.)	36.8	36.59	35.98			

The comparison between results of different techniques for determining operating temperatures of loaded conductors is quite valuable in that estimated values are verified against calculation and measurement. It provides a high confidence level that weather parameters can be used to determine the operating temperature of loaded conductors accurately. It paves the way for an easy method to determine if a transmission line is being underutilised. The subsequent section discusses the different thermal ratings and levels for the Apollo – Croydon line.

4.3.1 **Apollo – Croydon line ratings**

The system operator guideline as discussed in Section 4.2.1 defines line ratings for the Apollo – Croydon line. The line consists of a triple layer zebra conductor in a quad bundle arrangement for each phase with a templated temperature of 50 °C. Table 4.3.2 displays the thermal rating for the conductor used on the Apollo – Croydon line. The ratings dictate the maximum permissible current rating for zebra conductor for various operating temperatures. The probability of an unsafe condition arising associated with each rating is quantified and displayed. The probability of an unsafe

condition arising is kept constant for the conductor and rate A, B and C are determined at different operating temperatures.

Table 4.3.2 Thermal ratings for zebra conductor at different temperatures

ACSR Triple Layer				
Percentage		8.60%	42.97%	70.05%
Probability		1.05E-06	5.25E-06	8.56E-06
Triple		**Rate A**	**Rate B**	**Rate C**
ZEBRA	50	694	982	1616
ZEBRA	60	817	1124	1760
ZEBRA	70	916	1243	1889
ZEBRA	80	1003	1344	2018

The ampacity values in table 4.3.2 are used as a measure to determine if the line is underutilised in terms of operating temperature and loading. Figure 4.3.11 displays the 24 hour loading of the Apollo – Croydon line for the day that the LIDAR survey took place. The loading for the line during the time of the survey is circled in red. The comparisons between the measured and calculated temperature results for this instance are documented in Section 4.3. The thermal ratings in table 4.3.2 are compared with the loading of the line presented in Figure 4.3.11 and are regarded as the existing loading of the line. For example, the time for comparison was chosen at approximately 18:00 from Figure 4.3.11 when the loading on a line is usually higher due to the demand for electricity during peak periods. The same approach is used as in Section 4.2.1 and the results are summarised in Table 4.3.3.

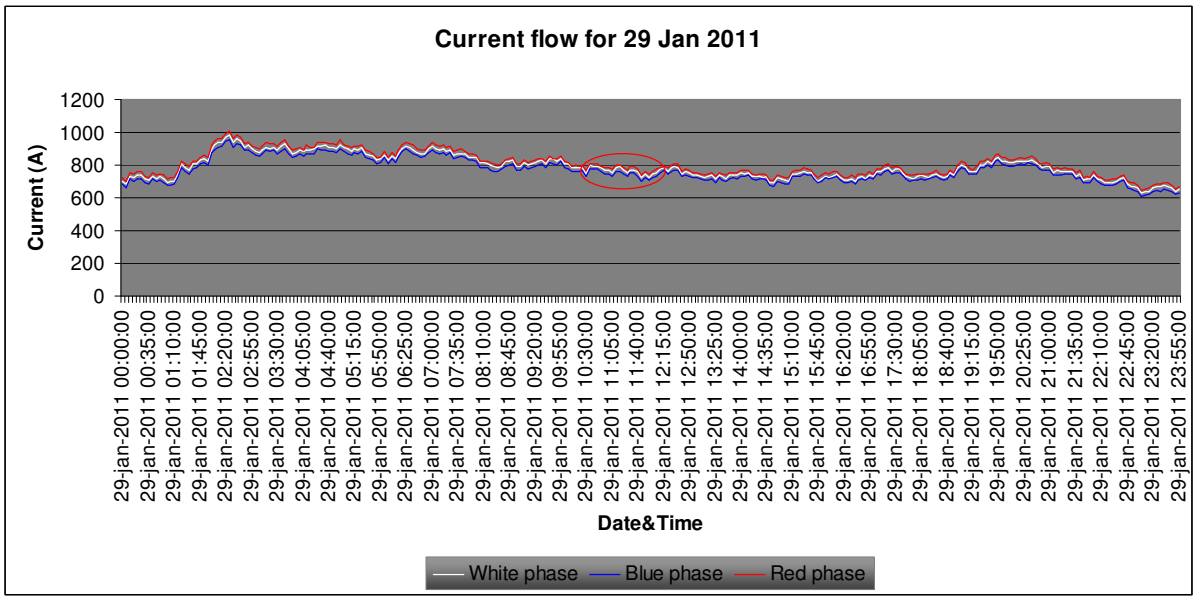

Figure 4.3.11: Actual loading of Apollo – Croydon on day of survey

The results show very good agreement between methods. It is noted that the conductor temperature rise for spans 1 – 2 in Table 4.3.3 is much lower than in Table 4.3.1. This is explained by the difference in weather parameters. There is a smaller wind angle present in Table 4.3.3 than in Table 4.3.1. Higher solar radiation is present in Table 4.3.1 than in 4.3.3 and results in greater solar heating. The loading of the line in Figure 4.3.11 suggests that at 726 A the line was operated between rate A and rate B. The templated temperature is determined using weather conditions that with full load current will result in the conductor surface temperature being equal to the templated temperature. The measured temperature during this period was on average around 22 ℃ with a loading of 726 A. This temperature was obtained during the continuous measurement of weather parameters and was used for both the Mathcad and PLS CADD temperature calculations. The results demonstrate that the line is underutilised in terms of operating temperature and loading.

Table 4.3.3: Temperature comparison for Apollo – Croydon at different loadings

	Span 1-2			Span 8-9		
	PLS CADD	**Mathcad**	**Measured**	**PLS CADD**	**Mathcad**	**Measured**
Wind speed (m/s)	3	3	3	4	4	4
Direction/Angle with conductor	31	31	31	0	0	0
Ambient Temperature (℃)	20.2	20.2	20.2	20.4	20.4	20.4
Solar radiation (Watt/m²)	153	153	153	46	46	46
Load current (A)	726	726	726	726	726	726
Single conductor current (A)	181.5	181.5	181.5	181.5	181.5	200
Conductor height above MSL (m)	1500	1500	1500	1500	1500	1500
Conductor Temperature (℃)	21	18.48	19.6	22.1	21.7	21.1
	Span 28-29			**Span 59-60**		
	PLS CADD	**Mathcad**	**Measured**	**PLS CADD**	**Mathcad**	**Measured**
Wind speed (m/s)	5	5	5	1	1	1
Direction/Angle with conductor	90	90	90	3	3	3
Ambient Temperature (℃)	20.6	20.6	20.6	19.8	19.8	19.8
Solar radiation (Watt/m²)	54	54	54	74	74	74
Load current (A)	726	726	726	795	795	795
Single conductor current (A)	181.5	181.5	181.5	198.75	198.75	198.75
Conductor height above MSL (m)	1500	1500	1500	1500	1500	1500
Conductor Temperature (℃)	21.3	20.29	21.48	23.3	23	22.28

	Span 65-66			Span 81-82		
	PLS CADD	**Mathcad**	**Measured**	**PLS CADD**	**Mathcad**	**Measured**
Wind speed (m/s)	8	8	8	1	1	1
Direction/Angle with conductor	40	40	40	0	0	0
Ambient Temperature (°C)	20.6	20.6	20.6	19.9	19.9	19.9
Solar radiation (Watt/m²)	76	76	76	120	120	120
Load current (A)	726	726	726	726	726	726
Single conductor current (A)	181.5	181.5	181.5	181.5	181.5	181.5
Conductor height above MSL (m)	1500	1500	1500	1500	1500	1500
Conductor Temperature (°C)	21.4	20.06	22.27	23.9	24.4	24.13
	Span 141-142					
	PLS CADD	**Mathcad**	**Measured**			
Wind speed (m/s)	6	6	6			
Direction/Angle with conductor	60	60	60			
Ambient temperature (°C)	20.9	20.9	20.9			
Solar radiation (Watt/m²)	35	35	35			
Load current (A)	726	726	726			
Single conductor current (A)	181.5	181.5	181.5			
Conductor height above MSL (m)	1500	1500	1500			
Conductor Temperature (°C)	21.5	21.35	22.34			

4.3.2 **Apollo – Croydon substation equipment ratings**

This section discusses the substation equipment ratings of both sending and receiving substations. Table 4.3.4 displays the 275 kV equipment ratings at Apollo substation. The thermal limits, short circuit current ratings as well as the MVA ratings are displayed. The power equipment ratings are all equal to a rated value of 1500 MVA or 3149 A rounded to 3150 A. Based on the power equipment ratings at Apollo substation the line can operate at line design rating A and cannot support higher ratings without sacrificing loss of equipment life. However, the equipment ratings of Croydon substation also need to be evaluated.

Table 4.3.4: Apollo substation equipment ratings

Equipment	Thermal ratings	MVA rating
Isolator BB1	3150A, 40 kA ,1s	1500 MVA
PG Isolator BB2	3150A, 40 kA, 1s	1500 MVA
Circuit breaker	3150A, 40 kA, 1s	1500 MVA
Current transformer	3150A, 40 kA, 1s	1500 MVA
Isolator line	3150A, 40 kA, 1s	1500 MVA
Line trap	3150A, 40 kA, 1s	1500 MVA
Capacitor voltage transformer	Voltage related equipment	Voltage related equipment
Surge Arrester	Voltage related equipment	Voltage related equipment

Note: The rated duration for fault currents of substation equipment were obtained from Eskom specification TSP41-595 [63], IEC 60694:2002 [64], IEEE Std C37.06:2009 [54].

Table 4.3.5 displays the 275 kV equipment ratings at Croydon substation. The thermal limits, short circuit current rating and the MVA ratings are displayed. The current ratings of the power equipment at Croydon substation are all equal except the rating of the circuit breaker and busbars which are higher. The busbar ratings at both substations are similar.

Table 4.3.5: Croydon substation equipment ratings

Equipment	Thermal ratings	MVA rating
Isolator BB1	2500A, 31.5 kA ,1s	1191 MVA
Isolator BB2	2500A, 31.5 kA, 1s	1191 MVA
Circuit breaker	3150A, 50 kA, 1s	1500 MVA
Current transformer	2500A, 50 kA, 1s	1191 MVA
Isolator line	2500A, 31.5 kA, 1s	1191 MVA
Line trap	2500A, 40 kA,1s	1191 MVA
Capacitor voltage transformer	Voltage related equipment	Voltage related equipment
Surge Arrester	Voltage related equipment	Voltage related equipment

Table 4.3.6 displays the line ratings for the Apollo – Croydon 275 kV overhead transmission line. In addition, the current rating of the limiting pieces of terminal equipment (2500A) is below the designed ratings of the line. This limits the maximum power flow, as the transmission line cannot operate at the designed ratings.

Table 4.3.6: Apollo – Croydon line ratings

Line	Conductor rating (A) Quad Zebra			Busbar rating (A) Twin bull			Terminal equipment (A)
Apollo – Croydon 275 kV	Rate A	Rate B	Rate C	Rate A	Rate B	Rate C	Lowest equipment rating
	2775	3928	6464	2298	3306	6090	2500

The substation equipment ratings at Croydon substation are well below those of line rating A, B and C. The substation equipment thermally limits this line. The ratings show that the majority of the equipment including busbars are underrated and cannot support the ratings of the line. This result in a thermal constraint and an economic decision must be made as to whether loss in equipment life to support thermal uprating is acceptable, or to invest capital to replace underrated equipment to match line ratings. Assessment of the ratings of both substations reveals that there is benefit in replacing the underrated substation equipment only at Croydon substation to alleviate congestion and to support higher power transfers and line ratings. Substation equipment can be replaced to match line rating B of 3928 A. Higher ratings for busbars also need to be determined.

Note: Un-used spare capacity already exists on the Apollo – Croydon 275 kV transmission line.

4.4 ESSELEN – JUPITER 275 KV THERMAL ANALYSIS

The Esselen – Jupiter line is approximately 36.53 km and the third line considered for thermal uprating. Figure 4.4.1 displays the topography of the line obtained from TxSIS. Four weather stations were installed at pre-identified spans at which the temperature of the conductor was also measured for the red, white and blue phases. The spans where the equipment was installed are:

- Spans 5 – 6 (3 temperature sensors and 1 weather station),
- Spans 125 – 126 (3 temperature sensors and 1 weather station,
- Spans 149 – 150 (3 temperature sensors and 1 weather station),
- Spans 182 – 183 (12 temperature sensors and 1 weather station).

The same rationale for the number of temperature sensors installed was used as defined in Section 4.2.1.

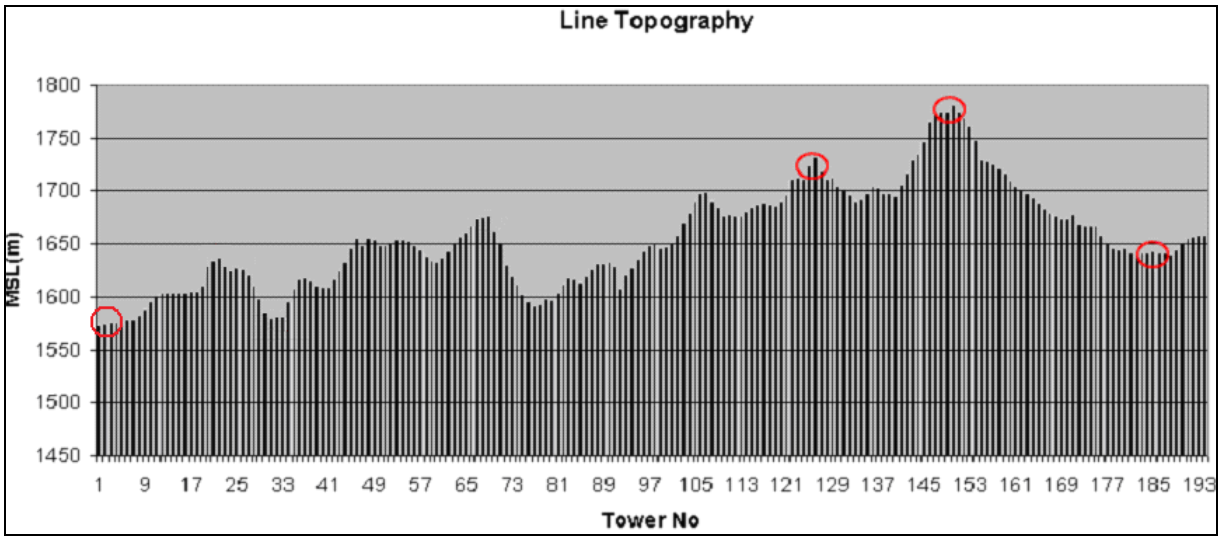

Figure 4.4.1: Line topography of Esselen – Jupiter 275 kV

Figures 4.4.2 to 4.4.7 display the conductor temperature measured during the LIDAR survey for the Esselen – Jupiter 275 kV line that took place on 29 January 2011 from

approximately 10:00 to 12:30. The figures show that the maximum operating temperature was experienced at spans 5 – 6 which was around 39 ℃. The rest of the spans experienced maximum temperatures that ranged between 30 ℃ to 39 ℃. On average, the minimum temperature is consistent across all the monitored spans with an average minimum of around 15 ℃. The templated temperature of 50 ℃ was never reached.

The temperature sensors overall measured the temperature of the conductor for a duration of approximately 1 month from 10 January 2011 to 18 February 2011. The results for the duration of the installation are displayed in Annexure D. In addition, weather stations were used to measure the weather parameters during the 1 month period at each section where the temperature measurements took place. The conductor temperature measured during the LIDAR survey is used to calibrate the representative PLS CADD model for the Esselen – Jupiter line. The calculated temperature as per PLS CADD and Mathcad is verified by the measured temperature.

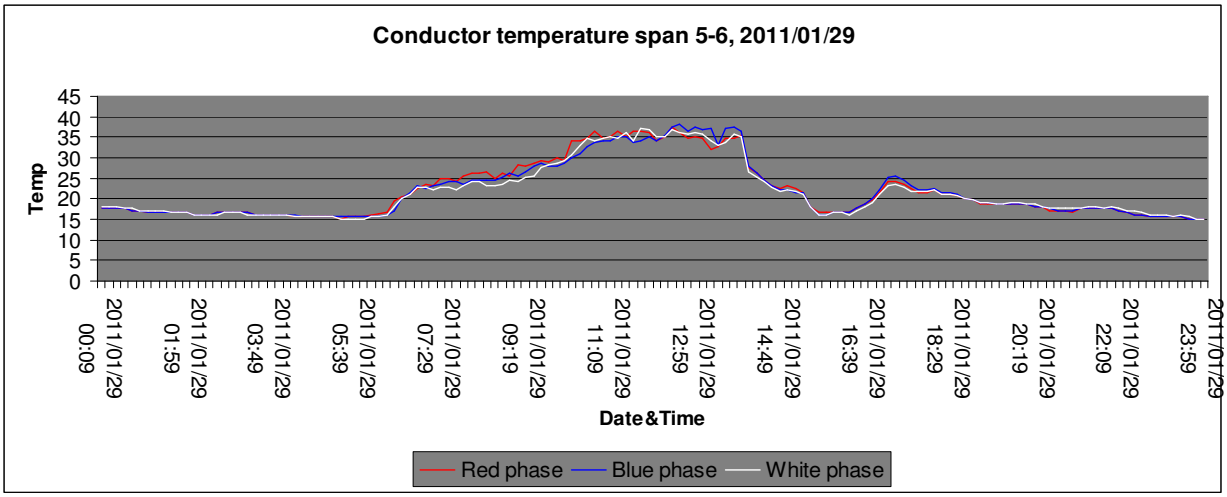

Figure 4.4.2: Actual measured conductor temperature, spans 5–6

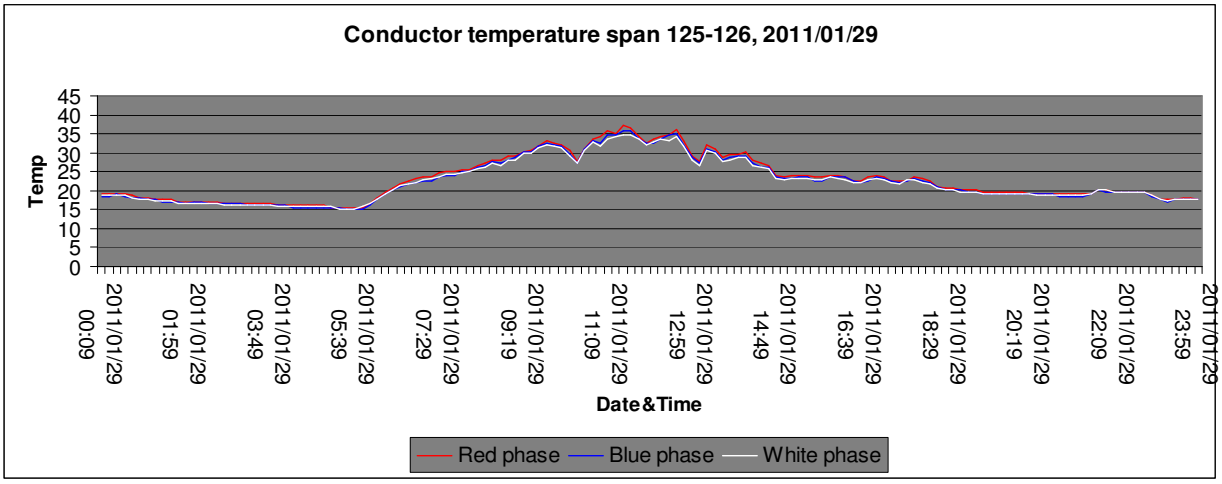

Figure 4.4.3: Actual measured conductor temperature, spans 125–126

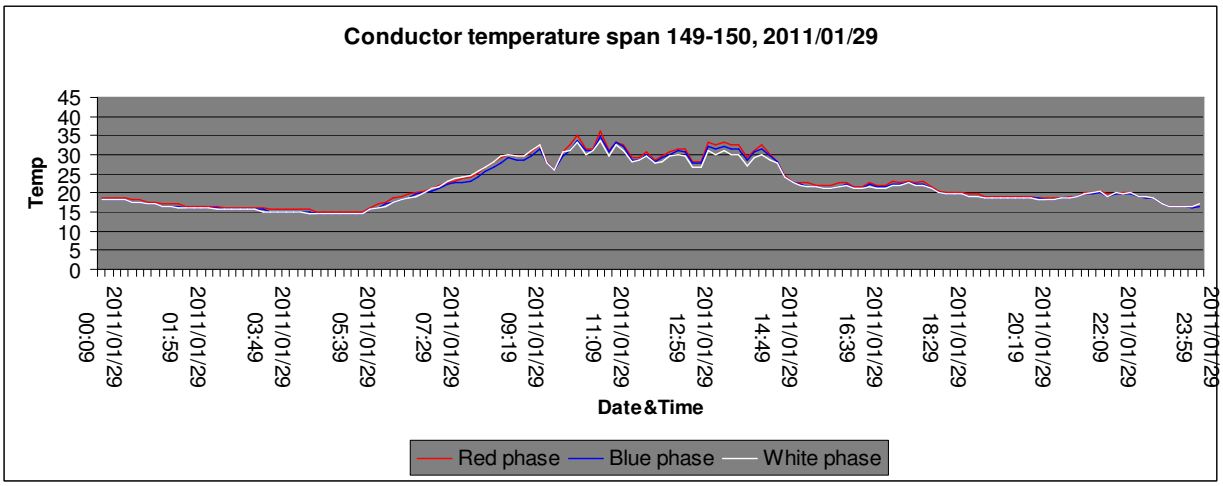

Figure 4.4.4: Actual measured conductor temperature, spans 149–150

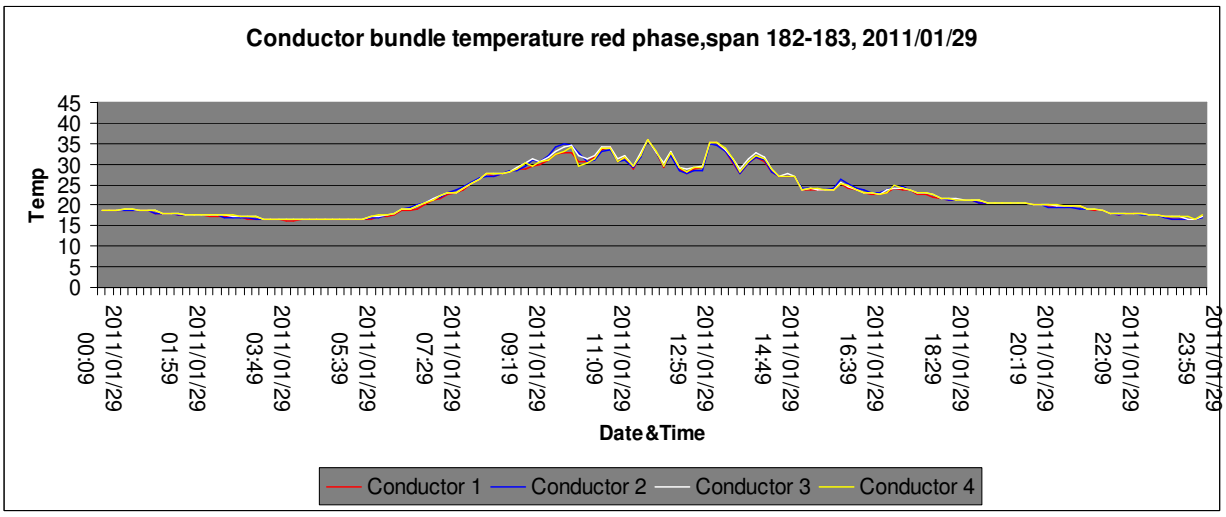

Figure 4.4.5:Actual measured conductor temperature red phase, spans 182–183

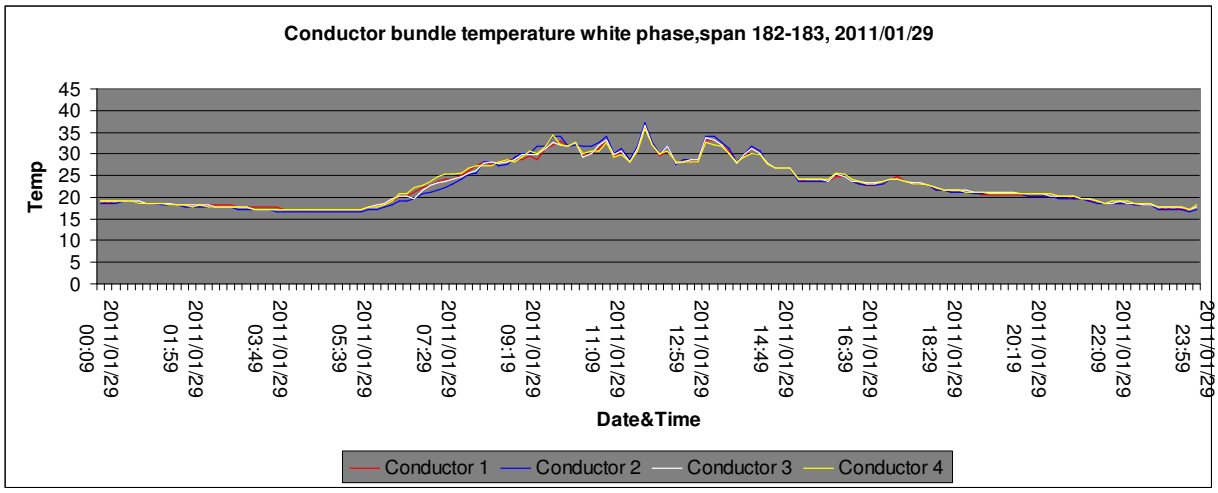

Figure 4.4.6: Actual measured conductor temperature white phase, spans 182–183

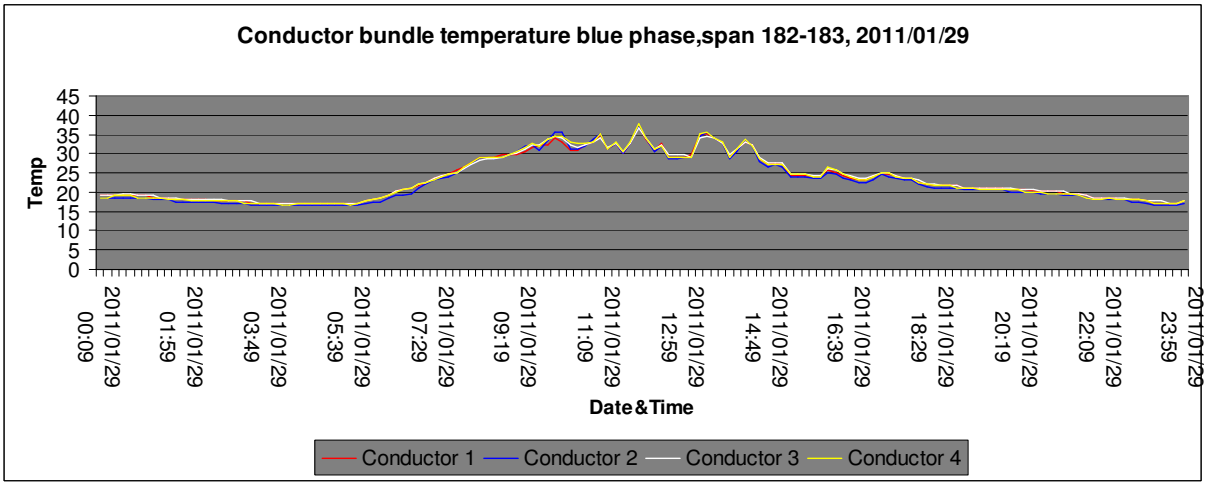

Figure 4.4.7: Actual measured conductor temperature blue phase, spans 182–183

Table 4.4.1 displays the comparison between the measured conductor temperature during the survey and the temperature calculated with Mathcad and PLS CADD for the various spans. The results in Table 4.4.1 show a good agreement between the temperatures measured and those obtained by means of calculation.

Table 4.4.1: Temperature comparison for Esselen – Jupiter 275 kV

	Span 5-6			Span 125-126		
	PLS CADD	**Mathcad**	**Measured**	**PLS CADD**	**Mathcad**	**Measured**
Wind speed (m/s)	2	2	2	2	2	2
Direction/Angle with conductor	34	34	34	10	10	10
Ambient Temperature (℃)	22.7	22.7	22.7	24.3	24.3	24.3
Solar radiation (Watt/m²)	891	891	891	1100	1100	1100
Load current (A)	649	649	649	618	618	618
Single conductor current (A)	162.25	162.25	162.25	154.5	154.5	154.5
Conductor height above MSL (m)	1500	1500	1500	1500	1500	1500
Conductor Temperature (℃)	29.4	29.5	30.2	35.7	35.49	35.63
	Span 149-150			**Span 182-183**		
	PLS CADD	**Mathcad**	**Measured**	**PLS CADD**	**Mathcad**	**Measured**
Wind speed (m/s)	3	3	3	4	4	4
Direction/Angle with conductor	44	44	44	17	17	17
Ambient Temperature (℃)	22.4	22.4	22.4	22.9	22.9	22.9
Solar radiation (Watt/m²)	1167	1167	1167	1125	1125	1125
Load current (A)	598	598	598	626	626	626
Single conductor current (A)	149.5	149.5	149.5	156.5	156.5	156.5
Conductor height above MSL (m)	1500	1500	1500	1500	1500	1500
Conductor Temperature (℃)	28.7	28.49	28.79	30	29.22	30.12

4.4.1 **Esselen – Jupiter line ratings**

The Esselen – Jupiter line consists of a triple layer zebra conductor in a quad bundle arrangement for each phase with a templated temperature of 50 ℃. Table 4.4.2 displays the thermal ratings for the conductor used on the Esselen – Jupiter transmission line. The ratings dictate the maximum permissible current rating for various templating temperatures.

Table 4.4.2 Thermal ratings for zebra conductor at different templating temperatures

ACSR Triple Layer				
Percentage		8.60%	42.97%	70.05%
Probability		1.05E-06	5.25E-06	8.56E-06
Triple		**Rate A**	**Rate B**	**Rate C**
ZEBRA	50	694	982	1616
ZEBRA	60	817	1124	1760
ZEBRA	70	916	1243	1889
ZEBRA	80	1003	1344	2018

Figure 4.4.8 displays the 24-hour loading or current flow of the line for the day that the LIDAR survey took place. The loading of the line during the time of the survey is circled in red. The comparison between the measured and calculated temperature results for this instance is documented in Table 4.4.3. The thermal ratings in table 4.4.2 are compared with the loading of the line presented in Figure 4.4.8 that is regarded as the existing loading of the line. For example, the time for comparison is chosen at approximately 18:00 from Figure 4.4.8 when the loading on a line is usually higher due to the demand for electricity during peak periods. The results are summarised in Table 4.4.3.

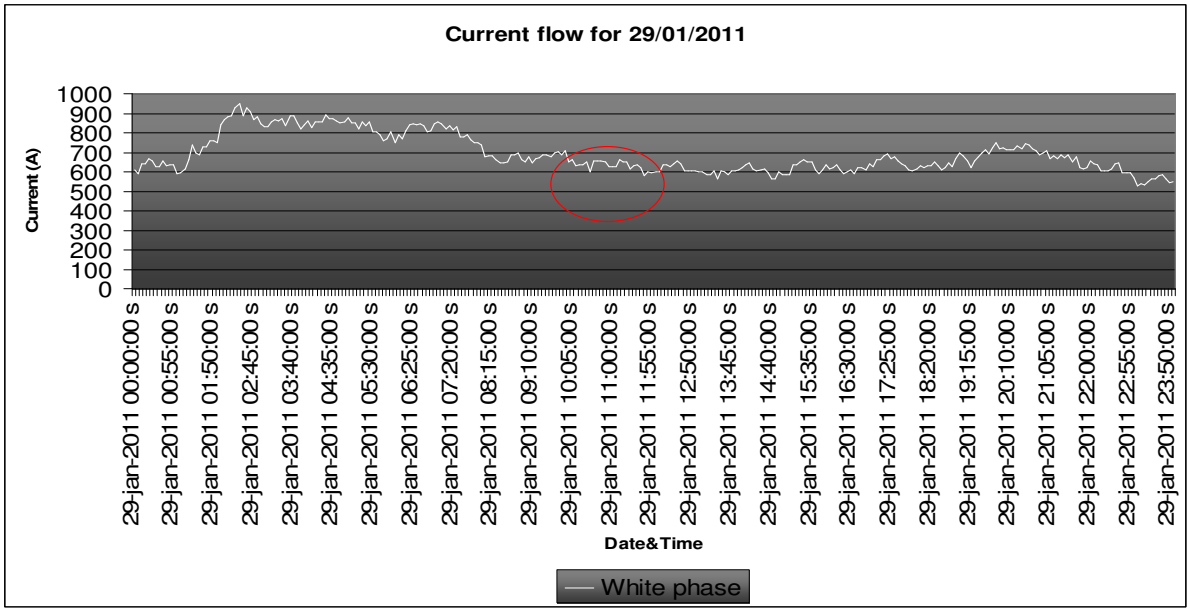

Figure 4.4.8: Actual loading of Esselen – Jupiter on day of survey

The results obtained for the conductor temperature from PLS CADD, Mathcad and the sensors show reasonable agreement. The loading of the line in Figure 4.4.8 suggests that at 612 A the line was operated at a loading level lower than rating A. The measured temperature during this time was on average approximately 22 ℃ with a loading of 612 A. This temperature was obtained during the continuous measurement of weather parameters and was used for both the Mathcad and PLS CADD temperature calculations. If the present loading of the line is compared with the thermal ratings in table 4.4.2, it shows that the line is underutilised.

Table 4.4.3: Temperature comparison for Esselen – Jupiter at a different loading

	Span 5-6			**Span 125-126**		
	PLS CADD	**Mathcad**	**Measured**	**PLS CADD**	**Mathcad**	**Measured**
Wind speed (m/s)	3	3	3	7	7	7
Direction/Angle with conductor	14	14	14	14	14	14
Ambient Temperature (℃)	20.2	20.2`	20.2	20.3	20.3	20.3
Solar radiation (Watt/m²)	153	153	153	44	44	44
Load current	612	612	612	612	612	612

(A)						
Single conductor current (A)	153.2	153.2	153.2	153.2	153.2	153.2
Conductor height above MSL (m)	1500	1500	1500	1500	1500	1500
Conductor Temperature (℃)	22.1	18.3	21.8	21.2	19.7	22.65
	Span 149-150			**Span 182-183**		
	PLS CADD	**Mathcad**	**Measured**	**PLS CADD**	**Mathcad**	**Measured**
Wind speed (m/s)	7	7	7	7	7	7
Direction/Angle with conductor	37	37	37	37	37	37
Ambient Temperature (℃)	20.4	20.4	20.4	20.4	20.4	20.4
Solar radiation (Watt/m²)	42	42	42	42	42	42
Load current (A)	612	612	612	612	612	612
Single conductor current (A)	153.2	153.2	153.2	153.2	153.2	153.2
Conductor height above MSL (m)	1500	1500	1500	1500	1500	1500
Conductor Temperature (℃)	20.9	20.69	21.2	20.8	20.8	21.93

4.4.2 **Esselen – Jupiter substation equipment ratings**

This section discusses the substation equipment ratings of both Esselen and Jupiter substations. Table 4.4.4 displays the 275 kV equipment ratings at Esselen substation. The thermal limits, short circuit current rating and the MVA ratings are displayed. The highest current rating is that of the circuit breaker. The remaining equipment all have equal current ratings. Based on the power equipment ratings at Esselen substation the line can operate safely at line rating A. Rating B for the line is 1871 MVA or 3928 A, which means that the circuit breaker and busbars at Esselen are the only pieces of equipment that can support line-rating B.

Table 4.4.4: Esselen substation equipment ratings

Equipment	Thermal ratings	MVA rating
Isolator BB1	3150A, 50 kA, 1s	1500 MVA
PG Isolator BB2	3150A, 50 kA, 1s	1500 MVA
Circuit breaker	4000A, 50 kA, 1s	1905 MVA
Current transformer	3150A, 50 kA, 1s	1500 MVA
Isolator line	3150A, 50 kA, 1s	1500 MVA
Line trap	3150A, 40 kA,1s	1500 MVA
Capacitor voltage transformer	Voltage related equipment	Voltage related equipment
Surge Arrester	Voltage related equipment	Voltage related equipment

Note: The rated duration for fault currents of substation equipment were obtained from Eskom specification TSP41-595 [63], IEC 60694:2002 [64], IEEE Std C37.06:2009 [54].

Table 4.4.5 displays the 275 kV ratings at Jupiter substation. The thermal limits, short circuit current rating and the MVA rating are displayed. The current ratings of the power equipment at Jupiter substation vary but the highest rating is that of the circuit breaker and the lowest that of the current transformer. The busbar configuration at Esselen is triple bull and the configuration at Jupiter is twin bull.

Table 4.4.6 displays the line ratings for the Esselen – Jupiter 275 kV overhead transmission line. The substation equipment ratings at Esselen substation are much higher than the equipment ratings at Jupiter substation. As explained, the power equipment at Esselen substation are suitable to support line rating A. However, a bottleneck exists at Jupiter substation because the equipment is underrated and line rating A is not achievable.

Table 4.4.5: Jupiter substation equipment ratings

Equipment	Thermal ratings	MVA rating
Isolator BB1	2500A, 31.5 kA,1s	1191 MVA
Isolator BB2	2500A, 31.5 kA, 1s	1191 MVA
Circuit breaker	3150A, 50 kA,1s	1500 MVA
Current transformer	2150A, 50 kA, 1s	1024 MVA
Isolator line	2500A, 31.5 kA,1s	1191 MVA
Line trap	2500A, 40 kA,1s	1191 MVA
Capacitor voltage transformer	Voltage related equipment	Voltage related equipment
Surge Arrester	Voltage related equipment	Voltage related equipment

Table 4.4.6: Esselen – Jupiter line ratings

Line	Conductor rating (A) Quad Zebra			Busbar rating (A) Triple bull			Terminal equipment (A)
Esselen-Jupiter 275 kV	Rate A	Rate B	Rate C	Rate A	Rate B	Rate C	Lowest equipment rating
	2775	3928	6464	3386	4727	9617	2150

The substation equipment at Jupiter substation thermally limits the Esselen – Jupiter transmission line. The ratings show that the majority of the equipment is underrated and cannot support the ratings of the line. Evaluation of the ratings of both substations reveals that there is benefit in replacing the underrated substation equipment to alleviate bottlenecks to accommodate higher power transfers safely. It is recommended to replace underrated equipment to match line rating B of 3928 A.

4.5 CONCLUSION

Higher power transfers are thermally limited by substation equipment ratings. In most cases the ratings of substation equipment is well below that of the line rating. For this reason it is important to identify underrated terminal equipment within the transmission circuit on which additional capacity is needed. Operating underrated terminal

equipment above their designed rating will result in a loss of life, excessive equipment damage and premature failure. By replacing underrated terminal equipment with higher ratings, one can increase transfer capacity on the circuit. The operating temperatures of the lines discussed are well below those of the designed rating. This results in underutilisation of the transmission circuits. By increasing the operating temperature of these lines, higher power transfers are safely achievable.

Chapter 5
Conclusion and recommendations

In this chapter, conclusions are drawn from the results obtained in the previous chapter. An overview of the PLS CADD models, operating temperatures and the ability of the transmission circuits to safely support increases in thermal transfer capacity is provided. Finally, recommendations for future research in the thermal uprating of transmission lines and substation equipment are provided.

5.1 CONCLUSION

The electricity transmission system of South Africa is owned by Eskom and operated by the national system operator, a division within the power utility. This regulated company provides electricity to the whole of South Africa. Power generation margins are tight and this results in a requirement to construct additional generating and transmission capacity. Environmental pressures and the difficulty of obtaining new rights of way restrict the latter. The electricity demands of Eskom's customers are increasing, which turns thermally limited transmission systems into bottlenecks. The results obtained from this research provide a non-intrusive method to alleviate congestion in transmission circuits by unlocking unused thermal capacity. Power transfer is safely increased and older transmission networks are thermally uprated to operate closer to design limits.

The following key outcomes of this work can be summarised as follows:

- It has been found that Eskom's existing 275 kV transmission line network was designed conservatively and is operating at temperatures significantly below the temperatures for which they were designed.
- The present loading of the transmission lines in relation to the designed loading has been established.
- It has been shown that it is possible to unlock spare thermal capacity on heavy loaded transmission lines by means of a non-intrusive method.

- Conductor-to-ground clearances of the transmission lines under present loading from the “as is” condition of the lines have been obtained.
- Conductor sag and clearances under increased loading conditions have been identified.
- The sensitivity of transmission circuits towards prevailing weather parameters has been estimated.
- The response of the transmission lines and substation terminal equipment to short-time emergency loads when thermal uprating is implemented has been investigated.
- Thermal ratings of power equipment were compared with line ratings to identify underrated equipment.
- Justification has been provided to thermally uprate heavily loaded networks to alleviate congestion within power networks, if sufficient margin exists.

The following conclusions are based on the results obtained from the Jupiter – Prospect 275 kV transmission circuit:

- The three-dimensional PLS CADD model created from LIDAR data input results in accurate information on the terrain, towers, conductors, ground wires and any other obstacles along the surveyed right of way.
- The model is used to accurately assess the conductor-to-ground clearances under existing loading conditions and under increased loading conditions.
- The maximum operating temperature was approximately 37 ℃ and the minimum 14 ℃. The templated temperature of 50 ℃ was never reached. The measured temperature of each conductor within the bundle shows good agreement. This implies that the current sharing in each conductor within the bundle is equal as equal operating temperatures were estimated, calculated and measured.
- No under clearances or infringements exist under existing and increased loading conditions. Therefore, the condition and height of all the conductors above ground is acceptable. The line is a good candidate for thermal uprating

but that would depend on the rating of terminal substation equipment and their condition.

- The combination of operating temperature, electrical loading and the graphical sagging of conductors shows that the transmission line is underutilised. The operating temperature can be increased. The templated temperature of 50 ℃ for the Jupiter – Prospect line was never reached.
- The steady state behaviour of conductor temperature and electrical current based on weather conditions were determined and illustrate that capacity can be unlocked by using real-time weather parameters. Historical weather parameters used when determining initial thermal ratings result in conservative ratings.
- The substation equipment ratings of the Jupiter substation are well below those of the line ratings. The highest current rating is that of the circuit breaker (3150 A) and the lowest current rating is that of the current transformer (2000 A) followed by the pantograph line isolator (2400 A) of the second busbar. Based on the power equipment ratings the Jupiter – Prospect line could not operate at the designed line ratings due to underrated terminal equipment and is therefore thermally limited by the substation equipment.
- The substation equipment ratings of the Prospect substation are also well below those of the line ratings. However, the current ratings of this substation are all equal (2500A). Based on these power equipment ratings the Prospect substation could support operation at line rating A without any replacement of substation equipment.
- The limiting pieces of terminal equipment are mostly situated at Jupiter substation. By replacing underrated equipment, line ratings could be achieved and transfer capacity unlocked.
- The line ratings of the Jupiter – Prospect could be increased by re-templating the line. However, substation equipment must match increased line ratings to ensure safe and reliable power transfer.
- The power utility would rather replace underrated terminal equipment than operate substation equipment beyond nameplate values, which would adversely affect the security of supply.

The following conclusions are based on the results obtained from the Apollo – Croydon 275 kV transmission circuit:

- The three-dimensional PLS CADD model created from LIDAR data input results in accurate information on the terrain, towers, conductors, ground wires and any other obstacles along the surveyed right of way.
- The maximum operating temperature was experienced at spans 65 – 66, which was approximately 40 °C. The remaining monitored spans experienced maximum temperatures that averaged 35 °C with a minimum of 15 °C. The templated temperature of 50 °C was never reached under the measured weather parameters and loading conditions.
- Conductor clearances under existing conditions and under increased loading conditions are obtained by graphical sag analysis. The Apollo – Croydon line has a few of minor infringements under existing as well as increased loading conditions. This may be due to previous heavy loading or the age of the conductor. The conductor must be re-tensioned to obtain necessary clearances to accommodate higher power transfers.
- Material experts must be consulted to confirm if the conductor has annealed over time and must assess the tensile strength and condition of this conductor. This has to take place prior to re-tensioning. However, the age of the conductor shows that the phase conductors have reached the end of their lifetime. Only an in-depth analysis will reveal if the condition of the conductors limits the potential of increased power transfer. The condition of the current carrying clamps, joints and fittings must also be identified during the conductor assessment.
- If the conductors are found to be in an acceptable condition, they can be re-tensioned. This would result in the conductors being raised to obtain necessary clearances to support increased operating temperature.
- The combination of operating temperature, electrical loading and the graphical sagging of the conductors shows that the transmission line is underutilised even though the line has minor clearance infringements, as expected. The minor infringements are mostly due to their age and possibly the cumulative effects of annealing and creep. The infringements could be rectified by means of re-

tensioning the conductor. The operating temperature could then be increased. The templated temperature of 50 ℃ for the Apollo – Croydon line was never reached during the periods of high demand.

- The steady state behaviour of conductor temperature and electrical current obtained by PLS CADD thermal analysis illustrates that capacity could be unlocked by using existing weather parameters to determine higher ratings. Historical weather parameters used when determining initial thermal ratings result in conservative ratings for this line. If the conductor is re-tensioned, higher operating temperatures could be safely achieved.
- The substation equipment ratings of the Apollo substation are all equal to a rated value of 3150 A. Based on the power equipment ratings at Apollo substation the line could operate at line design rating A but could not support higher ratings without sacrificing loss of equipment life.
- The substation equipment ratings of the Croydon substation are well below those of line ratings A, B and C. The ratings show that the majority of the equipment including busbars are underrated and could not support the ratings of the line. Based on the power equipment ratings at Croydon substation the line could not operate at the designed ratings due to existing underrated terminal equipment and is therefore thermally limited. However, by replacing underrated equipment or by operating equipment at higher loadings for short periods with a small acceptable loss of equipment life, congestion could be alleviated.
- The substation equipment at both Apollo and Croydon thermally limits power transfer in relation to the line ratings. However, the equipment at Apollo can safely support line-rating A but the equipment at Croydon cannot. If the underrated equipment at Croydon is replaced to match the circuit breaker rating of 3150 A, a minimum of 630 A of transfer capacity could be unlocked. However, if underrated equipment is replaced to match line rating B current carrying capacity can be increased.

The following conclusions are based on the results obtained from the Esselen – Jupiter 275 kV transmission circuit:

- The three-dimensional PLS CADD model created from LIDAR data input results in accurate information on the terrain, towers, conductors, ground wires and any other obstacles along the surveyed right of way.
- The operating temperature for the Esselen – Jupiter line was obtained by means of direct measurement and compared with calculation.
- The energised conductors experienced maximum temperatures that range between 30 °C and 40 °C. The minimum temperature was consistent across all the monitored spans with an average minimum of 15 °C. The templated temperature of 50 °C was never reached.
- Conductor clearances under existing conditions and under increased loading conditions were obtained by means of graphical sag analysis. A few of infringements on the clearance line were reported under increased loading conditions. This was identified by the graphical sag analysis using PLS CADD. The conductors have to be re-tensioned to support higher operating temperatures.
- As in the case of the Apollo – Croydon line, the condition of the conductors on the Esselen – Jupiter line must be determined prior to re-tensioning. The condition of the current carrying clamps, joints and fittings must also be identified during the conductor assessment. This is accomplished by an infrared scan of the hardware. Re-tensioning would raise the height of the conductor above ground and increase clearance to accommodate higher operating temperatures.
- The combination of operating temperature, electrical loading and the graphical sagging of the conductors shows that the transmission line is underutilised even though the line has minor clearance infringements. The infringements could be rectified by re-tensioning the conductor. The templated temperature of 50 °C for the Esselen – Jupiter line was never reached during the periods of high demand.
- The steady state behaviour of conductor temperature and electrical current obtained by PLS CADD thermal analysis illustrates that capacity could be unlocked on the Esselen – Jupiter line. If conductor is re-tensioned, higher operating temperatures could be safely achieved.

- The substation equipment ratings of Esselen substation are matched to meet line rating A. The highest current rating is that of the circuit breaker and the other equipment has equal current ratings. Based on the power equipment ratings at Esselen substation the line can operate safely at line rating A. Rating B for the line is 3928 A, which means that the circuit breaker and busbars at Esselen are the only substation equipment that can safely support the B line-rating. Line ratings B and C could not be achieved without sacrificing equipment insulation and life. If operated for prolonged periods at ratings B and C the power equipment could prematurely fail due to over-heating.
- The current ratings of the power equipment at Jupiter substation vary but the highest rating is that of the circuit breaker and the lowest that of the current transformer.
- The busbar configuration at Esselen is triple bull and the configuration at Jupiter is twin bull. This limits power transfer as line ratings are not achievable.
- The majority of underrated equipment is within the Jupiter substation boundaries and cannot support the ratings of the line without sacrificing equipment insulation and lifetime. The security of supply is affected if equipment is operated for long periods beyond nameplate values. By replacing underrated equipment to match the highest equipment ratings, line ratings are still not achievable but thermal capacity is definitely unlocked.
- System operators must balance the risk of sacrificing equipment lifetime against customer demand. In a situation where loss of supply could be experienced the power utility would rather operate equipment beyond nameplate ratings before shedding load. A case where substation equipment is operated beyond nameplate ratings is mainly an economic decision.

The research documented in this dissertation has investigated the thermal uprating of transmission lines and substation equipment. The verification of conductor clearances under existing and increased loading conditions, 3D modelling, determination of conductor temperatures and thermal ratings of substation equipment has allowed an opportunity to remove thermal constraints and maximise the use of existing transmission assets. Using the results and information obtained from this research the

thermal uprating of transmission lines and substation equipment could easily be implemented and would prove to be beneficial to power utilities.

5.2 RECOMMENDATIONS

The following are the recommendations for future research:

- A thorough transmission network or line evaluation must always precede the decision to uprate existing transmission circuits. The “as is” condition must be established and conductor-to-ground clearances must always be assessed by following responsible engineering practice.
- If the line found to be a good candidate for thermal uprating, the reliability of compression joints, clamps and fittings must be checked,. The condition of the transmission line hardware and existing substation equipment must also be checked to ensure that it will accommodate any increases in transfer capacity. This can be verified for instance by means of infrared scanning of the equipment.
- The results show the suitability of LIDAR technology for collecting the necessary data with sufficient accuracy in a fast and reliable way. It could be a great advantage in determining the operating temperature of the conductor and the conditions of joints, fittings and clamps simultaneously from an airborne platform using infrared technology.
- The nameplate ratings of substation equipment do not represent the maximum loading capability of the equipment as the influence of the actual environmental parameters are not considered during operation. By evaluating the operating environment, loading limits can be determined which will take full advantage of the capability of the equipment before infringing on loss of insulation and equipment lifetime. Infra-red scanning of equipment can be performed to identify hotspots.
- By using the actual or local weather parameters along the right of way, increased thermal ratings for both conductors and substation equipment can be determined.

- Real-time monitoring of environmental weather conditions can enhance thermal ratings for transmission circuits. Real time ratings reflect the actual capability of the transmission line at any given time.
- If re-tensioning is needed to obtain sufficient clearances for higher thermal ratings, the structural integrity of towers should be checked against existing design methodologies.
- Operating the existing 275 kV network at a higher voltage, for example 300 kV, would increase the MVA loading without increasing the current.
- The possibility of uprating and re-conductoring existing lines with high temperature and low sag conductors (HTLS) without modifying existing structures must be investigated. The electrical losses at very high operating temperatures must also be determined. Economic justification is needed for the use of HTLS conductors.
- It may not always be practical to uprate substation equipment. However, in some cases, where increased capacity is required and the expansion of substations is restricted due to lack of space, existing equipment should be replaced.
- Substation equipment studies with the scope of identifying and implementing methods of safely uprating existing equipment and their practical demonstration would be a valuable addition to the research documented in this dissertation.
- A power transformer is the most expensive piece of equipment within the substation boundaries. It is recommended that there should be close collaboration with manufacturers when intending to increase capacity in a transformer. Historical loading criteria must be identified if the equipment has been underutilised. Original design calculations are also needed. Methods of increasing capacity within power transformers would for instance be to add bigger radiators and fans for cooling. For a short term solution where a unit is oil cooled additional pumping and cooling of oil may increase capacity. A longer term solution would imply an additional or larger transformer.
- Most Eskom transmission transformers are only loaded to approximately 40% where two transformers are operated in parallel and 60% if three transformers

are used. If transformers have ONAN cooling they can be changed to ONAF, creating 25% more capacity by adding cooling fans.

- Current transformers are used for metering, protection and relaying purposes. Uprating CT's is normally not possible. However, in many cases it would be easier and more economical to replace the device.
- Line traps are mainly used for power line carrier protection and communication. A line trap is a current rated device and is not designed to operate at higher than nameplate ratings. Short-time emergency loadings for line traps were identified in this dissertation. Replacement of this component might be the best solution to increase capacity.
- This research revealed that circuit breaker ratings are generally higher than existing line ratings. Increasing transmission line ratings may require increased circuit breaker ratings. Existing circuit breakers can be uprated with the cooperation of manufacturers.
- It is recommended to replace underrated circuit breakers with new circuit breakers to accommodate higher fault currents.
- The influence of demand side management (DSM), relative to uprating of transmission lines and substation equipment has not been discussed. However it could be possible to short term overload transmission circuits to assist with maintenance.

REFERENCES

[1] R. Stephen, “Description and evaluation of options relating to the uprating of overhead transmission lines”, presented at the CIGRE conference, Paris, France, 2004, Paper B2-201.

[2] J.M. Zulu, “A real-time monitoring system for the optimisation of power transmission line’s loading capabilities”, M.Sc thesis, University of Warwick, United Kingdom, 2002.

[3] R. Inglesi, A. Pouris, “Forecasting electricity demand in South Africa: A critique of Eskom’s projections”, South African Journal of Science, 106(1/2), Art. #16, 4 pages. DOI: 0.4102/sajs. V106i1/2.16, 2010.

[4] Integrated report, Eskom Holdings SOC Limited, South Africa, 2010. [Online]. Available: http://www.financialresults.co.za/2010/eskom_ar2010

[5] P. Lloyd, B. Cowan, N. Mohlakoana, “Improving access to electricity and stimulation of economic growth and social upliftment”, Energy Research Centre, University of Cape Town, Rondebosch, 2004.

[6] J. Swan, “Determination of conductor ampacity – a probabilistic approach”, Magister technology dissertation, School of electrical engineering, Vaal Triangle Technicon, 1994.

[7] A.R. Fitzpatrick, G.A. Davidson, “Increasing the capacity of transmission line systems”, Proceedings of the American Power Conference, Volume 1, USA, p288, 1992.

[8] Siemens Power Technology International, Overhead transmission line uprating training course notes, unpublished.

[9] P.S. van Staden, K. Thejane, E. Mathebula, “275 kV Thermal line uprating study”, Eskom Research, Test and Development, Technical Report. PRJ10-01322700-3632, 20 April 2010.

[10] B Dalle, N Bell, Study committee SC B2 CIGRE, Action plan of CIGRE study committee B2, “Overhead lines”, March 2006.

[11] Increased Power Flow Guidebook: Increasing Power Flow on Transmission and Substation Circuits. EPRI, Palo Alto, CA: 1010627, 2005.

[12] Eskom Holdings SOC Ltd, “The planning, design and construction of overhead power lines”, Crown publications, South Africa, Johannesburg, February 2005.

[13] Working Group SC 22-12 CIGRE. “Probabilistic determination of conductor current rating”, Electra No. 164, pp.103-119, February 1996.

[14] B Chakrabarti, C. Callaghan, V. Krichtal, D. Goodwin, M. Mistry, “Beat the heat”, IEEE Power and Energy, pp. 67-71, 2011.

[15] J. Seymour, T. Horsley, “The seven types of power problems”, American power conversion, 2005. [Online]. Available:http://www.apc.com/prod_docs/ results.cfm?DocType=White%20Paper&Query_Type=3&Value=21

[16] J. Duncan Glover, M.S. Sarma, “Power system analysis and design”, 3rd edition. Pacific Grove. California: Brooks and Cole, 2002.

[17] Mrinal K Pal, “Lecture notes on power system stability”, Edison, New Jersey, June 2007, unpublished.

[18] A. Xémard, S. Dennetière, I. Uglesic, V. Milardic, B. Milesevic, P. Grand, F. Sauvegrain, P. Stevenin, M. Mesic, “The protection against lightning of an overhead line uprated from 225 kV to 400kV”, presented at the International Conference on Power Systems Transients, Kyoto, Japan June 2009.

[19] V.J. Gosbell, “Harmonic distortion in the electric supply system”, Integral power quality centre, Technical note No 3, March 2000, unpublished.

[20] R. D Dunlop, R. Gutman, and P. P. Marchenko, “Analytical Development of Loadability Characteristics for EHV and UHV Transmission Lines.” IEEE Transactions on Power Apparatus and Systems. Volume 98. Number 1.pp. 606-617, March/April 1979.

[21] H. P. St. Clair, “Practical Concepts in Capability and Performance of Transmission Lines.” AIEE Transactions on Power Apparatus and Systems. Volume 72. Part III. pp. 1152-1157, December 1953.

[22] Central station engineers, Electrical transmission and distribution reference book, 4th edition. East Pittsburgh. Pennsylvania: Westinghouse Electric Corporation, 1964.

[23] R Dugan, M. McGranaghan, S. Santoso, H. Beaty, “Electrical power systems quality”, 2nd edition. New York: McGraw-Hill, 2002.

[24] EPRI AC Transmission Line Reference Book—200 kV and Above, Third Edition. EPRI, Palo Alto, CA: 1011974, 2005.

[25] A.A. Nimje, C. Kumar Panigrahi, A.Kumar Mohanty. “Enhanced power transfer capability by using SSSC”. Journal of Mechanical Engineering Research. Vol. 3 (2), pp. 48-56, February 2011. Available: http://www.academicjournals.org/jmer

[26] N. Ritter, P. Bird. Course note 238 Module 8, Topic: “Generator and line stability”, unpublished. Available: http://*www.nuceng.ca/canteachmirror/library/20042908.pdf*

[27] B. Dolly, M. Anthony, G. Hurford,” Practical Implementation of Probabilistic Line Ratings in an Operational Environment,” System Operations and Planning Division, Eskom, unpublished.

[28] S.P. Hoffmann, A.M. Clark, “The approach to thermal uprating of transmission lines in the UK,” presented at the CIGRE conference, Paris, France, Paper B2-317, 2004.

[29] R.C. Hibbeler, “Mechanics of materials”, 6th edition. Upper Saddle River. New Jersey: Pearson Prentice Hall, 2005.

[30] M.Tullmin, “Galvanic corrosion,” corrosion-club.com, para. 4, 2001. [Online]. Available: http://www.corrosion-club.com/images/corrosioncell.gif/. [Accessed: February, 28, 2012].

[31] Electrical connections for power circuits, facilities instructions, standards and Techniques 3-3 11/91, August, 2000.

[32] Working group B2.12, “Conductors for the uprating of overhead lines,” February 2004.

[33] AA Burger, H. Vosloo, E. Shunmagum, Determination of conductor current ratings within Eskom, Unique standard identifier EST32-319, February, 2009.

[34] Electrical Machinery regulations 15, Clearance of power lines- minimum clearances, Operational safety Act 85 of 1983.

[35] Working Group SC 22-12 CIGRE. “The thermal behaviour of overhead conductors section 1 and 2: Mathematical modelling for evaluation of conductor temperature in the steady state and the application thereof,” Electra No. 144, pp. 107 – 125, October, 1992.

[36] V.T. Morgan, “The thermal rating of overhead line conductors, Part 1: the steady state thermal model”. International Journal of Electrical Power Systems Research. pp. 119 – 139, 1982.

[37] A.P.B. Kersting, M. Müller, J.N. Hoffmann, “Transmission line uprating design using survey data from airborne LIDAR,” presented at the CIGRE conference, Paris, France, Paper B2-D2-317, 2004.

[38] Power line system incorporated, Power line computer aided design and drafting, Version 10.6, 2010.

[39] Dallas Semiconductor, DS1920 Temperature iButton®, 19-4886 Rev 8/09, pp 1 – 22, 2009.

[40] J.H. Cronin, R.S. Bayliss, “Rate substation equipment for short-time overloads”, Electrical world, Transmission and Distribution. pp. 44 -47, 15 April 1972.

[41] I.S. Benko, D.E. Cooper, D.O. Craghead, P.Q. Nelson. “Loading of substation electrical equipment with emphasis on thermal capability Part II – application.” Presented at IEEE PES Winter Meeting, New York, January. 1978.

[42] Eskom Holdings SOC Ltd, “Theory, design, maintenance and life management of power transformers,” Crown publications, South Africa, April, 2008.

[43] IEC standard 60076-2, “Loading guide for oil-immersed power transformers”, 2005.

[44] ANSI standard. C57.91. Annex B. “Effect of loading transformers above rating on, tap changers, and auxiliary components”, 1995b.

[45] IEC standard 60044-1, Instrument transformers, 2003.

[46] ANSI. Standard C57.13-1993. Requirements for instrument transformers, 1993.

[47] PJM, PJM interconnection task force of the transmission and substation subcommittee, “Guide for determination of current transformers ratings”, February 1999.

[48] ABB, Application Guide, ABB instrument transformers. [Online]. Available: http://www05.abb.com/.../1hsm%209543%204000en%20it%20application%20guide%20ed3.pdf

[49] IEC standard 60044-2, Instrument transformers Part 2: Inductive voltage transformers, 2003.

[50] IEEE committee report, “New IEEE temperature limitations for disconnecting switches,” IEEE Trans. Power Apparatus and Systems, Vol. PAS-88, No. 09, pp. 1412 – 1423, Sept. 1969.

[51] ANSI standard C37.37, Loading guide for AC high- voltage air switches in excess of 1000 volts, 1979.

[52] ABB, Application Guide, ABB circuit breakers. [Online]. Available: http://www05.abb.com/global/scot/scot209.nsf/.../$file/1sxu400142m0201.pdf

[53] B.J. Conway, D.W. McMullen, A.J. Peat, J.M. Scofield, “Loading of substation electrical equipment with emphasis on thermal capability, Part 1 – Principles,” IEEE Trans. Power apparatus and systems. Vol. PAS-88. No. 4. pp. 1394 – 1402, August. 1979.

[54] IEEE standard C37.06, AC high-voltage circuit breakers, 2009.

[55] ANSI. standard C93.3, Requirements for power line carrier line traps, 1981.

[56] PJM, PJM Interconnection Planning and Engineering Committee. “Air disconnect switch ratings.” February 1999.

[57] PJM, PJM Interconnection Planning and Engineering Committee, “Guide for determination of line trap normal and emergency ratings.” August 1999.

[58] IEC standard 60076-7, Loading guide for oil immersed power transformers, 2005

[59] IEC standard 60076-1, Power transformers – General 2011.

[60] IEEE Power Africa 2012 Conference tutorial notes, Power transfer capacity of overhead lines, July 2012.

[61] NRS standard 048-2, Electricity supply – Quality of supply, Part 2: Voltage characteristics, compatibility levels, limits and assessment methods, 2003.

[62] Eskom internal directive EED 15/6/1-1 Thermal limits of transmission line and busbar conductors, 1970.

[63] Eskom specifications TSP41-595, Power line carrier line traps and associated post support insulators, November 2008.

[64] IEC Standard 60694, Common specifications for high voltage switchgear and controlgear standards, 2002.

[65] P.S. van Staden, J.A. de Kock, “The practical comparison of conductor operating temperatures against IEEE and CIGRE ampacity calculations”, IEEE PES PowerAfrica 2012 Conference and Exposition, July 2012.

ANNEXURE A: – WEATHER MONITORING EQUIPMENT

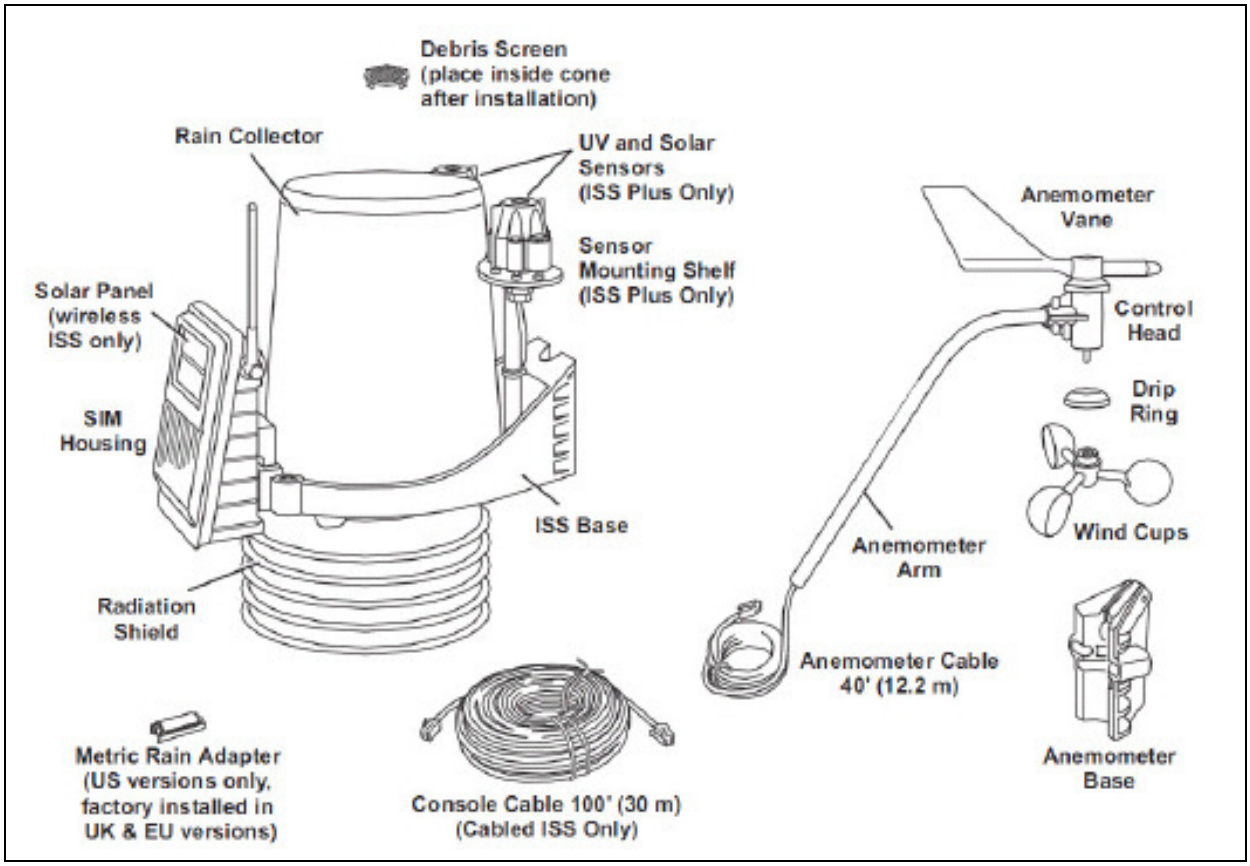

Figure A1: Weather monitoring inventory

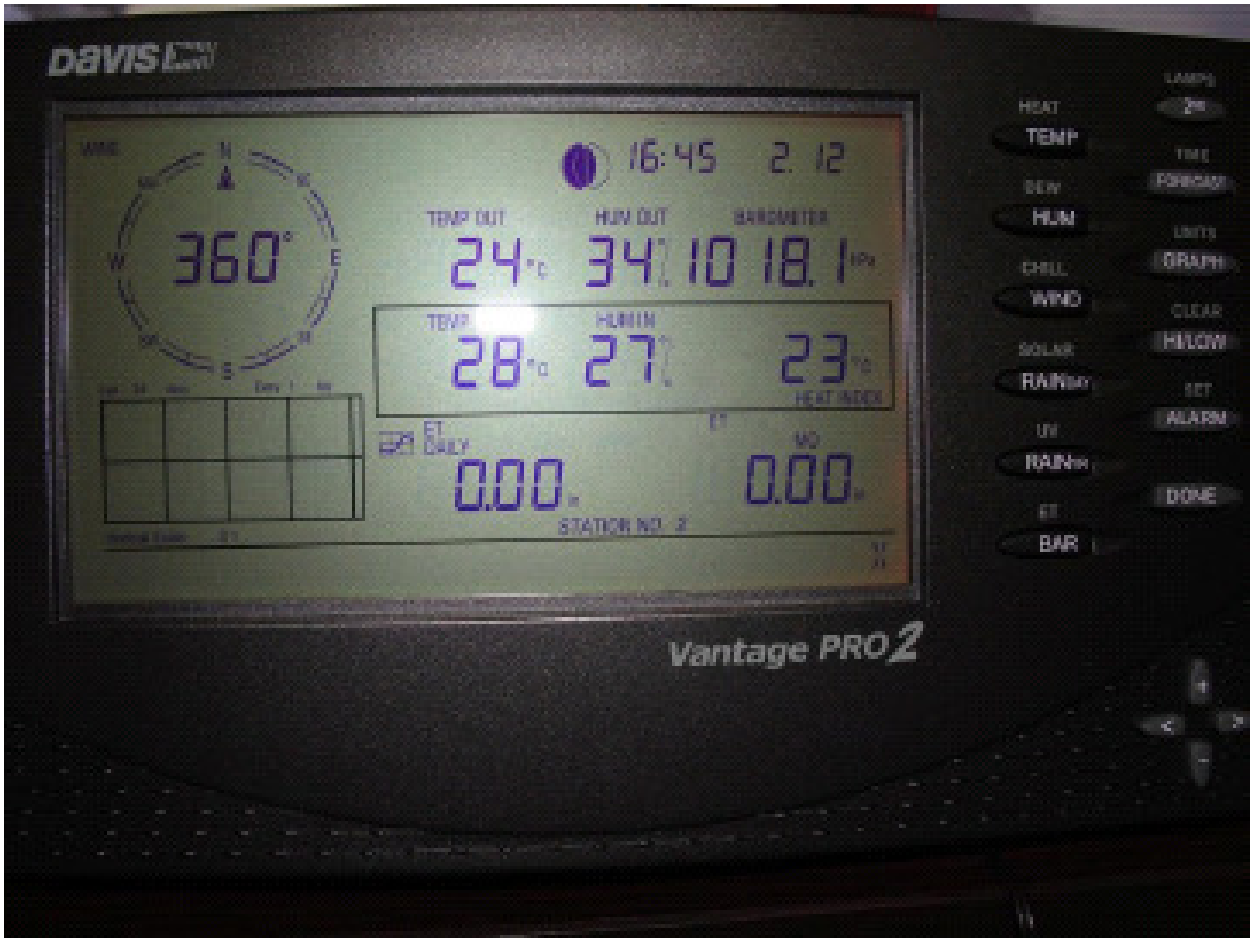

Figure A2: Weather console displaying weather data

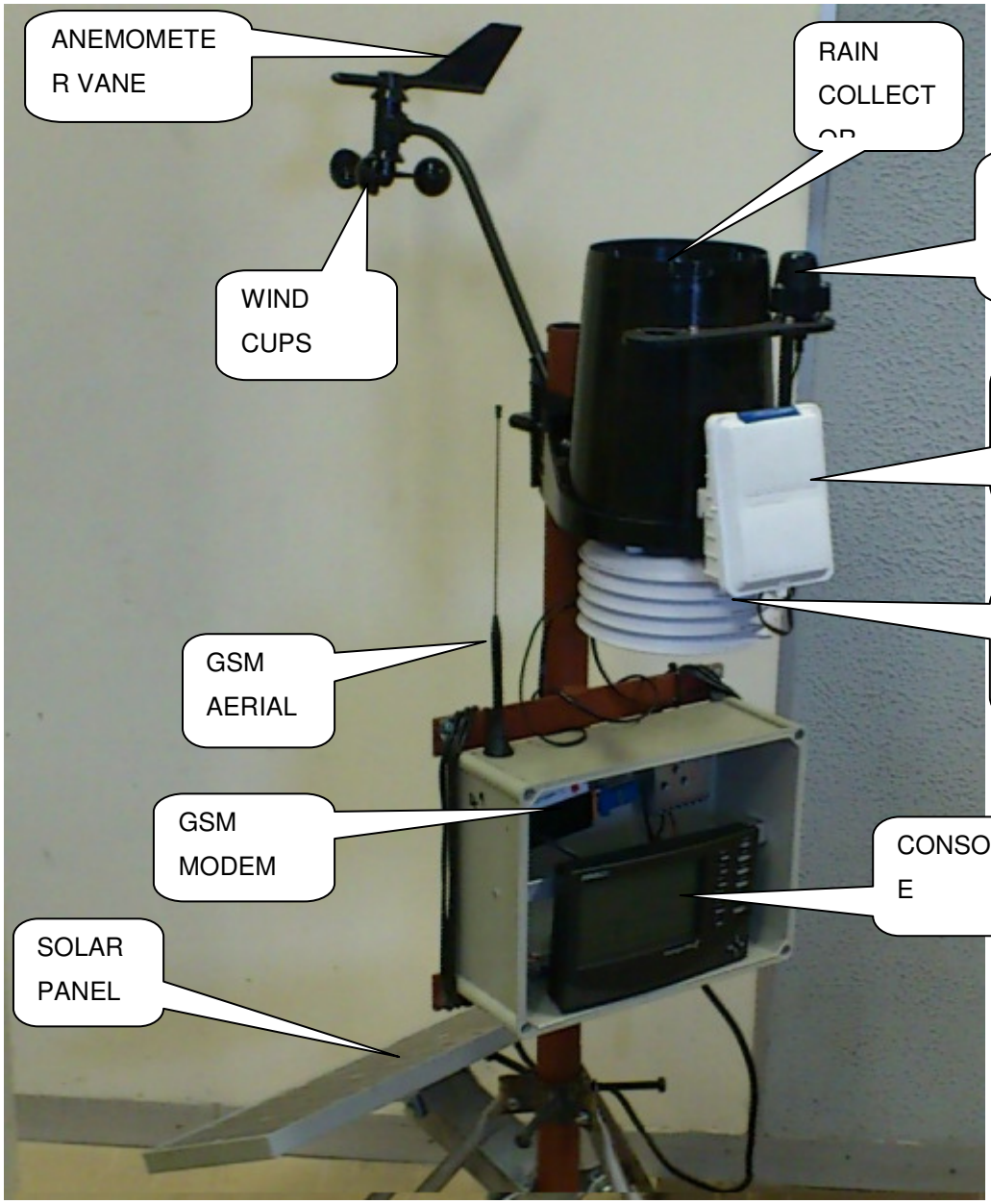

Figure A3: Weather station on tripod assembly

ANNEXURE B: APOLLO – CROYDON TRANSMISSION LINE MODEL

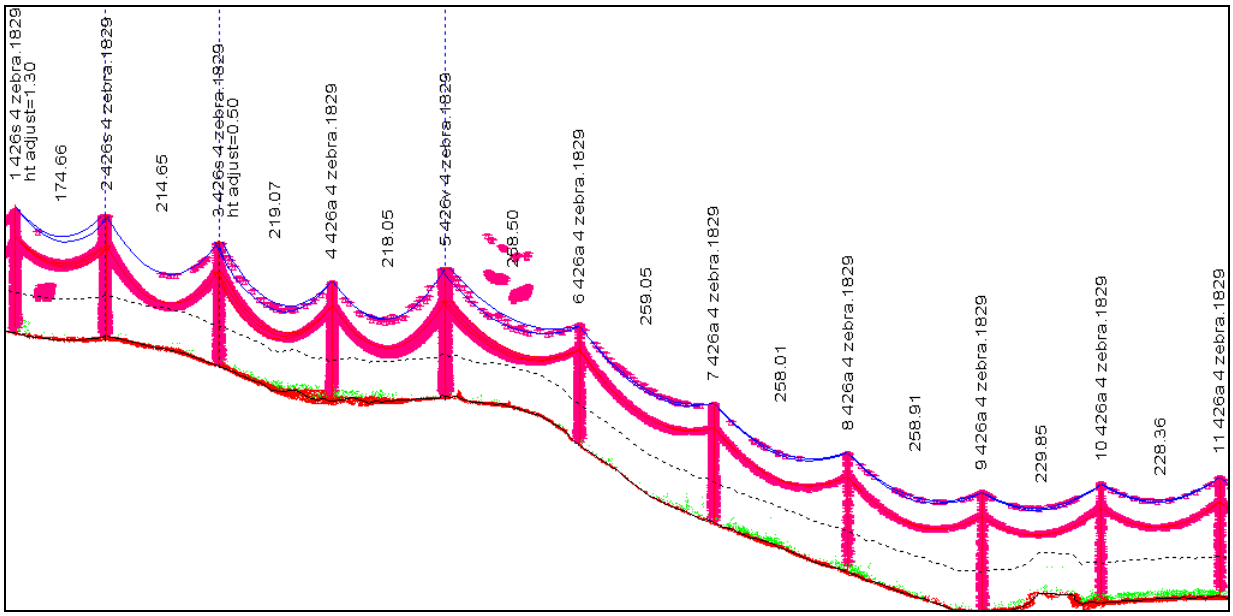

Figure B1: Transmission line model towers 1 – 11

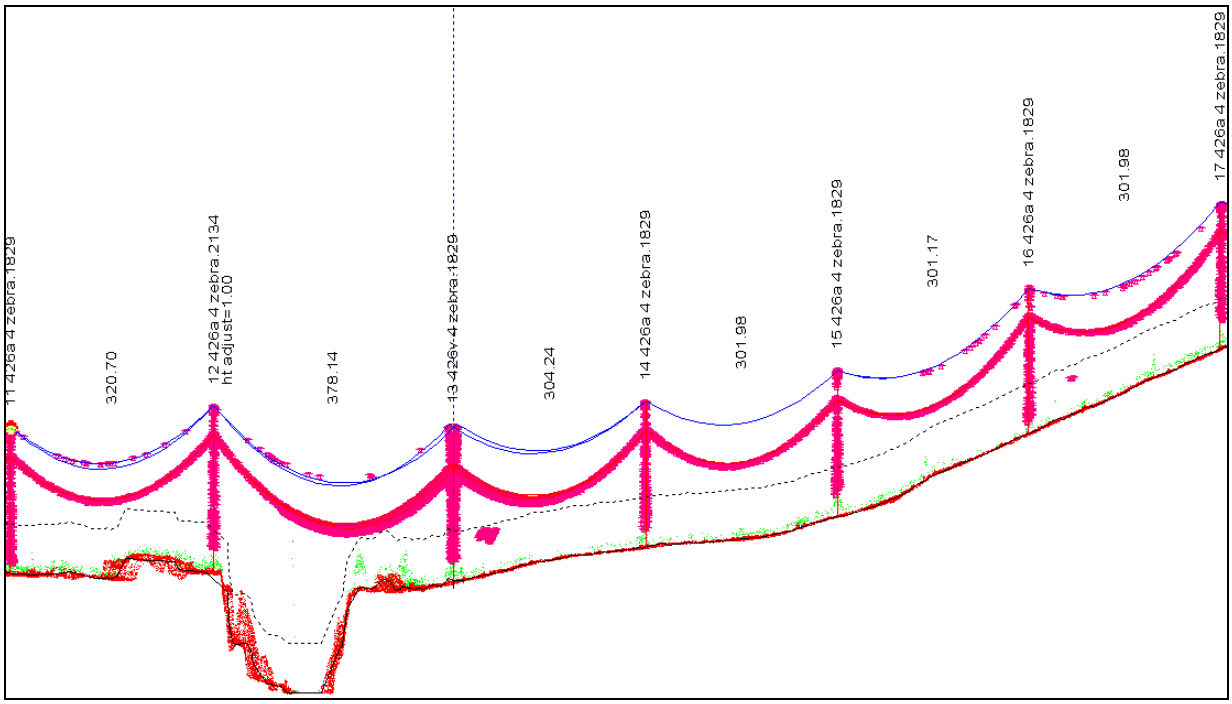

Figure B2: Transmission line model towers 11 – 17

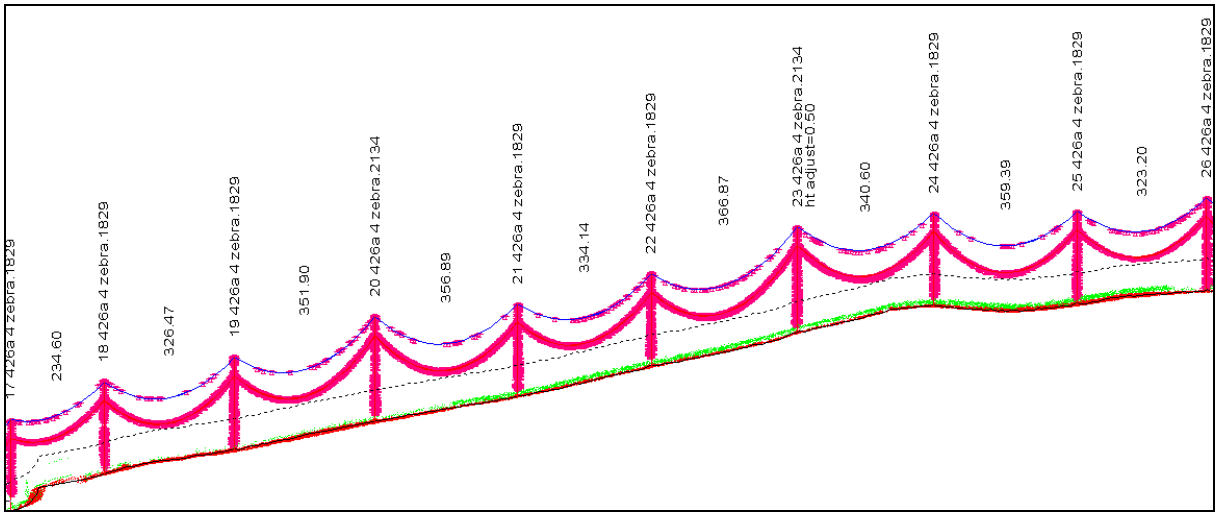

Figure B3: Transmission line model towers 17 – 26

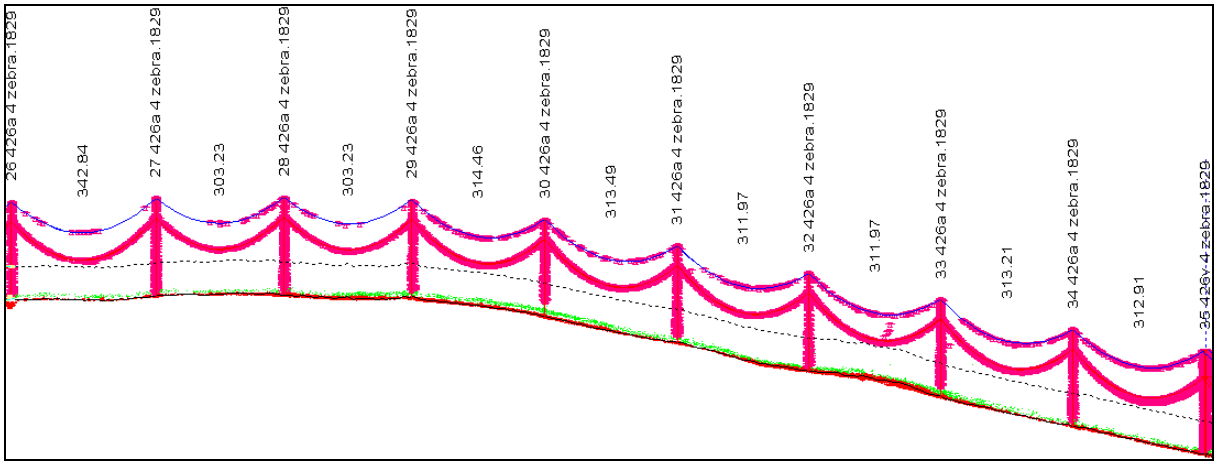

Figure B4: Transmission line model towers 26 – 35

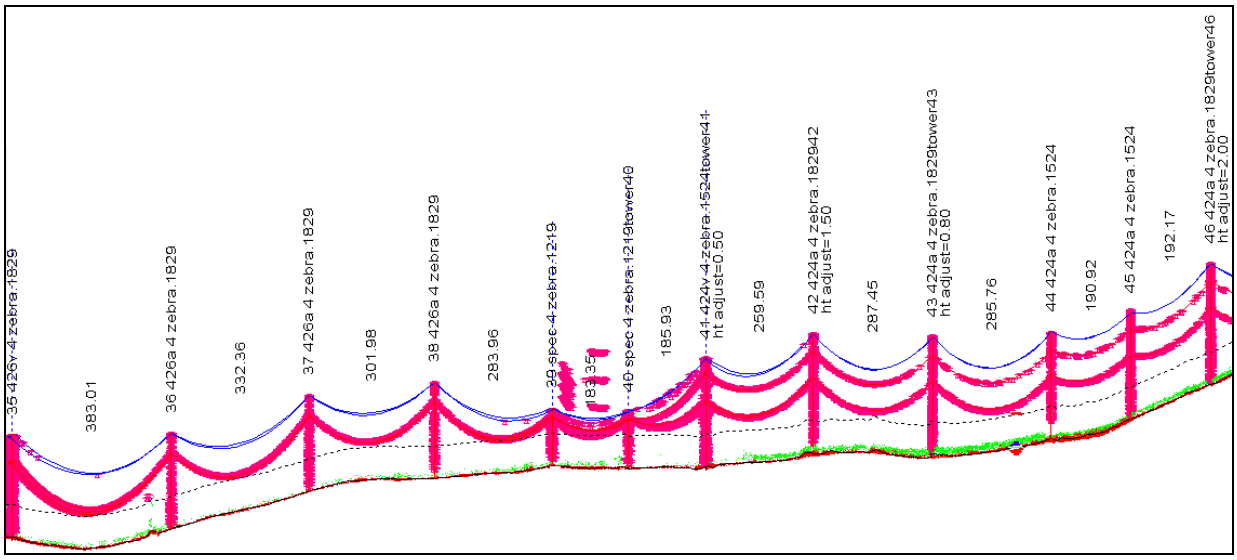

Figure B5: Transmission line model towers 35 – 46

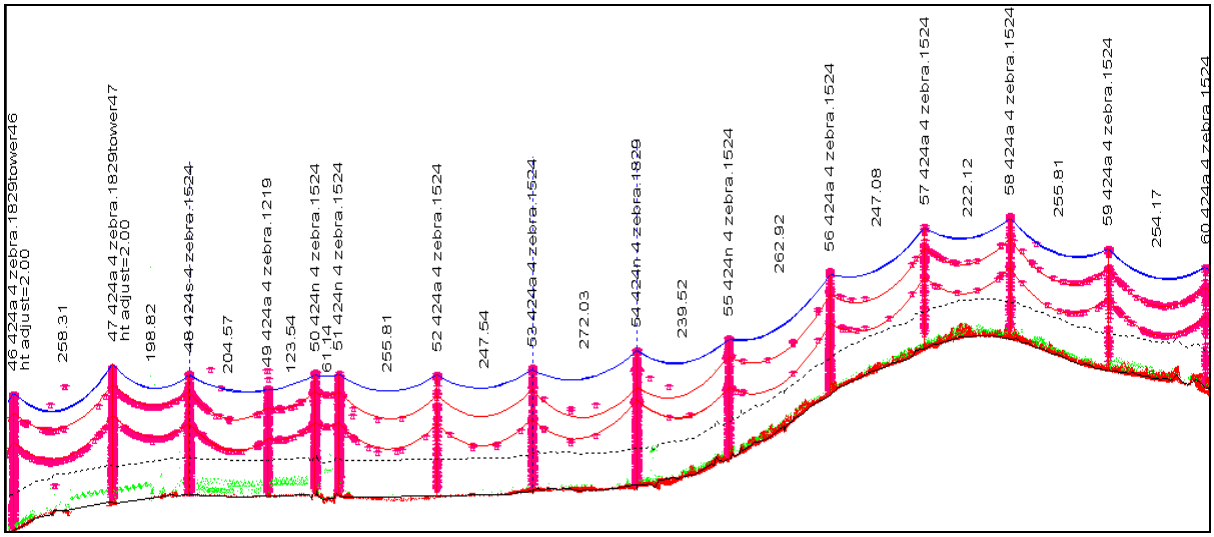

Figure B6: Transmission line model towers 46 – 60

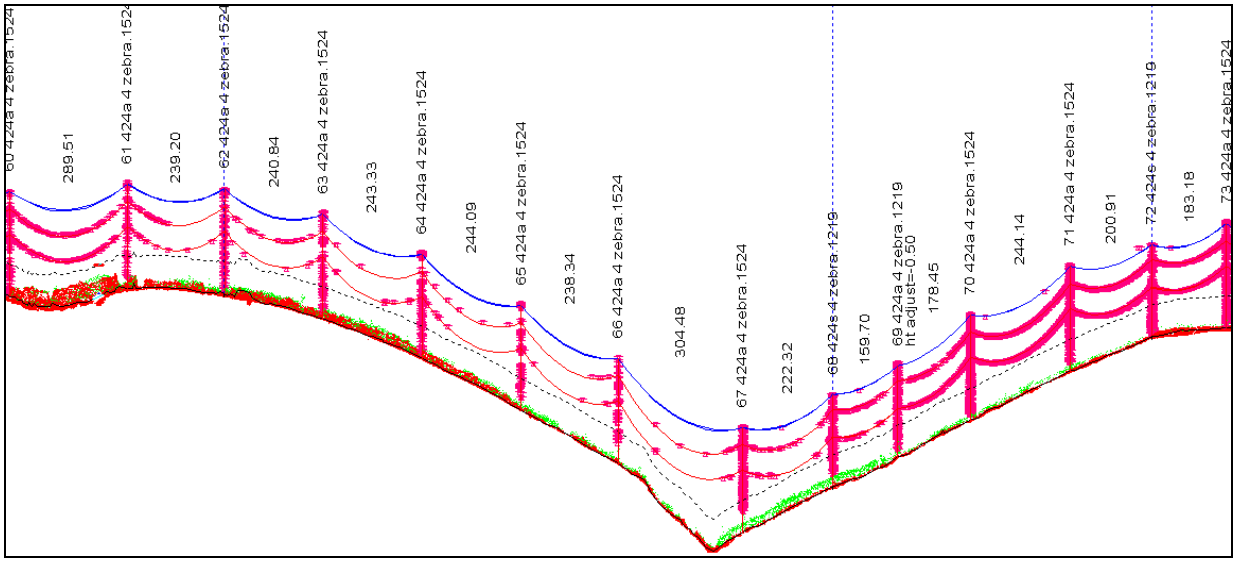

Figure B7: Transmission line model towers 46 – 60

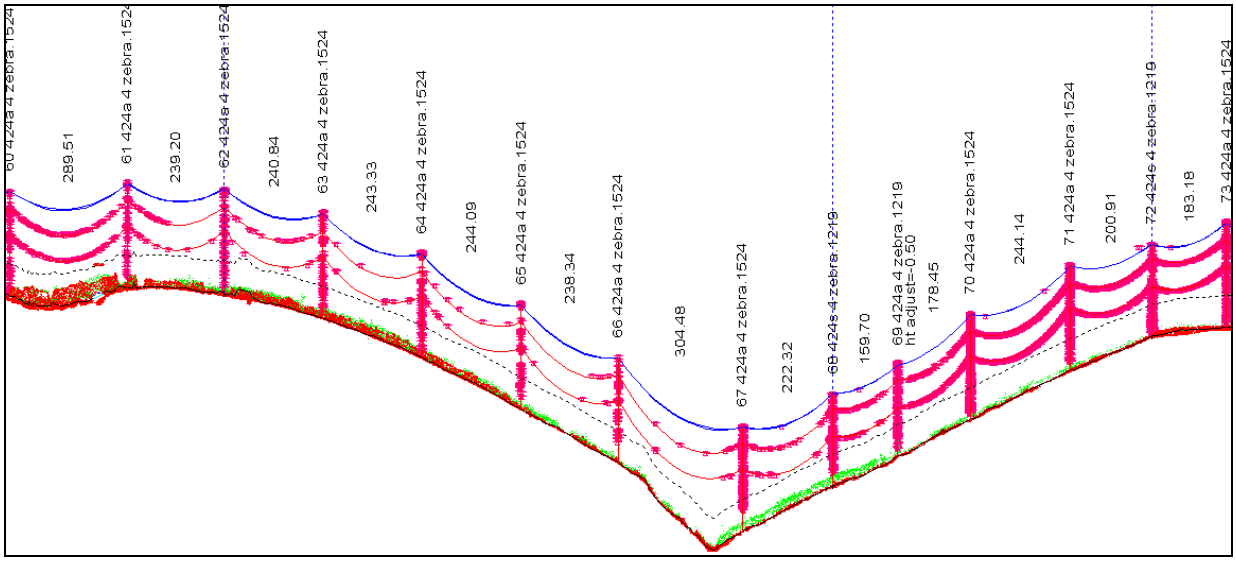

Figure B8: Transmission line model towers 60 – 73

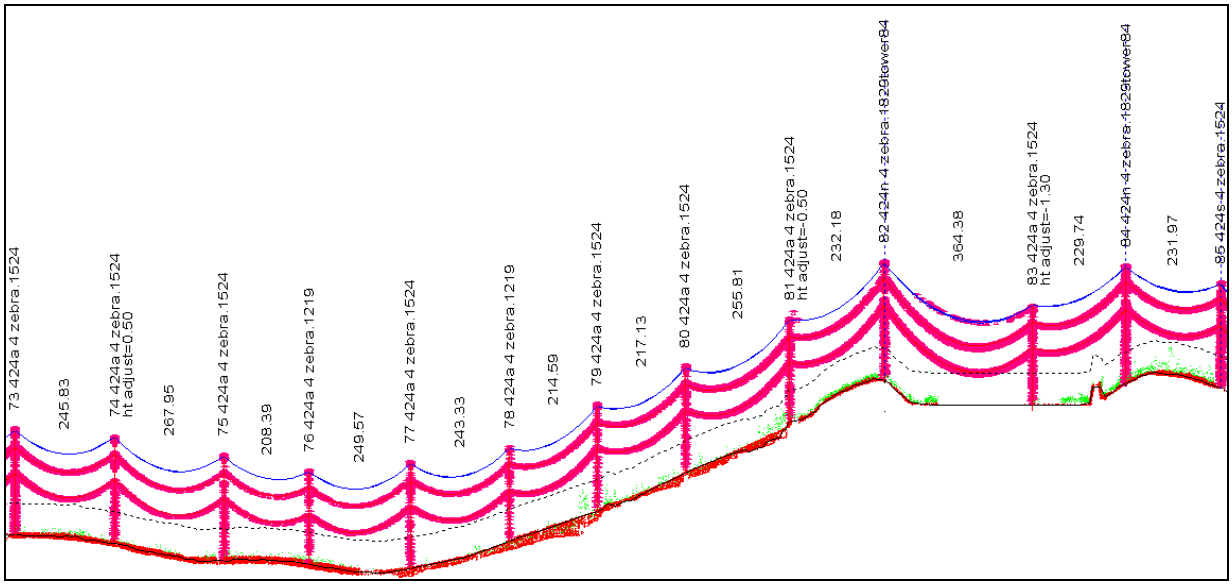

Figure B9: Transmission line model towers 73 - 85

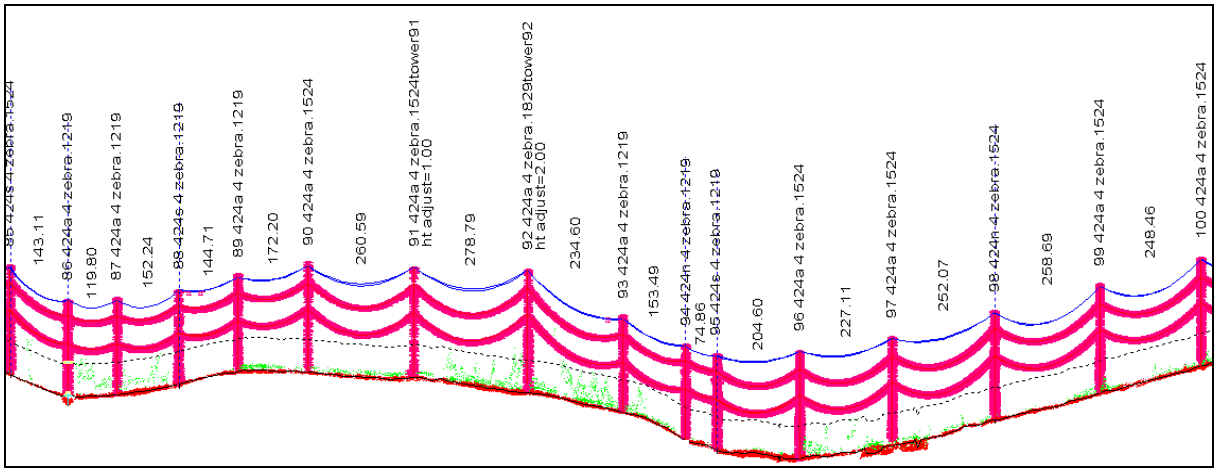

Figure B10: Transmission line model towers 85 – 100

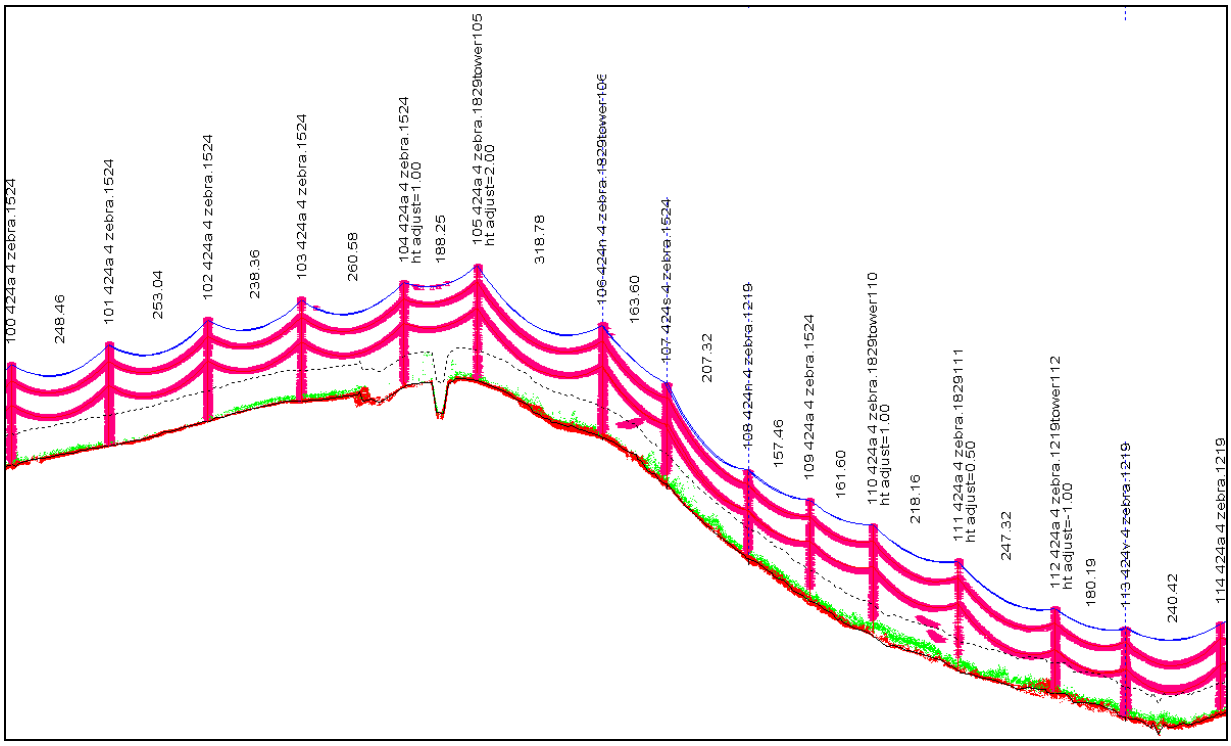

Figure B11: Transmission line model towers 100 – 114

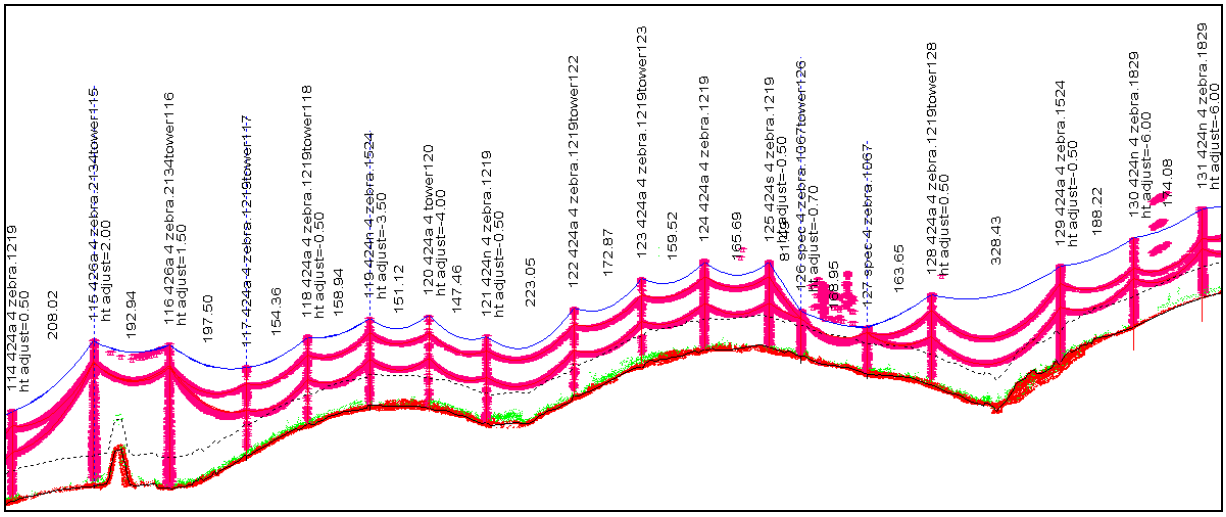

Figure B12: Transmission line model towers 114 - 131

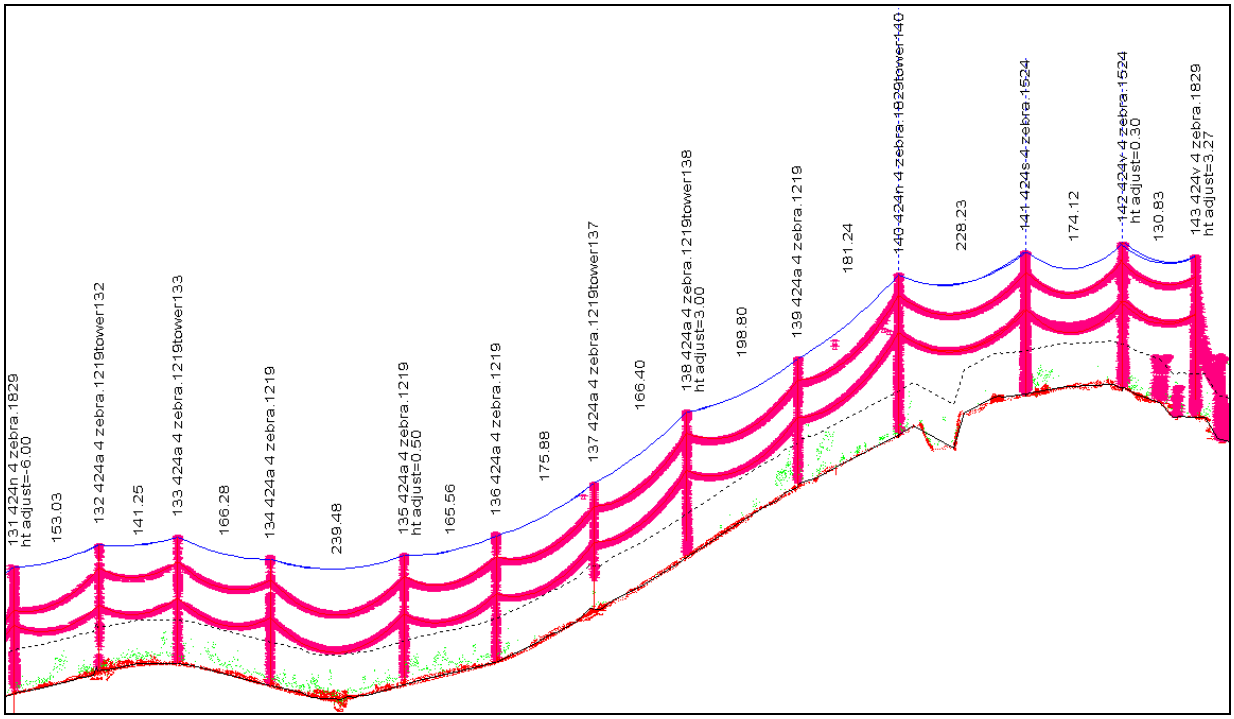

Figure B13: Transmission line model towers 131 - 143

ANNEXURE C: ESSELEN – JUPITER TRANSMISSION LINE MODEL

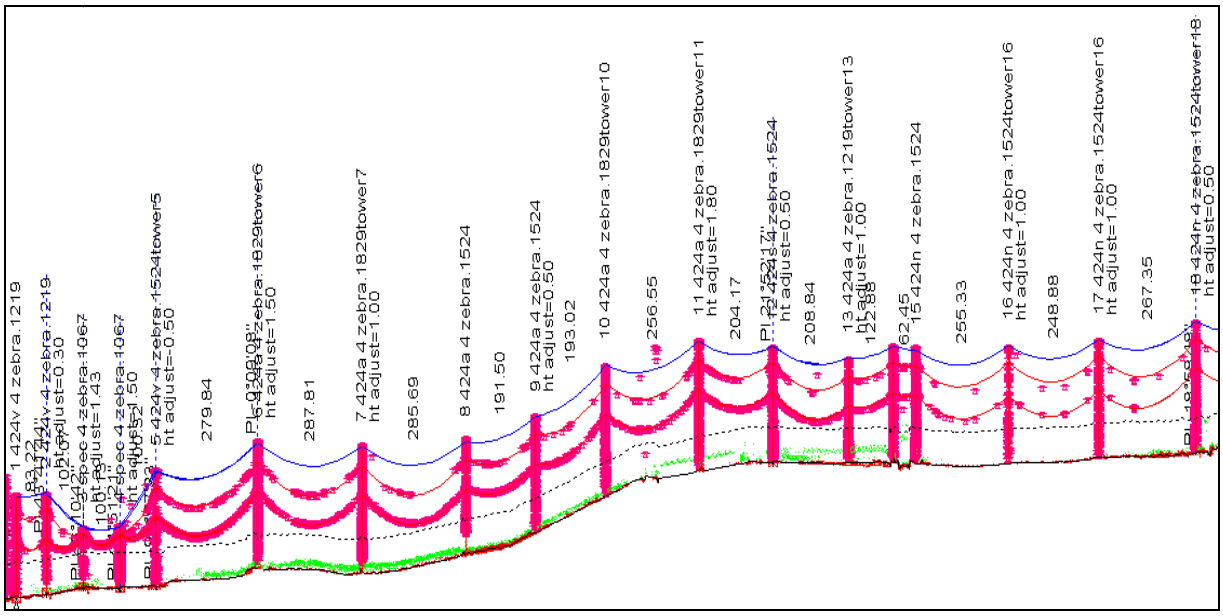

Figure C1: Transmission line model towers 1 - 18

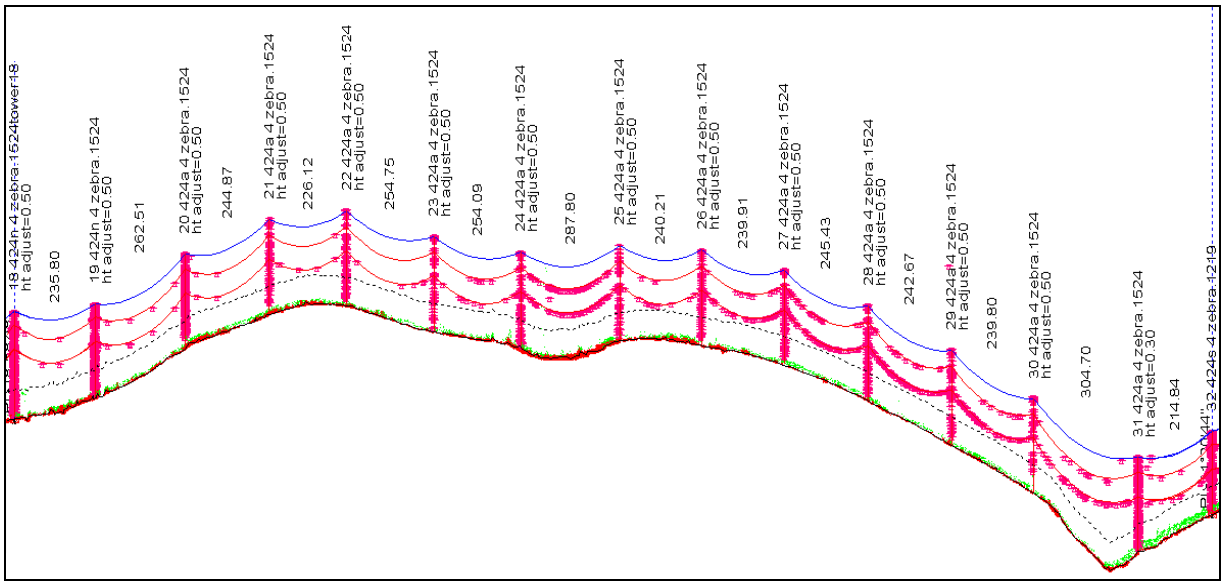

Figure C2: Transmission line model tower 18 - 32

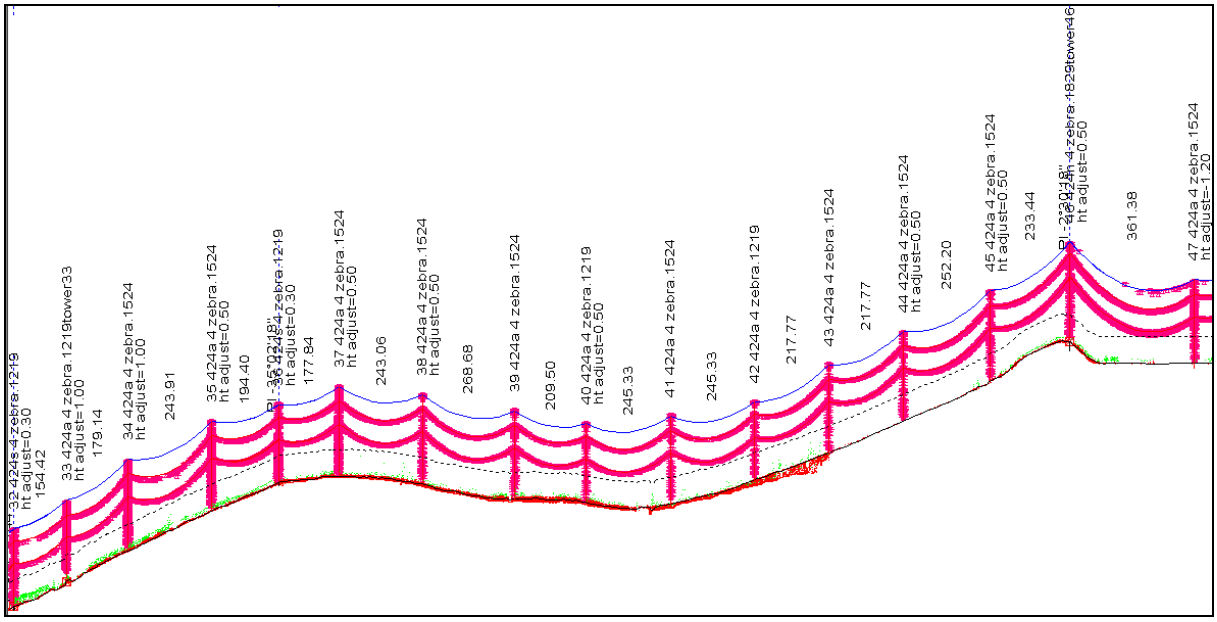

Figure C3: Transmission line model towers 32 – 47

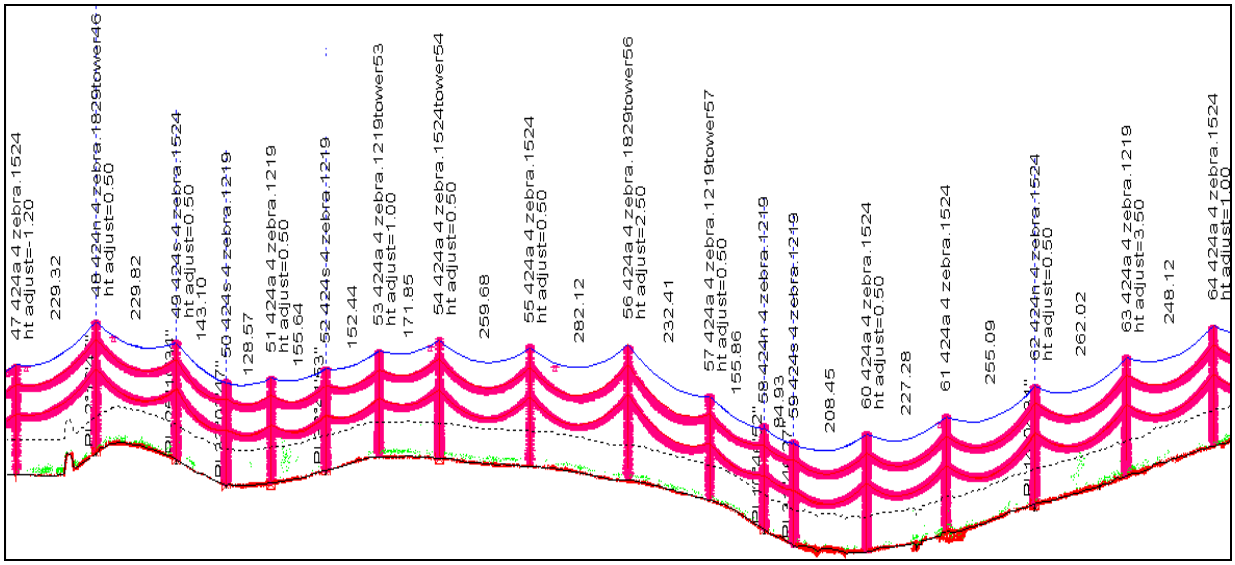

Figure C4: Transmission line model towers 47 – 64

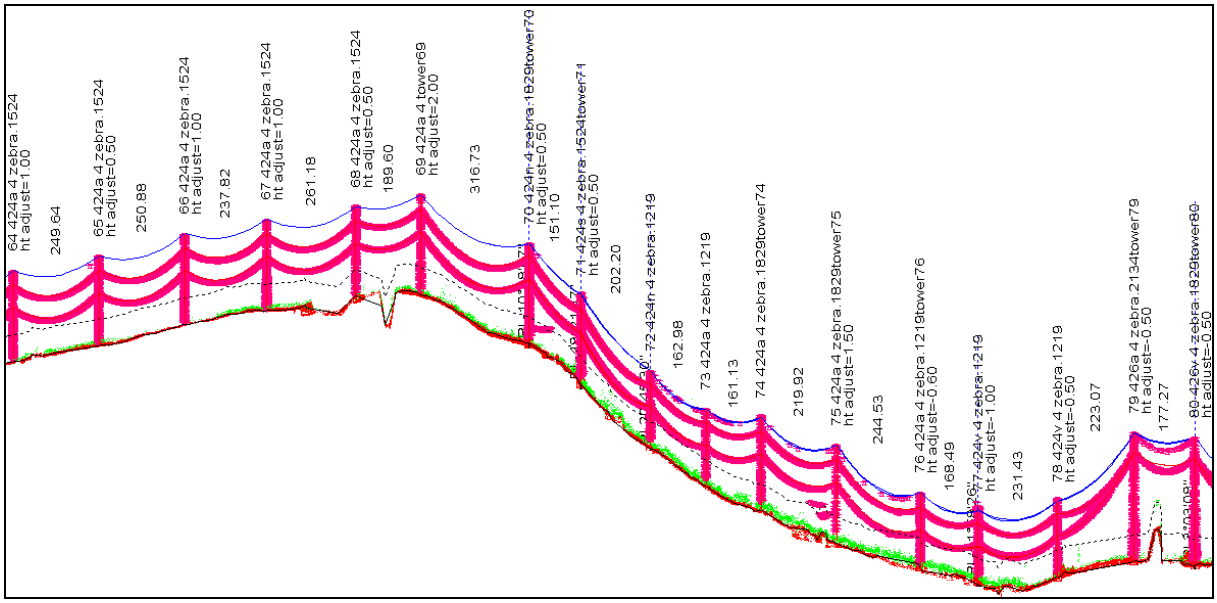

Figure C5: Transmission line model towers 64 – 80

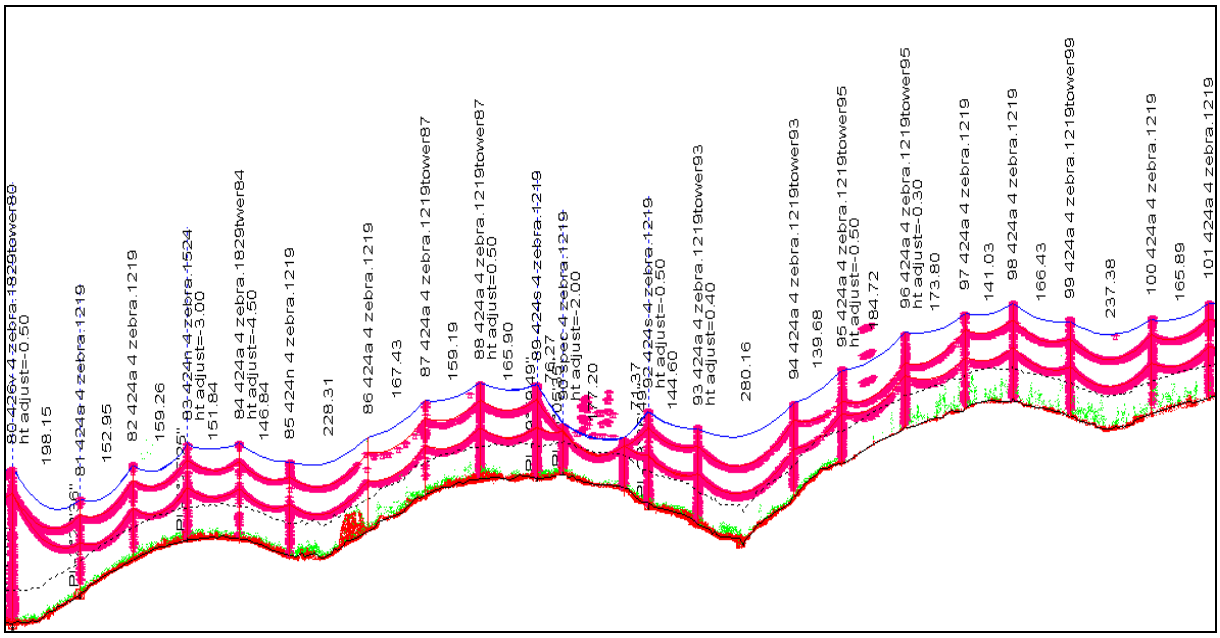

Figure C6: Transmission line model tower 80 – 101

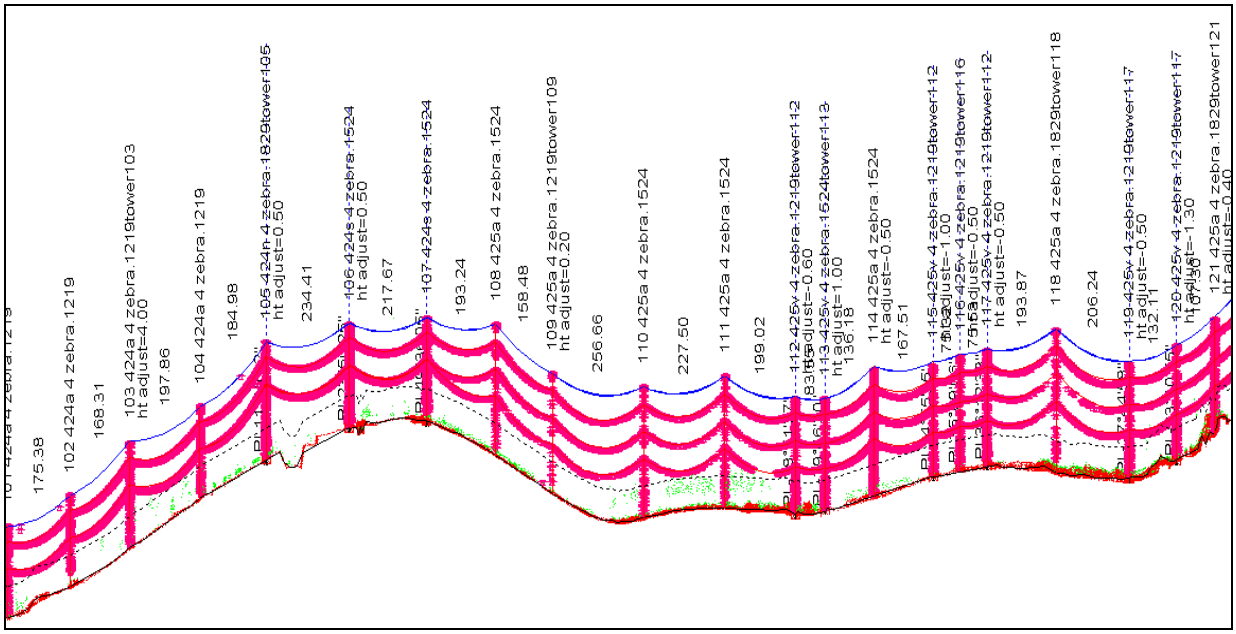

Figure C7: Transmission line model towers 101 – 121

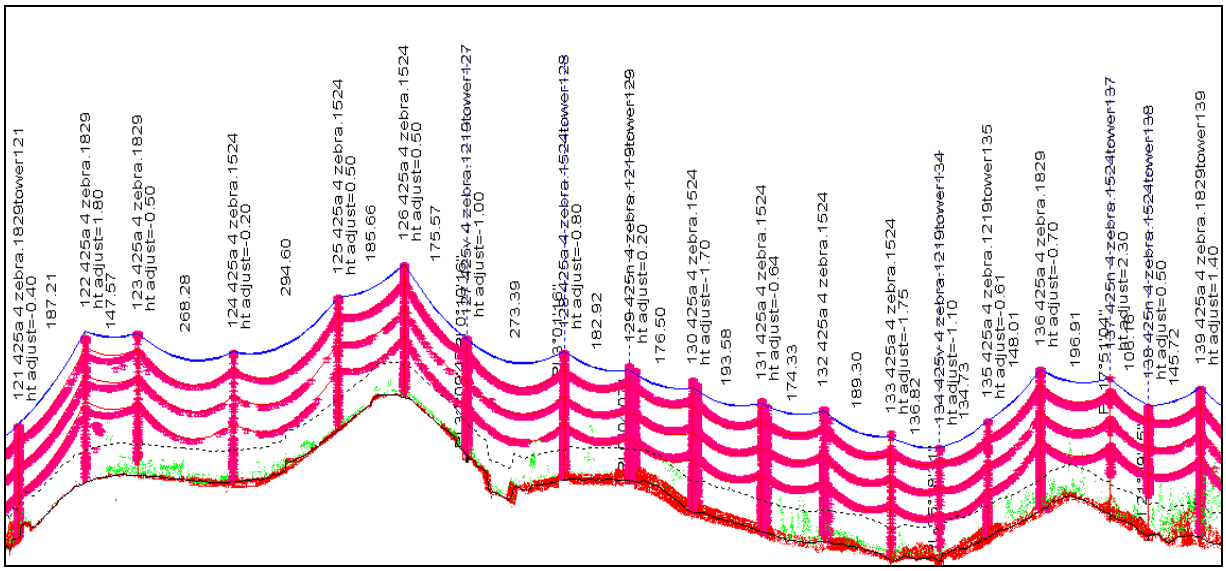

Figure C8: Transmission line model towers 121 – 139

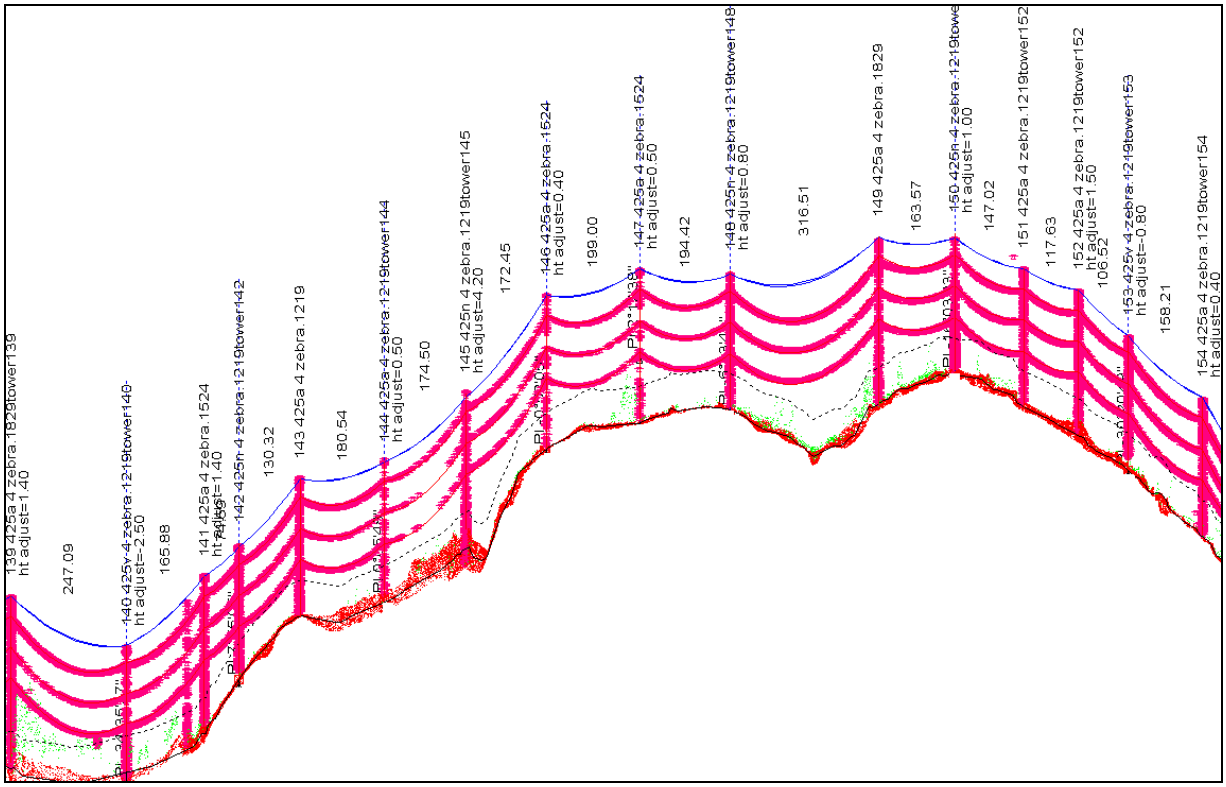

Figure C9: Transmission line model towers 139 – 154

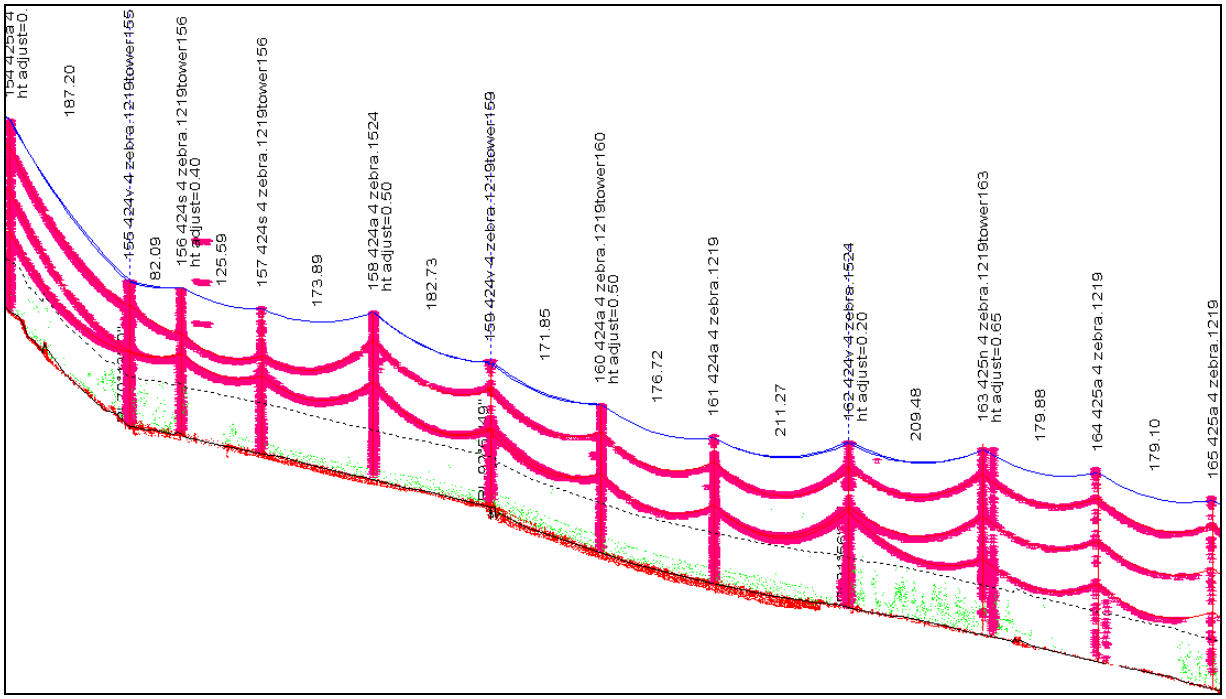

Figure C10: Transmission line model towers 154 – 165

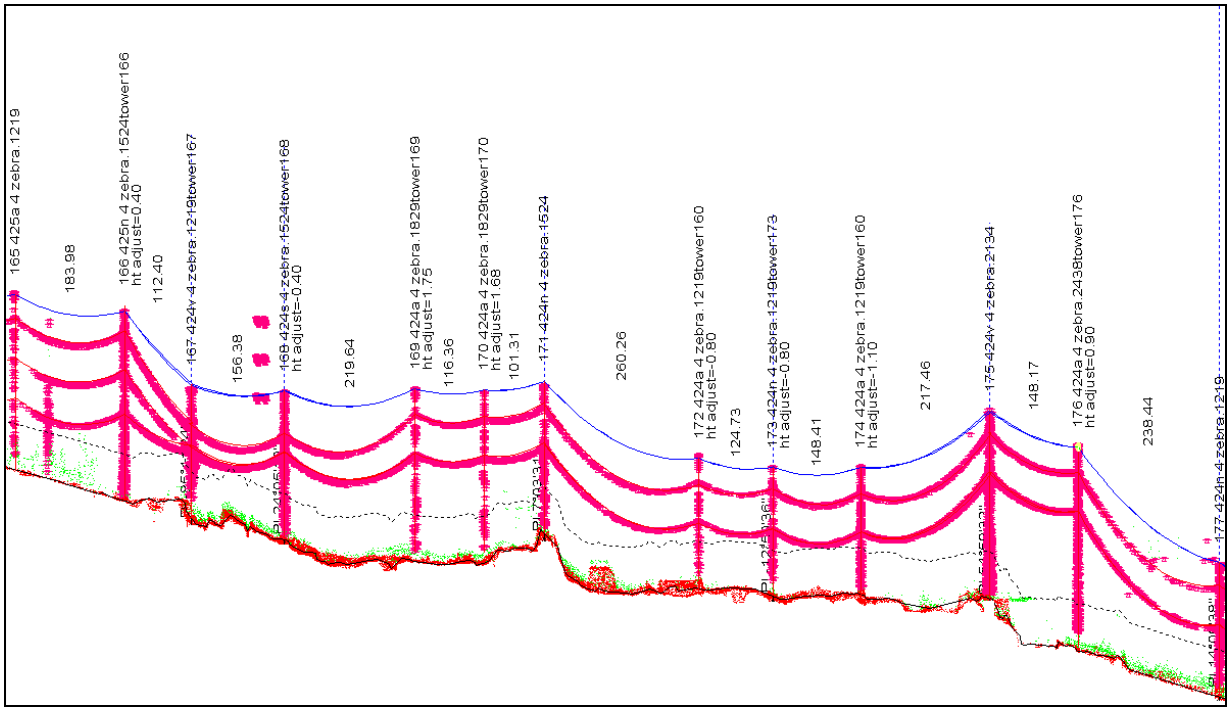

Figure C11: Transmission line model towers 165 – 177

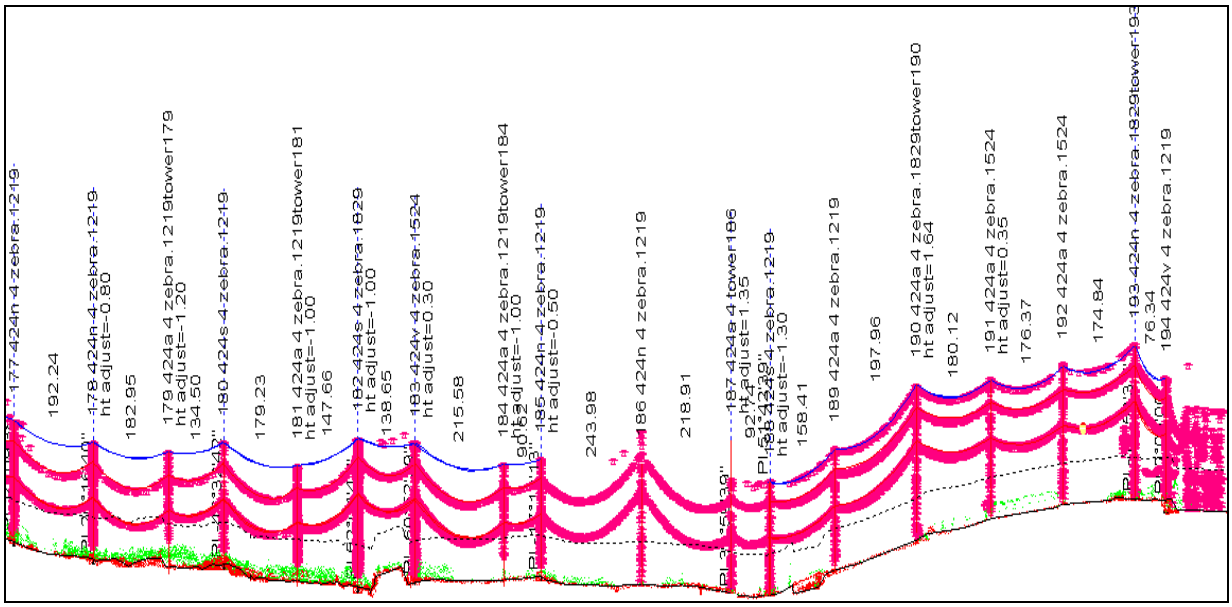

Figure C12: Transmission line model towers 177 – 194

ANNEXURE D: JUPITER – PROSPECT OPERATING TEMPERATURES

SPAN 5-6 (12 SENSORS)

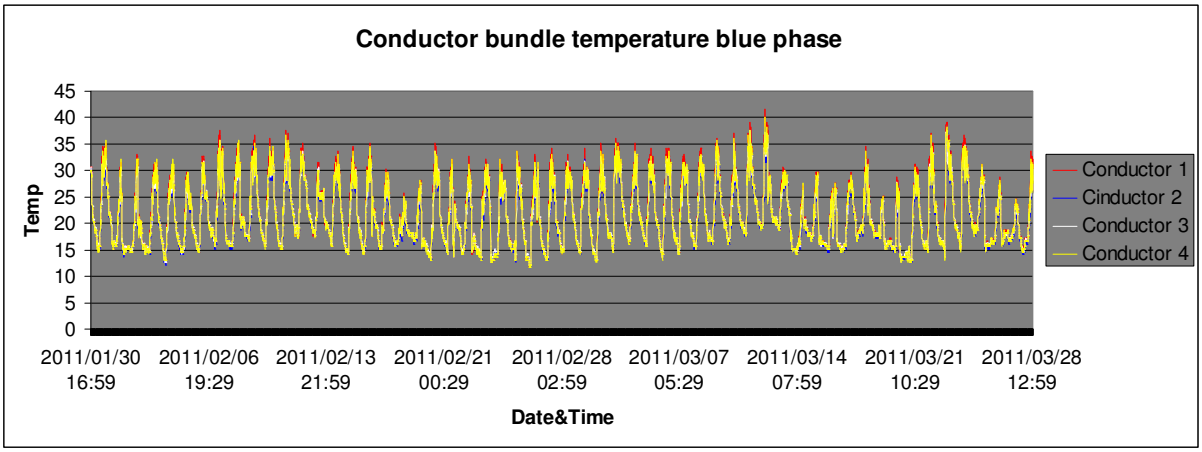

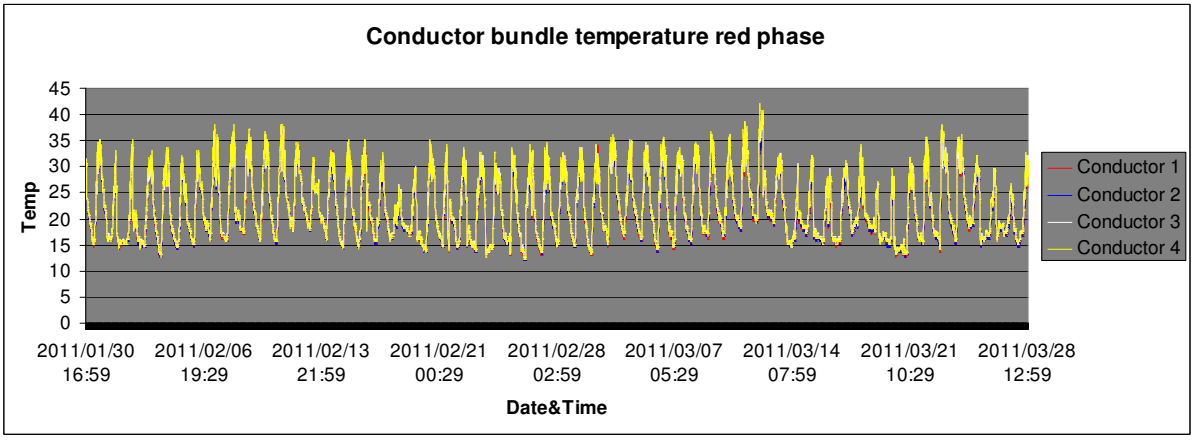

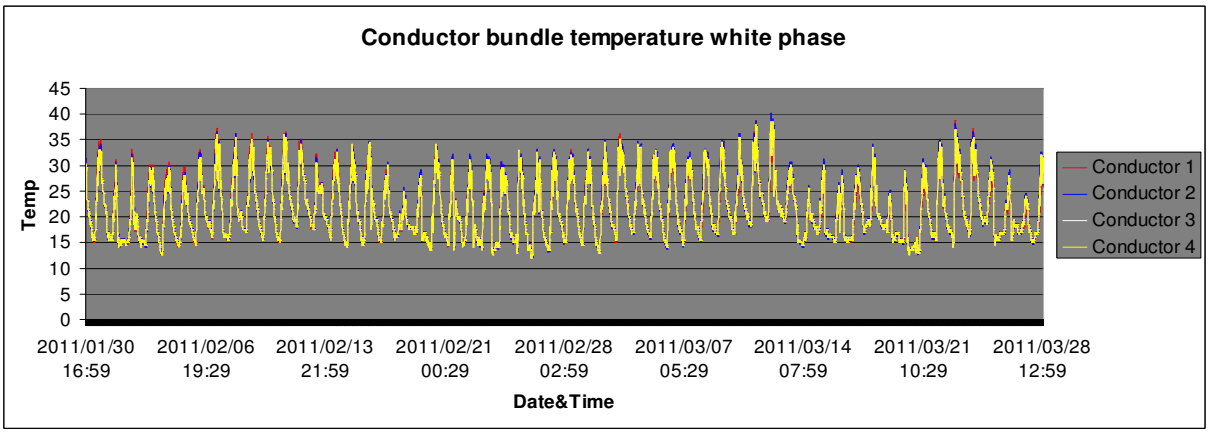

ANNEXURE E: APOLLO – CROYDON OPERATING TEMPERATURES

SPANS 1 – 2 (12 SENSORS)

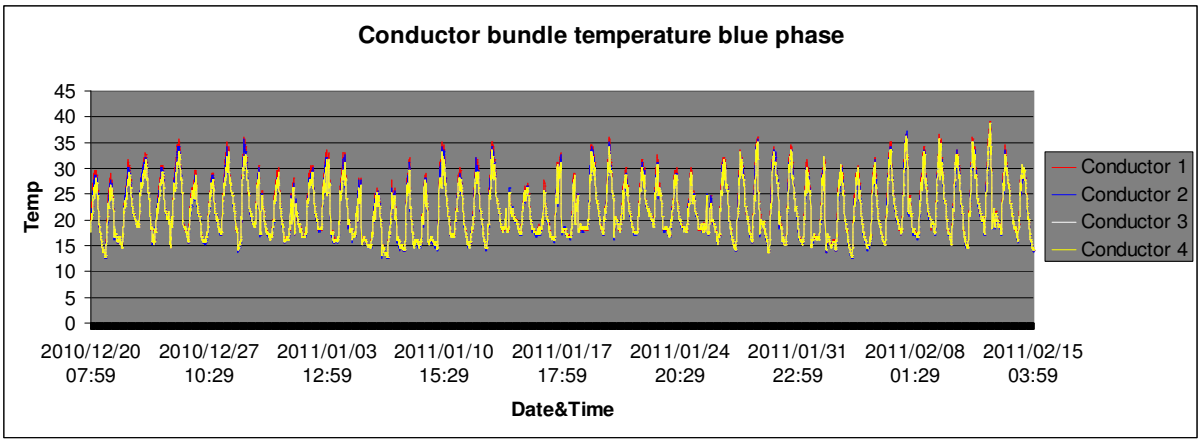

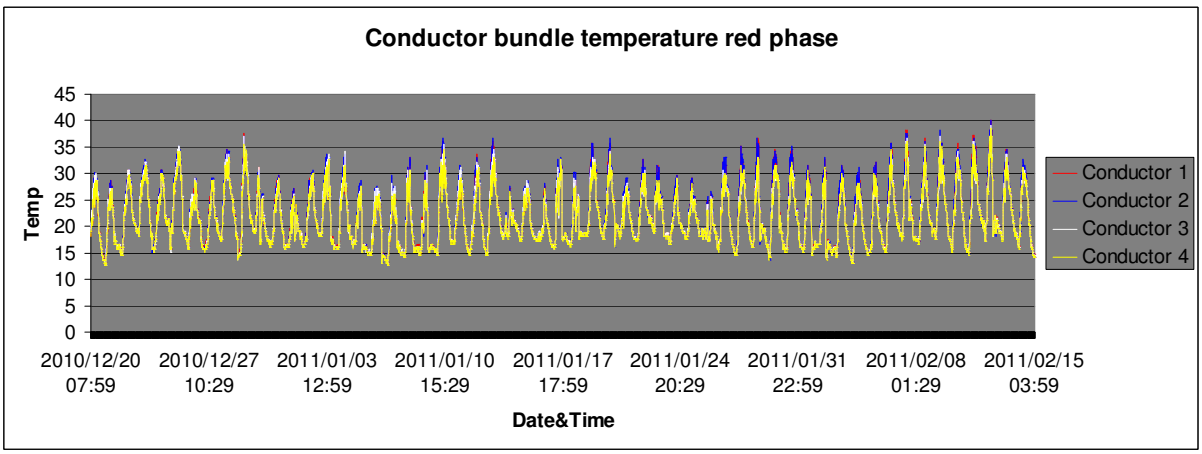

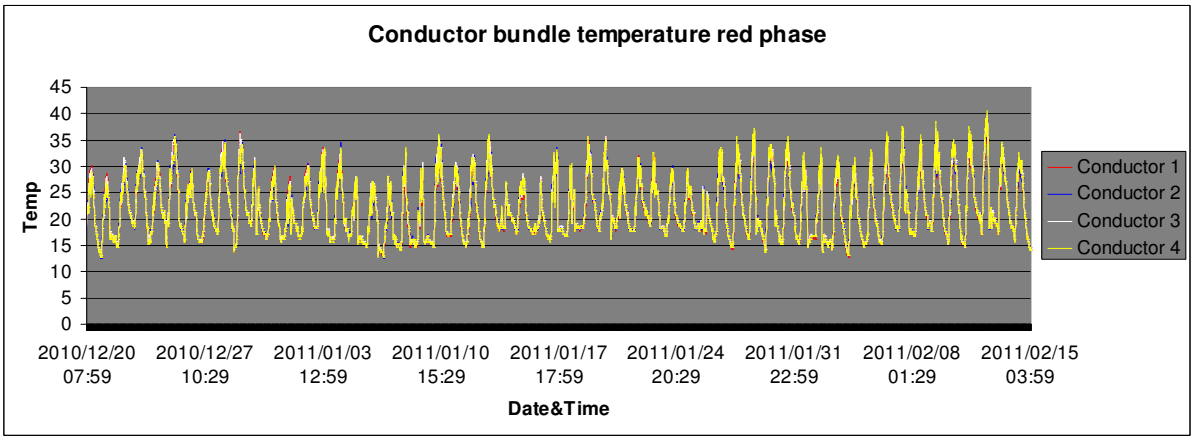

SPANS 8 – 9 (3 SENSORS)

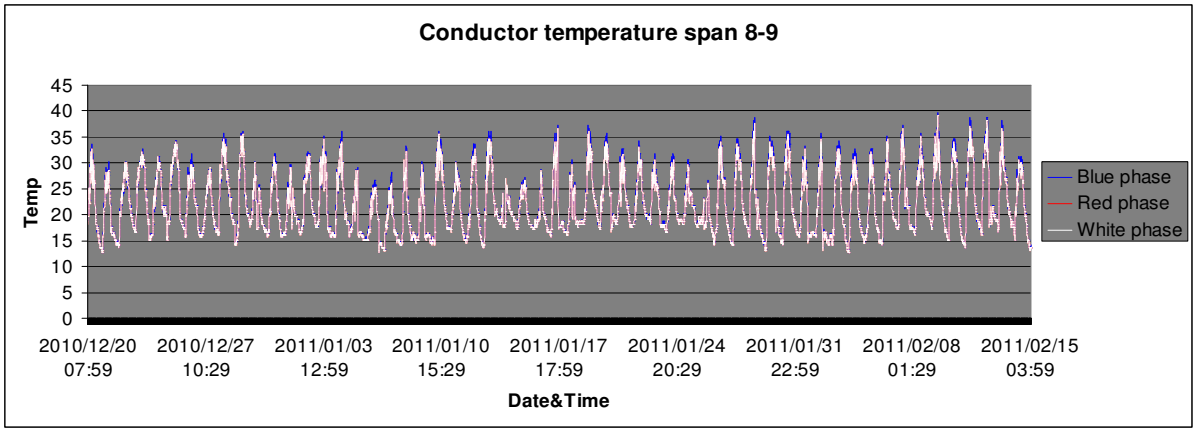

SPANS 28 – 29 (3 SENSORS)

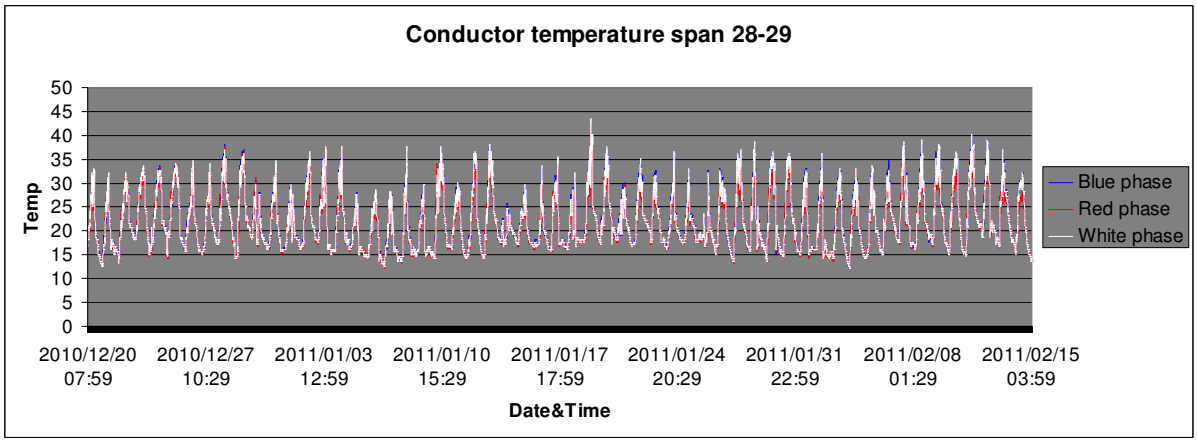

SPANS 59 – 60 (3 SENSORS)

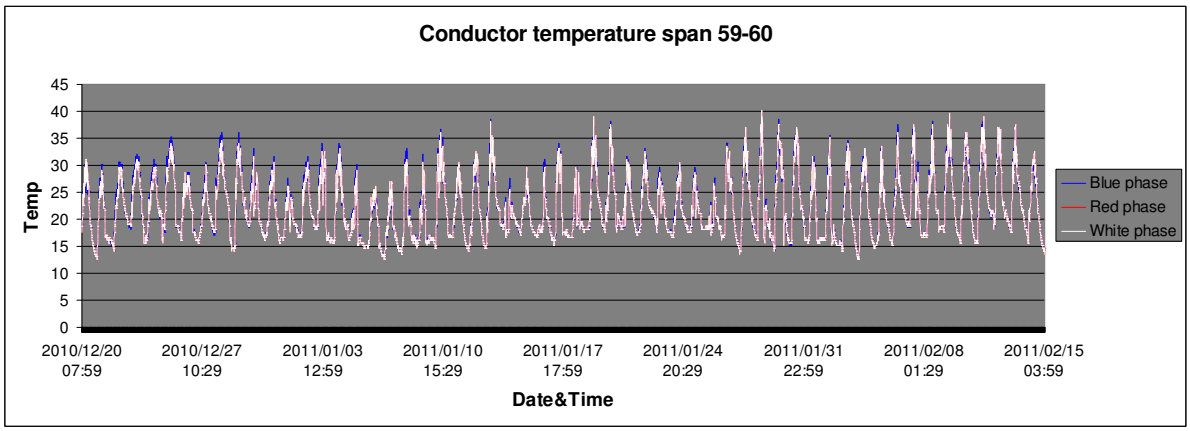

SPANS 65 – 66 (3 SENSORS)

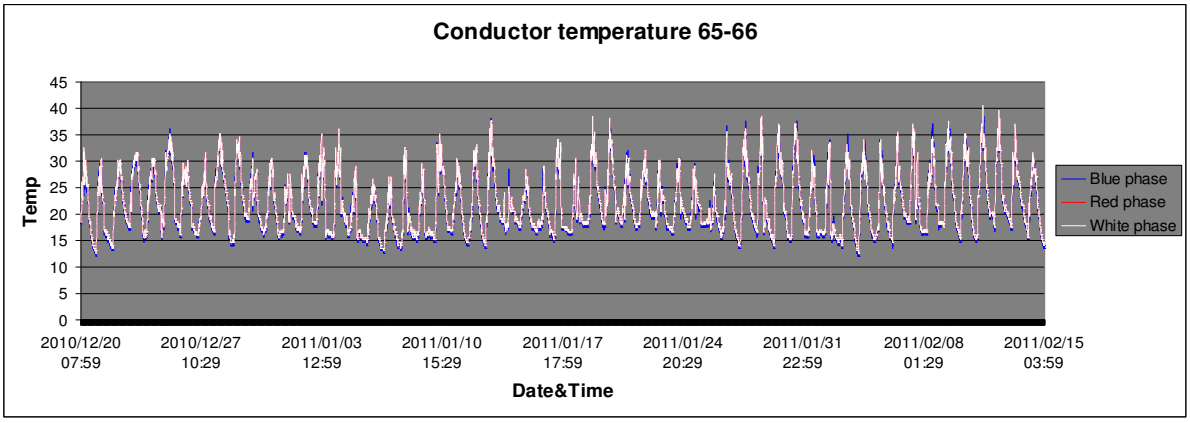

SPANS 81 – 82 (3 SENSORS)

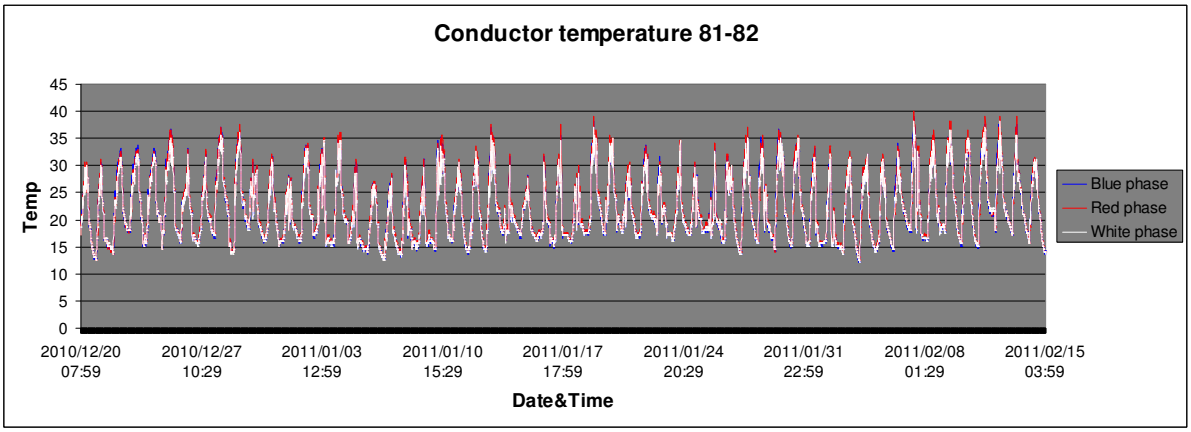

SPANS 149 – 150 (3 SENSORS)

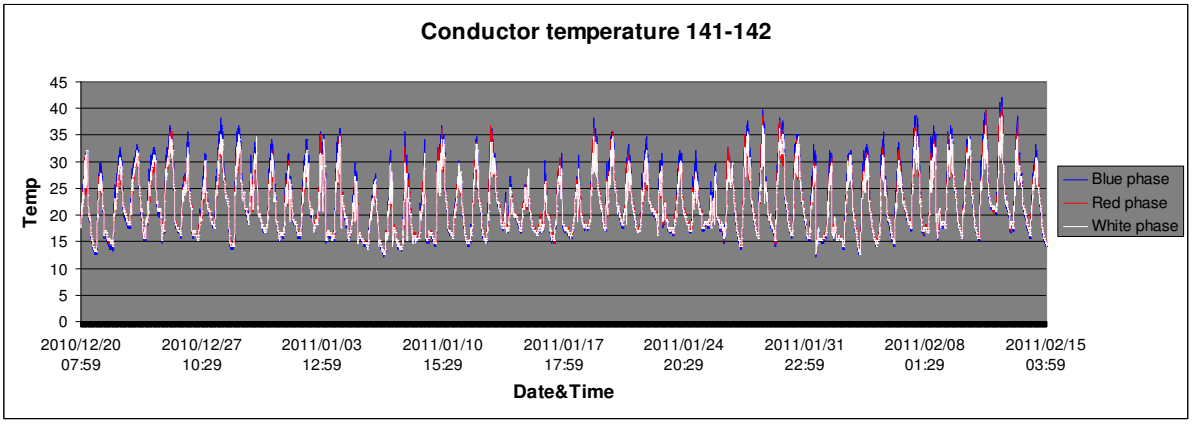

ANNEXURE F: ESSELEN – JUPITER OPERATING TEMPERATURES

SPANS 5 – 6 (3 SENSORS)

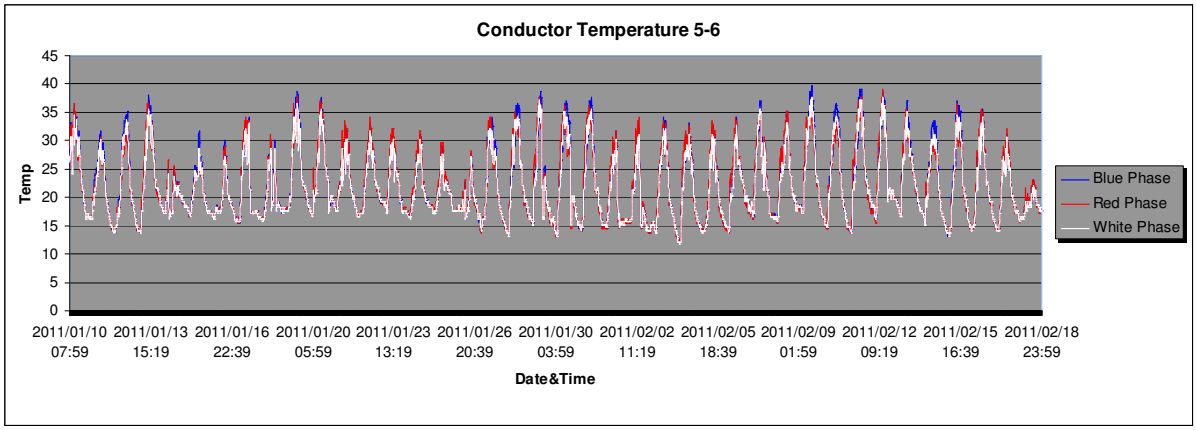

SPANS 125 – 126 (3 SENSORS)

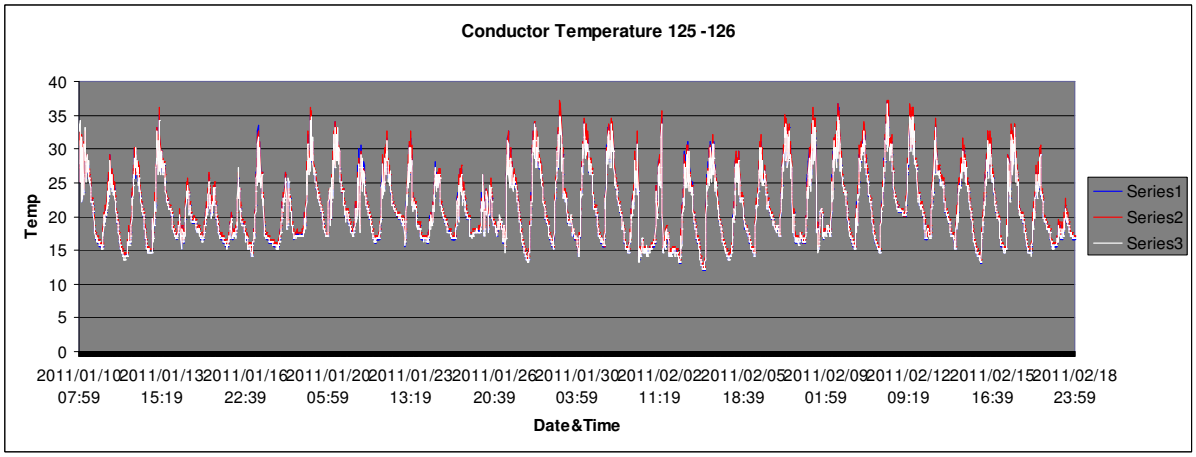

SPANS 125 – 126 (3 SENSORS)

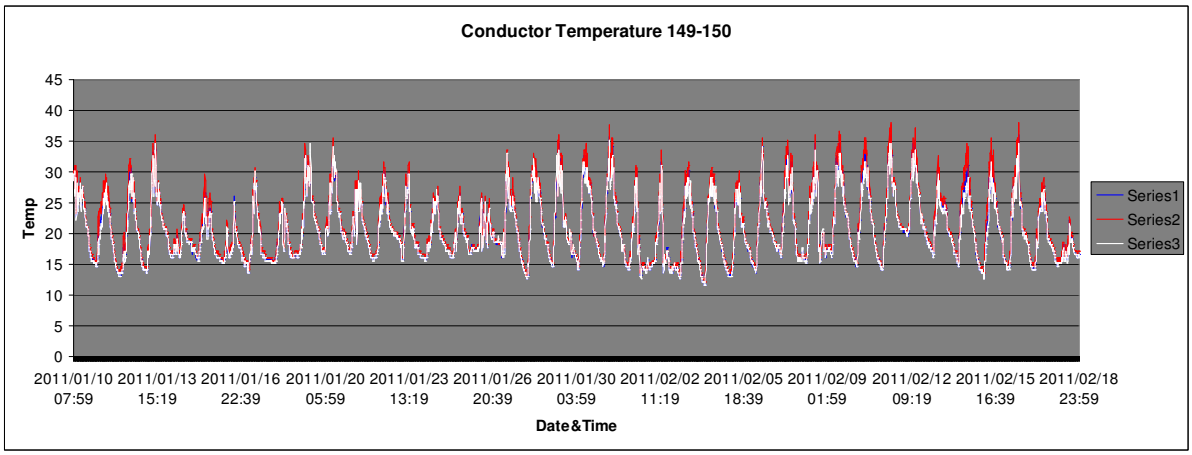

SPANS 182 – 183 (12 SENSORS)